2016

EXPERIMENTAL AND THEORETICAL INVESTIGATION OF SUSTAINABLE FAST PYROLYSIS BIOFUELS FROM WOODY BIOMASS

Bethany Jean Klemetsrud
Michigan Technological University, bjklemet@mtu.edu

EXPERIMENTAL AND THEORETICAL INVESTIGATION OF SUSTAINABLE FAST PYROLYSIS BIOFUELS FROM WOODY BIOMASS

By

Bethany J. Klemetsrud

A DISSERTATION

Submitted in partial fulfillment of the requirements for the degree of

DOCTOR OF PHILOSOPHY

In Chemical Engineering

MICHIGAN TECHNOLOGICAL UNIVERSITY

2016

This dissertation has been approved in partial fulfillment of the requirements for the Degree of DOCTOR OF PHILOSOPHY in Chemical Engineering.

Department of Chemical Engineering

Dissertation Advisor: *Dr. David Shonnard*

Committee Member: *Dr. Michael Mullins*

Committee Member: *Dr. Ezra Bar-Ziv*

Committee Member: *Dr. Julio Sacramento Rivero*

Department Chair: *Dr. S. Komar Kawatra*

Table of Contents

Preface

This doctoral dissertation contains material previously reviewed and published in scientific journals along with material currently submitted to scientific journals. Full citation of these are as follows:

Chapter 2

Reprinted with permission from SHONNARD D, KLEMETSRUD B, SACRAMENTO-RIVERO J, NAVARRO-PINEDA F, HILBERT J, HANDLER R , SUPPEN N, AND DONOVAN R. 2015. A REVIEW OF ENVIRONMENTAL LIFE CYCLE ASSESSMENTS OF LIQUID TRANSPORTATION BIOFUELS IN THE PAN AMERICAN REGION. ENVIRONMENTAL MANAGEMENT 56(6): 1356-1376.

DOI Link: 10.1007/s00267-015-0543-8

Author Contributions

Shonnard	Project lead, writing of the paper, interpretation of data, case study, review of the paper
Klemetsrud	Organized collaborative efforts, literature review, analysis of qualitative results, writing of the paper, in charge of submission and review of the journal article
Sacramento-Rivero	Interpretation of data, review of the paper
Navarro-Pineda	Literature review, analysis of quantitative results, writing of the paper, review of the paper

Hilbert	Interpretation of the data and review of the paper
Handler	Review of the paper,
Suppen	Review of the paper
Donovan	Review of the paper and collected data for case study

Chapter 3:

DOI: 10.1021/acssuschemeng.6b00610

Author Contributions

Klemetsrud	Experimental planning, collection of data, analysis and interpretation of data, writing of the paper, responsible for submission and review of journal article
Ukaew	Experimental planning, collection of data, analysis and interpretation of data, writing of the paper
Thompson V	Experimental planning, interpretation of data, paper review and editing
Thompson D	Interpretation of data, paper review and editing

Klinger	Experimental planning, analysis and interpretation of data, writing of the paper
Li	Collection and analysis of data
Eatherton	Collection and analysis of data
Puengprasert	Collection of data
Shonnard	Experimental planning, analysis and interpretation of data, paper review and editing

Chapter 4:

Submitted to ACS ENERGY AND FUELS KLEMETSRUD, B, EATHERTON, D, SHONNARD, D. EFFECT OF LIGNIN CONTENT AND TEMPERATURE ON THE PROPERTIES OF HYBRID POPLAR BIO-OIL, CHAR, AND GAS VIA FAST PYROLYSIS. ACS ENERGY AND FUELS

Author Contributions

Klemetsrud	Experimental planning, collection of data, analysis and interpretation of data, writing of the paper
Eatherton	Collection of data, analysis and interpretation of data,
Shonnard	Experimental planning, analysis and interpretation of data, paper review and editing

Chapter 5:

Will be submitted to JOURNAL OF ANALYTICAL AND APPLIED PYROLYSIS KLEMETSRUD, B, KLINGER , J, BAR ZIV, E, SHONNARD, D A KINETIC STUDY OF THE FAST MICRO-PYROLYSIS OF HYBRID POPLAR. JOURNAL OF ANALYTICAL AND APPLIED PYROLYSIS

Author Contributions

Klemetsrud	Experimental planning, collection of data, analysis and interpretation of data, application of models to data, writing of the paper
Klinger	Analysis of six stage degradation model, paper review and editing
Bar Ziv	Paper review and editing
Shonnard	Experimental planning, analysis and interpretation of data, paper review and editing

Acknowledgements

I would like to first acknowledge the financial support I received from the King-Chavez Parks Future Faculty Fellowship program. I would also like to acknowledge the financial support received from National Science Foundation's Sustainable Energy Pathway (MPS/CHE – ENG/ECCS –1230803) and a Research Collaboration Network on Pan American Biofuels and Bioenergy Sustainability (CBET-1140152"RCN-SEES) and the Richard and Bonnie Robbins Endowment.

I would like to express my utmost gratitude to my advisor and mentor, Dr. David Shonnard. Without your guidance, support and patience I would not be the researcher I am today. Thank you for all of the discussions, questions, and extra projects you have given me over the past 4 years. Thank you for all of the opportunities and helping to break down barriers for underrepresented minority students. A special thanks for participating in the AGEP, Individual Development Plan study. This was incredibly valuable and will help future URM students. I would like to acknowledge the support and guidance of my committee members, Dr. Ezra Bar Ziv, Dr. Julio Sacramento Rivero, and Dr. Michael Mullins. Thank you for your thoughtful questions, discussions and review of my research. A huge thank you to the staff in the Department of Chemical Engineering, especially Tanna Kallianen and Alexis Snell for your help with all of paper work and Jerry Norkol for your help fixing all of the things I broke. I

I am incredibly grateful to my research group throughout these past 4 years. Thank you for being available to brainstorm, vent or help in anyway possible. A special thanks to Olumide Winjobi, Suchada Ukaew, Rui Shi and Ulises Gracida Alvarez. I am

incredibly grateful to Jordan Klinger for helping guide me through graduate school, answering my endless questions and always being available for moral support. I would like to acknowledge all of the contributions of my undergraduate research assistants (Matthew Coel, Joshua Patton, Leanne Bregni, Dominic Eatherton, Adeline Koerner and Lucia Li) your work was invaluable.

Thank you to my family for supporting me in this endeavor. Never in my wildest dreams did I expect to obtain my doctorate. Thank you for all of the encouragement, the stressed out Facetime calls and for there being no shortage of laughter. Thank you so much to all of my friends here at Michigan Tech and in the Houghton community. You have truly made this place seem like home. Your constant encouragement, pep talks, meals, coffee breaks and meaningful discussions have brightened each and every day. I would especially like the thank all of my friends at Canterbury House and Good Shepherd Lutheran Church. From the minute I walked through the door, you all felt like family.

Abstract

Biofuels are an important advancement in alternative energy that can provide substantial environmental benefits compared to their conventional fossil fuel counterparts Said benefits are usually measured using life cycle assessments. However, it is not well understood yet how different methodological choices such as system boundaries, biomass feedstocks, conversion pathways, geographical data, etc. affect the conclusions drawn from biofuels LCA. This research shows large variability in life cycle assessment results and limits comparison across different biofuel pathways due to methodological choices set forth by policy and certification schemes. Advanced biofuels have not reached large scale production due to a limited understanding of thermochemical conversion of various feedstocks and the cost of these feedstocks.

To address the issues of feedstock cost, municipal solid waste (MS) was evaluated as a feedstock for the production of bio-oil via fast pyrolysis. MSW (paper waste, grass clippings, fiberboard, waferboard, microllam, plywood) produced similar yields as that of its traditional feedstocks (switchgrass, corn stover and hybrid poplar). Bio-oil yields ranged from 58% to 77% for the MSW feedstocks. The woody waste had the highest yields and the largest production of lignin derived compounds while the paper waste had higher levels of carbohydrate derived compounds and lower yields.

To understand how controlled variations in feedstock affected bio-oil speciation, 8 genetically different hybrid poplar samples with increasing lignin content from 17%-22% were pyrolyzed at 500°C, 550°C and 600°C. The purpose of this work was to evaluate how the effect of increasing lignin content with respect to increasing temperature affects

product distribution and bio-oil speciation. With increasing lignin content at 500°C the char yield increased from 17.5% to 27.2% and the bio-oil yield decreased from 73% to 65%. With increasing temperature the increase in lignin, allowed for a higher percentage of lignin derived compounds within the bio-oil.

To gain a better understanding into biomass degradation, kinetic data was obtained using a micropyrolysis GC/MS experimental set-up. This data was quantified and the mass of bio-oil species produced with respect to time was calculated. The kinetic data showed that hemicellulose derived bio-oil compounds such as acetic acid was produced in large quantities initially, whereas lignin derived compounds such as methyl syringol had a delay in production and took a longer time to reach maximum production. Application of a first order exponential decay model and a six-step degradation model were applied to the data. The first order exponential decay model was insufficient for capturing the initial production of the bio-oil compounds. The six stage degradation model fit the data very well and was able to give insight into biomass degradation with respect to the stoichiometric parameters. These parameters showed that hemicellulose degrades first and then cellulose and lignin degrade at later times agreeing with previous literature. These data along with the application of the six stage degradation model gives a better understanding of biomass degradation with the use of a semi-empirical model. Overall this work shows that MSW and hybrid poplar bio-oil produced via fast pyrolysis are a viable option for the production of biofuels and contributes to the overall knowledge needed for the implementation and advancement within the biofuel industry

1. Introduction

1.1 Overview of Research

Biofuels are considered an integral part of the world's renewable energy portfolio. Biofuels are derived from plant or animal material and can be converted through one of two pathways; biochemical and thermochemical. These pathway categories also offer conventional and advanced technologies, depending on feedstock type [1]. Biofuels are considered advantageous due to their potential to offset greenhouse gas emissions compared to their fossil fuel counterparts. Biofuels have gained market share in the US and globally due to their market demand from policies set forth by governments to reduce greenhouse gas emissions, create rural jobs, and promote national energy independence [2-5] . Despite momentum gained in commercial production of biofuels, barriers remain in large-scale adoption of biofuels due to technological and sustainability challenges.

This dissertation has two main emphases. The first is on a review of the overall biofuel sustainability in the Pan American region in the context of environmental life cycle assessment (LCA). The goal in this is to gain a better understanding of the reasons for variability in LCA methods and results for a wide range of biofuel pathways in different countries and locations. The second focus is on the conversion of municipal solid waste and woody materials to an energy rich bio-oil through fast pyrolysis. Fast pyrolysis is one of the main thermochemical platform process technologies that could allow for the use of woody biomass as biofuel feedstock, one of the most abundant forms of biomass on Earth.

1.2 Policy

According to the USEPA's RFS2 there are mandates which require that by 2022, 21 billion gallons of biofuel produced must be considered advanced. In 2015 the United States produced 14.8 million gallons of corn ethanol, however there was no significant production of advanced biofuels[6]. There are several other policies around the world that influence the production of biofuels across the globe. The most common policies that influence biofuel production are the European Union's Renewable Energy Directive and the Roundtable for Sustainable Biomaterials. The US RFS2 and the EU-RED are both government policies whereas the RSB is a voluntary certification. These policies all have different criteria set forth for biofuels to qualify or obtain certification from these policies and schemes. The EU-RED requires to meet 35% reduction in greenhouse gas emissions compared to its fossil fuel alternative. On the other hand, for a biofuel to be considered advanced within the US RFS2 it must meet 50% reduction in GHG emission. To comply with the RSB biofuels must also meet a 50% reduction. A brief comparison is shown in Table 2.1.

In order to achieve these mandates set forth by the United States government there are several technical advances that must be met, along with environmental assessment methods that must follow. Aside from the national mandate set forth by the EPA, 29 out of 50 states, along with Washington D.C. have set forth renewable portfolio standards (RPS). The RPS goal is to encourage and increase production of renewable electricity from solar, wind, geothermal and biomass. These goals are set forth at the state level. For

example the state of Michigan passed legislation stating that 10% of its electricity must come from renewable resources. [7]

To encourage the production of renewable electricity, most states offer a tax incentive for companies helping achieve these policy requirements. One issue when evaluating the effect of policy on the production of biofuels is that the status of biofuels adhering to renewable energy standards is not well known. One way to evaluate if biofuels are meeting requirements set forth by policy is to employ life cycle assessment, so that achieving the targeted greenhouse gas emission savings can be documented for each qualified biofuel.

1.3 Life Cycle Assessment

Life cycle assessment (LCA) is a tool that allows for the tracking of inputs, outputs and environmental impacts throughout a process or product's entire life cycle, from cradle (extraction) to grave (disposal). LCA is mandated by government policy such as RFS2 and RED to qualify biofuels based on sustainability targets such as reductions in greenhouse gas emissions compared to fossil fuels. LCA adheres to a standard methodology set forth by the International Organization for Standardization (ISO 14040-14044) [8-11]. These standards allow for LCAs to be conducted in a consistent manner to ensure results are accurate, comprehensive, and can be compared among different products. However there are areas where the standards are not clear and variability may occur due to regulatory mandates, such as the RFS2 and the European Union's Renewable Energy Directive (RED) different methods of handling co-products from biofuel production [12, 13]. Areas of potential variability include, allocation (how the

coproducts are handled with respect to sharing the pathway environmental burdens), functional unit (the basis for conducting the LCA and equivalence among different products that are compared), as well as quality and availability of data. Geographical and system boundaries also are large factors when considering the variability in LCA's conducted, as well as the technology and time relevance of the data.

Several studies have been done to look at sustainability of biofuel production and use employing LCA's conducted in the European context, however little attention has been paid to the Pan American region, even with their dominance in global biofuel production [14]. The variabilities of methodology used to assess the sustainability of advanced biofuels is not well understood especially within the context of other countries renewable fuel mandates. One of the barriers that is needed to overcome the increase in demand of biofuels and mandates is to understand where the variability in assessment comes from. When focusing on the US EPA's mandate it is very straightforward, but when comparing these biofuel pathways to those implemented in other countries, such as Brazil or Sweden, it becomes much more difficult. Therefore, a study assessing the variability of LCA's is needed in the Pan American context.

1.4 Biomass and Conversion Technologies

The second thing that is needed to reach the 21 billion gallon goal, is the actual production of advanced biofuels. By definition, advanced biofuels are biofuels produced from renewable biomass (excluding corn starch) that reduce GHG emissions by 50%. Traditionally biofuels in the United States have been produced from corn, and the ethanol industry has been well established and subsidized by the U.S. government. There are

several pathways that are being investigated and assessed in biofuel research to achieve these mandates set forth. Figure 1.1 below shows several different pathways that are currently being explored.

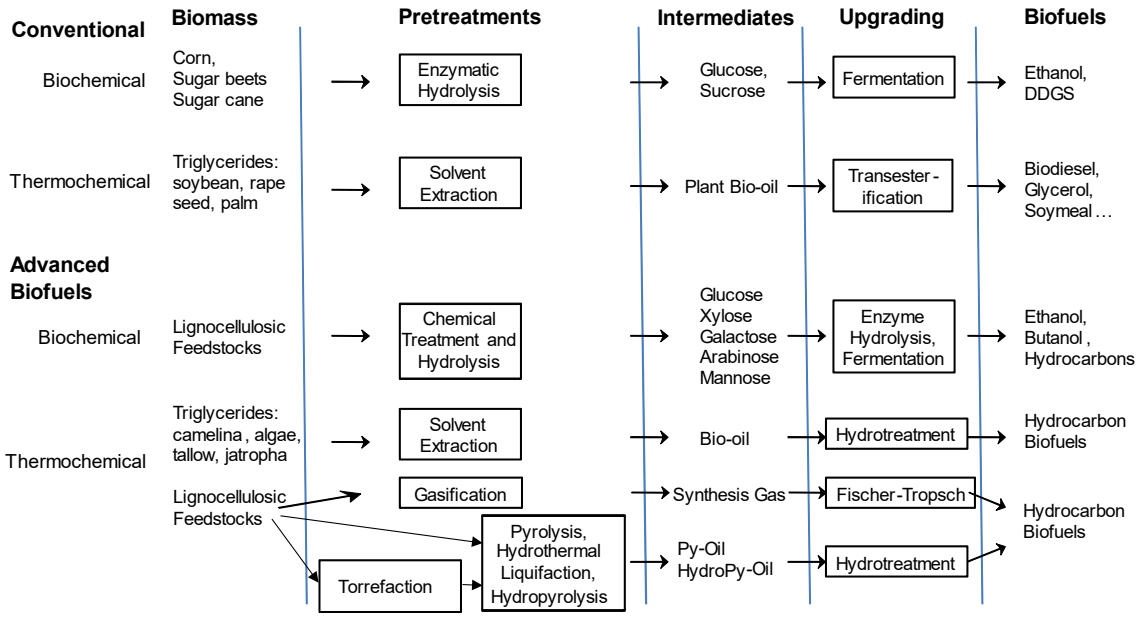

Figure 1.1: Different pathways of conventional and advanced biofuel processing routes adapted from [5]

As shown above there are 2 main pathways that are currently being evaluated, biochemical and thermochemical. Advanced biochemical pathways focus on freeing up the sugars present in lignocellulosic biomass through hydrolysis. Once the sugars are readily available they then undergo fermentation in which the sugars are converted into a bio-alcohol, generally ethanol, but metabolic engineering research is leading to hydrocarbon fermentation products that are not produced naturally.. This is the same method in which corn and sugarcane ethanol are produced, however for this pathway to

be considered advanced the feedstock must be derived from a renewable lignocellulosic feedstock. This becomes much more difficult for conversion compared to corn and sugarcane, due to sugars being much more difficult to free up from the wood structure. Conventional biochemical conversion is well studied and its mechanisms are well understood. Another pathway for producing biomass is thermochemical conversion. Thermochemical conversion is the process of using heat in the absence of oxygen to turn renewable biomass into a renewable liquid fuel.

The primary method employed in thermochemical conversion for liquid biofuel production is fast pyrolysis. Fast pyrolysis occurs at temperatures between 400-600 °C, in the absence of oxygen, at a rapid heating rate, which generally requires finely ground biomass (1mm dimension) and a low residence time (<2 seconds). When biomass is pyrolyzed the main product that is formed once the vapors are condensed is bio-oil, with a yield of between 60-85%, char with a yield of 5-20% and gas with a yield of 5-20% [15, 16]. Several studies have focused on looking at the decomposition of individual components of biomass (hemicellulose, cellulose and lignin) rather than on whole raw biomass [17-24] Hemicellulose degrades to form pyrolysis vapors at temperatures between 200-260 °C and generally produces compounds such as carbon dioxide, carbon monoxide, water, low molecular weight ketones, aldehydes, organic acids and furans. These compounds are highly oxygenated and difficult to upgrade to a transportation fuel in the gasoline, diesel, and jet ranges. Cellulose degrades at higher temperatures of between 240-350°C and produces carbon dioxide, carbon monoxide, water, some lower molecular weight species such as acetol and primarily anhydrosugars such as levoglucosan. Anhydrosugars can be upgraded to a liquid transportation fuel. However,

these compounds contain a lot of oxygen and therefore require more hydrogen to upgrade them, compared to less oxygenated compounds such as plant oils. Lignin degrades in a wide temperature range of 300- 500°C. Lignin is primarily comprised of different phenolic structures cross linked into the structural support of the biomass. When lignin is pyrolyzed it produces some gases and water, but produces monomers of its phenolic rings and tars (large phenolic structures composed of dimers, trimers) and char (a solid higher carbon solid which cannot be easily volatilized).

Some of the major drawbacks of pyrolysis oil is that compared to fossil fuel it has a lower heating value (due to the large amount of oxygen present), is unstable (due to repolymerization of the bio-oil components from the presence of reactive low molecular weight compounds), is corrosive (presence of organic acid and large oxygen content), and it has high viscosity(due to repolymerization and presence of tars). In order to overcome these drawbacks of pyrolysis oil, there needs to be a focus at producing compounds with a lower oxygen content, compounds within the gasoline and diesel carbon range, and the reduction of low molecular weight species. When looking at the compounds produced from the chemical components listed above, it is observed that phenolic structures are more easily upgraded [25] and have a lower amount of oxygen. The oxygen present is more easily removed, compared to anhydrosugars and lower molecular weight species. Also, phenolics are well within the molecular range of hydrocarbon transportation fuel. However, lignin, the source of the phenolics in biooil, does produce a significant amount of char, and therefore the relationship of char produced and phenolics present in bio-oil needs to be understood. Also, an overall understanding of how varying lignin, cellulose, and hemicellulose composition within the biomass affects the overall quality of bio-oil

needs to be better understood. Several studies have looked at comparing the composition of bio-oil produced from different biomass types. However, these studies have not looked at how differing composition within the same biomass species affects the quality of bio-oil produced.

In addition to the experimental issues discussed, there are several kinetic models that exist for understanding the mechanisms of degradation and the rates of pyrolysis of biomass [26-31]. Some of these models have focused on the volatilization of the biomass and how it changes with respect to time. Most models use a thermogravimetric analysis (TGA) approach to measure mass loss from the biomass solid over time in the presence of increasing temperature and also to the volatiles produced, with little attempt on product speciation of the volatile compounds. Several studies have looked at the mechanisms of biomass degradation and have focused primarily on the degradation of the structural components of the biomass (hemicellulose, cellulose and lignin) [17-24].

Several review articles have evaluated different aspects of biomass pyrolysis kinetics [32-36]. These review articles focus on three main types of reactions: 1) single component model, often based off of mass loss data, 2) multicomponent models and 3) activation energy distribution models. Each of these models is useful in its own way to understanding the mechanisms of how biomass degrades. The single component model can evaluate individual biomass component (hemicellulose, cellulose and lignin) or the entire biomass as a whole. One of the most popular single component models was described by the Shafizadeh and Chin model [26] and is shown below in Figure 1.2a. The wood is decomposed to chars, tars and gas and the total kinetic value for this reaction is

the sum of those 3 reactions. The multicomponent models focus on the biomass degrading with respect to intermediates formed. Di Blasi and Lanzetta first described this type of model from the degradation of xylan and its formation of an intermediate solid product before finally reacting to form its final char, they further developed this model by evaluating the pyrolysis of wheat and corn straw [30, 37]. This idea laid the ground work for the Klinger et al. [27] model which is shown below in Figure 1.2b. Instead of there being one solid intermediate, the six step degradation model has five solid intermediates. Distributed activation energy models (DAEM) assumes that there are infinite parallel first order reactions occurring with the kinetic model and all reactions have the same activation energy. DAEM kinetic models appear similar to single component models but they include a function of the activation energy. The function used to determine the activation energy is complex, compared to the Arrhenius equation.

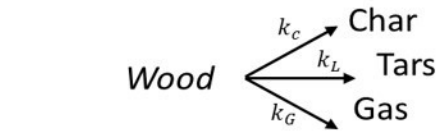

$$k = k_C + k_L + k_G \qquad \textbf{(a)}$$

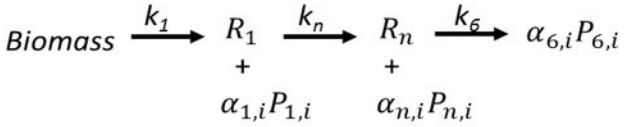

$$R = Reaction\ intermediate$$

$$\sum \alpha_{n,i}P_{n,i} = Products\ formed \qquad \textbf{(b)}$$

Figure 1.2: a) Single component model adapted from [26] **b)** multicomponent model developed by Klinger et al. [27]

The Klinger et al. [27] model assumes that the biomass is broken into solid intermediates as the biomass continues to degrade producing bio-oil. The α represents the stoichiometric amount of each bio-oil product being formed with each reaction. Therefore the total amount of bio-oil species produced is the sum of the production within each of these reactions governed by its stoichiometric coefficient.

These models and mechanisms allow for a better understanding of how biomass is degrading but there has not been any work that looks at production of individual species within the bio-oil with respect to time and within the context of the mechanisms of degradation proposed in literature.

1.5 Research Objectives and Proposal Dissertation Structure

The purpose of this dissertation is to look at the status of biofuel sustainability on the Pan American region and ways =for improving biofuel sustainability by developing a greater knowledge on how biofuels are transformed from biomass to an energy rich liquid through pyrolysis. The research objectives for this dissertation are as follows

1. Understand the status of biofuel life cycle assessments in the Pan American region
2. Understand how different methodological factors affect greenhouse gas emissions calculated using life cycle assessment for the production of biofuels
3. Determine if certain MSW samples are suitable feedstocks for thermochemical conversion through fast-pyrolysis

4. Understand how feedstock composition and acid washing of MSW affects bio-oil properties
5. Evaluate the effect of varying lignin content of hybrid poplar on pyrolysis products
6. Understand how increasing temperature along with increasing lignin content affects pyrolysis product distribution among liquid bio-oil, solid char, and gas, and the properties of the bio-oil.
7. Gain a better understanding of biomass degradation rates during pyrolysis by evaluating individual chemical species within the bio-oil produced with respect to time
8. Evaluate the suitability of previous kinetic models for describing the rates of production of species within hybrid poplar bio-oil with respect to increasing severity of treatment at constant temperature.

This dissertation is divided into 4 parts. The first part focuses on the variability in how biofuels are assessed across the Pan American region and how LCA methodology affects the final result (Chapter 2). The second part focuses on the use of MSW as a feedstock for bio-oil conversion via fast pyrolysis (Chapter 3). Chapter 4 looks at how changes in the composition (varying lignin content) of hybrid poplar affect the bio-oil products that are produced through pyrolysis and on how changes in reaction temperature to improve bio-oil product yields and properties. Finally, Chapter 5 evaluates the kinetics of hybrid poplar fast-pyrolysis, looking at how key products are evolved with respect to time and comparing them to kinetic models in literature.

By assessing the theoretical sustainability of bio-oils across the Pan American region through life cycle assessment and evaluating the use of MSW and hybrid poplar as a potential sustainable feedstock for biofuel, this work adds to the greater knowledge of sustainable biofuel technologies and helps to address and provide resources for meeting the advanced biofuel mandates set forth by the Renewable Fuel Standard 2 (RFS2) in the US and mandates from other national jurisdictions.

1.6 References

1. Shonnard, D.R., et al., *Chemical Engineering of Bioenergy Plants: Concepts and Strategies*. Vol. 1 Handbook of Bioenergy Crop Plants, ed. C. Kole, Joshi, C., Shonnard, D.R. . 2012, Boca Raton, FL: CRC Press-Taylor.
2. Jensen, J.R., K.E. Halvorsen, and D.R. Shonnard, *Ethanol from lignocellulosics, US federal energy and agricultural policy, and the diffusion of innovation.* Biomass and Bioenergy, 2011. **35**(4): p. 1440-1453.
3. Solomon, B.D., et al., *Policies for the Sustainable Development of Biofuels in the Pan American Region: A Review and Synthesis of Five Countries.* Environmental Management, 2015. **56**(6): p. 1276-1294.
4. Solomon, B.D. and R. Bailis, *Introduction*, in *Sustainable development of biofuels in Latin America and the Caribbean*, Solomon B. D. and Bailis R, Editors. 2014, Springer: New York. p. 1-26.
5. Shonnard, D.R., et al., *Chemical Engineering of Bioenergy Plants: COncepts and Strategies*, in *Handbook of Bioenergy Crop Plants*, C. Kole, Joshi, C., Shonnard, D.R., Editor. 2012, CRC Press.
6. RFA, R.F.A. *World Ethanol Production*. 2015 October 15,2016]; Available from: http://ethanolrfa.org/resources/industry/statistics/#1454098996479-8715d404-e546
7. Legistlatures, N.C.o.S. *State Renewable Portfolio Standards and Goals*. 2016 [cited 2016 October 15, 2016]; Available from: http://www.ncsl.org/research/energy/renewable-portfolio-standards.aspx

8. ISO 14040, *Environmental Management - Life Cycle Assessment - Principles and Framework.* 1997.

9. ISO 14041, *Environmental Management - Life Cycle Assessment - Life Cycle Interpretation.* 1998.

10. ISO 14043, *Environmental Management - Life Cycle Assessment - Life Cycle Interpretation.* 1998.

11. ISO 14044, *Environmental Management - Life Cycle Assessment - Requirements and Guidelines.* 2006.

12. RED, *Directive 2009/28/EC of the European Parliament and of the Council of 23 April 2009 on the promotion of the use of energy from renewable sources and amending and subsequently repealing Directives 2001/77/EC and 2003/30/EC*. 2009.

13. RED, *Directive of the European Parliament and the Council amending Directive 98/70/EC relating to the quality of petrol and diesel fuels and amending Directive 2009/28/EC on the promotion of the use of energy from renewable sources*, COM, Editor. 2012.

14. OECD, *Chapter 2 Biofuels*, in *OECD-FAO Agricultural Outlook 2013* 2014.

15. Mohan, D., C.U. Pittman, and P.H. Steele, *Pyrolysis of wood/biomass for bio-oil: a critical review.* Energy & Fuels, 2006. **20**(3): p. 848-889.

16. Kan, T., V. Strezov, and T.J. Evans, *Lignocellulosic biomass pyrolysis: A review of product properties and effects of pyrolysis parameters.* Renewable and Sustainable Energy Reviews, 2016. **57**: p. 1126-1140.

17. Patwardhan, P.R., R.C. Brown, and B.H. Shanks, *Product distribution from the fast pyrolysis of hemicellulose.* ChemSusChem, 2011. **4**(5): p. 636-643.

18. Shen, D. and S. Gu, *The mechanism for thermal decomposition of cellulose and its main products.* Bioresource Technology, 2009. **100**(24): p. 6496-6504.

19. Huang, Y., et al., *Study on structure and pyrolysis behavior of lignin derived from corncob acid hydrolysis residue.* Journal of Analytical and Applied Pyrolysis, 2012. **93**: p. 153-159.

20. Collard, F.-X. and J. Blin, *A review on pyrolysis of biomass constituents: Mechanisms and composition of the products obtained from the conversion of cellulose, hemicelluloses and lignin.* Renewable and Sustainable Energy Reviews, 2014. **38**: p. 594-608.

21. Isahak, W.N.R.W., et al., *A review on bio-oil production from biomass by using pyrolysis method.* Renewable and sustainable energy reviews, 2012. **16**(8): p. 5910-5923.

22. Kelkar, S., et al., *Pyrolysis of North-American grass species: Effect of feedstock composition and taxonomy on pyrolysis products.* biomass and bioenergy, 2014. **64**: p. 152-161.

23. Patwardhan, P.R., et al., *Product distribution from fast pyrolysis of glucose-based carbohydrates.* Journal of Analytical and Applied Pyrolysis, 2009. **86**(2): p. 323-330.

24. Patwardhan, P.R., R.C. Brown, and B.H. Shanks, *Understanding the fast pyrolysis of lignin.* ChemSusChem, 2011. **4**(11): p. 1629-1636.

25. Hilten, R.N., et al., *Effect of torrefaction on bio-oil upgrading over HZSM-5. Part 1: Product yield, product quality, and catalyst effectiveness for benzene, toluene, ethylbenzene, and xylene production.* Energy & Fuels, 2013. **27**(2): p. 830-843.

26. Shafizadeh, F. and P.P. Chin. *Thermal deterioration of wood*. in *ACS Symposium Series American Chemical Society*. 1977.

27. Klinger, J., E. Bar-Ziv, and D. Shonnard, *Unified kinetic model for torrefaction–pyrolysis.* Fuel Processing Technology, 2015. **138**: p. 175-183.

28. Klinger, J., E. Bar-Ziv, and D. Shonnard, *Kinetic study of aspen during torrefaction.* Journal of Analytical and Applied Pyrolysis, 2013. **104**: p. 146-152.

29. Di Blasi, C. and C. Branca, *Kinetics of primary product formation from wood pyrolysis.* Industrial & engineering chemistry research, 2001. **40**(23): p. 5547-5556.

30. Lanzetta, M. and C. Di Blasi, *Pyrolysis kinetics of wheat and corn straw.* Journal of Analytical and Applied Pyrolysis, 1998. **44**(2): p. 181-192.

31. Sonobe, T. and N. Worasuwannarak, *Kinetic analyses of biomass pyrolysis using the distributed activation energy model.* Fuel, 2008. **87**(3): p. 414-421.

32. Sharma, A., V. Pareek, and D. Zhang, *Biomass pyrolysis—A review of modelling, process parameters and catalytic studies.* Renewable and Sustainable Energy Reviews, 2015. **50**: p. 1081-1096.

33. Bridgwater, A.V., *Review of fast pyrolysis of biomass and product upgrading.* Biomass and Bioenergy, 2012. **38**: p. 68-94.

34. Di Blasi, C., *Modeling chemical and physical processes of wood and biomass pyrolysis.* Progress in Energy and Combustion Science, 2008. **34**(1): p. 47-90.

35. White, J.E., W.J. Catallo, and B.L. Legendre, *Biomass pyrolysis kinetics: A comparative critical review with relevant agricultural residue case studies.* Journal of Analytical and Applied Pyrolysis, 2011. **91**(1): p. 1-33.

36. Papari, S. and K. Hawboldt, *A review on the pyrolysis of woody biomass to bio-oil: Focus on kinetic models.* Renewable and Sustainable Energy Reviews, 2015. **52**: p. 1580-1595.

37. Di Blasi, C. and M. Lanzetta, *Intrinsic kinetics of isothermal xylan degradation in inert atmosphere.* Journal of Analytical and Applied Pyrolysis, 1997. **40**: p. 287-303.

2. A Review of Environmental Life Cycle Assessments of Liquid Transportation Biofuels in the Pan American Region

Reprinted with permission from SHONNARD D, KLEMETSRUD B, SACRAMENTO-RIVERO J, NAVARRO-PINEDA F, HILBERT J, HANDLER R , SUPPEN N, AND DONOVAN R. 2015. A REVIEW OF ENVIRONMENTAL LIFE CYCLE ASSESSMENTS OF LIQUID TRANSPORTATION BIOFUELS IN THE PAN AMERICAN REGION. ENVIRONMENTAL MANAGEMENT 56(6): 1356-1376.

2.1 Abstract

Life Cycle Assessment has been applied to many biofuel and bio-energy systems to determine potential environmental impacts, but the conclusions have varied. Different methodologies and processes for conducting LCA of biofuels make the results difficult to compare, in-turn making it difficult to make the best possible and informed decision. Of particular importance are the wide variability in: country-specific conditions, modeling assumptions, data quality, chosen impact categories and indicators, scale of production, system boundaries, and co-product allocation. This study has a double purpose: conducting a critical evaluation comparing environmental LCA of biofuels from several conversion pathways and in several countries in the Pan American region using both qualitative and quantitative analyses, and making recommendations for harmonization with respect to biofuel LCA study features, such as study assumptions, inventory data, impact indicators, and reporting practices. The environmental management implications

---

1 The material contained in this chapter was previously published in *Environmental Management*

are discussed within the context of different national and international regulatory environments using a case study. The results from this study highlight LCA methodology choices that cause high variability in results and limit comparability among different studies, even among the same biofuel pathway, and recommendations are provided for improvement.

2.2 Introduction to issues of LCA of biofuels

Life cycle assessment (LCA) is a well-established methodology to comprehensively determine potential environmental and human health impacts of a product throughout its life cycle; starting with extraction of raw materials, then including manufacturing, transport and use, and ending with disposal of residues at end of life (Allen and Shonnard 2002). LCA is useful to gain an understanding of a product system, to identify the most relevant environmental impacts, to guide product improvement, for stakeholder communication, and decision-making. It has emerged as an important part of environmental management since the first studies were conducted in the 1960s focusing on the cumulative energy demand for chemical intermediates and products (SAIC 2006). Due to the energy crisis in the early 1970s, energy applications of LCA increased, and when global environmental challenges emerged in the late 1980s, interest in LCA again increased. The first formal LCA methodology guidance documents (SETAC 1993) were followed by the publication of the internationally agreed-upon LCA standards, the ISO 14040 series which laid a general framework and requirements (ISO 14040 1997; ISO 14041 1998; ISO 14042 1998; ISO 14043 1998; ISO 14040 2006; ISO 14044 2006;

SETAC 1991; SETAC 1993). These documents have provided critical guidelines in research and helped establish LCA as a professional practice.

Interest in achieving environmental sustainability for biofuels and bioenergy has provided additional momentum to study biofuel pathways using LCA. Partly in response to policy and regulation, emissions of anthropogenic (man-made) greenhouse gases (GHG) have been a common feature of biofuel LCA. There is little doubt that biofuel policy and regulation have in turn been influenced by a scientific consensus that the Earth's atmosphere and oceans have warmed, extent of snow and ice cover has diminished, sea level has risen, and concentrations of CO_2 and other GHG have increased since about 1850 (IPCC 2013). As presented in Solomon and others in this special feature, energy policy in many Pan American countries mandates the use of LCA to demonstrate savings of GHG emissions for biofuels. These eligible biofuels will count toward production targets that transportation fuel producers are obligated to achieve (Moser and others 2014). For example, in the United States the Renewable Fuels Standard 2 (RFS2) defines a methodology to assess GHG emissions of biofuel pathways, including indirect land-use change emissions of CO_2 (emissions resulting from conversion of natural lands to food production as a result of biofuel expansion). Furthermore, RFS2 mandates 20% GHG emission savings for conventional biofuels (corn ethanol, soybean biodiesel), 50% for advanced biofuels (sugar cane ethanol, hydrotreated esters of fatty acids, HEFA), and 60% for cellulosic biofuels (cellulosic ethanol, pyrolysis-based hydrocarbon biofuels, gasification-based hydrocarbon biofuels) (Moser and others 2014) - and see Shonnard and others (2012) for a summary of biofuel processing options. These LCA requirements

will likely affect production systems throughout the Pan American region for countries exporting biofuels to the U.S. through the RFS2 guidelines, or to the European Union, through their Renewable Energy Directive (EU-RED). This has already been demonstrated in Argentina, where exports of soybean biodiesel to the EU were restricted before new calculations were certified and due to restrictions on GHG emissions as calculated under EU-RED guidelines (Hilbert and Galligani 2014).

The two main established governmental standards that influence the practice of LCA for biofuels globally (Moser and others 2014) are RFS2 and the EU Renewable Energy Directive 2009/28/EC and Fuel Quality Directive 98/70/EC through 2009/30/EC (RED 2009; RED 2012). The RFS2 mandates consequential biofuel LCA modeling, in which effects beyond the biofuel pathway, such as indirect land use change and displacement of existing market items with co-products, are added to the GHG inventory attributed to the biofuel (EPA 2010). The U.S. Environmental Protection Agency (EPA) is responsible for determining whether biofuel pathways achieve GHG reduction targets mandated in the RFS2. In carrying this out, EPA uses several LCA models and sub-models. The Greenhouse gases, Regulated Emissions, and Energy use in Transportation (GREET) model from Argonne National Laboratory (ANL 2014) is used for assessing the direct biofuel pathway, while the DAYCENT model provides soil biogeochemical process emissions such as N_2O from N fertilizer application and soil carbon dynamics (CFR 2010). Indirect land use change effects and their emissions are determined using domestic and global commodity market models, such as the Forestry and Agricultural Sector Optimization Model (FASOM) and the integrated Food and Agricultural Policy and

Research Institute (FAPRI) models (CFR 2010). EPA RFS2 LCA approach employs "system expansion" to account for co-products generated during biofuel production and credits avoided GHG emissions from co-product displacement effects to the Renewable Identification Number (RIN) generating biofuels (see Solomon et al. in this special feature for a discussion of RIN in RFS2).

The EU-RED differs from the RFS2 biofuel LCA approach in several ways. The EU-RED employs energy allocation to distribute GHG emissions among products and co-products in a biofuel pathway. Direct land use change (dLUC, emissions when land converts to biofuels) GHG emissions are included using the IPCC "tier 1" estimation method and carbon stock data for different land types (IPCC 2006a; IPCC 2006b), but iLUC effects are not currently included. Finally, whereas in RFS2 the US-EPA determines each pathway's GHG emissions and qualifies biofuel pathways, the EU-RED allows compliance with mandated sustainability criteria using voluntary certification standards (Moser and others 2014). There currently are six voluntary certificates that may qualify under the EU-RED meta-standard. A review of 13 Latin American and Caribbean countries showed that of a total 177 certified biofuel entities (biomass growers, biofuel facilities, supply chain companies, etc.) a large majority (139) qualified under EU-RED (Solomon and Bailis 2014). A competent review of sustainability standards and certification of biofuels is provided in Moser et al. (2014) and Diaz-Chavez (2014).

Biofuel LCA can be a very complicated analysis and, depending on study scope, may include over 100 unit processes, thousands of inventory elements, and multiple mid-point or end-point impact categories. Aspects of LCA methodology such as choice of system

boundary, source of inventory data for unit process inputs, and decisions on co-product allocation can all have a profound effect on study results (Allen and Shonnard 2002; Cherubini and others 2009; Larson 2006). Larson (2006) reviewed a number of liquid biofuel LCAs from the North America and the European Union (EU). That study revealed a wide range of GHG emissions and energy demand results due to variability of several study features, such as climate-active species included, N_2O emission assumptions, co-product allocation method, and soil carbon dynamics. Beyond these biofuel LCA topics, Cherubini and others (2009) evaluated key issues influencing LCA outcomes for liquid biofuel and bioenergy systems (biopower, and heat) and the need to model them accurately. These issues included biomass type and supply chains, soil carbon pools, CH_4 emissions, effects of residue removal on soil N and C balances, fossil reference system features, functional unit selection (a preference for land area), crop yields, and fertilizer inputs. They also noted the potential for trade-offs between GHG emissions and fossil energy reductions and potential increases in acidification, eutrophication, and local air pollutants when bioenergy replaces fossil energy systems. Cherubini and Strømman (2011) reviewed 94 LCAs of biomass energy, mostly from the EU and with contributions from North America, Asia, but with very few from South America, Africa, and Oceania. The study provided qualitative rather than quantitative evaluations of the LCA results from this literature, it discussed the key LCA issues and features as well as the approaches taken to address them. Information was presented on the study locations, biofuel and bioenergy pathways, feedstock types, choice of functional unit, impact categories, allocation method, fossil reference system, and land use change. Relations of methodology choices with policy maker's requirements were described,

highlighting shortcomings and future research directions. Within the study reported in this article, the focus is not only on the qualitative differences within the context of biofuel LCAs, but also on the quantitative differences between different feedstocks biofuel pathways, and with a dedicated focus on the Pan American region, which has not occurred before.

As noted previously, choice of system boundary will have a large effect on study results depending on whether only impacts directly linked to the biofuel pathway are considered (attributional LCA modeling) or whether indirect effects beyond the pathway are considered (consequential LCA modeling) (Allen and others 2009). Indirect effects are most often associated with indirect land use change (iLUC) emissions of CO_2 due to the market-driven demand for more land to compensate for food production lost to biofuels (Fargione and others 2008; Searchinger and others 2008). In addition to that, inventory data within life cycle inventory databases, [ecoinvent™ (SCLCI 2014), US Life Cycle Inventory (NREL 2014), GREET (ANL 2014), GaBi (PE International 2014), among others], are not necessarily compatible with each other due to differences in data formatting and quality requirements, geographical and technological coverage, allocation procedures, and time relevance. Several studies concluded that the choice of method to allocate inventory data among biofuel pathway products and co-products has an overwhelming effect on LCA results (Bailis and Baka 2010; Larson 2006; Wang and others 2011b). Finally, LCA software packages (SimaPro, GREET, GaBi, GHGenius, BioGrace) may yield variable results for the same biofuel pathway because of differences in life cycle inventory databases, in their treatment of biogenic carbon, in how recycle of

material is handled, impact assessment methods used, and because there is no common agreement in relation to emission factors for such items as electricity and N_2O emissions from soil (Fan and others 2012).

2.2.1 Research objectives

Despite the fact that there are some good reviews discussing the variation of LCA results due to methodological differences as discussed above, an in-depth review for the Pan American region is missing in the literature. The Pan American region is of particular interest as a study focus because of its dominance in global biofuel production (OECD 2014). Yet despite the large number of Pan American biofuel LCAs, no comprehensive review of the literature has occurred, in contrast to what occurs for the US and EU biofuel and bioenergy LCA literature (Larson, 2006; Cherubini and others, 2009). This review builds on prior work and expands the scope of study with a more detailed review and analysis including aspects of policy-driven LCA approaches (through the case study presented), more impact categories, and statistical analyses of LCA results, especially for GHG emissions. Furthermore, in this work we focus on two research questions to address in the reviewed articles, in the context of Pan American countries: (1) What LCA methodology choices are used to determine the potential environmental impacts of the biofuel production systems in the Pan America region? (2) How frequently is policy-driven LCA employed in Pan American biofuel and what is the magnitude of change in LCA results when it is employed? One Pan American case study directly addresses the latter question. The article ends with recommendations for improving biofuel LCA through research and other actions.

2.3 Research Methods

To answer the two research questions, we conducted a literature review by means of search engines of scientific publishers including Elsevier/ScienceDirect, SpringerLink, Redalyc, and the American Chemical Society, and then performed a case study. Studies not reported in journals, such as governmental analyses, were searched by means of the Google Scholar search engine. Studies performed in countries out of the Pan American region were discarded. We considered studies in English, Spanish, and Portuguese languages, since these are the main languages in the Pan American region. The time frame considered articles published from 2000 to the present in order to consider the most recent studies.

A total of 74 articles were found and analyzed according to a number of LCA features (see Introduction section), including the geographic location, feedstock used, the types of biofuel produced, the functional unit, the chosen life cycle impact assessment methodology and impact categories, the allocation criteria, the system boundaries, and the regulatory frameworks guiding the studies. These articles represent LCA studies of biofuels production in Argentina, Brazil, Canada, Colombia, Cuba, Chile, Costa Rica, Ecuador, Mexico, Peru and the US. *Qualitative analyses* of the articles determined how often the articles aligned with certain LCA features. An overview of the evaluated studies is provided in **Table A.1** in Appendix A. To undertake a *quantitative analysis* of the environmental profile of biofuels, the results on GHG emissions were conveyed in "box and whisker plots" showing the medians, interquartile ranges, minimums, maximums, and non-typical data (Cleary 2009; Muench and Guenther 2013). The medians separates

the higher and lowers halves of a set of results, the interquartile ranges represent the points lying between the lower and upper quartiles, Q_1 and Q_3, respectively. The whiskers represent the maximums and minimums of a sample. Non-typical data are shown with a × symbol and represent points that lie outside of $Q_1 - 1.5 \cdot (Q_3 - Q_1)$ and $Q_3 + 1.5 \cdot (Q_3 - Q_1)$.

2.4 Qualitative Results

2.4.1 Geographic locations

The distribution of articles among different geographic (country) locations is shown in **Figure 2.1a**, with some articles evaluating more than one geographic area. The majority of studies were on biofuel production in the United States (32/74 articles-US) and Brazil (21/74-BR), with fewer studies on biofuels produced in Colombia (8/74-CO), Argentina (5/74-AR), Chile (3/74-CL), Mexico (3/74-MX), Canada (2/74-CA), Costa Rica (2/74-CR), Cuba (1/74-CU), Ecuador (1/74-EC) and Peru (1/74-PE). Brazil's large number of studies is a result of their long history of ethanol production and the need to understand its environmental implications. The higher number of studies in the United States is likely a result of the active research programs investigating many types of advanced biofuels and the interest by funding agencies to understand the environmental implications of future biofuel production systems with respect to meeting regulatory standards for savings in GHG emissions and other sustainability criteria.

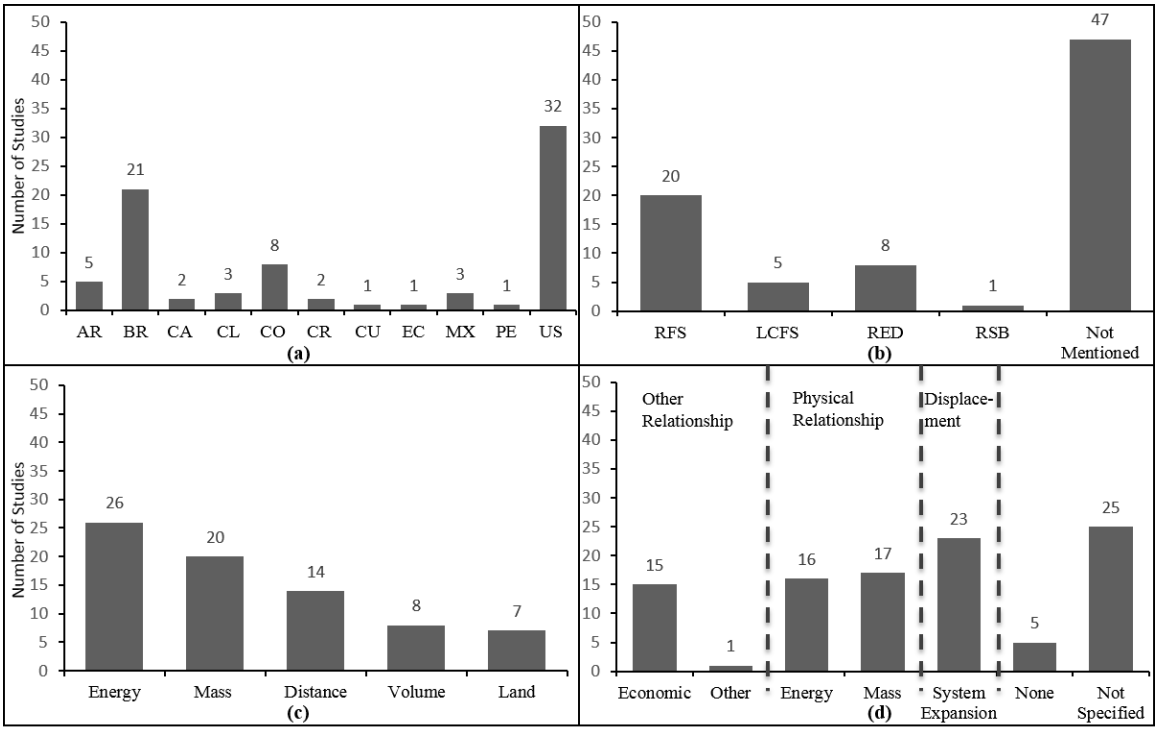

Figure 2.1 Number of studies in the reviewed articles: a) geographic locations (74 studies, 79 scenarios), b) selected framework and methodology (74 studies, 82 scenarios), c) functional units used (74 studies, 75 scenarios d) allocation methods (74 studies, 102 scenarios).

2.4.2 Regulatory framework for LCA

The ISO 14040 standards establish that the scope, assumptions, description of data quality, methodologies and output of LCA studies should be transparent (ISO 14044 2006). The transparency of an LCA is what allows for reproduction of the work by others and for accurate comparisons and conclusions to be made, therefore good documentation calls for a more transparent study. Nearly all the papers reviewed use ISO 14040 standards to conduct their LCAs.

Nearly half of the reviewed studies use a regulatory framework (which have predetermined functional units and allocation methods) as a guideline to perform the

LCA, as shown in **Figure 2.1b**. Of the studies mentioning regulatory framework the most common is the RFS (20/74) due to the abundance of LCAs conducted in the US. The Low-Carbon Fuel Standard (LCFS) of the state of California in the United States provided guidance for LCAs in 5/74 articles in this review. The few LCAs that used the EU-RED framework (8/74) and only 1/74 used the Roundtable on Sustainable Biofuels (now Biomaterials) (RSB) metrics. Sixty-three percent of the studies did not mention regulatory-driven LCA guidance. Because a large amount of articles (27/74) mentioned some regulatory-driven guidance, this can be interpreted as policy having a significant influence on the methodology aspects of current LCAs of biofuel production systems. There are no frameworks specifically for Latin American and the use of U.S. and European frameworks for assessing the environmental sustainability of biofuels may reflect the interest of exportation of biofuels rather than local use. This concept that regulatory frameworks affect production and certification of Latin American biofuels is elaborated in the case study located at the end of this article.

2.4.3 Functional units

An LCA should clearly specify the functional unit, which provides a reference to which the input data and output results are normalized and allows for comparisons among different fuel production systems (ISO 14044 2006). The review showed that the preferred functional unit is energy content of the biofuel (26/74) such as the lower heating value followed by mass of fuel (20/74), distance traveled by a vehicle (14/74) operated on pure biofuel, volume of fuel (8/74), and land area (7/74) (**Figure 2.1c**). Most of the studies that used the energy functional unit compared the GWP of the biofuel with

that of the fossil reference or against GHG emission savings targets stated by either the EU-RED or the US-RFS. Studies that used a distance-based functional unit meant to compare biofuel or their blends with the fossil reference. Studies that used a land-based functional unit compared different cropping scenarios or estimated the carbon payback time of the biofuel production system. Finally, the few studies that did not use any functional unit showed percentages of GHG reductions achieved by substituting fossil-based fuels by biofuels. The variation in functional units used makes comparison of LCA results difficult between biofuel pathways and even between the same biofuel pathway in studies conducted by different research groups. Over 60% of the reviewed studies quantify the performance of biofuels in terms of energy giving confidence as a suitable functional unit; additionally targets for meeting global warming potential thresholds are expressed in g CO_2 eq/ MJ. Thus it would be useful to have LCA results based on MJ of produced energy. This is perhaps an area where policy-driven LCA frameworks can help (see **Table 2.1**) by standardizing the functional unit definition.

2.4.4 Allocation methods

The partitioning of the inventory from input or output flows of a process or a product system between one or more products is called allocation (ISO 14044:2006). When the LCA study follows the recommendations of a regulatory framework such as RSB, US-RFS or EU-RED, the allocation procedure is fixed (see **Table 2.1**). **Figure 2.1d** shows the frequency of allocation procedures reported in the reviewed studies. These results indicate that system expansion (23/74) followed by mass allocation (17/74), energy allocation (16/74) and economic allocation (15/74) are the most common methods.

However, the largest number of studies (25/74) did not report the allocation method used, which was surprising because most biofuel production systems include one or more co-products which may be used as animal feed, power or heat production, or chemical intermediates. In some studies the regulatory framework was discussed, but there was no clear indication of allocation or adhering to that framework. Different allocation criteria lead to considerably different results on the impacts even when considering the same agricultural and/or industrial assumptions (Amores and others 2013; Bailis and Kavlak 2013; Bailis and Baka 2010; Consorcio 2012; Hilbert and Galbusera 2011; Iriarte and others 2012; Krohn and Fripp 2012; Luo and others 2009). When possible, different allocation criteria (mainly mass and energy) should be used in biofuel LCAs, to allow for proper comparisons among LCA results across different regulatory frameworks, and for evaluation of the final results when considering emission thresholds.

2.4.5 Biofuel pathway inputs and sources of inventory data

The quality of LCA pathway inputs and inventory data will determine the quality of the study results, and it is always preferred to have site specific inputs from biofuel producers along the supply chain. However, because advanced biofuels are not yet a commercial reality, availability of high quality inputs are often lacking, and estimation methods are largely relied on. **Figure 2.2a** shows the large variety of input and inventory sources chosen for LCA studies in the Pan American region. The most commonly cited sources of process inputs and inventory data are from literature sources (65/74). Ecoinvent is the most commonly used life cycle inventory database for this study group. SimaPro was considered a "data source" in **Figure 2.2a**, when studies failed to report what databases

were used within SimaPro. A discussion of LCA software used, such as SimaPro, is in A.4.5 of Appendix A. Lifecycle inventory sources that are important in LCAs include: land use change models (such as GTAP), biogeochemical models for predicting soil organic carbon and nitrogen emissions (such as DAYCENT), and IPCC emission factors for dLUC emissions, among others. Wide variance with respect to data sources and primary data gathering methods demonstrates the need for LCAs to have the most current temporal and spatial data possible in order to generate the most accurate conclusions.

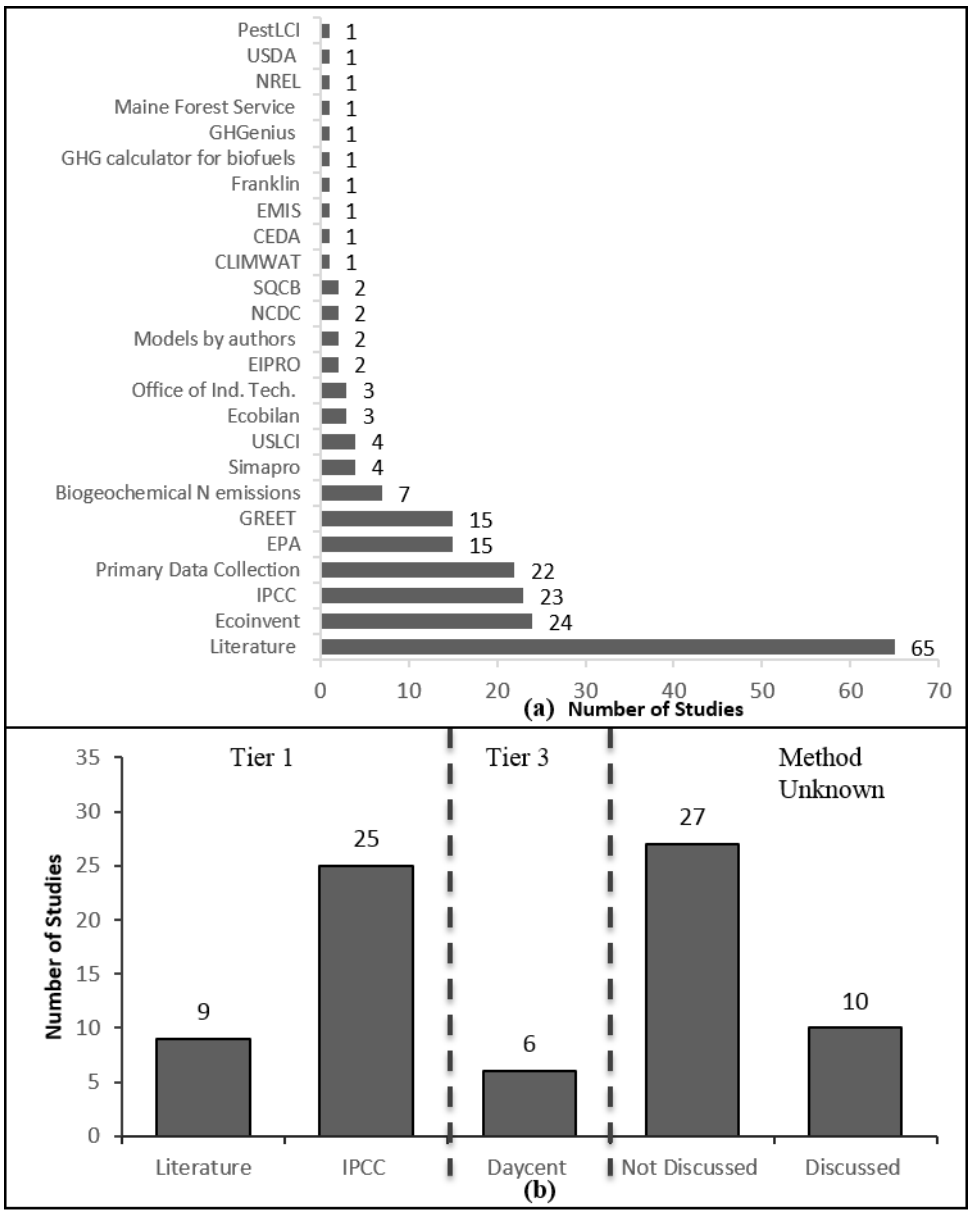

Figure 2.2 a) Number of articles using different sources of inputs and inventory data, b) Number of N_2O methodologies used according to IPCC tier categories. See Appendix A glossary for more information on inputs and inventory data sources.

2.4.5.1 N_2O emissions

Application of N fertilizers to biomass cultivation systems for biofuels can be an important source of GHG emissions, an important cause of groundwater contamination, and a primary reason for eutrophication of receiving waters (Cherubini and Stromman 2011). Subject to variation in nitrogen fertilizer requirements, biofuel GHG results can often be dominated by N_2O emissions. N_2O emissions are dependent on a number of soil and biomass production system parameters; soil properties, climate, irrigation and tillage practice, and annual versus perennial crops (Cherubini and Stromman 2011). Type of N fertilizer can also impact biofuel GHG results because of the large differences in upstream emissions among different fertilizer types (Adom and others 2012). In the impact assessment methodologies studied in this evaluation, N_2O is reported to have a global warming potential ranging from 276-310 times higher than that of CO_2, providing another source of variability in GHG results. **Figure 2.2b** shows the distribution of N_2O emission estimation methods categorized according to the IPCC as Tier 1, Tier 2, and Tier 3. Tier 1 is the simplest and most common method, employing a constant emission factor for both direct and indirect (NO_3^- leaching, NH_4^+ volatilization) mechanisms, 1.325% of applied N is emitted as N in N_2O. Also, climate types are cataloged in a very wide classification that may lead to conclusions that are unrepresentative of actual conditions. For example, in a study comparing predicted emissions in two different climates, a 300% difference was predicted between temperate-dry and temperate-humid climates (Galbusera and Hilbert 2011), none of which are representative of the actual locations, according to the authors.

Tier 2 and 3 methods are more detailed and depend heavily on site-specific data such as soil type, precipitation, climate information, etc. DAYCENT, CENTURY, and EPIC are examples of Tier 3 biogeochemical models which predict not only nitrogen cycle reactions, but also soil carbon, crop yield, and other system outcomes. Some studies use factors embedded within LCA software such as GREET and EBAMM, which use the IPCC tier 1 method. Twenty seven of the articles do not discuss N_2O, and thus it is unclear if these were included in the overall GHG emissions. Of the articles discussed, 10/74 mentioned how the application of fertilizer is very GHG intensive due to N_2O emissions but omit mentioning the method used to calculate those emissions. Allocation of N_2O emissions is highly dependent on yields of the crops, with most studies relying on single yield numbers, and year-to-year variations are rarely considered. Tier 1 methods were used 34/74, or 46% of the time, whereas Tier 3 methods were only used in 8% or 6/74 of the reviewed studies. Comparing the amount of studies that used Tier 1 over Tier 2 or 3 methods suggests that relative ease at calculating these values may be a factor. Using Tier 2 or 3 methods requires a vast amount of data and software. The lack of studies discussing N_2O emissions should be a reminder of the need for meticulous documentation of all GHG emissions.

2.4.6 Impact assessment categories and methods

Impact categories are classified as midpoint or endpoint. The first approach focuses on potential environmental problems in the middle of the environmental cause and effect chain, while the second approach models additional mechanisms to estimate actual damage to human health, ecosystem quality, and resource depletion. Midpoint analyses

are easier to model, but require more knowledge of human health and ecosystem damage mechanisms by decision makers, and endpoint analyses are easier to interpret and to communicate.

Depending on the goal and scope of the study, one or more impact categories may be included in the life cycle impact assessment (LCIA). While global warming potential (GWP) and energy consumption are often included in biofuel LCAs, a full environmental evaluation should consider other categories related to impacts to soil, water, air, human health, and ecosystems (Muench and Guenther 2013; Cherubini and Stromman 2011). The occurrence of the various impact categories in the reviewed articles is shown in **Figure 2.3**. The articles included a wide range in impact categories and an analysis was done to determine whether biofuels outperformed or underperformed fossil fuels most of the time. The most common categories found in these articles were GWP (GHG emissions), and energy demand (fossil and total), and both of these show biofuels generally out performing fossil fuel systems. As in other reviews of biofuel and bioenergy LCA literature (Larson 2006; Cherubini and Stromman 2011), biofuels were found in our study to underperform overall compared to fossil fuels in many categories, including acidification, eutrophication, dLUC, iLUC, and land occupation. **Table A.2** in Appendix A shows the impacts assessed for each reviewed article.

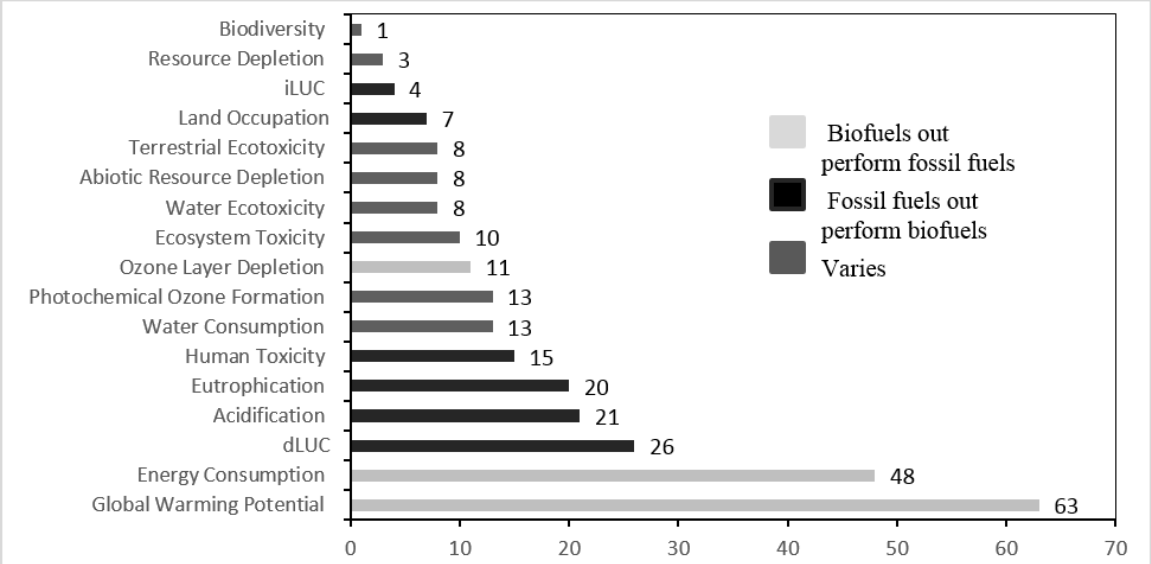

Figure 2.3 Number of mid-point impacts studied within this assessment. See Appendix A glossary for more information on impacts used.

Figure 2.4 shows the frequencies of the various LCIA methodologies used in the reviewed studies, and divides these into midpoint and endpoint impact indicator methods. Each of these methodologies considers a specific set of environmental impacts. For example, IPCC GWP 100a only includes GWP whereas EPA's TRACI also considers ozone depletion, acidification, cancer health impact, non-cancer effects, eutrophication, smog formation, eco toxicity, fossil fuel, land, and water uses. The GREET model and the Centrum voor Milieukunde Leiden (CML) and the Ecological Scarcity life cycle impact assessment methods consider midpoint impact categories, while Ecoindicator 99 considers endpoint impact categories. The GREET model includes GWP, energy, and emissions of regulated pollutants contributing to acidification, smog formation, and health effects. Compared to the GREET model, CML includes also ecotoxicity related environmental impacts. The Ecological Scarcity method generates a single environmental

index which requires that the impact categories be normalized according to a critical annual flow in the reference area and a set of factors that include data adapted for Switzerland. Ecoindicator 99 expresses the resource depletion as the surplus energy required for the extraction of mineral and fossil fuels in the future, the damage to ecosystem quality as the loss of species in a certain area and period of time, and the damage to human health as the number of years life lost and lived disabled (combined as Disability Adjusted Life Years, DALY) (PRé-consultants 2011). Both Ecological Scarcity and Ecoindicator 99 use varying ranges of impact categories and weighting factors for determining a single environmental score. Some methodologies such as CML 2001 and TRACI have similar categories (i.e. acidification, eutrophication) but the units used for analysis differ making comparisons between them difficult.

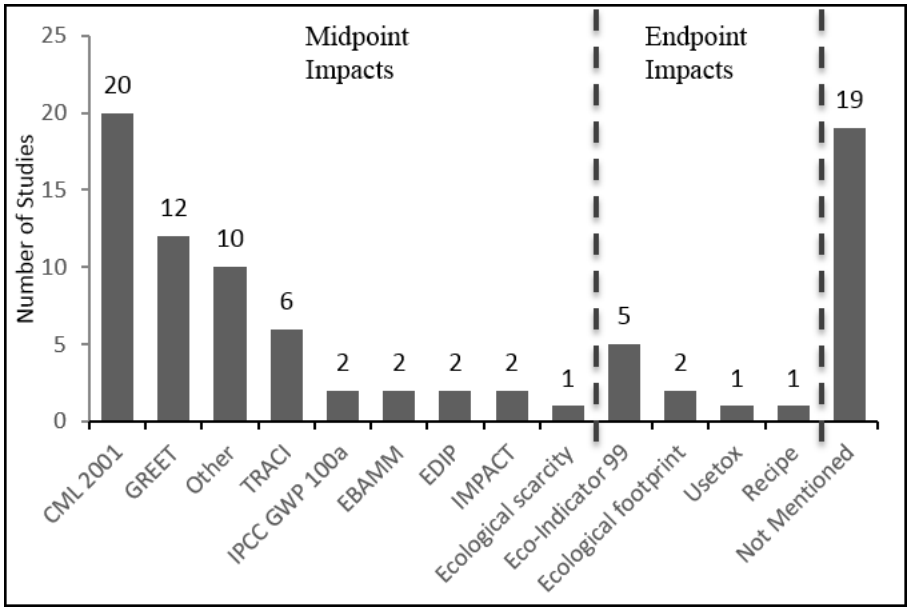

Figure 2.4 Number of the articles studied using different impact assessment methods. See Appendix A glossary for more information on impact assessment methods.

The single impact category present in nearly all reviewed LCAs was GWP. This was to be expected since one of the primary goals of biofuels is to reduce GHG emissions compared to conventional fossil fuels. The few studies which do not include the GWP instead focus on the energy consumption (Bruinsma 2009; da Costa and others 2006; Pradhan and others 2011; Velásquez and others 2010) or water consumption (Mishra and Yeh 2011). The vast majority of biofuels outperform conventional fossil fuels within these two impacts. In other impact categories, especially those that are less studied (acidification and eutrophication) conventional fossil fuels outperform the majority of biofuels. This is mainly due to the large requirement of fertilizers for most biofuel feedstocks. In other impact categories the results vary due to factors such as feedstock production, system boundaries, input data, transportation distances, energetic content and blending.

Only 8 of the articles looked at the overall endpoint impacts (Cavalett and others 2013; Consorcio 2012; Emmenegger and others 2011; Koch 2003; Neupane and others 2011; Yang and others 2012), with the Cavelett et al. (2013) study performing multiple analyses comparing endpoint results from different LCA methodologies. Eco-Indicator 99 is the most common LCIA method for analyzing endpoint impacts. Under this approach, biofuels seem to present a worse endpoint environmental impact than fossil fuels in part due to normalization and weighting factors strongly affecting the final results of end-point impacts. Moreover, the factors are site specific and most are based on European conditions. No particular normalization and weighting factors for the Pan American region exist, which makes the use of the endpoint approach difficult and uncertain for this

region. On the other hand, normalization values (Bare and others 2006) and weighting factors (Thomas and others 2007) are available for the US.

2.4.7 Water consumption

Fresh water is considered a renewable, though finite, resource and as such its sustainable management must be considered. In LCAs of biofuels, some attention has been paid to land use change, and to some aspects of water degradation such as eutrophication, acidification and aquatic ecotoxicity, but water consumption is seldom included. In the reviewed studies, less than 18% or 13/74 papers considered water consumption, with one study comparing US and Brazilian scenarios (Chavez-Rodriguez and Nebra 2010). Most studies considering water consumption are from countries with an extensive and well-developed biofuel sector, such as the US and Brazil. Eight analyses were conducted in the United States (Chavez-Rodriguez and Nebra 2010; Chiu and others 2012; Chiu and others 2009; Clarens and others 2010; Mishra and Yeh 2011; Yang and others 2011; Yang and others 2012; Zaimes and Khanna 2013) , 3 in Brazil (Cavalett and others 2013; Chavez-Rodriguez and Nebra 2010; Ometto and others 2009), 2 in Chile (Iriarte and others 2010; Iriarte and others 2012) and 1 in Argentina (Emmenegger and others 2011). Water consumption is of particular importance where water scarcity is a prevalent issue (e.g. southwestern US, the northern region of Mexico and the Norte Grande in Chile all deal with arid climates) and can be a limiting factor. In order to give an accurate view of the sustainability of biofuels, water consumption and its potential environmental impacts related to pressure on water availability (from ISO 14046) must be assessed, especially in water scarce and/or arid regions.

2.5 Quantitative results

In this section the quantitative impact that assumptions on allocation criteria and inventory data have on LCA results will be described. The focus of this section will be on GWP since most of the studies reviewed analyzed this impact category. This in no way implies that other environmental impacts are less important, and is done to illustrate the source of variability in LCA studies conducted in the Pan American region. The terms agricultural stage and industrial stage used here refer to all the activities involved in biomass production and biomass transformation into biofuels, respectively. The GHG emissions were analyzed as g CO_{2eq}/MJ. The article's original values expressed per kg of biofuel were then transformed considering a lower heating value of 26.8 MJ/kg for ethanol (Garcia and others 2011) and of 37.1 MJ/kg for biodiesel (Iriarte and others 2012). LCA results expressed in other functional units (such as land area) were not considered.

2.5.1 Effects of allocation method, biomass yields, and pathway inputs

This analysis considered 100 scenarios present in 32 articles. **Figure 2.5** shows the life-cycle GHG emissions associated with biofuels production from different types of feedstock without including the dLUC emissions. Calculated GHG emissions using economic, energy, mass, or no specified allocation (**Figure 2.5a**) tend to be greater than when using system expansion (**Figure 2.5b**), which can even result in negative emissions (relative to the substituted system). Under system expansion it is assumed that the co-products generated by the biofuels production system displace current products available in the market. Thus, the (relatively high) GHG emissions generated by the conventional

products in the market are subtracted from the (relatively lower) total GHG emissions derived from the biofuel production system, which leads to lower GHG emissions than for attributional allocation. Variations in the GHG emission results may also be attributed to the assumptions on the agricultural stage (biomass yield and fertilizers required) and/or the technical level of the industrial stage (efficiency of the equipment). It is difficult and uncertain to identify whether allocation or differences in the inputs to the biofuel pathway causes a larger effect on the final results, however some trends were uncovered as described next.

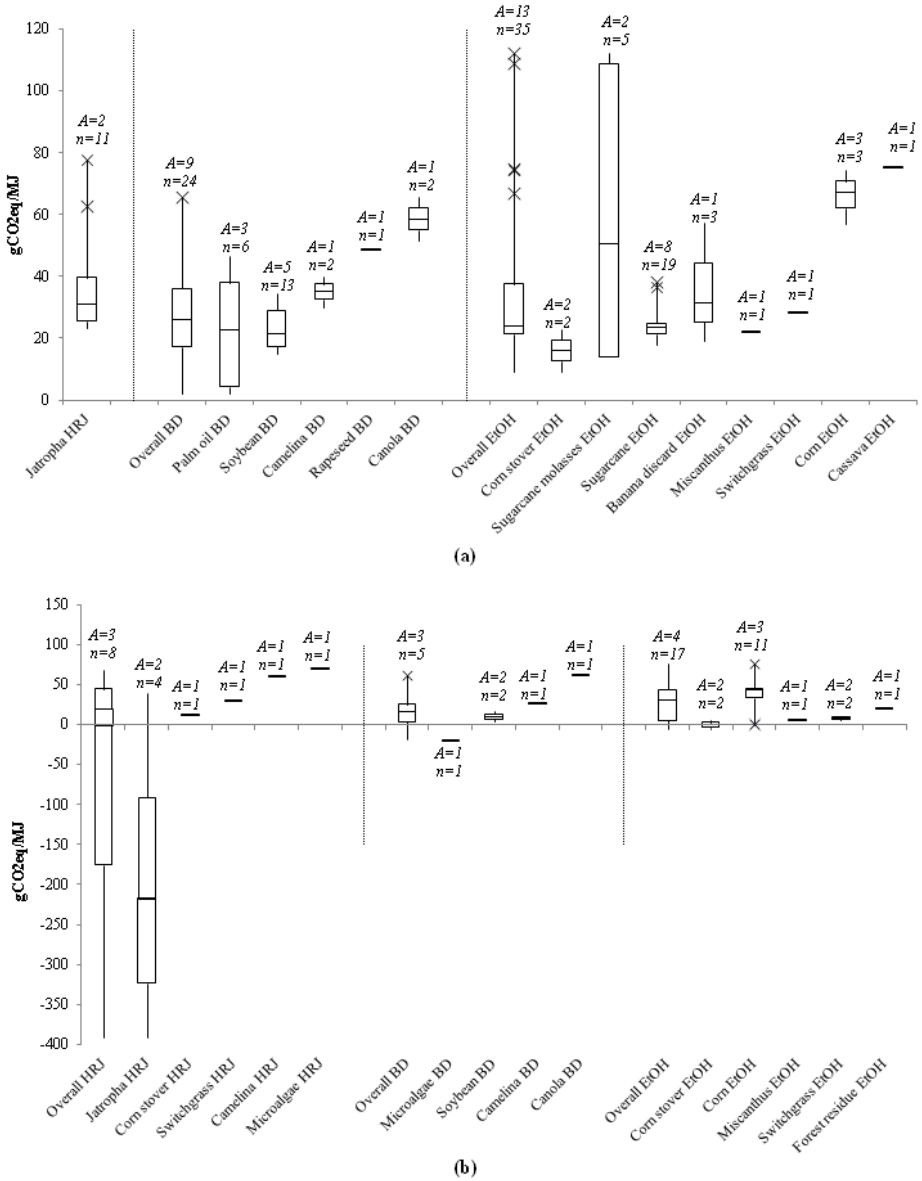

Figure 2.5 Box and Whisker plot showing the minimum, maximum, and non-typical data of the GHG emissions not including the LUC effect (a) from studies considering mass, energy, economic, or no allocation (b) from studies considering system expansion. *A* refers to the number of articles and *n* to the number of analyses.

Allocation criteria and different assumptions on biomass cultivation and yields are responsible for the bulk of the variations on the GHG emissions from jatropha-based hydro-renewable jet (HRJ) production. Mass, economic, energy, and no specified allocation criteria present GHG emissions of 23 – 33 (first and second quartiles), 27 – 29 (second quartile), 28 – 40 (third quartile), and 45 – 78 g CO_{2eq}/MJ (fourth quartile), respectively (**Figure 2.5a**). System expansion may generate GHG emissions benefits depending on the use of the co-products. Using these as substitutes of soybean meal or as boiler fuel resulted in GHG emission benefits of 300 – 391(first and second quartiles), and 134 g CO_{2eq}/MJ (third quartile), respectively, while using them as fertilizers lead to GHG emissions of 40 g CO_{2eq}/MJ (fourth quartile) (Bailis and Baka 2010; Bailis and Kavlak 2013).

Allocation criteria and different assumptions on biomass cultivation and yields are also responsible for the variations on the GHG emissions of the biodiesel production from camelina, and canola (Krohn and Fripp 2012). A similar situation occurs with the soybean-based biodiesel production. This biofuel presents GHG emissions of 15 – 20 (first quartile), 21 – 31 (second and third quartiles), and 23 – 35 g CO_{2eq}/MJ (third and fourth quartiles) under mass, not specified, economic, and energy allocation criteria, respectively (Hilbert and Galbusera 2011). Under system expansion, the soybean-based biodiesel achieves relatively lower GHG emissions of 4 – 17 g CO_{2eq}/MJ (Huo and others 2008; Krohn and Fripp 2012).

Different assumptions on both the agricultural and industrial stages are responsible for the variations of the GHG emissions derived from the palm oil-based biodiesel

production reaching GHG emissions of 2– 46 and 10 g CO_{2eq}/MJ under Colombian (Castanheira and Freire 2011; Consorcio 2012), and Brazilian (de Souza and others 2010) conditions, respectively.

The presence of non-typical data (denoted by the × symbol) for the overall ethanol production in **Figure 2.5a** suggests that the estimated average of 24 g CO_2-eq/MJ is not representative of all feedstock sources, with the largest differences for corn, cassava, and sugarcane molasses. Allocation criteria and different assumptions on the industrial stage explain the variations on the corn-based ethanol production. Estimations of net GHG emission are 57 (first quartile) and 67 – 75 g CO_2-eq/MJ (second to fourth quartiles) under energy and not specified allocation criteria, respectively (Chavez-Rodríguez and Nebra 2010; Wang et al. 2012; Wu et al. 2006). Under system expansion and using natural gas for energy purposes makes corn-based ethanol reach GHG emissions of 30 – 47 (first to fourth quartile). Different geographic locations within the US are responsible for this variation. The use of coal instead of natural gas makes the GHG emissions rise to 76 gCO_{2eq}/MJ (Liska and others 2009).

Under Colombian conditions, the sugarcane molasses-based ethanol production reaches net GHG emissions of 14 g CO_{2eq}/MJ (first and second quartiles) with no significant differences between energy and economic allocation criteria (Consorcio 2012).The net GHG emissions of the sugarcane-molasses-based ethanol production under Mexican conditions, and considering the energy allocation criteria, are 50 – 112 g CO_{2eq}/MJ (third and fourth quartiles) (Garcia and others 2011). Different assumptions on the industrial

stage, such as the boiler efficiencies, the electricity requirements, and the ethanol yield per ton of cane, are responsible for this variation.

There seem to be a consensus on the GHG emissions derived from the ethanol production from the sugarcane juice in Brazil. Such emissions range between 18 and 28 g CO_{2eq}/MJ (first to third quartiles) depending on the cultivation and industrial conditions assumed. Higher GHG emissions of 29 and 37 – 38 g CO_{2eq}/MJ (fourth quartile) are estimated for Argentinean and Mexican conditions, respectively.

The banana discard-based ethanol production under Costa Rica conditions reaches GHG emissions of 19 g CO_{2eq}/MJ if no fertilizers are required, while under Ecuador conditions the resulting GHG emissions for an organic farm and a conventional farm are 31 and 57 g CO_{2eq}/MJ, respectively (Graefe and others 2011).

The low GHG emissions attributed to lignocellulosic ethanol (produced from corn stover, miscanthus, switchgrass, or forest residue) are mainly due to the assumption of using the residual lignin for process heat and power co-generation (Wang and others 2011a; Wang and others 2007) and export of excess electricity to displace coal-derived or grid mix electricity.

Overall, the variability in GHG emissions suggests that process inputs, rather than LCA methodology differences, are more important for these studies. Since many LCA inputs such as crop yields undergo significant changes throughout the years from random variation in annual weather conditions, it is important to also focus on long-term studies, rather than single “snapshot” LCAs of a given biofuel pathway.

Regarding the breakdown of the GHG emissions by stage, there is significant variability in the data resulting mainly from the relatively low number of articles that analyzed this issue (see Figure A.2 in Appendix A), which hinders reaching conclusions about the individual contributions. While in general the agricultural stage appears to be the largest contributor to the net GHG emissions, in the case of lignocellulosic-based and soybean-based biofuels it is lower than the industrial stage because these feedstock sources are considered as either crop residues or N-fixing crops needing low N fertilizer inputs (Agusdinata and others 2011; Bailis and Baka 2010; Graefe and others 2011; Luo and others 2009).

2.5.2 Direct land-use change (dLUC) effects

This analysis considered 61 scenarios present in 15 articles. Initially, we will refer to the GHG emissions that do not consider the dLUC effect as the base GHG emissions **(Figure 2.5).** The GHG emissions that do include dLUC emissions of CO_2 will be referred as the net GHG emissions. **Figure 2.6** shows the net GHG emissions by the biofuels production from different types of feedstock. Similar to results in **Figure 2.5**, the net GHG emissions using economic, energy, mass, or not specified allocation criteria (**Figure 2.6a**) tend to be larger than when using system expansion (**Figure 2.6b**). Most of the biodiesel LCAs consider low-carbon-content soils such as savannah, pastureland, or grassland as reference land-types (Castanheira and Freire 2011; Galbusera and Hilbert 2011; Iriarte and others 2012; Iriarte and Villalobos 2013), while studies on ethanol production also consider forest deforestation (Amores and others 2013; Consorcio 2012; Garcia and others 2011). This helps explain the apparently lower net GHG emissions for biodiesel

than for ethanol (**Figure 2.6a**). Studies that employ the GREET model (Kim and Dale 2009; Krohn and Fripp 2012; Wang and others 2012; Wang and others 2011a) include both domestic and international direct and indirect LUC, and it is not possible to extract only the dLUC portion. Overall, the effect of the dLUC is either an increase or a reduction of the base GHG emissions of the biofuel production depending on the dLUC scenario assumed.

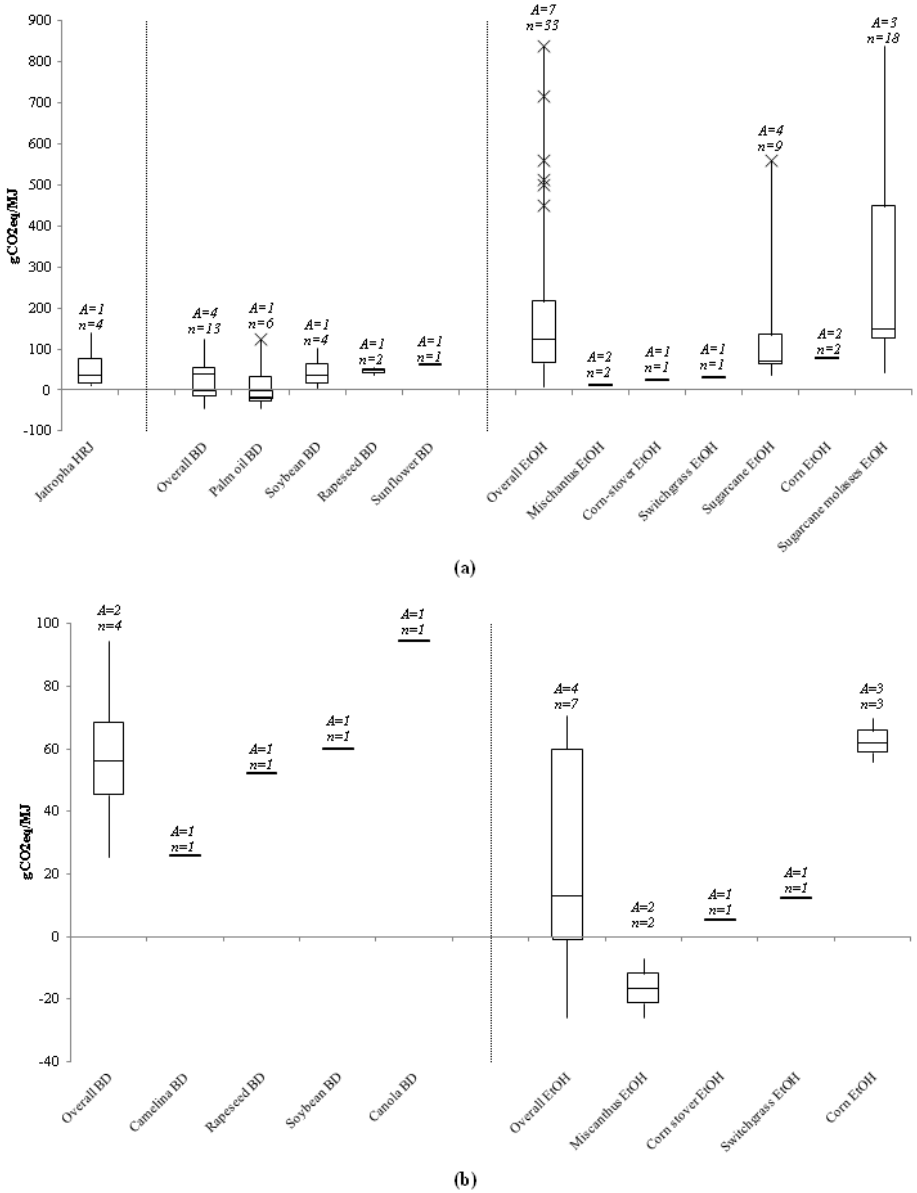

Figure 2.6 Box and Whisker plot showing the minimum, maximum, and non-typical data of the GHG emissions including the dLUC effect (a) from studies considering mass, energy, economic, or no allocation (b) from studies considering system expansion. *A* refers to the number of articles and *n* to the number of analysis. Corn, corn stover, miscanthus, and switchgrass include also iLUC GHG emissions.

For the jatropha-based HRJ production, the effect of the dLUC on the base GHG emissions is a reduction of about 11 – 27 g CO_{2eq}/MJ when the cultivation takes place on pasturelands, reaching net GHG emissions of 13 – 17 g CO_{2eq}/MJ (first and second quartiles). However, the cultivation on grasslands and shrub lands lead to net GHG emissions of 56 (third quartile) and 140 g CO_{2eq}/MJ (fourth quartile), respectively, which means an increase of about 16 – 112 g CO_{2eq}/MJ compared to base GHG emissions (Bailis and Baka 2010).

For the palm oil-based biodiesel production in Colombia, the cultivation on savannah results in net GHG benefits of 13 – 43 g CO_{2eq}/MJ (first to third quartiles) depending on the degradation level of the soil, in other words, its effect is a reduction of about 52 – 82 g CO_{2eq}/MJ in the base GHG emissions. On the other hand, the effect of the cultivation on displaced forests is an increase of about 4 – 85 g CO_{2eq}/MJ in the base GHG emissions, reaching net GHG emissions of 49 – 124 g CO_{2eq}/MJ (fourth quartile) (Castanheira and Freire 2011).The challenge in multipurpose crops that are not produced specifically for biofuel production is trying to calculate the impact on dLUC of the derivation of a co-product of the crop as in the case of soybean oil (18 % of oil in the seed) (Galbusera and Hilbert 2011). A similar situation occurs with the ethanol production from sugarcane (Amores and others 2013) and sugarcane-molasses (Amores and others 2013; Consorcio 2012; Garcia and others 2011). The net GHG emissions of the soybean-based biodiesel, considering the economic allocation criteria, are 7 – 21 (first and second quartiles) and 52 – 105 g CO_{2eq}/MJ (third and fourth quartiles) when the cultivation takes place on agricultural lands (changing the crop) and on pastureland,

respectively. The effect of the dLUC on the base GHG emissions is then a decrease of about 1- 15 g CO_2eq/MJ and an increase of about 30 – 83 g CO_{2eq}/MJ when cultivation takes place on agricultural land and on pasturelands, respectively (Galbusera and Hilbert 2011). However, soybean cultivation on agricultural lands may incur iLUC emissions as other lands, such as forestlands, can be converted to croplands in an attempt to tradeoff the area used for the soybean biofuel cultivation, which is a topic that requires further studies. The dLUC effect on the base GHG emissions of the rapeseed-based biodiesel production in Chile is an increase of about 7 g CO_{2eq}/MJ considering that the cultivation takes place on non-degraded grasslands, reaching net GHG emissions of 56 g CO_{2eq}/MJ (Iriarte and others 2012).The sugarcane-based ethanol production in Brazil reaches net GHG emissions of 36 – 45 g CO_2eq/MJ (first quartile) when the cultivation takes place on typical savannah and/or pasturelands. The effect of the dLUC is an increase of about 17 g CO_2eq/MJ in the base GHG emissions (Souza and others 2012). Under Mexican conditions the GHG emissions are 65 – 67 (second quartile), 72 – 74 (third quartile), and 135 – 137 g CO_2eq/MJ (fourth quartile) when performing the cultivation on tropical dry forests, grasslands, and rainforests, respectively. In other words, the effect of the dLUC is an increase of 32 – 100 g CO_2eq/MJ on the base GHG emissions (Garcia and others 2011). Considering direct deforestation of rainforest, the sugarcane-based ethanol production in Argentina reaches net GHG emissions up to 560 g CO_2eq/MJ (Amores and others 2013).

The net GHG emissions of the sugarcane molasses-based ethanol production depend on the assumptions on both the industrial stage conditions and the dLUC scenarios

considered. The use of all of the sugarcane molasses leads to net GHG emissions ranging between 43 and 123 g CO_{2eq}/MJ (first quartile) depending on the dLUC scenario assumed (Consorcio 2012; Garcia and others 2011). Similarly, the use of a portion of the molasses leads to net emissions of 140 – 224 g CO_2eq/MJ (second and third quartiles) (Garcia and others 2011). These trends were estimated for Mexico and Colombia. When the dLUC involves direct deforestation under Argentinean conditions, the net GHG emissions range from 440 to 839 g CO_2eq/MJ (third and fourth quartiles) depending on the allocation criteria used (Amores and others 2013) (**Fig 6a**). Overall, the effect of the dLUC on the base GHG emissions of the sugarcane molasses-based ethanol production in Colombia is an increase of about 27 g CO_{2eq}/MJ when cultivation takes place on shrublands (Consorcio 2012). In the case of Mexico, the effect of the dLUC is an increase of about 97 – 116, 28 – 32, and 24 – 41 g CO_2eq/MJ when cultivation takes place on rainforests, tropical dry forests, and grasslands, respectively (Garcia and others, 2011).

Studies on the ethanol production from corn, corn stover, miscanthus, and switchgrass did not specify the LUC scenario considered. Furthermore, two studies gathered both the dLUC and the iLUC emissions of GHG as simply LUC GHG emissions (Wang and others 2011; Wang and others 2012). Thus, Kim and Dale (2009) estimated that the corn-based ethanol production reaches average net GHG emissions of 56 g CO_2eq/MJ, while Wang and others (2011) and Wang and others (2012) estimated total GHG emissions of 62 – 70 g CO_2eq/MJ when including both dLUC and iLUC GHG emissions. The effect of the dLUC and the iLUC on the base GHG emissions derived from the corn-based ethanol production is an estimated 9 g CO_2eq/MJ increase (Wang and others 2012). Other

studies, however, have estimated that the dLUC and the iLUC emissions of GHG derived from the corn-based ethanol production may be higher, ranging from 20 up to 104 CO_2eq/MJ depending on the above- and below-ground carbon content of the soil and the treatment of the emissions at different times (Wang and others 2011). The net GHG emissions of the ethanol production from corn stover and switchgrass are 5 and 12 g CO_2eq/MJ (Wang and others 2012), respectively including both the dLUC and the iLUC effects. On the other hand, the miscanthus-based ethanol production results in GHG emissions benefits (negative emissions) of 7 and 26 g CO_2eq/MJ considering and not considering the iLUC effect, respectively (Scown and others 2012; Wang and others 2012). Overall, the LUC effect on the base GHG emissions (including both the dLUC and the iLUC effect) of ethanol production from switchgrass and corn stover is almost null, while for miscanthus the effect is a reduction of 12 g CO_2eq/MJ (Wang and others 2012).

Regarding the breakdown of the GHG emissions by stage, adding the GHG emissions derived from the dLUC to the agricultural emissions makes this stage the major contributor to net GHG emissions for biofuels production for all types of feedstock, with the exception of corn and corn stover (see **Figure A.3 in Appendix A)**. In the case of corn, some analyses assume old industrial conditions that require coal for energy production (Kim and Dale 2005), which explains the high contribution of the industrial stage. However, the use of more recent data that reflect the current corn-based ethanol production leads to a different trend where the agricultural stage is the major contributor to the net GHG emissions (Wang and others 2011; Wang and others 2012). On the other hand, considering corn stover as a residue results in GHG emissions of the agricultural

stage coming mainly from the supplement of fertilizers to compensate the nutrient loss from stover removal (Wang and others 2011a; Wang and others 2012).

2.5.3 Regulatory frameworks and certification schemes for biofuel sustainability

Currently, several regulatory frameworks and certification schemes are available that aim to assess the sustainability of biofuels production. The Testing Framework for Sustainable Biomass (TFSB) or "Cramer Criteria", and the EU-RED are examples of regulatory frameworks, while the Roundtable on Sustainable Biomaterials (RSB), the International Sustainability & Carbon Certification (ISCC), and the Global Bioenergy Partnership (GBEP) are examples of certification schemes (BEFSCI 2011). These initiatives analyze a range of factors associated with the biofuel's supply chain including air quality, biodiversity, energy security, GHG emissions, land use change, soil quality, and water use, and in all cases rely on LCA results. The most critical factor in these certification schemes and regulatory frameworks is the GHG emissions. The main regulatory framework and certificateion schemes explicitly state the guidelines to be used in the LCA.

Table 2.1 shows a brief comparison of these metrics along with those developed by the RSB. The guidelines developed by the US EPA and the EU-RED are the most commonly employed in LCAs conducted in the Pan American countries, as shown in **Figure 2.1b**. Several of the certification schemes listed above require production to meet or exceed the regulatory frameworks of the EU-RED. Section A.5.3 in Appendix A discusses how dLUC can affect the ability of biofuels to meet certification schemes, such as EU-RED.

The use of certification schemes and/or regulatory frameworks allows for comparison and assessment of environmental management between biofuel production systems. Several of the certification schemes (RSB, ISCC, Bonsucro), have criteria that must be met concerning land use, soil, water, air, waste, and several other social and environmental indicators (Solomon and Bailis 2014). These certification schemes with a focus on environmental quality could help ensure that the best possible environmental management of these biofuel systems across the Pan American region is being used.

Table 2.1 Methodological metrics to estimate the GHG balance. Adapted from van Dam et al., (2010).

Initiative	Functional unit	Allocation	Default factors	Selected time period	GHG emission reduction required
EU-RED	energy content of fuel	Energy	Typical and default values	Annualized emissions over 20 years.	35%[a]
US-RFS2	Energy content of fuel	System expansion	EPA results to producer	100 years with 2% discount rate or 30 year with 0% discount rate.	Conventional biofuel: 20%[b] Advanced biofuels: 50% Biomass-based diesel: 50% Cellulosic biofuel: 60%
RSB	energy content of fuel	Economic[c]	Ecoinvent Emission factors[c]	IPCC metrics	50% for a blend of biofuels[c]

[a] This value will rise to 50% on January 2017 and will be 60% on 2018 for those facilities which production starts on or after January 2017.
[b] Below gasoline.
[c] RSB (2011).

2.6 Case study: The GWP of jatropha HRJ production in the Yucatan state of Mexico: Effects of regulation-driven allocation requirements

2.6.1 Introduction

Sections 2.4 and 2.5 presented a wide range of biofuel LCA results when different study assumptions are used. In addition, it was mentioned in section 2.5.3 that certification

schemes and regulatory frameworks have the potential to standardize biofuel LCA around a set of accepted practices. This section presents a case study LCA of hydro-renewable jet (HRJ) produced from *Jatropha* oil in Mexico using LCA methods required by US EPA RFS2 and EU RED, and compares GHG results to each other and to fossil jet. Rather than making LCA results agree, the LCA results diverge because the LCA methods are different between the regulatory frameworks in the US and the EU.

Jatropha curcas (referred to as jatropha) is a shrub plant that produces seeds with high oil (40% wt) content that can be grown on marginal soils and therefore can help restore eroded areas. The tallest variety grows to 6 m height, has adapted to a variety of climate conditions (from subtropical to arid) and can grow in low fertility soil (FACT 2010). The most suitable climate conditions for jatropha cultivation are within a belt extending from 30 °N to 35 °S straddling the equator. Seed productivities have historically been between 0.3 to 6 dry ton / ha / yr depending on rainfall and soil quality. The entire plant has been used for erosion control, as a hedge plant, medicinal use, and for firewood. The fruit of the plant has been used as a combustion source and fertilizer. The seed oil has been used in lamps, for cooking, as an engine fuel, and for soap making; the seed cake has been used as a fertilizer, an input for biogas and charcoal production, and for combustion (FACT 2010).

This case study presents results from a jatropha cultivation project in the Yucatan region of Mexico with conversion of extracted oil to hydro-renewable jet (HRJ) fuel in Cancun. The effects of LCA allocation method are explored - system expansion versus energy allocation conducted, according to both US and EU frameworks.

2.6.2 LCA Methods

2.6.2.1 Goal and scope

The goal of this limited LCA is to evaluate the greenhouse gas emissions associated with the production of HRJ derived from jatropha oil grown on marginal agriculture lands in the Yucatan peninsula of Mexico. The study scope is cradle-to-grave starting with jatropha cultivation and concluding with combustion of HRJ in jet engines. Both attributional and consequential modelling were done depending on allocation (energy and system expansion, respectively). Results of the LCA for the proposed HRJ are compared with impacts of producing and using fossil jet-fuel and savings of GHGs are computed.

2.6.2.2 Production site and carbon stocks

Figure 2.7 shows the locations of jatropha cultivation, oil extraction at Uman, and HRJ production at Cancun. The land area bordered by green in this figure is the location of the proposed plantations of jatropha. A report by the Universidad Autonoma de Chapingo from June 2010 cataloged the canopy cover and carbon content of above- and below-ground biomass of native vegetation in the jatropha plantation area. **Table A.3** in Appendix A details the carbon content for several land categories from acreage in the green bordered area from **Figure 2.7**. The carbon stock values are used to estimate direct land use change (dLUC) emissions in this study. This analysis assumes cultivation on 55,000 ha with an average annual yield of 10 metric ton/ha of wet seeds to produce a total wet weight of 550,000 ton of seeds. No indirect LUC effects are included because Jatropha will not be grown on agricultural lands. The study assumes oil extraction will

occur at Uman and the resulting jatropha oil will be transported by truck to Cancun for processing to HRJ.

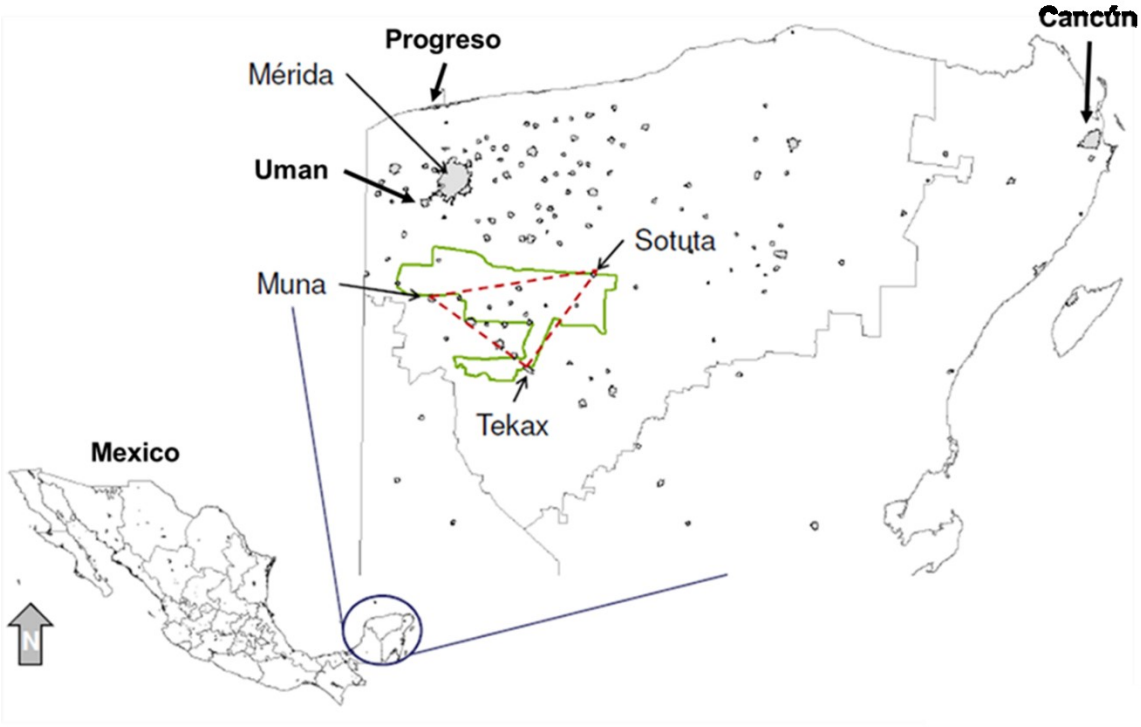

Figure 2.7 Locations of jatropha cultivation, oil extraction at Uman, and HRJ production at Cancun.

2.6.2.3 Biofuel pathway, functional unit, and allocation methods

The major life cycle stages for this study are shown in **Figure 8**; jatropha cultivation and harvesting, jatropha seed and shell transport, jatropha oil extraction at Uman, jatropha oil transport, jatropha HRJ production in Cancun, and HRJ combustion. The study assumes that the seed will be dried at the site of harvesting using natural gas and transported by truck along with the shell and husk to a processing plant in Uman; 95 km distant on average from harvesting sites. The plantation will utilize wastewater from adjacent pig farms for irrigation and soil nitrogen amendment. Additional chemical fertilizer will also

be required — data for this requirement was provided by the company "KUO Bioenergía". The jatropha oil is extracted from the seeds at the plant through mechanically pressing the seeds, application of heat, and hexane extraction.

The base line analysis assumes that the residual shell, husk and seed cake are combusted to generate electricity for internal use in oil extraction and for export to the Yucatan grid. The functional unit for this LCA is 1 MJ of energy released upon combustion of each fuel product, HRJ and petroleum jet-fuel. Energy allocation was used to attribute environmental burdens to pathway co-products (see **Figure 2.8**); system expansion was also employed as an alternative allocation scenario to conform to the US EPA RFS2. A pathway diagram for system expansion, along with further details of the allocation methods and factors are presented in Appendix A (**Figure A.5**)

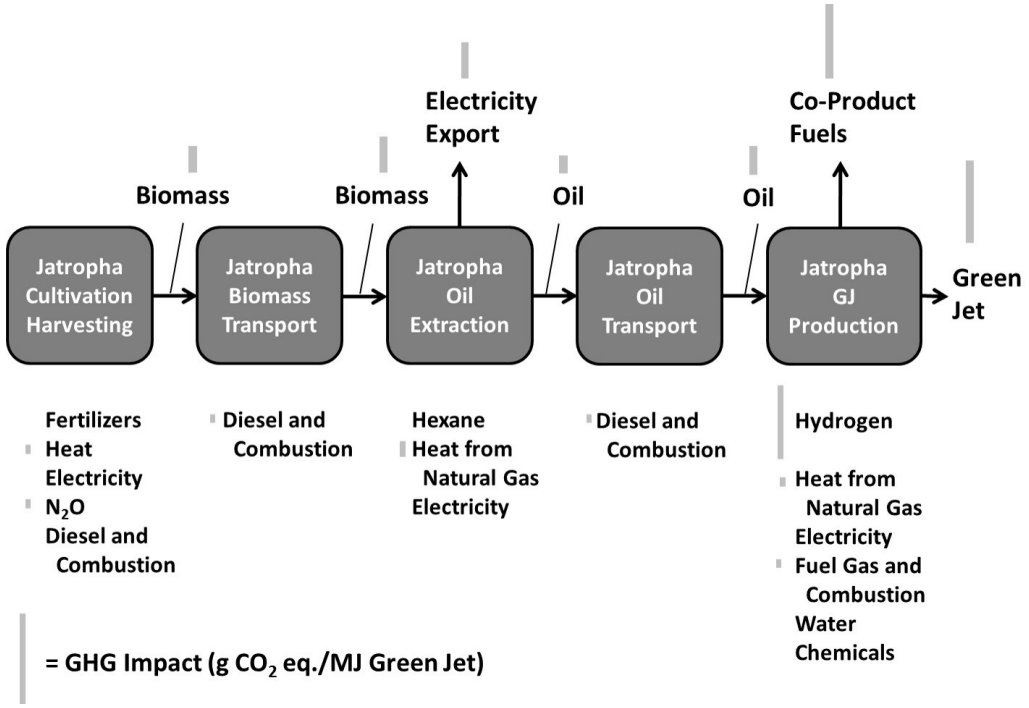

Figure 2.8 Life cycle stages for the analysis of HRJ from jatropha using energy allocation according to the USA framework. The red bars indicate greenhouse gas (GHG) emission impacts and height of bar is proportional to the degree of impact. GHG impacts accumulate as material moves through the life cycle due to the input and use of material and energy (shown below each stage). Impacts exit the HRJ product life cycle when co-products are created and exported, and are allocated to HRJ and co-products using energy allocation by considering the material flows of products and their lower heating value.

2.6.2.4 Process inputs and inventory data

Inputs at each stage of the HRJ life cycle were developed on an annual basis for all 55,000 ha of jatropha plantation and conversion of the entire amount of jatropha oil to HRJ. All input data to the HRJ life cycle were obtained from original documents of the company KUO Bioenergía, and from the company UOP for the HRJ production processes, and standards based upon IPCC guidelines for N_2O emissions from fertilizer application. Unless otherwise noted the ecoinvent™ database from SimaPro 7.2 was

utilized to develop inventory data for all inputs to the life cycle. Input tables for each stage of the pathway are included in Appendix A (**Tables A.3-8**). The allocation according to energy of the inventory data to HRJ from the various life cycle stages is shown in Appendix A in **Table A.9**.

2.6.2.5 Impact assessment

Environmental impacts are limited to global warming which was calculated using the IPCC 2007 GWP 100a method in SimaPro 7.2 version. In this method, CO_2 has a global warming potential (GWP) of 1, CH_4 = 25, and N_2O = 298. A full accounting of the GWP of solvents and refrigerants is included in the analysis using inventory elements from the ecoinvent^{TM} database in SimaPro 7.2. The annual GHG emissions are divided by the energy content (in MJ) of the annual HRJ production to arrive at the desired result; g CO_2 eq/MJ HRJ. Emissions of CO_2 from combustion processes involving biomass fuel or HRJ are *not* counted toward the GHG totals, because they are considered carbon neutral, unlike fossil CO_2 emissions which *are* counted.

2.6.3 GHG results

The GHG emissions for Yucatan jatropha HRJ for the different allocation methods are shown in **Table 2.2** along with savings compared to fossil jet-fuel. The GHG results are organized based on major stages of production along the biofuel pathway. Allocation methods are correlated with regulatory frameworks in the US and EU. The US Department of Energy (US DoE) uses energy allocation in which all co-products are included in the allocation factor calculations. US EPA uses system expansion which is the method employed to determine whether biofuels qualify toward targets established in

the RFS2. EU-RED is energy allocation in which co-products from oil extraction are considered as products with negligible value (wastes) and are not included in the calculation of allocation factors. As explained in Appendix A ("Energy allocation according to the EU-RED" section), the allocation case of EU-RED includes some minor changes to inputs to the HRJ pathway relative to the US DoE and US EPA cases , but otherwise the same inputs were used (see **Tables A.11-12**).

The highest emission stages are HRJ production and jatropha cultivation, with all other stages, including dLUC, being of minor importance. In the cultivation stage, diesel fuel use, electricity, fertilizers, and N_2O emissions are the most important inputs and source of inventory data. In the HRJ production stage, H_2 generation and process heat, both from natural gas, are the two dominant inputs. In the US-EPA case using system expansion, very large emission credits for co-products from oil extraction and HRJ production dominate the results. Savings of GHG emissions compared to fossil jet-fuel are greater than ~80% for all cases and significantly larger for the system expansion case.

Table 2.2 GHG Emissions for Jatropha HRJ for three allocation methods compared to petroleum jet fuel.

GHG emissions	Fossil jet[a]	US DoE	US-EPA	EU-RED
Jatropha cultivation/harvest (HRA)	6.8	1.5	7.8	1.8
Jatropha seed, shell transport (RMT)	1.3	0.5	2.5	0.4
Jatropha oil extraction		1	5.2	0.2
Jatropha oil transport		0.7	1.3	0.7
HRJ production from jatropha oil (LFP)	6	16.4	30.7	14.6
Co-product credit extraction stage			-61.4	
Co-product credit GJ production stage			-70	
Final production transport	1			
Fossil jet fuel combustion	77.7			
dLUC		-0.8	-4.1	-3.2
Total	92.9	19.3	-88.0	14.5
GHG emissions savings (%)		79.2	194.7	84.4

[a] From Skone and Gerdes (2008), RMA = Raw Material Acquisition, RMT = Raw Material Transport, LFP = liquid fuel production. US DoE: Energy allocation, US EPA: System expansion (Displacement) allocation, EU-RED: Energy allocation; electricity export from oil extraction not included.

2.6.4 Interpretation of GHG results

The GWP results from this study achieve large savings compared to fossil jet-fuel and would qualify as an advanced biofuel under the RFS2 standard (>50% savings) and also under EU-RED (>35% savings). The different requirements for each of the allocation approaches add effort and complexity to the LCA. The US-DoE energy allocation is an often-used approach in which all co-products of economic value are allowed in the calculation of the allocation factors. The EU-RED case does not allow energy allocation for certain co-products such as extraction residues which are considered wastes according to the regulation, though they may be economically viable as a renewable energy source in certain cases. In system expansion (the US-EPA case), the calculated changes to the environment are attributed to the system as a whole, with no possibility of dividing the total impact among co-products. Attributional modeling, on the other hand, does not

attempt predicting actual changes to the environment due to limited modeling of market product displacements, however all products and co-products are assigned environmental burdens, proportionally to their mass, volume, energy content, or market price. Each allocation has advantages and limitations and therefore for the near term it is likely that biofuel environmental LCAs for any potential biofuel feedstock pathway will have to conform to one or more regulatory frameworks with regard to allocation and other LCA methodology aspects. As a final note, cultivation of jatropha at this study site was halted in 2013 due to lower than acceptable yields from these marginal lands. This testifies to the importance of updating system inputs through time before considering LCA results representative of real conditions. As of this writing, cultivation of jatropha for the purpose of evaluation for feasibility as a biofuel feedstock continues at other study sites in the state of Yucatan.

2.7 Recommendations for research and other efforts to enhance LCA and improve environmental management of biofuels and bioenergy

This critical evaluation of biofuel LCAs in the Pan American region reveals a wide range of important study features; such as regulatory-driven frameworks, modeling assumptions (study scope, functional units, and allocation), inventory databases, environmental impacts assessed, and biofuel pathways in different countries. When considering the most commonly encountered potential environmental impact, global warming potential, these LCA characteristics caused a wide range in GHG emission results, even when the results are converted to the same basis (g CO_2 eq./MJ biofuel). Normally, these complications make it very difficult to compare environmental performance between different biofuel

pathways in different locations, and more importantly, makes it difficult to understand the main drivers for environmental damage so that improvements to biofuel production systems can be achieved. However, in our quantitative analysis of GHG emission results from many of the articles studies we were able to determine the magnitude of change in emissions for two main study features, allocation and LUC, admittedly with some significant effort. Other aspects of biofuel LCA such as crop yield, inputs to the agricultural and industrial stages, could have been quantified on a statistical basis, but were beyond the scope of this study. It is also important to note that while the bioenergy sector has adopted many of the best practices of conducting LCAs, broader adoption of more progressive mandates such as peer review of industrial process LCAs prior to certification, will require higher confidence in the results of the methodology.

In order to take full advantage of LCA as an environmental management tool, we offer a number of recommendations to guide future research with the goal of improving the quality and utility of study results.

- Biofuel LCA Guidance Frameworks: A number of regulatory-driven biofuel LCA frameworks and certification schemes are currently in effect throughout the Pan American region. Based on our evaluation of the literature and the case study, these frameworks and schemes are one of the most important reasons for divergence in LCA study results. Future research should quantify the impact of these frameworks and schemes for the same pathways in order to isolate this single study variable. The use of Product Category Rule (PCR) for biofuel production can help with comparisons between different pathways and feedstocks due to the data collection

and other LCA methods being standardized. PCR's follow ISO standards and can therefore be used within other frameworks and certification schemes. Understanding the variations within other frameworks and certification schemes will become increasingly important as the research community develops new methods for incorporating local sociological values and the wide variety of sustainability metrics into LCAs.

- Life Cycle Inventory Data Quality: There is a need to improve inventory data quality so that the output from LCA of biofuels and bioenergy systems are more accurate and useful. Inventory data resides in the industrial sphere and also in the context of cultivation systems and ecosystems. In the past, industry-funded confidential benchmarking studies have shown that there is a wide range of energy efficiency and extent of pollution control for industrial production of key inputs needed for biofuel and bioenergy production (fertilizers, industrial chemicals, electricity, etc.). There is also a great need of field validated data for carbon stocks and N_2O emissions from fertilizer use, both of which have a large impact on GHG emissions and water quality. Research is needed to understand this variability and to incorporate it on a statistical basis for use in uncertainty analysis in LCA. This will be particularly challenging with respect to the need to incorporate sociological indicators and metrics associated with labor rights, land use change and other impacts on rural communities.
- Cultivation Systems: Important changes will occur to soils when land transitions into bioenergy cropping on a large scale. These changes will affect inputs to biofuel and bioenergy LCA in the form of inventory data used in the analysis of GHG emissions

and other important categories of environmental sustainability. Research needs to continue and to be expanded in regional scope in both experimental and modeling aspects on soil properties such as organic matter, carbon, cycling of nutrients (N, P, K), management of water, erosion, emissions, and yields. This research should be conducted in a coordinated way on multiple cropping systems, various climates and in multiple locations throughout the Pan American region in order to capture the effects of local conditions that impact a variety of processes (e.g. transpiration rates, water yield relationships drought tolerances.)

- Life Cycle Impact Categories: The focus in biofuel and bioenergy LCA has been on GHG emissions due to the mandates in regulatory frameworks. However, LCA should anticipate future environmental issues and therefore the scope of environmental impacts must expand. Future research should continue with GHG emissions, but also expand with increasing momentum into water availability and degradation issues (nutrient runoff and management), biodiversity, criteria air pollutants (PM, H_2S, Hg, etc.), and human/ecosystem toxicity.
- Systems Analysis for Sustainability: Although beyond the scope of topics in this review, it is worth noting that in the opinion of the authors LCA is an ideal platform to integrate information and data across the entire biofuel pathways, and depending on system boundary, may also include data from technical and natural systems outside of the direct pathway. LCA is capable of including this indirect data into the analysis, but also is able to contribute to meta analyses by contributing environmental assessments for a full spectrum sustainability analysis. The meta analyses would include techno-economic analyses, regional and global economic

analyses, environmental impact analyses, and societal impact analyses. Future research should address the data, framework, and methodology issues in systems analysis for sustainability. This will become increasingly important as biofuels and bioenergy in general become deeply imbedded in the global energy markets which will make it more difficult to understand coupling between the integrated systems (e.g. water-energy nexus.)

- Carbon Neutrality: Most of the articles reviewed assumed carbon neutrality in the carbon cycle of the biofuel production. The carbon neutrality assumption eases the analysis towards the GWP impact. However, this assumption does not consider the timing of the CO_2 emissions, since when the biofuel is burned the carbon stored is released instantly as CO_2 to the atmosphere while the carbon sequestration process in the next cycle of biomass production can take a longer time period.
- Outreach: Another topic beyond the scope of issues in this LCA review is outreach, but the authors consider this a high priority. Programs should be considered for translating LCA research out to the professional communities who are impacted by study results, to policy makers, and also to the general public. As done effectively in agricultural and forestry industries, outreach into the biofuels production community would be an effective mechanism to disseminate the best sustainable practices.

2.8 Acknowledgements

This material is based upon work supported in part by the U.S. National Science Foundation grant CBET-1140152"RCN-SEES: A Research Coordination Network on Pan American Biofuels and Bioenergy Sustainability". We would like to thank the U.S. National Science Foundation for partial support in writing this paper under Award

Number 1105039, "OISE-PIRE Sustainability, Ecosystem Services, and Bioenergy Development Across the Americas". The article benefited greatly from the comments of three anonymous reviewers

Acronyms

Acronym	Meaning
BD	Biodiesel
HRJ	Hydrorenewable jet-fuel
DAYCENT	Daily Century
dLUC	Direct land-use change
EBAMM	ERG Biofuel Analysis Meta-Model
EPA	Environmental Protection Agency
EtOH	Ethanol
EU-RED	European Union – Renewable Energy Directive
GHG	Greenhouse gases
GREET	Greenhouse gases, Regulated Emissions, and Energy use in Transportation
GWP	Global warming potential
IPCC	Intergovernmental Panel on Climate Change
ISCC	International Sustainability & Carbon Certification
LCA	Life cycle assessment
LCI	Life cycle inventory
LCIA	Life cycle impact assessment
RSB	Roundtable on sustainable biomaterials
US-RFS	United States – Renewable Fuel Standard

2.9 References

Adom F, Maes A, Workman C, Clayton-Nierderman Z, Thoma G, Shonnard D (2012) Regional Carbon Footprint of Dairy Feed Rations for Milk Production in the United States Inter Jour Life Cycle Assess 17:520-534

Agusdinata DB, Zhao F, Ileleji K, DeLaurentis D (2011) Life cycle assessment of potential biojet fuel production in the United States Environmental Science & Technology 45:9133-9143 doi:10.1021/es202148g; 10.1021/es202148g

Allen DT and others (2009) Framework and Guidance for Estimating Greenhouse Gas Footprints of Aviation Fuels. http://caafi.org/information/pdf/AFRL-RZ-WP-TR-2009-2206.pdf

Allen DT, Shonnard DR (2002) Green Engineering: Environmentally Conscious Design of Chemical Processes. Prentice-Hall. Upper Saddle River, NJ

Amores MJ, Mele FD, Jimenez L, Castells F (2013) Life cycle assessment of fuel ethanol from sugarcane in Argentina The International Journal of Life Cycle Assessment 18:1344-1357 doi:10.1007/s11367-013-0584-2

ANL (2014) GREET1_2013 Model, Transportation Technology R&D Center. Argonne, IL, USA

Bailis R, Kavlak G (2013) Environmental Implications of Jatropha Biofuel from a Silvi-Pastoral Production System in Central-West Brazil Environmental science & technology 47:8042-8050 doi:10.1021/es303954g

Bailis RE, Baka JE (2010) Greenhouse gas emissions and land use change from Jatropha curcas-based jet fuel in Brazil Environmental science & technology 44:8684-8691 doi:10.1021/es1019178; 10.1021/es1019178

Bare J, Thomas G, Norris G (2006) Development of the Method and U.S. Normalization Database for Life Cycle Impact Assessment and Sustainability Metrics Environmental science & technology 40:5108-5115 doi:10.1021/es052494b

BEFSCI (2011) A compilation of bioenergy sustainability initiatives overview vol 2013.

Bruinsma B (2009) Producción de biodiesel de palma aceitera y jatropha en la Amazona del Peru y el impacto para la sostenibilidad. Open Universiteit Nederland

Castanheira EG, Freire FM Environmental performance of palm oil biodiesel - a life cycle persepctive In: IEEE International Symposium on Sustainable Systems and Technology (ISSST), 2011. pp 1-6. doi:10.1109/ISSST.2011.5936843

Cavalett O, Chagas MF, Seabra JEA, Bonomi A (2013) Comparative LCA of ethanol versus gasoline in Brazil using different LCIA methods The International Journal of Life Cycle Assessment 18:647-658 doi:10.1007/s11367-012-0465-0

CFR (2010) Regulation of Fuels and Fuel Additives: Changes to Renewable Fuel Standard Program.

Chavez-Rodriguez MF, Nebra SA (2010) Assessing GHG emissions, ecological footprint, and water linkage for different fuels Environmental science & technology 44:9252-9257 doi:10.1021/es101187h; 10.1021/es101187h

Cherubini F, Bird ND, Cowie A, Jungmeier G, Schlamadinger B, Woess-Gallasch S (2009) Energy-and greenhouse gas-based LCA of biofuel and bioenergy systems: Key issues, ranges and recommendations Resources, Conservation and Recycling 53:434-447

Cherubini F, Strømman AH (2011) Life cycle assessment of bioenergy systems: state of the art and future challenges Bioresource technology 102:437-451

Chiu Y, Wen., Suh S, Pfister S, Hellweg S, Koehler A (2012) Measuring ecological impact of water consumption by bioethanol using life cycle impact assessment The International Journal of Life Cycle Assessment 17:16-24 doi:10.1007/s11367-011-0328-0

Chiu YW, Walseth B, Suh S (2009) Water embodied in bioethanol in the United States Environmental science & technology 43:2688-2692

Clarens AF, Resurreccion EP, White MA, Colosi LM (2010) Environmental life cycle comparison of algae to other bioenergy feedstocks Environmental science & technology 44:1813-1819 doi:10.1021/es902838n; 10.1021/es902838n

Cleary J (2009) Life cycle assessments of municipal solid waste management systems: A comparative analysis of selected peer-reviewed literature Environment International 35:1256-1266 doi:http://dx.doi.org/10.1016/j.envint.2009.07.009

Consorcio CUE (2012) Evaluacion del ciclo de vida de la cadena de produccion de biocombustibles en Colombia vol ATN/JC-10826-CO y ATN/JF-10827-CO. Medellin

da Costa RE, Yanez E, Torres EA (2006) The energy balance in the production of palm oil biodiesel-two case studies: Brazil and Colombia:1-5

de Souza S, Pereira, , Pacca S, de Avila M, Turra ,, Borges JL, B., (2010) Greenhouse gas emissions and energy balance of palm oil biofuel Renewable Energy 35:2552-2561 doi:http://dx.doi.org/10.1016/j.renene.2010.03.028

Diaz-Chavez R (2014) Indicators for socio-economics sustainability assessment. Springer, Switzerland

Ecoinvent 3 Database (2014) http://www.ecoinvent.org/. .

Emmenegger FM, Pfister S, Koehler A, Giovanetti L, Arena A, Pablo,, Zah R (2011) Taking into account water use impacts in the LCA of biofuels: an Argentinean case study The International Journal of Life Cycle Assessment 16:869-877 doi:10.1007/s11367-011-0327-1

EPA (2010) Renewable Fuel Standard Program (RFS2) Regulatory Impact Analysis, U.S. Environmental Protection Agency, Office of Transportation and Air Quality.

FACT (2010) The Jatropha Handbook: From Cultivation to Applications FACT Foundation http://wwwfact-foundationcom/en/Knowledge_and_Expertise/Handbooks

Fan J, Handler RM, Shonnard DR, Kalnes TN (2012) A review of life cycle greenhouse gas emissions of hydroprocessed jet fuels from renewable oil and fats International Journal of Environmental Science and Engineering Research (IJESER) 3:114-138

Fargione J, Hill J, Tilman D, Polasky S, Hawthorne P (2008) Land clearing and the biofuel carbon debt Science 319:1235-1238

GaBi Databases (2014) http://www.gabi-software.com/america/databases/.

Galbusera S, Hilbert JA (2011) Analisis de emisiones de gases de efecto invernadero de la produccion agricola extensiva y estudio de la "huella de carbono" de los productos derivados de la soja en la Republica de Argentina. INTA, Argentina

Garcia CA, Fuentes A, Hennecke A, Riegelhaupt E, Manzini F, Masera O (2011) Life-cycle greenhouse gas emissions and energy balances of sugarcane ethanol production in Mexico Applied Energy 88:2088-2097 doi:http://dx.doi.org/10.1016/j.apenergy.2010.12.072

Graefe Sand others (2011) Energy and carbon footprints of ethanol production using banana and cooking banana discard: A case study from Costa Rica and Ecuador Biomass and Bioenergy 35:2640-2649 doi:http://dx.doi.org/10.1016/j.biombioe.2011.02.051

Hilbert JA, Galbusera S (2011) Analisis de emisiones produccion de biodiesel - AG-Energy. Instituto Nacional de Tecnologia Agropecuaria,

Hilbert JA, Galligani S (2014) Argentina. Springer, New York

Huo H, Wang M, Bloyd C, Putsche V (2008) Life-cycle assessment of energy and greenhouse gas effects of soybean-derived biodiesel and renewable fuels.

IPCC (2006a) Chapter 2: Generic Methodologies Applicable to Multiple Land-Use Categories. In: Aalde H, Gonzalez, P., Gytarsky, M., Krug, T., Kurz, W.A., Lasco, R.D., Martino, D.L., McConkey, B.G., Ogle, S., Paustian, K., Raison, J., Ravindranath, N.H., Smith, P., Somogyi, Z., Amstel, A.V., Verchot, L. (ed) IPCC guidelines for national greenhouse gas inventories Volume 4: Agriculture, Forestry, and Other Land Use.

IPCC (2006b) Chapter 5: Cropland. IPCC guidelines for national greenhouse gas inventories Volume 4: Agriculture, Forestry, and Other Land Use.

IPCC (2013) Summary for Policymakers. In: Climate Change 2013: The Physical Science Basis. Contribution of Working Group I to the Fifth Assessment Report of the Intergovernmental Panel on Climate Change In: Stocker TF, D. Qin, G.-K. Plattner, M. Tignor, S.K. Allen, J. Boschung, A. Nauels, Y. Xia, V. Bex and P.M. Midgley (ed). Cambridge University Press, Cambridge, United Kingdom and New York, NY, USA,

Iriarte A, Rieradevall J, Gabarrell X (2010) Life cycle assessment of sunflower and rapeseed as energy crops under Chilean conditions Journal of Cleaner Production 18:336-345 doi:http://dx.doi.org/10.1016/j.jclepro.2009.11.004

Iriarte A, Rieradevall J, Gabarrell X (2012) Transition towards a more environmentally sustainable biodiesel in South America: The case of Chile Applied Energy 91:263-273 doi:http://dx.doi.org/10.1016/j.apenergy.2011.09.024

Iriarte A, Villalobos P (2013) Greenhouse gas emissions and energy balance of sunflower biodiesel: Identification of its key factors in the supply chain Resources, Conservation and Recycling 73:46-52 doi:http://dx.doi.org/10.1016/j.resconrec.2013.01.014

ISO 14040 (1997) Environmental Management - Life Cycle Assessment - Principles and Framework

ISO 14040 (2006) Environmental Management - Life Cycle Assessment - Principles and Framework

ISO 14041 (1998) Environmental Management - Life Cycle Assessment - Life Cycle Interpretation

ISO 14042 (1998) Life Cycle Assessment - Impact Assessment

ISO 14043 (1998) Environmental Management - Life Cycle Assessment - Life Cycle Interpretation

ISO 14044 (2006) Environmental Management - Life Cycle Assessment - Requirements and Guidelines

Kim S, Dale B, E (2009) Regional variations in greenhouse gas emissions of biobased products in the United States - corn-based ethanol and soybean oil The

International Journal of Life Cycle Assessment 14:540-546 doi:10.1007/s11367-009-0106-4

Kim S, Dale BE (2005) Environmental aspects of ethanol derived from no-tilled corn grain: nonrenewable energy consumption and greenhouse gas emissions Biomass and Bioenergy 28:475-489 doi:http://dx.doi.org/10.1016/j.biombioe.2004.11.005

Koch S (2003) LCA of biodiesel in Costa Rica: An environmental study on the manufacturing and use of palm oil methyl ester. San Jose

Krohn B, J.,, Fripp M (2012) A life cycle assessment of biodiesel derived from the "niche filling" energy crop camelina in the USA Applied Energy 92:92-98 doi:http://dx.doi.org/10.1016/j.apenergy.2011.10.025

Larson ED (2006) A review of life-cycle analysis studies on liquid biofuel systems for the transport sector Energy for Sustainable Development 10:109-126

Liska A, J.,, Yang H, S.,, Bremer V, R.,, Klopfenstein T, J.,, Walters D, T.,, Erickson G, E.,, Cassman K, G., (2009) Improvements in life cycle energy efficiency and greenhouse gas emissions of corn-ethanol Journal of Industrial Ecology 13:58-74 doi:10.1111/j.1530-9290.2008.00105.x

Luo L, van der Voet E, Huppes G, Udo de Haes H, A., (2009) Allocation issues in LCA methodology: a case study of corn stover-based fuel ethanol The International Journal of Life Cycle Assessment 14:529-539 doi:10.1007/s11367-009-0112-6

Mishra G, S.,, Yeh S (2011) Life cycle water consumption and withdrawal requirements of ethanol from corn grain and residues Environmental science & technology 45:4563-4569 doi:10.1021/es104145m; 10.1021/es104145m

Moser C, Hildebrandt T, Bailis R (2014) International Sustainability Standards and Certification. Sustainable development of biofuels in Latin America and the Caribbean. Springer. New York

Muench S, Guenther E (2013) A systematic review of bioenergy life cycle assessments Applied Energy 112:257-273

Neupane B, Halog A, Dhungel S (2011) Attributional life cycle assessment of woodchips for bioethanol production Journal of Cleaner Production 19:733-741 doi:http://dx.doi.org/10.1016/j.jclepro.2010.12.002

NREL (2014) U.S. Life Cycle Inventory Database, National Renewable Energy Laboratory

OECD (2014) Chapter 2 Biofuels. doi:http://dx.doi.org/10.1787/888932861168

Ometto AR, Hauschild MZ, Nelson Lopes RW (2009) Lifecycle assessment of fuel ethanol from sugarcane in Brazil The International Journal of Life Cycle Assessment 14:236-247 doi:10.1007/s11367-009-0065-9

Pradhan A, Shrestha DS, McAloon A, Yee W, Hass M, Duffield JA (2011) Energy life-cycle assessment of soybean biodiesel revisited American Society of Agricultural and Biological Engineers 5:1031-1039

PRé Consultants (2011) SimaPro 7.2. http://www.earthshift.com/software/simapro.

RED (2009) Directive 2009/28/EC of the European Parliament and of the Council of 23 April 2009 on the promotion of the use of energy from renewable sources and amending and subsequently repealing Directives 2001/77/EC and 2003/30/EC vol 2013.

RED (2012) Directive of the European Parliament and the Council amending Directive 98/70/EC relating to the quality of petrol and diesel fuels and amending Directive 2009/28/EC on the promotion of the use of energy from renewable sources.

RSB (2011) Indicadores de cumplimiento de los principios y criterios de la RSB vol 2013.

SAIC (2006) Life Cycle Assessment: Principles and Practice, report to U.S. Environmental Protection Agency.

Searchinger Tand others (2008) Use of US croplands for biofuels increases greenhouse gases through emissions from land-use change Science 319:1238-1240

SETAC (1991) A Technical Framework for Life Cycle Assessment.

SETAC (1993) Guidelines for Life Cycle Assessment: A 'Code of Practice. In: Consoli F, Allen, D., Boustead, I., Fava, J., Franklin, W., Jensen, A.A., Oude, N., Parrish, R., Perriman, R., Postlethwaite, D., Quay, B., Seguin, J., and Vigon, B. (ed)

Shonnard DR, Campbell MB, Martin-Garcia AR, Kalnes TK (2012) Chemical Engineering of Bioenergy Plants: Concepts and Strategies. Vol. 1 Handbook of Bioenergy Crop Plants. CRC Press-Taylor, Boca Raton, FL

Skone, Gerdes (2008) Development of Baseline Data and Analysis of Life Cycle Greenhouse Gas Emissions of Petroleum-Based Fuels. November 26, 2008

Solomon BD, Bailis R (2014) Introduction. Springer, New York

Souza S, Pereira, de Avila M, Turra,, Pacca S (2012) Life cycle assessment of sugarcane ethanol and palm oil biodiesel joint production Biomass and Bioenergy 44:70-79 doi:http://dx.doi.org/10.1016/j.biombioe.2012.04.018

Thomas PG, Lippiatt BC, Cooper J (2007) Life Cycle Impact Assessment Weights to Support Environmentally Preferable Purchasing in the United States Environmental science & technology 41:7551-7557 doi:10.1021/es070750+

van Dam J, Junginger M, Faaij APC (2010) From the global efforts on certification of bioenergy towards an integrated approach based on sustainable land use planning Renewable and Sustainable Energy Reviews 14:2445-2472 doi:http://dx.doi.org/10.1016/j.rser.2010.07.010

Velásquez HI, Ruiz AA, de Oliveira S (2010) Análisis energético y exergético del proceso de obtención de etanol a partir de la fruta del banano Revista Facultad de Ingenieria Universidad de Antioquia 51:87-96

Wang M, Han J, Dunn JB, Cai H, Elgowainy A (2012) Well-to-wheels energy use and greenhouse gas emissions of ethanol from corn, sugarcane and cellulosic biomass for US use Environmental Research Letters 7:045905

Wang M, Han J, Haq Z, Tyner W, E.,, Wu M, Elgowainy A (2011a) Energy and greenhouse gas emission effects of corn and cellulosic ethanol with technology improvements and land use changes Biomass and Bioenergy 35:1885-1896 doi:http://dx.doi.org/10.1016/j.biombioe.2011.01.028

Wang M, Huo H, Arora S (2011b) Methods of dealing with co-products of biofuels in life-cycle analysis and consequent results within the U.S. context Energy Policy 39:5726-5736

Wang M, Wu M, Huo H (2007) Life-cycle energy and greenhouse gas emission impacts of different corn ethanol plant types Environmental Research Letters 2:024001

Yang J, Xu M, Zhang X, Hu Q, Sommerfeld M, Chen Y (2011) Life-cycle analysis on biodiesel production from microalgae: Water footprint and nutrients balance Special Issue: Biofuels - II: Algal Biofuels and Microbial Fuel Cells 102:159-165 doi:http://dx.doi.org/10.1016/j.biortech.2010.07.017

Yang Y, Bae J, Kim J, Suh S (2012) Replacing gasoline with corn ethanol results in significant environmental problem-shifting Environmental science & technology 46:3671-3678 doi:10.1021/es203641p; 10.1021/es203641p

Zaimes GG, Khanna V (2013) Microalgal biomass production pathways: evaluation of life cycle environmental impacts Biotechnology for biofuels 6:88-6834-6836-6888 doi:10.1186/1754-6834-6-88; 10.1186/1754-6834-6-88

3. Characterization of Products from Fast Micro-Pyrolysis of Municipal Solid Waste (MSW) Biomass

3.1 Abstract

Biomass feedstock costs remain one of the largest impediments to biofuel production economics. Municipal solid waste (MSW) represents an attractive feedstock with year-round availability, an established collection infrastructure paid for by waste generators, low cost and the potential to be blended with higher cost feedstocks to reduce overall feedstock costs. Paper waste, yard waste and construction and demolition waste (C&D) were examined for their applicability in the pyrolysis conversion pathway. Paper waste consisted of non-recyclable paper such as mixed low grade paper, food and beverage packaging, kitchen paper wastes and coated paper; yard waste consisted of grass clippings and C&D wastes consisted of engineered wood products obtained from a construction waste landfill. The waste materials were tested for thermochemical conversion potential using a bench scale fast micro-pyrolysis process. Bio-oil yields were the highest for the C&D materials and lowest for the paper waste. The C&D wastes had

[2] The material in this chapter was previously published in *ACS Sustainable Chemistry & Engineering*

the highest level of lignin derived compounds (phenolic and cyclics) while the paper waste had higher levels of carbohydrate derived compounds (aldehydes, organic acids, ketones, alcohols and sugars). However, the paper material had higher amounts of lignin derived compounds than expected based upon lignin content that is likely due to the presence of polyphenolic resins used in paper processing. The paper and yard wastes had significantly higher levels of ash content than the C&D wastes (14-15% versus 0.5-1.3%), which further correlated to higher levels of alkali and alkaline earth metals, which are known to reduce the amount of pyrolysis bio-oil produced. The effect of acid washing was evaluated for grass clipping and waste paper and the amount of bio-oil produced was increased from 58% to 73% and 67% to 73%, respectively.

3.2 Introduction

MSW is attractive as a biofuel feedstock because it is available year-round, it already has an established infrastructure for collection and handling, and it has the potential to be low cost. MSW currently is a negative cost feedstock because municipalities paid an average of $49.27/ton in 2012 for landfilling, with a range from $18.43 in Idaho to $105.40 in Massachusetts[1]. While it is unlikely that these negative costs of MSW will be available for biorefineries due to the preprocessing required—to separate out the fractions of interest, upgrade the quality and alter particle size—it will likely be available at lower cost than other herbaceous feedstocks. Beyond the potential cost benefits, use of organic components in MSW for biofuels has the potential to reduce greenhouse gas emissions, as landfills are the third largest anthropogenic source of methane from the decomposition of organics in MSW[2]. An average composition of MSW generated in the United States is

provided in Table 3.1[3], showing that many components in MSW are organic and may be suitable feedstocks for bio-based fuels and chemicals (e.g. paper and paperboard, wood, yard trimmings, and some plastics).

Table 3.1. National average municipal solid waste composition [3] .

Material	% Total MSW before recycling (251 mil tons)	% Total MSW after recycling (164 mil tons)
Paper and paperboard	27.4%	14.8%
Glass	4.6%	5.1%
Steel	6.7%	6.8%
Aluminum	1.4%	1.6%
Other nonferrous metals	0.8%	0.4%
Plastics	12.6%	17.6%
Rubber and leather	3.0%	3.8%
Textiles	5.6%	7.2%
Wood	6.3%	8.2%
Other materials	2.0%	2.3%
Food	14.52%	21.1%
Yard trimmings	13.5%	8.8%
Misc. inorganic waste	1.6%	2.4%

Of these, paper and paperboard are likely to have more value when recycled than as a feedstock for fuels. However, there is still a significant fraction of paper and paperboard that is non-recyclable, including coated paper and cardboard, polycoat material, glossy papers in magazines, food-contaminated papers and cardboards, and any material with binders such as phone books. Yard waste is often collected separately from other MSW in many municipalities making it an attractive option. Construction and demolition (C&D) waste is also a potential feedstock. This stream consists of waste materials

generated during construction, renovation, and demolition from both residential and nonresidential sources. In a 2009 report [4], the Environmental Protection Agency (EPA) estimated that approximately 170 million tons of C&D waste was generated in 2003 in the United States, going to an EPA-estimated 1,900 C&D landfills, although more recently many localities are setting recycling targets for C&D projects [5]. The composition of this waste stream is primarily wood, drywall, metal, plastics, roofing, masonry, glass, cardboard, concrete, and asphalt debris. The relative amounts of these materials vary greatly depending on the relative percentages of new construction versus renovation and demolition, as well as the type and size of structures being built, renovated, or demolished. The only fraction relevant to a biorefinery would be the woody material that consists of both untreated and treated (e.g., painted, stained, or varnished) materials. In this report, only untreated woody materials were utilized, because it is unknown whether the treated material would affect downstream processing of these materials. C&D waste is generally handled separately from residential waste, although a separation step may also be necessary to remove non-organic materials.

MSW biomass can be considered a renewable resource which can be converted to valuable products through fast pyrolysis processing [6]. Fast pyrolysis is a thermal degradation process for converting biomass to a liquid fuel. This process occurs at temperatures of 450-700°C in the absence of oxygen and in a reaction environment that assures rapid heat transfer. The products of biomass fast pyrolysis are generally composed of 30-70 wt% liquid bio-oil, 20-30 wt% solid char, and 20-30 wt% gas, and the chemical speciation within the oil product varies, depending on MSW type and process operating conditions.

MSW biomass with high lignin are expected to have higher concentrations of phenolic compounds in bio-oil[7, 8]; higher cellulose should produce more anhydrosugars such as levoglucosan[7, 9] ; and higher hemicellulose should produce more furan and lighter, highly oxygenated compounds such as organic acids[10]. Ash and mineral content will also affect product distribution. MSW biomass potentially contains high amounts of alkaline metals, which can cause secondary cracking reactions, resulting in more gaseous products and smaller organic molecules within the pyrolysis oils[11]. In addition, MSW biomass can have a significant portion of non-biomass components such as adhesives and resins in manufactured wood products, resulting in unique chemical species.

This research employed micro-pyrolysis coupled with gas chromatography and mass spectroscopy (GC/MS) to rapidly evaluate small samples of MSW biomass for their suitability as biofuel feedstocks. This work aims to identify and compare fast pyrolysis product distributions for bio-oil, gaseous species, and solid char for several MSW types. MSW biomass samples are compared to traditional feedstocks such as switchgrass and corn stover based on their pyrolysis product distribution. The effect of ash content and abundance of alkaline earth metals (calcium) on product distribution and the amount of bio-oil produced was evaluated. We also evaluated the effects on pyrolysis bio-oil composition of dilute acid washing to remove ash components on high-ash MSW samples, as other recent works have indicated a strong connection between oil production/quality and mineral content [12-15] .

3.3 Materials and Methods

3.3.1 Samples and Feedstock Characterization

The construction and demolition (C & D) waste materials were collected from a C & D landfill and included plywood, fiberboard, Microllam and wafer board, and were subsequently ground to 1.25 inches (3.2 cm) (Vermeer HG 200). Corn stover was harvested single-pass as bales which were ground with a Vermeer BG480 grinder (Pella, Iowa) fitted with a 6-inch screen (15.2 cm) and dried to approximately 8.3% moisture. Alamo switchgrass bales were size reduced to 2 inches (5.1 cm) and later ground through a Bliss Hammermill (Eliminator E4424; Ponca City, OK) fitted with a 1-inch (2.5 cm) screen and were dried to approximately 10% moisture. Kentucky bluegrass clippings were collected and dried from approximately 60% to 10% moisture. The non- recyclable fraction of municipal solid waste paper was collected by Cascadia Consulting (Seattle, WA) during a waste characterization study being conducted for the city of Seattle. This material consisted of mixed/low grade paper including magazines, colored paper, junk mail and bound paperback books; aseptic and polycoats such as paper packaging materials that include plastic or metal layers and any type of food-soiled paper. These materials were shredded using a commercial HSM Securio P36 shredder (Frickingen, Germany). Hybrid poplar was obtained directly from Michigan Tech's School of Forest Resources to provide a traditional feedstock to compare the woody MSW pyrolysis product distribution and its bio-oil speciation to. The hybrid poplar was ground and sized to approximately 200 microns. All materials, except hybrid poplar, were then characterized by Huffman Laboratories Inc. (Golden, CO) to determine fuel characteristics (proximate, ultimate, and calorimetric analysis). Hybrid poplar proximate

and ultimate analysis data was obtained from the bioenergy feedstock library from Idaho National Laboratory[16]. Metal content data for hybrid poplar was taken from literature data[17-19] and is shown in Table 3.3. The proximate and ultimate analysis and metals content for different types of samples are present in Table 3.2 and Table 3.3. The woody biomass samples all have similar amounts of carbon (49%-51%), hydrogen (~6%), have lower ash contents than other MSW samples, but vary significantly on the amounts of nitrogen, which is likely due to binders used in the manufacture of the wood products. Comparing grass clippings to corn stover and switchgrass the HHV and LHV are nearly identical (~18 MJ/kg and ~15 MJ/kg respectively). Comparing the ash content, grass clippings and waste paper contain a factor of 3-4 times higher ash content, compared to corn stover and switchgrass. Grass clippings has the lowest volatile content, however waste paper has similar volatile content as the switchgrass and corn stover. Waste paper has the lowest amount of carbon and fixed carbon, due to the removal of lignin during the Kraft process.

The amount of bio-oil produced will also be compared to ash content to observe how higher ash contents of certain biomass, such as grass and waste paper, affect conversion. The metal content shown in Table 3.3 will allow for a comparison of chemical speciation and mineral content; and to determine if mineral content correlates with bio-oil composition. For example, it has been shown that higher levels of calcium promote the production of smaller organic fractions through a type of cracking mechanism over the calcium [20].

Table 3.2: Proximate and ultimate analysis of different types of MSW biomass samples

Sample	%						HHV	LHV
	C	H	N	Fixed C	Volatile	Ash	(MJ/kg)	(MJ/kg)
Fiberboard	49.08	6.13	3.84	17.06	82.49	0.45	20.48	17.20
Gr. Clippings	43.88	5.67	3.70	12.08	73.53	14.39	18.34	15.34
Microllam	50.91	6.01	BDL[a]	19.49	79.16	1.34	20.72	17.44
Waste Paper	38.88	5.18	BDL[a]	5.14	79.03	15.83	16.47	13.77
Plywood	50.87	6.14	0.06	15.31	84.19	0.50	20.78	17.44
Waferboard	49.72	6.00	0.13	13.85	84.94	1.21	20.52	17.33
Corn Stover	48.70	5.70	0.70	16.70	79.00	4.27	18.58	15.38
Hybrid Poplar[16]	48.9-51.1	5.9-6.1	0.18-0.42	14.5-14.7	82.3-85.3	0.8-1.8	8441-8781	7048-7382
Switchgrass	47.20	5.70	0.50	15.60	80.20	4.20	18.79	15.70

[a]BDL=below detectable limit

Table 3.3: Metals content in different types of MSW biomass samples, parenthesis indicate standard deviation in the literature data

Sample	ppm										
	Al	Ca	Fe	K	Mg	Mn	Na	P	Si	Ti	S
Fiberboard	49.12	1208	68.62	453.3	165.5	67.75	373.7	39.20	265.7	2.995	71.24
Gr. Clippings	2497	9716	1324	17915	2914	66.64	457.5	3504	36207	137.5	1855
Microllam	60.33	1444	47.77	524.4	91.08	27.40	3845	87.66	393.9	4.455	71.78
Waste Paper	18234	48943	892.3	496.8	835.8	73.19	1367	54.99	17970	1397	1104
Plywood	78.14	497.4	98.72	259.7	70.65	16.13	1207	51.88	578.4	4.420	62.40
Waferboard	54.81	2866	89.32	1434	342.8	9.168	1036	106.2	274.0	6.605	117.3
Corn Stover	62.99	2731	332.9	9307	1561	29.62	25.22	517.5	10328	2.548	374.5
Hybrid Poplar[17-19]	120.0	5832 (1510)	264.4	1848 (548)	417.9 (300)	--	128.1 (44.7)	563.8 (161)	744.7	48.55	220.6
Switchgrass	54.52	2170	469.7	6002	2432	60.63	492.1	800.1	10308	2.470	450.5

3.3.2 Fast micro-pyrolysis experiments

Fast pyrolysis of MSW samples occurred in a micro-pyrolysis reactor (CDS analytical model 5200HP pyroprobe), as shown in Figure 3.1 and the results were analyzed using GC/MS. For all experiments, approximately 0.2 mg of each MSW sample were placed in the middle of a quartz pyrolysis tube under a helium (99.999% purity) atmosphere (Figure 3.1). Prior to each experiment, the vials were de-volatilized at 600ºC for 10 min. within the pyroprobe to ensure that all recorded compounds were from the MSW samples. This was verified by real-time measurement of only instrument background signal by the GC/MS. Initial MSW and final char weights were measured using a microbalance (Orion Cahn microbalances, Model C-35 by Thermo) with a resolution of 1 µg. To ensure the water characterized in the chromatogram was produced entirely from pyrolysis, the sample was dried for 10 minutes at 120ºC in the pyroprobe. To verify that there was no thermochemical conversion occurring at 120ºC the samples were weighed before and after drying. The mass loss was negligible indicating that the biomass had not accumulated any water since it was obtained and processed. It was then heated to 500 °C with a heating rate of 1,000°C/s, and held for 20 seconds. The volatile products were transported to a gas chromatograph (GC, model K8880181 by ThermoFisher) and mass spectrometer (MS, model DSQII by Thermo Scientific) through a heated transfer line (>300°C) with a helium carrier gas (~20 mL/min). The GC injection port, at 275°C, was directly fed from the pyrolyzer transfer line, and was operated in split-mode to ensure a constant 1mL/min flow rate. The GC was furnished with a Restek RXI-5MS 30m fused silica column (low polarity phase, crossbond 5% diphenyl/95% dimethyl polysiloxane, 30m x 0.25 mm, 0.25 µm film thickness) for product separation. After initiation of pyrolysis, the GC oven temperature was initially held at 35

°C for 3 minutes, then increased at 15 °C/min to 210 °C, followed by an increase at 12 °C/min to 275 °C for 5 min. The mass spectrometer was set-up to capture ion fragments 15-400 m/z at a detector ionizing voltage of 70 eV, with the ion source temperature set to 275 °C. These experiments were conducted in triplicate. This experimental set-up was operated at the maximum temperatures for the transfer line, GC inlet and column oven temperatures. However due to temperature limitations larger dimer and trimer units may be condensing within the transfer line. The experimental set-up was optimized to look at the majority of components within the bio-oil, which include lower molecular weight species, anhydrosugars and phenolic monomers[21].

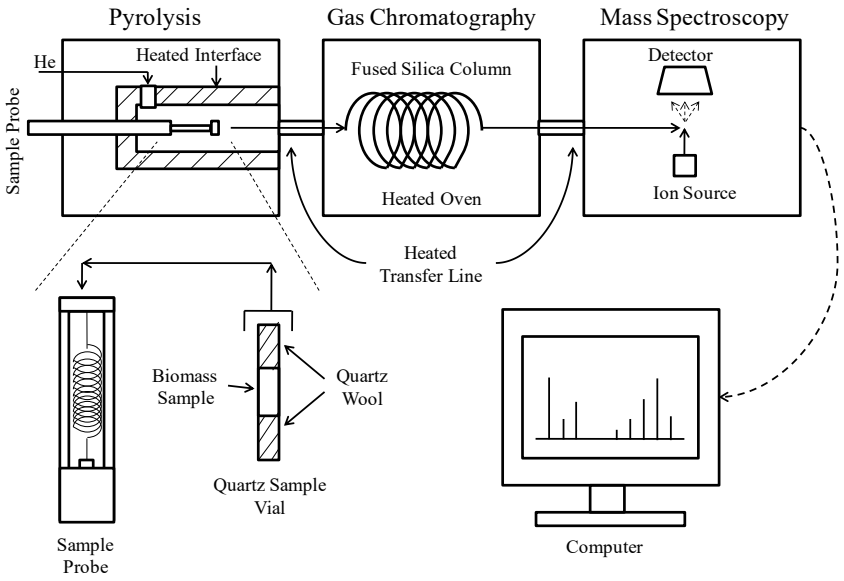

Figure 3.1: Experimental diagram for fast pyrolysis of MSW samples in a micro-pyrolysis reactor[22]

3.3.3 Peak identification and characterization of micro-pyrolysis products

The solid char mass was determined gravimetrically by difference between initial MSW weight and final char weight. The product distribution of gas and bio-oil obtained from

fast pyrolysis of MSW samples was analyzed using GC-MS. It is important to note that there are limitations to using GC/MS for the analysis of bio-oil; primarily some compounds are not able to be volatilized within this system, such as large tars and it is difficult to distinguish between molecular isomers, etc.[23]. Some compounds condense at temperatures higher than 400 °C and may not even be making it to the GC. In this work, approximately 30-60% by mass of the bio-oil species were identified and quantified with the use of chemical standards. It is on this basis that comparisons between feedstock species are made and not necessarily on a complete analysis of all bio-oil species. The samples' sizes and particles were small (< 1 mm in dimension) to avoid significant heat/mass transport limitations and yield repeatable results.

To characterize the pyrolysis products, the char yield, and relative abundance of bio-oil and gas were determined. Char yield was calculated based on the initial and final mass of the biomass and char, respectively. A number of organic species found within the pyrolysis oils were quantified with chemical standards (discussed further below). Only individual peaks that contributed 1% or greater to total peak area were considered significant to the overall product quantification and resulted in a range of 66-78% peak area closure. For peaks having standards, bio-oil mass yields were calculated using response factors from the calibration curves. To account for water, gas and the unknown compounds, the char mass and bio-oil mass (from identified compounds) were subtracted from the original sample mass. It is difficult to characterize and account for the hundreds of compounds that are produced during pyrolysis. The gas and water compounds as well as bio-oil compounds with no standards were unable to be characterized on a mass basis. For this study, the water, gas and unknown compounds were weighted equally based on

peak area, and used for comparative purposes between feedstock. These peak areas, after the characterized bio-oil mass was subtracted, were used to determine a relative abundance between MSW samples and traditional biomass samples. The relative abundance of water was based on 18 m/z, the CO_2 on 44 m/z, and the CO on 28 m/z within the early retention large gas peak. The unknown compounds included those that fell within the >1% peak area and were not able to be identified as described above, and those that were not included in the analysis due to having peak areas below 1%. There are limitations to this method in not being able to complete a full mass balance, but it allows for direct comparisons of the MSW samples and traditional biomass samples that were evaluated as a pyrolysis feedstock in this study. It is important to note the distinction between compounds that are quantified within all bio-oil samples, and those left on a relative basis (peak area), and compared between sample without a complete quantification. Specific compounds and quantification strategies are described further below.

The areas of chromatographic peaks of three trials were normalized by their initial sample masses to place them on a comparable basis. These normalized peak areas were used with chemical standards to quantify mass of each compound and to calculate the relative abundance of gas, bio-oil, and product distribution. If peak area closure of 65% could not be achieved using a 1% cut off, 0.5% was used to determine the peaks for analysis; grass clippings and fiber board were the only species that resulted in using a 0.5% peak area cutoff. Peak area closure refers to the sum of characterized peaks compared to the total sum of all peaks detected. Peaks that contributed less than 1% of

the total peak area were difficult to identify and distinguish above the chromatogram baseline, and were considered as insignificant for the methods used in this study.

Based on the ion spectra from the MS detector, peaks were identified and assigned to one parent fraction in the biomass: (1) carbohydrate, (2) lignin, (3) resin, or (4) unknown. When positive peak matches were made in accordance with spectra established and published by NIST, they were assigned to areas (1-3) respectively based on their structure and functional groups. For example, sugar, anhydrosugars, aldehydes, organic acids, ketones and alcohols are typically formed from the carbohydrate fractions, while cyclic, phenolic, and larger molecular weight compounds generally originate from the lignin fraction. If a peak identification contained non-biomass matter in its structure (eg. nitrogenous compounds), these compounds were assumed to be generated from the urea-formaldehyde based adhesives or laminates in certain MSW samples. Primary gases and reaction-formed water were categorized as originating from the carbohydrate fraction [24, 25] as they are formed in smaller quantities from lignin. These major categories were then divided into smaller subcategories. Within the carbohydrate fraction there are 1) light weight organics, which is a group comprised of small alcohols, carboxylic acids, ketones, etc., 2) small sugars, which is comprised of furan compounds, and 3) large (6+ carbon) sugars such as anhydrosugars like levoglucosan. The lignin fraction was divided between smaller lignin compounds, consisting of single phenolic rings and large lignin compounds, commonly referred to as tars. Some peaks were not identified using the NIST webbook, but were associated into groups based on the unique mass charge fragments that exist for the several types of compounds. 73, 60 and 57 m/z are representative of anhydrosugars (similar to levoglucosan), and therefore any peak

prevalently containing these three characteristic m/z charges was identified as a sugar. If a peak only prevalently contained a 57 m/z peak at early retention times (5-10 minutes), it was labeled as a light sugar fraction. If a peak was within the 8-20 minute range and contained 124, 157,167, and/or 168 m/z fragments, it was labeled as a lignin species. Large peaks that occurred after 20 minutes and did not contain 73, 60 or 57 m/z fragments were labeled as tars (large lignin fractions) and were not able to be identified. Any remaining peaks were allotted to the unidentified (unknown) category and were not quantifiable with standards.

3.3.4 Standards

Several (18) species that have been identified in bio-oil [21, 26], were used as standards for quantifying the pyrolysis bio-oil in this research. These compounds were separated into groups of mixtures based on their retention index and solubility in acetonitrile and DMSO. Therefore, compounds soluble in the same solvent but possessing distinctly dissimilar retention indices (to prevent co-elution of peaks) were grouped together.

The first two standard solutions used acetonitrile as a solvent and contained between 7-9 compounds within that solution. The last two solutions used DMSO as a solvent and contained only one sugar species. This prevented co-elution of sugars and generated the best quality calibration curve. To generate the stock solution, 2 mL of each liquid phase and 1 gram of each solid phase standard compound was used. Solvent was then added to achieve the high end of the calibration mass as shown in Table 3.4. The samples were diluted and then injected in triplicates via an autosampler (Thermofisher AI 1310**).** Eight different dilution ratios of 1:1; 2:1; 5:1; 10:1; 25:1; 50:1; 75:1; 100:1 (low end of

calibration mass shown in Table 3.4) were used to generate a range of masses for calibration. The compounds within the mixture were identified based on their NIST retention index and mass charge spectra. The peak areas were determined via ICIS integration within the Xcalibur software. The mass of each compound injected was then plotted with respect to peak area to determine a response factor.

Table 3.4: Analytical Standards used to interpret GC/MS results of pyrolysis oil

	Standards	**Solvent**	**Calibration Mass Range (µg)**	**Retention Index[27]**	**r^2**
Standard Solution 1	acetic acid	acetonitrile	17.23-0.34	600-650	0.99
	pyridine	acetonitrile	16.08-0.32	730-772	0.99
	furfural	acetonitrile	18.92-0.38	815-830	0.99
	anisole	acetonitrile	16.23-0.32	~918	0.99
	m-cresol	acetonitrile	16.52-0.33	1070-1100	0.98
	methyl syringol	acetonitrile	8.87-0.18	1308-1317	0.90
	syringaldehyde	acetonitrile	8.87-0.18	1643-1670	0.99
Standard Solution 2	acetol	acetonitrile	16.87-0.33	522-526	0.87
	2-butanone	acetonitrile	13.93-0.28	550-622	0.98
	3-pentanone	acetonitrile	13.97-0.28	688-695	0.99
	toluene	acetonitrile	15.00-0.30	750-790	0.98
	furfuryl alcohol	acetonitrile	19.26-0.38	813-865	0.99
	phenol	acetonitrile	8.24-0.16	980-1000	0.99
	2-methoxyphenol	acetonitrile	9.03-0.18	1070-1095	0.99
	3-methoxycatechol	acetonitrile	9.12-0.18	~1272	0.99
	eugenol	acetonitrile	18.34-0.36	1348-1370	0.99
Solution 3	levoglucosan	DMSO	5.40-0.98	~1491	0.75
Solution 4	d-xylose	DMSO	40.29-7	--	0.98

3.3.5 Acid Washing

To understand the effects that high ash content and alkali and alkaline earth metals have on fast pyrolysis product distribution, the high ash samples (grass clippings and waste paper) were washed with acid solution in order to decrease metal content[28]. Twenty ml of 0.1 M H_2SO_4 was used to wash 1g of sample with stirring at room temperature for 4 hours. Afterwards, the mixture was filtered, washed with distilled water to neutrality and dried at 105°C for 24 hours.

3.4 Results and Discussion

3.4.1 Pyrolysis products

Pyrolysis product distributions were calculated by measuring the char yield gravimetrically and then subtracting that from initial sample mass to obtain the amount of volatiles (bio-oil+gas+water) produced. To quantify the bio-oil, the identified peaks with their respective peak areas were correlated to a mass basis from the response factors determined with the standards. The poplar samples were run at a later time and therefore the standards response factor was adjusted to the sensitivity of the instrument, using the mass spectrometers internal calibration compound. It was observed from the standards that compounds within the same chemical class and with similar chemical structure had similar response factors. Therefore, if an organic acid peak was identified, an average organic acid response factor could be used to determine the mass created from fast pyrolysis. This also applied to phenolic and sugar species. The bio-oil mass was determined for each trial using the response factors. Finally, the bio-oil and char mass were subtracted from the original biomass to give the relative abundance of the remaining

substances; water, gas and unidentified bio-oil (those above and below the 1% peak area percent cutoff). For the species that were not identified, peak area percent was used to calculate the relative abundance of that species. Although this method is a partial mass balance (char plus bio-oil peaks with standards), relative abundance of the remaining peaks allows a comparison between one MSW sample to another and also to the conventional feedstocks.

The first peak in the chromatogram is a mixture of non-condensable gases (CO, CO_2 – no H_2 or CH_4 were detected in any samples) and water, as shown in Figure 3.2. Therefore, the relative abundance of combined gas + water was calculated using the peak area percent of this first (gas+water) peak compared to the total area of the uncharacterized peaks. To distinguish between water and gases, the 18 m/z peak area was calculated as a percentage of the total gas+water peak area. Among all species over this initial retention time, 18 m/z uniquely belongs to water, which in turn almost entirely produces an ion form of the parent molecule (18-) in the mass spectrometer (with very small contribution from formation/detection of a hydroxyl group, 17-). The relative abundance of gas was calculated by difference of the relative abundance of water from the relative abundance of gas + water . The relative abundance of unidentified bio-oil mass was then calculated by difference from the previously determined relative abundance of gas and water, the characterized bio-oil and the char yield. There are limitations to this method in not being able to complete a full mass balance, but it allows for the direct comparison of the MSW samples to each other and to traditional biomass sample that were pyrolyzed in this study.

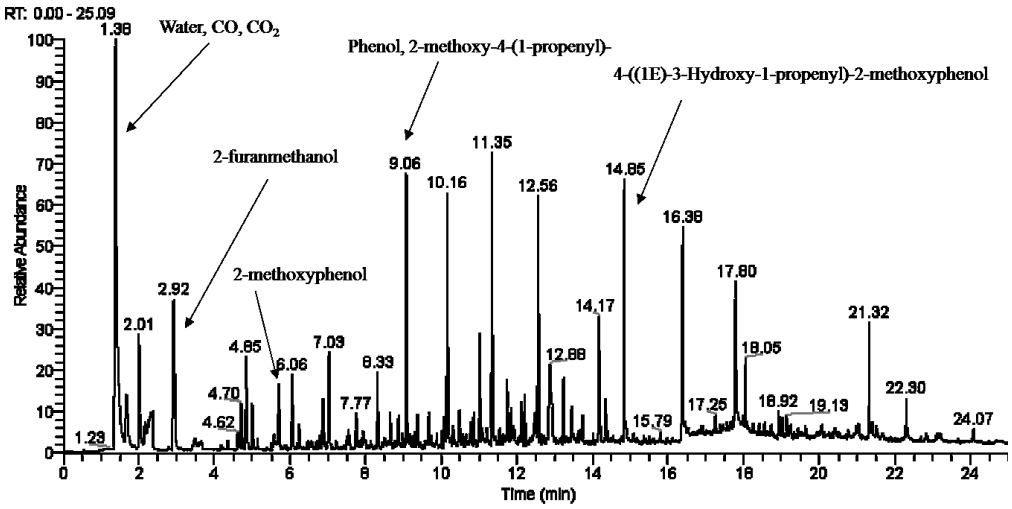

Figure 3.2: Example of a chromatogram from pyrolysis of Microllam MSW

Figure 3.3 shows the pyrolysis bio-oil product distribution of the 6 MSW samples with a comparison to traditional feedstocks. Bio-oil yields are between 60.5-77.2% for all samples, relative abundance of gas plus water between 1.5-8.2%, and char yields between 17-31%. Waferboard and plywood show the highest amount of bio-oil produced as compared to waste paper, corn stover, and grass clippings, which have the lowest amounts of bio-oil produced. The high amounts of bio-oil for waferboard and plywood are likely due to the higher amounts of lignin, the lack of coatings, and mineral content. The waste paper appeared to be heavily coated, which likely contributed to the high char yield (presumably with ash in the char) and the lower production of bio-oil. Comparing these values to the hybrid poplar and literature[29, 30] , it is observed that the waste construction materials (fiberboard, waferboard, Microllam) have similar product distributions (relatively high oil and low gas), whereas the grass clippings sample is similar to that of corn stover (lower oil and higher gas). The error bars represent the

standard deviation of triplicate trials. The bars are the average values of the triplicate runs.

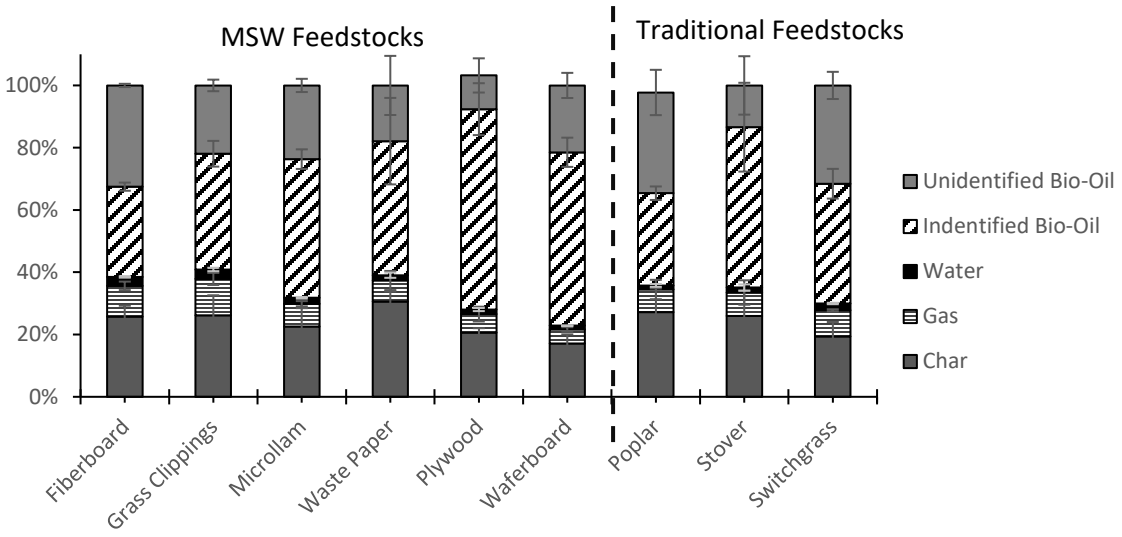

Figure 3.3: Product distribution of char yield, identified bio-oil yield, relative abundance of gas, water and unidentified bio-oil, from MSW and traditional biomass feedstocks. Error bars are standard deviation from triplicate experiments.

3.4.2 Effect of MSW type on bio-oil composition

Figure 3.4 shows the sum of bio-oil compounds derived from carbohydrate, lignin, resin, and unspecified fractions generated from fast pyrolysis. This figure shows the amount of bio-oil produced for each MSW sample along with the breakdown of different bio-oil fractions. Note that the error bars represent the standard deviation between the triplicate experiments. The waste paper, in principle, contains mostly cellulose and hemicellulose, with very little lignin. This supports why carbohydrate derived compounds were observed in the highest relative abundance within waste paper, and between all samples. There is likely small amounts of lignin remaining from the Kraft process, in addition to poly-phenolic resins that generate the observed 'lignin derived' compounds. Styrene compounds

were found in bio-oil from waste paper. This resin is likely from styrene butadiene for binding pigmented coatings[31]. In the fiberboard samples, some nitrogen-containing organic compounds were detected with small peak areas, suggesting resin of the urea-formaldehyde type. Fiberboard, Microllam, plywood, and waferboard showed the highest amount of lignin derived compounds among the MSW types. This is likely due to their similarity to woody biomass sources, as compared to the hybrid poplar results shown. Fiberboard and Microllam likely have a similar product distribution to the plywood, but due to smaller lignin peaks being below the 0.5-1% peak area cut off, they are not specified. In comparison to agricultural residues (stover), herbaceous crops (clippings, switchgrass), and certainly the waste paper just discussed, woody MSW types have a much greater lignin content. The product distribution of the MSW reasonably compares to literature results (bio-oil yields of 60-90%) for micro-pyrolysis[20]. Not surprisingly, the sample with presumably the highest carbohydrate fractions (those most closely resembling woody biomass like plywood and waferboard), exhibit the highest amount of bio-oil produced. The detailed compositions of compounds and mass percents for MSW samples are located in the bio-oil composition section of Appendix B in Tables B.1-B.11.

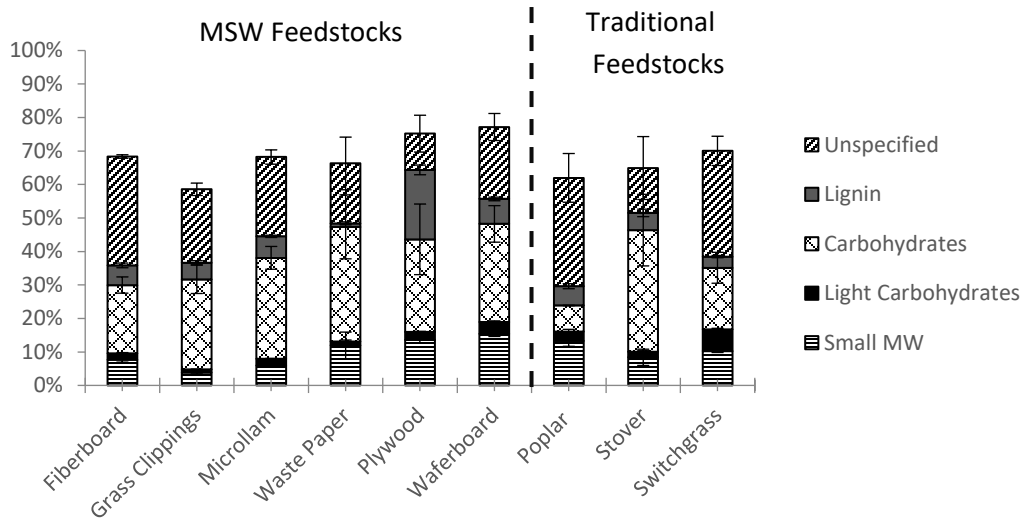

Figure 3.4: Compounds derived from the pyrolysis of different types of MSW and traditional biomass feedstocks

3.4.3 Effect of mineral content

High alkali and alkaline earth metals in MSW biomass are expected to cause cracking reactions which would generate less bio-oil and increase the amount of gas generated during pyrolysis[11, 20, 28]. As mentioned previously, the calcium present in the waste paper biomass is likely due to the coatings adhered to the biomass in oxidized form such as CaO, unlike the calcium ion present in the other MSW biomass which is present in its cation structure and bound within the biomass. Therefore, the calcium present in waste paper does not have the same catalytic (cracking) effect on the biomass structure compared to the other MSW biomass samples. In further support of the alkali metal induced cracking reactions, the samples with generally higher ash content (grass clippings, corn stover, etc.) on average produce more non-condensable gas and less oil and carbohydrate species as observed in Figure 3.3 and 3.4. It is often particularly noted in literature that these alkaline minerals degrade the carbohydrate fraction [10,20]. One

method used to reduce the amount of alkaline earth minerals is to acid wash the biomass samples before pyrolysis.

3.4.4 The effects of acid washing on fast pyrolysis products

The same fast pyrolysis conditions were used to study the effects of acid wash on the fast pyrolysis product distributions of grass clippings and waste paper. In this study, grass clippings and waste paper (due to their relatively high ash content) were treated with 0.1 M H_2SO_4 in order to remove ash and mineral content. Similar acid washing studies done at Idaho National Laboratory showed that the reduction of ash content to be approximately 37% with an almost complete reduction of alkaline and alkaline earth metals, 91% for K, 93% for Ca and 100% for Mg, but no change in the amount of Na present. The product distribution results of pretreated and un-pretreated grass clippings and waste paper obtained from fast pyrolysis are shown in Figure 3.5. For grass clippings and waste paper, the increase in bio-oil yield for the acid treated sample was achieved due to either a reduction in char and/or gas due to removal of either mineral or ash content, as shown below in Figure 3.5.

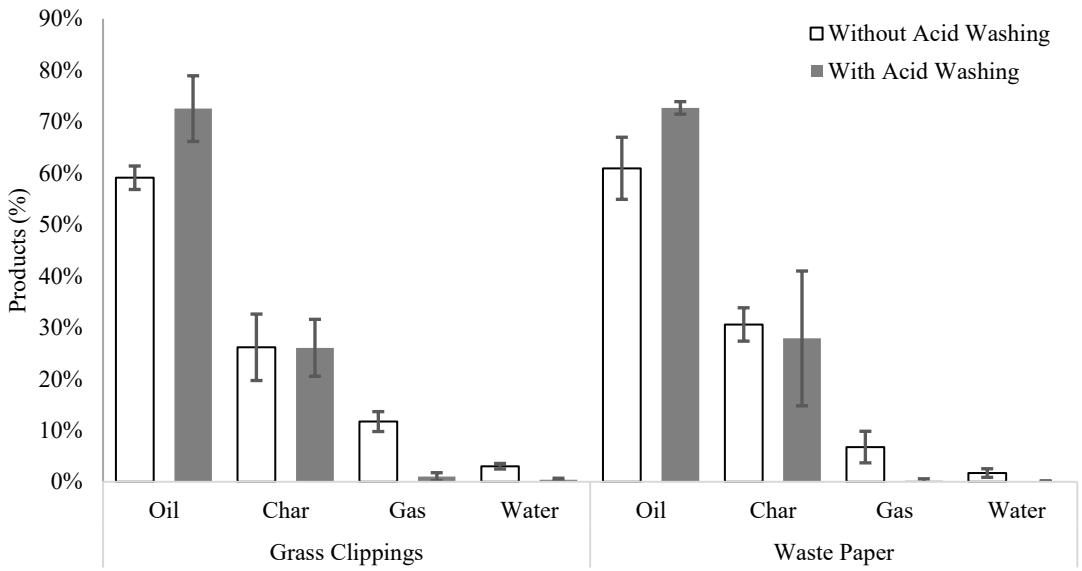

Figure 3.5: Comparison of fast pyrolysis products for acid washed and raw grass clippings and waste paper

From Figure 3.5, after acid washing and rinsing with distilled water the grass clippings and waste paper showed improvement of bio-oil produced. The chromatograms from these experiments are shown in appendix B and show a clear increase in leveoglucosan (RT 13 minutes) and other sugars. Carbohydrates and their derivatives appearing in bio-oil have been shown to be particularly susceptible to the catalytic effect of mineral cations[14]. The bio-oil mass from grass clippings increased from 59% to 73% and increased from 61% to 73% for waste paper; in both cases greater than the standard deviations. The acid wash results were in agreement with studies in literature[7, 32], which looked at the effects of minerals content in biomass on pyrolysis product distribution, and showed an increase in bio-oil production and reduction in pyrolysis gases. Again, these results look at the relative abundance of the unidentified bio-oil, distribution, water and gas results. When looking at

the water and gas yields, this is the relative abundance and should be viewed as showing the qualitative change in gas and water production due to the effect of acid washing.

Acid washing of biomass prior to fast pyrolysis had significant impact on the pyrolysis bio-oil composition and spectral/compounds mass for grass clippings and waste paper, as seen in Tables B.12 and B.13 in Appendix B. The effect of acid treatment is primarily seen in the large increase of sugar-derived compounds, especially for levoglucosan, which increased from 0% to 25.41% for grass clippings and 5.10% to 23.36% for waste paper. The small molecular weight species from acid washed grass clippings and waste paper (organic acids, aldehydes, etc.) decreased from 3.8% to 1.9% and 10.5% to 4.2%, respectively, compared to raw samples. The increase of sugar-derived compounds from acid washed grass clippings and waste paper corresponded to results in Patwardhan, et al. [14]. They studied the influences of alkali and alkaline earth metals on the pyrolysis products of pure cellulose, hemicellulose, and lignin [14]. They found that low amounts of alkaline metal in cellulose, as little as 0.1 wt%, can greatly reduce levoglucosan present in bio-oil, whereas no significant difference in lignin was found. This occurs because the metal species react with the sugar rings by promoting ring-opening of carbohydrates, whereas the metal species are less coordinated with aromatic rings [14].

In support of this, our work found that sugar-derived compounds increased in acid washed grass clippings and waste paper. However, lignin-derived compounds decreased in both acid washed grass clippings and waste paper, from 1.01% to 0.68% for grass clippings and 1.06% to 0.25% for waste paper, as shown in Tables B.12 and B.13 in the supporting information. This may have resulted from the long period (4 hours) of acid washing, which

may have cause the degradation of lignin structure in grass clipping and waste paper. Zhou, et al. [33] studied the effect of sulfuric acid within biomass at concentrations of 0, 0.0005, 0.001, 0.003, and 0.005 g H_2SO_4/g dry biomass on the yield and composition of lignin derived oligomers for fast pyrolysis of Douglas-fir wood at a temperature of 500 °C. They found that with increasing addition of H_2SO_4 the production of anhydrosugar increased, but the yield of methoxylated phenolic compounds (i.e., isoeugenol, eugenol, 4-ethyl-guaiacol, guaiacol, 4-vinyl-guaiacol, 4-methyl-guaiacol, vanillin, and acetoguaiacone) decreased. The reduction of pyrolysis lignin products in grass clippings and waste paper after acid wash may have resulted either from the degradation of lignin structure or the presence of H_2SO_4 in samples after the wash step.

Raveendran, et al. [32] reported that removal of mineral content, through acid washing using HCl and washing using NaOH for samples with high silica content, made a difference on the pyrolysis products of wood and twelve biomass types (such as coconut shell, corncob, corn straw, millet straw, rice straw, wheat straw, rice husk, and others) in a packed bed reactor. The amount of bio-oil increased and the relative abundance of gas decreased for all pretreated biomass samples [32]. Wannapeera, et al. [28] studied the effect of metal species on the pyrolysis weight loss of different types of agricultural biomass, through the use of a drop tube reactor. The weight losses of pretreated biomass was higher than un-pretreated biomass[28] due to the removal of metal species which reduced cross-linking reactions, while increasing the formation of volatile products and reducing char formation [28].

3.5 Conclusions

This micro-pyrolysis-based work shows that several types of MSW biomass are viable feedstocks for the production of pyrolysis bio-oil due to the relatively high production of bio-oil observed. This is particularly true for the "wood" MSW types; plywood, fiberboard, Microllam, and waferboard. Differences in the gaseous, liquid, and solid product distributions between the different feedstocks were large and could have arisen from (1) distribution between carbohydrate/lignin fractions, (2) mineral content, and (3) non-biomass organic matter inherent to MSW. These differences pose unique challenges when upgrading the bio-oil to a liquid transportation fuel. Due to the similar nature of the bio-oil produced from woody MSW feedstock, compared to hybrid poplar, the hydrotreatment will likely be the same. Therefore when performing thermochemical conversion of woody biomass, woody MSW could be incorporated as feedstocks. Paper and grass, showed a large generation of lower molecular weight compounds, this will make upgrading difficult, therefore the idea of using MSW blends could prove advantageous. We also conclude that mild processing with dilute acid and washing is an effective approach to boost bio-oil in high ash MSW types such as grass clippings and waste paper. The feasibility of acid washing has yet to be determined as to whether the increased amount of bio-oil can overcome the added economic and environmental impacts of this step. We also conclude that micro-pyrolysis is a beneficial and efficient way for relatively rapidly and inexpensively screening of biomass feedstocks. This work has allowed for the comparison of MSW feedstocks to their traditional counterparts and shown that they possess similar bio-oil qualities and product distributions. Using MSW biomass as

advanced biofuel feedstocks provides additional biomass supply beyond production on agricultural and forest lands and may increase the overall sustainability by turning waste into fuel and, importantly, by avoiding landfill emissions of greenhouse gases from the decomposition of biomass-derived components in MSW.

3.6 Acknowledgements

This work was supported by the US Department of Energy, Office of Energy Efficiency and Renewable Energy under Department of Energy Idaho Operations Office Contract No. DE-AC07-05ID14517. This manuscript has been co-authored by Battelle Energy Alliance, LLC under Contract No. DE-AC07-05ID14517 with the US Department of Energy. The US Government retains and the publisher, by accepting the article for publication, acknowledges that the US Government retains a nonexclusive, paid-up, irrevocable, world-wide license to publish or reproduce the published form of this manuscript, or allow others to do so, for US Government purposes.

3.7 References

1. KleanIndustries. Tipping fees vary across the U.S. *Market News* [Online], 2015. http://www.kleanindustries.com/s/environmental_market_industry_news.asp?ReportID=538710 (accessed November 20, 2015).

2. EPA Climate Change web site, Greenhouse Gas Emissions-Methane. , http://www3.epa.gov/climatechange/ghgemissions/gases/ch4.html (accessed January 31, 2016).

3. EPA *Municipal Solid Waste Generation, Recyling, and Disposal in the United States: Facts and Figures for 2010*; EPA-530-F-11-005; 2010.

4. EPA *Estimating 2003 Building-Related Construction and Demolition Materials Amounts* EPA530-R-09-002; 2009.

5. DDC, C. o. N. Y., Construction & Demolition Waste Manual Construction, C. o. N. Y. D. o. D. a., Ed. Gruzen Samton LLP with City Green Inc. : 2003.

6. Valkenberg, C., Gerber, MA., Walton, CW., Jones, SB., Thompson, SB., Stevens,DJ., Muncipal Solid Waste (MSW) to Liquid Fuels Synthesis, Volume 1: Availability of Feedstock and Technology. Energy, U. S. D. o., Ed. Pacific Northwest National Laboratory 2008.

7. Patwardhan, P. R., Understanding the product distribution from biomass fast pyrolysis. **2010**.

8. Bu, Q.; Lei, H.; Zacher, A. H.; Wang, L.; Ren, S.; Liang, J.; Wei, Y.; Liu, Y.; Tang, J.; Zhang, Q., A review of catalytic hydrodeoxygenation of lignin-derived phenols from biomass pyrolysis. *Bioresource technology* **2012,** *124*, 470-477.

9. Scott, D. S.; Piskorz, J.; Radlein, D.; Majerski, P., Process for the production of anhydrosugars from lignin and cellulose containing biomass by pyrolysis. Google Patents: 1995.

10. Patwardhan, P. R.; Brown, R. C.; Shanks, B. H., Product distribution from the fast pyrolysis of hemicellulose. *ChemSusChem* **2011,** *4* (5), 636-643.

11. Nik-Azar, M.; Hajaligol, M.; Sohrabi, M.; Dabir, B., Mineral matter effects in rapid pyrolysis of beech wood. *Fuel Processing Technology* **1997,** *51* (1), 7-17.

12. Fahmi, R.; Bridgwater, A. V.; Donnison, I.; Yates, N.; Jones, J., The effect of lignin and inorganic species in biomass on pyrolysis oil yields, quality and stability. *Fuel* **2008,** *87* (7), 1230-1240.

13. Lv, D.; Xu, M.; Liu, X.; Zhan, Z.; Li, Z.; Yao, H., Effect of cellulose, lignin, alkali and alkaline earth metallic species on biomass pyrolysis and gasification. *Fuel Processing Technology* **2010,** *91* (8), 903-909.

14. Patwardhan, P. R.; Satrio, J. A.; Brown, R. C.; Shanks, B. H., Influence of inorganic salts on the primary pyrolysis products of cellulose. *Bioresource Technology* **2010,** *101* (12), 4646-4655.

15. Wang, X.; CHEN, H.-p.; WANG, J.; XIN, F.; YANG, H.-p., Influences of mineral matters on biomass pyrolysis characteristics. *Journal of Fuel Chemistry and Technology* **2008,** *36* (6), 679-683.

16. Energy, U. S. D. o., Bioenergy Feedstock Library. Laboratory, I. N., Ed. bioenergylibrary.inl.gov.

17. Jenkins, B.; Baxter, L.; Miles, T., Combustion properties of biomass. *Fuel processing technology* **1998,** *54* (1), 17-46.

18. Sannigrahi, P.; Ragauskas, A. J.; Tuskan, G. A., Poplar as a feedstock for biofuels: a review of compositional characteristics. *Biofuels, Bioproducts and Biorefining* **2010,** *4* (2), 209-226.

19. Tharakan, P.; Volk, T.; Abrahamson, L.; White, E., Energy feedstock characteristics of willow and hybrid poplar clones at harvest age. *Biomass and Bioenergy* **2003,** *25* (6), 571-580.

20. Mohan, D.; Pittman, C. U.; Steele, P. H., Pyrolysis of wood/biomass for bio-oil: a critical review. *Energy & Fuels* **2006,** *20* (3), 848-889.

21. Milne, T.; Agblevor, F.; Davis, M.; Deutch, S.; Johnson, D., A review of the chemical composition of fast-pyrolysis oils from biomass. In *Developments in thermochemical biomass conversion*, Springer: 1997; pp 409-424.

22. Klinger, J.; Bar-Ziv, E.; Shonnard, D., Kinetic study of aspen during torrefaction. *Journal of Analytical and Applied Pyrolysis* **2013,** *104*, 146-152.

23. Evans, R. J.; Milne, T. A., Molecular characterization of the pyrolysis of biomass. *Energy & Fuels* **1987,** *1* (2), 123-137.

24. Khelfa, A.; Bensakhria, A.; Weber, J. V., Investigations into the pyrolytic behaviour of birch wood and its main components: Primary degradation mechanisms, additivity and metallic salt effects. *Journal of Analytical and Applied Pyrolysis* **2013,** *101*, 111-121.

25. Stefanidis, S. D.; Kalogiannis, K. G.; Iliopoulou, E. F.; Michailof, C. M.; Pilavachi, P. A.; Lappas, A. A., A study of lignocellulosic biomass pyrolysis via the pyrolysis of cellulose, hemicellulose and lignin. *Journal of Analytical and Applied Pyrolysis* **2014,** *105*, 143-150.

26. Diebold, J. P. *A review of the toxicity of biomass pyrolysis liquids formed at low temperatures*; National Renewable Energy Lab., Golden, CO (United States): 1997.

27. Stein, S. E., Retention Indices In *NIST Chemistry WebBook, NIST Standard REference Database Number 69*, Linstron, P. J., Mallard, W.G., Ed. National Institute of Standards and Technology Gaithersburg, MD 20899.

28. Wannapeera, J.; Worasuwannarak, N.; Pipatmanomai, S., Product yields and characteristics of rice husk, rice straw and corncob during fast pyrolysis in a drop-tube/fixed-bed reactor. *Songklanakarin Journal of Science and Technology* **2008,** *30* (3), 393.

29. Bridgwater, A. V., Review of fast pyrolysis of biomass and product upgrading. *Biomass and Bioenergy* **2012,** *38*, 68-94.

30. Jones, S., Holladay, JE., Valkenburg, C., Stevens, DJ., Walton, CW., Kinchin, C., Elliot, DC., Czernik, S *Production of Gasoline and Diesel from Biomass via Fast Pyrolysis, Hyrdotreating and Hydrocracking: A Design Case*; PNNL-18284; US DOE: PNNL, 2009.

31. Stilbert, E. K.; Young, A. E., Pigment coated paper. Google Patents: 1951.

32. Raveendran, K.; Ganesh, A.; Khilar, K. C., Influence of mineral matter on biomass pyrolysis characteristics. *Fuel* **1995,** *74* (12), 1812-1822.

33. Zhou, S.; Osman, N. B.; Li, H.; McDonald, A. G.; Mourant, D.; Li, C.-Z.; Garcia-Perez, M., Effect of sulfuric acid addition on the yield and composition of lignin derived oligomers obtained by the auger and fast pyrolysis of Douglas-fir wood. *Fuel* **2013,** *103*, 512-523.

4. Effect of Lignin Content and Temperature on the Properties of Hybrid Poplar Bio-Oil, Char, and Gas via Fast Pyrolysis

Submitted to ACS ENERGY AND FUELS KLEMETSRUD, B, EATHERTON, D, SHONNARD, D. EFFECT OF LIGNIN CONTENT AND TEMPERATURE ON THE PROPERTIES OF HYBRID POPLAR BIO-OIL, CHAR, AND GAS VIA FAST PYROLYSIS. ACS ENERGY AND FUELS[3]

4.1 Abstract

Fast pyrolysis of woody biomass has been identified as a potential means for the production of advanced transportation fuels. During fast pyrolysis the three main components of biomass (cellulose, hemicellulose, and lignin) thermochemically degrade to produce bio-oil. Prior studies have investigated fast pyrolysis of these individual components, however the manner in which variations in feedstock composition affect product distribution are not well understood. The purpose of this work is to assess the properties of bio-oil as lignin content is varied in hybrid poplar and how temperature of pyrolysis affects these results. The properties of bio-oil are assessed by calculating bio-oil yield relative to dry biomass and relative to char and gas, as well as changes in relative abundance of lignin-derived compounds in the bio-oil. Eight genetically different poplar samples with varying lignin content were pyrolyzed at 500℃ using a micro-pyrolysis unit, which was directly connected to a GC/MS. Four of these hybrid poplar samples over a range of lignin content were then pyrolyzed at temperatures of 550℃ and 600℃ to determine effects of pyrolysis temperature on product distribution

[33] The material in this chapter was submitted to *ACS Energy & Fuels*

among bio-oil, char, and gas. At a pyrolysis temperature of 500℃ an increase of poplar lignin content from 17% to 22% decreased relative bio-oil yield from 73% to 65% and increased char yield from 17.5% to 27.2% along with a decrease in abundance of lignin-derived phenolic species in bio-oil by 3%. With a higher pyrolysis temperature of 600°C, there was no decline in yield of bio-oil, nor an increase in char yield, and there was an increase in bio-oil phenolics compared to 500°C. From these results, higher temperatures are needed to increase the yield of bio-oil and of phenolic species in bio-oil.

4.2 Introduction

By 2022, the United States is required by the Renewable Fuels Standards Act (RFS2), to produce 36 billion gallons of blended transportation fuel. In 2012, the United States produced 13.8 billion gallons of biofuels, where 94% of the biofuel produced came from corn ethanol[27]. The RFS2 requires that by 2022, 21 billion gallons must be advanced biofuels derived mostly from lignocellulosic biomass instead of the currently used starch, sugars, and fats. Therefore, nearly all growth in the biofuels sector needs to be focused within the development of advanced biofuels.

A viable method for the production of advanced biofuels is the thermochemical conversion of biomass to a liquid transportation fuel [5,8,24]. Studies on thermochemical conversion have focused on bio-oil properties, reaction conditions, and the quality of the bio-oil produced via fast pyrolysis and how this is governed by the types of biomass processed[14]. Hybrid poplar has been identified as a potential feedstock for biofuel

production due to its ability to be genetically altered, its relatively quick growth rate, and that it is suitable for thermochemical conversion[7].

Previous studies have shown that biomass feedstock properties have a significant effect on the quality of bio-oil produced via fast pyrolysis[4,9,14]. Specifically, the mineral content and ash content of biomass have been shown to affect the quality of bio-oil. Higher ash content has shown lower bio-oil yields as an overall trend[2,19,23], whereas higher mineral content has been shown to increase lower molecular weight products produced in bio-oil. This is due to the pyrolysis products being cracked or broken down by alkali earth metals such as sodium and calcium[19],[16,29].

Biomass is comprised of 3 main components; cellulose, lignin and hemicellulose. Patwardhan et al[22] have studied these individual components to evaluate what products are produced when they are individually pyrolyzed. This previous work has shown that hemicellulose generally produces lower molecular weight gases, organic acids, and furans. Hemicellulose is also one of the first components of biomass to begin degradation, which can occur at temperatures as low as 250°C. Cellulose generally produces anhydrosugars, such as levoglucosan, and decomposes at a higher temperature, generally around 350-400ºC. Lignin, when pyrolyzed, generally gives a bio-oil that is rich in phenolic structures and has lower organic acid concentrations when compared to hemicellulose. The interactions between cellulose-lignin and cellulose- hemicellulose have been studied[3,12,28], however, there is not an overall understanding of how these components interact within the entirety of the biomass structure and how these individual components of biomass can be altered to generate a better quality bio-oil.

Bio-oil has received several criticisms, especially when compared to its fossil fuel counterpart. Bio-oils produced via fast pyrolysis generally has poor volatility, high viscosity, high corrosivity, and coking within the reactor[1]. Due to the presence of low molecular weight molecules, especially organic acids, bio-oil is generally acidic, causing it to be corrosive[16]. These low molecular weight molecules are not easily upgradable due to having high oxygen content and the possible need to be recombined to generate a larger molecule to be within gasoline range. One of the largest disadvantages of bio-oil is its high oxygen content. The high oxygen content requires an energy and hydrogen rich catalytic upgrading process[11]. Much of the oxygen rich products are generated from the hemicellulose and cellulose fractions. The lignin fraction does contribute to the oxygen content, but due to the nature of the phenolic ring, the lignin fraction contributes significantly to the carbon content of the bio-oil. Phenolic structures are easier to upgrade than carbohydrate derived bio-oil compounds, have a higher carbon to oxygen ratio and therefore can produce a more energy dense biofuel product[11].

Previous studies have looked at different kinds of biomass, their characteristics, and bio-oil properties [9,10,25,30]. Some studies have compared these biomass characteristics and bio-oil properties across different species[2,16] to evaluate what are key biomass characteristics to focus on. When looking across different biomass species, an increase in lignin content, from 18% to 35 % reduced the oxygen content of bio-oil, decreased bio-oil yields (due to an increase in bio-char yields) and increased the average molecular weight of the bio-oil.[16] However, prior studies have not conducted lignin related pyrolysis experiments

with a single species, and therefore there is no clear understanding of what occurs when an individual biomass species is evaluated across its genotype, which has been crossbred to change the biomass components.

In this study we obtained hybrid poplar that had been crossbred to increase the amount of lignin present in these hybrid poplar clones. Therefore, in this research we performed micropyrolysis experiments on hybrid poplar species with a range of lignin content. Our hope is that the results will allow for an improved understanding of how changing lignin content of hybrid poplar affects the quality of bio-oil produced and distribution of products among gas, liquid and solid char. This research allows for a systematic way of evaluating at the changing biomass composition of lignin of the same genetic species of hybrid poplar at varying temperatures. The objective of this study is to understand how changes in the biomass structure will affect fast-pyrolysis product distribution and the chemical composition of the bio-oil produced at various reaction conditions. This work evaluates 8 hybrid poplar samples and evaluates how char, gas and bio-oil yield change with respect to lignin composition. Bio-oil and char composition are also evaluated with respect to the poplar samples initial biomass composition.

4.3 Materials and Methods

4.3.1 Biomass Preparation

8 hybrid poplar clones ((*P.trichocarpa* x *P.deltoids*) x (*P. trichocarpa* x *P.deltoids)*) were obtained from a University of Florida study[20]. These cuts were then grown on the Baraga Plains at the Ford Forestry Center located in Alberta, MI by researchers in Michigan Tech's School of Forest Resources. Cuts from these tree plantings occurred after 3 years

of growth. The cuts were debarked and chipped using a coffee grinder. The samples were then sieved and sized to a range of 180-250 microns (80-60 Tyler mesh). After the samples were sized, they were then dried in a drying oven at 105°C for 24 hours and stored in a Ziplock bag. 2 mg of each of the 8 hybrid poplar samples, sized to 180-250 microns were then sent to the University of Georgia in Athens to determine the amount of lignin content and the syringol to guaiacol ratio by using PY-MBMS (Pyrolysis - Molecular Beam Mass Spectroscopy). The carbon content of these samples were measured, using an elemental analyzer (Costech 4010).

4.3.2 Pyrolysis Experiments

The 8 hybrid poplar samples were used to understand the effect of lignin content on fast-pyrolysis product distribution. These experiments were conducted in triplicate at 500°C. Four of these poplar samples were then used to understand the effect of temperature on lignin content and were pyrolyzed at 550°C and 600°C. Table 4.1 shows the samples, their lignin content, syringol to guiacol (S/G) ratio, and which experiments were performed on each sample. Lignin content ranged from 17% to 22%. Hardwoods, such as hybrid poplar, beech, chestnut, generally have lignin contents from 15-25%, whereas softwoods, such as pine, redwood, douglas fir, have lignin contents ranging from 25-40%. The syringol and guiacol ratio increased with increasing lignin content. This indicated that more syringol was being generated within the biomass structure for the genotypes that had increased lignin content. Sample numbers remain the same as the University of Florida study, however due to different growing conditions the lignin content varied from the original study.

Table 4.1: Hybrid poplar samples lignin content, S/G ratio and experimental matrix

Sample	Lignin Content (%)	S/G Ratio	Temperature Dependence
645	17.52	1.29	
695	19.76	1.48	
648	19.91	1.42	x
705	20.46	1.65	
765	20.50	1.34	x
506	21.50	1.54	x
635	21.65	1.73	
603	22.07	1.53	x

4.3.3 Effect of Lignin Content and Pyrolysis Temperature

Hybrid poplar samples ranging from 200-600 μg with thickness of approximately 200 microns were placed in a quartz vial held between 2 pieces of quartz wood, as shown below in Figure 4.1. The poplar fiber sample was then loaded into a CDS 5200 HP/HT pyroprobe where it was dried at 105°C for 10 minutes to remove free moisture and to ensure that any water detected in the experiments was from chemically bound and chemically formed water. The pyroprobe reactor was kept inert with a helium flow rate of 20 ml/min. The interface of the pyroprobe was then heated to 300°C. Once the interface temperature was achieved, the platinum coil was then rapidly heated to its predetermined reaction temperature (ranging from 500°C to 600°C). The platinum coil achieved the reaction temperature at a rate of 1000ºC/sec and used radiative and convective heat transfer for the biomass sample to undergo fast pyrolysis.

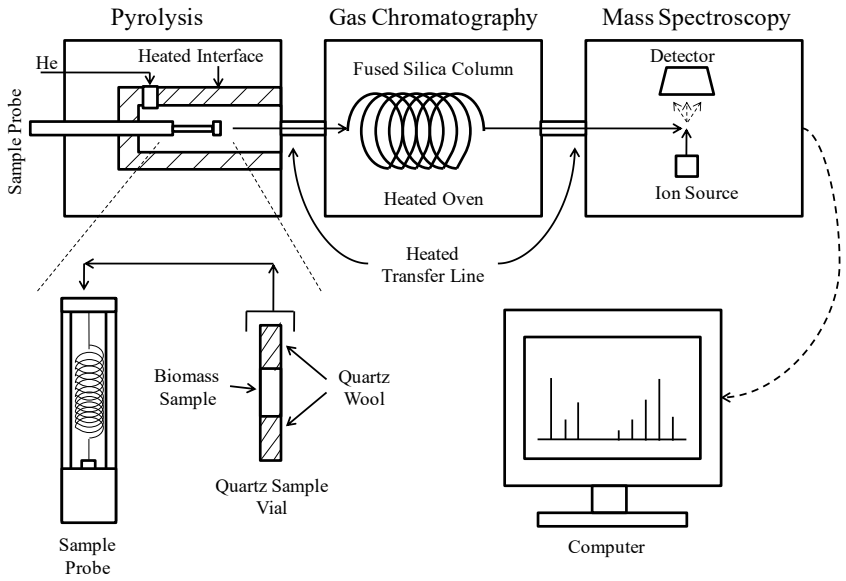

Figure 4.1: Experimental diagram for fast pyrolysis of hybrid poplar samples in a micro-pyrolysis reactor[15]

The gaseous vapors were then swept through the transfer line, which was kept at a temperature of 300°C, to the GC (Thermo Fisher Trace GC Ultra). The gaseous vapors were then condensed onto the GC column (Restek, Rxi-5ms, 30m x 0.25 mm, 0.25 um film thickness) which was held at a temperature of 35° C for 2 minutes. The column then was heated at a rate of 5°C/min, and once it reached 150°C, it was heated to 275°C at a heating rate of 10 °C/min. Once it reached 275°C it was held for 2 minutes to ensure heavier compounds were eluted through the column. After eluting through the column, the compounds were then sent to Thermo Fisher DSQII Mass Spectrometer (MS) and their mass ion fragments were measured. The ion source was kept at 275°C with an electron ionization potential of 70 eV. The data was recorded using Thermo Fisher's Xcalibur software. Experiments were conducted in triplicate. In-between experiments the pyroprobe containing an empty quartz vial was heated to 600°C and the GC to 275℃ several times to ensure that no residual pyrolysis oil existed within the pyroprobe or GC.

This method was used for all hybrid poplar samples, the GC/MS conditions remained the same, with the only change being the reaction temperature of the pyroprobe which was run additionally at 550°C and 600°C.

4.3.4 Bio-Oil Product Identification

To analyze the bio-oil and vapors that were produced during bio-oil, only chromatogram peaks that contributed to 1% or greater of total peak area were analyzed and identified. This approach contributed to approximately 70% of the total peak area. Peaks that contribute to less than 1% peak area were difficult to distinguish from the baseline and generally co-eluted with other species, making it difficult to de-convolute these small peaks. Products that contributed to 1% or greater of peak area were identified based on their mass charge spectra using the NIST spectra library included in the Xcalibur software. If products could not be clearly identified using the Xcalibur software, the mass spectra was compared to that of literature, and then confirmed comparing the compound spectra to that of the NIST webbook[26]. Compounds that were not identified using these methods were grouped into their classes based on their unique mass charge fragments. Table 4.2, shows the main fractions for specific compounds[20].

Table 4.2: Classes of compounds commonly found in pyrolysis liquid along with their characteristic m/z peaks from GC/MS analysis[20]

Classes	Characteristic m/z peaks
Five carbon hemicellulose (furans)	57+73+85+96+114
Six Carbon cellulose sugar (anhydrosugar)	57 + 60 + 73 + 98 + 126 + 144
Syringyl lignin monomer	154 + 167 + 168 + 182 + 194 + 208 + 210
Gualacyl Lignin Monomer	124 + 137 + 138 + 150 + 164 + 178

Compounds were then grouped into six different categories: lignin (those containing phenolic structures), small sugars (those containing furans), large sugars (primarily anhydro sugars), low molecular weight species (eluting during the first 5 minutes containing aldehydes, ketones and organic acids), gaseous products (the first peak in the chromatogram containing primarily CO_2 and CO), and water (contained within the first peak and separated out using the 18 m/z fragment). The char weight was measured using a microbalance (Orion Cahn microbalances, Model C-35 by Thermo) with a sensitivity of 1 ug. The char weight was then subtracted from the original mass and the remaining mass was allocated between, bio-oil, gas and water based on the identified peak area. The char was then analyzed using an elemental analyzer (Costech 4010) to determine the amount of carbon present.

4.4 Results and Discussion

4.4.1 Temperature of 500°C

The hypothesis for this research is that as the amount of lignin present in the same species of poplar increases, the amount of phenolics present in the bio-oil will increase. This hypothesis is supported by the literature which shows that bio-oil from coniferous sources with increasing lignin content have substantially more phenolics present in bio-oil, but a lower bio-oil yield due to the increase char yield[21]. Therefore, in our study, it was expected that with an increase in poplar lignin there would be an increase in phenolics present in the bio-oil and higher char yield.

As shown in Figure 4.2a with the triangle symbols, the relative bio-oil yield of the 8 hybrid poplar samples of between 17.5-22% lignin at 500°C decreased between 5-10% with increase in lignin content. The char yield, as shown in Figure 4.3a, depicts the

opposite trend as the lignin content is increased in that the char yield increases. From previous studies[3,6,17] it was observed that wood samples with higher lignin are likely to produce more char and therefore reduce the bio-oil yields (also observed in this study in Figures 4.2a and 4.3). The relative gas yields in our study did not change substantially as shown below in Figure 4.4, at the top of the bar charts. Therefore, the main tradeoff with increase in lignin came with decreasing the relative bio-oil yield and an increasing char yield.

Figure 4.5a shows the variation in amount of lignin derived compounds within the bio-oil with respect to the poplar lignin content. It was observed that with increasing lignin content of the biomass samples at 500°C, lignin derived compounds within the bio-oil decreased, though admittedly the size of error bars do not assure absolute confirmation of this trend. These results then suggest that instead of volatilizing from the poplar lignin structure into the bio-oil, lignin is preferentially remaining fixed in the char. At 500°C with increasing lignin in poplar, the other categories of compounds present in the bio-oil, such as low molecular weight compounds or carbohydrate-derived compounds, do not change substantially, as shown below in Figure 4.4.

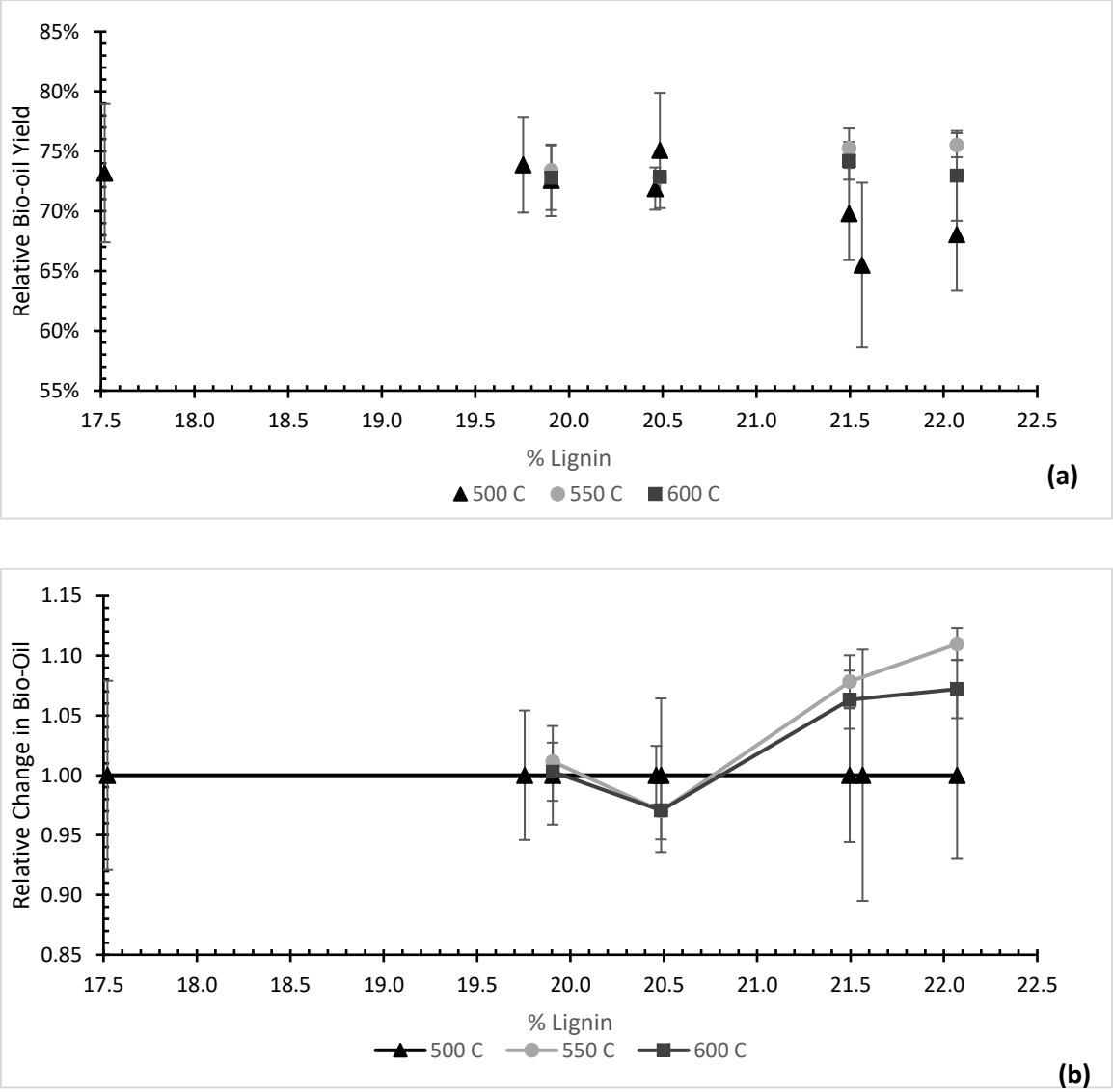

Figure 4.2: a) Bio-oil yield of different hybrid poplar clones at 500 °C, 550 °C and 600ºC b) Relative change of bio-oil yield with respect to 500°C

4.4.2 Effect of Increasing Fast-Pyrolysis Temperature

A set of experiments was performed on 4 of the hybrid poplar samples at 550ºC and 600°C to determine if the lignin could be volatilized more effectively with increasing temperature to boost bio-oil yield and the amount of lignin derived phenolics compounds in the bio-oil. Prior studies[2,14,16] show that as the temperature is increased, the char yields

will decrease, along with bio-oil yields, but the gas produced may increase. When pyrolyzing these poplar samples at higher temperatures, there was little to no change in bio-oil yield for two lower lignin poplar samples, but an increase in bio-oil yield for the higher lignin content poplar samples as shown in Figure 4.2a and b. The hybrid poplar sample at 20.5% lignin, actually showed a slight decrease. The char yield, with respect to lignin content did decrease significantly from 500ºC to 550°C, as shown in Figure 4.3a and b. This indicates that with increase in temperature more of the lignin was volatilized into the bio-oil instead of remaining fixed in the char. There is a significant change (because error bars do not overlap) in char yield from 500°C to 550°C and 600°C at the higher lignin containing species, than at the lower lignin contents. Indicating that more of the lignin was remaining fixed in the char at 500°C and higher temperature were needed for a more complete pyrolysis of the biomass. Jia, et al. [13] suggests that there are two reaction steps that occur with the degradation of the lignin structure; the first in which larger oligomers and smaller gases break off and lead to a more stable char. The char can further be degraded with an increase in residence time or reactor temperature leading to a larger production of lignin monomers[13]. The results from this study, suggest that at higher temperatures the second reaction is occurring at a much higher rate than at 500°C.

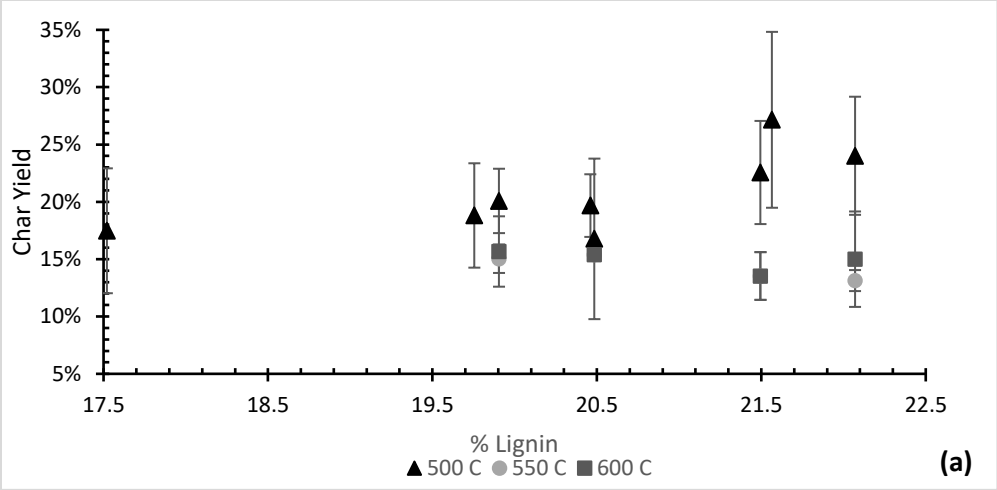

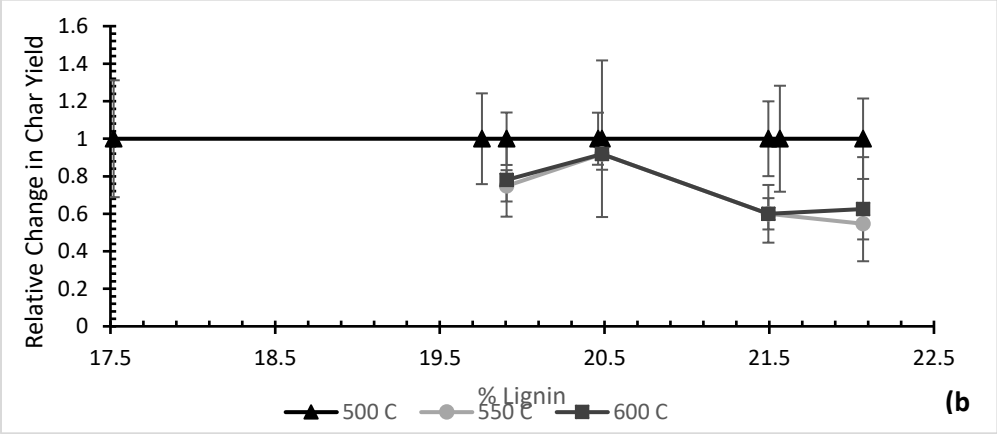

Figure 4.3: a) Char yield with respect to varying lignin content pyrolyzed at 500°C, 550°C, 600°C b) Relative change of char yield with respect to 500°C

The relative peak area data from the pyrolysis gc-ms experiments were organized into chemical categories in order to show any trends with change in lignin and temperature. The categories include gases (CO_2, CO, H_2O), bio-oil compound categories (low molecular weight (LMW), holocellulose-derived carbohydrates, lignin-derived phenolics, unspecified compounds)), and char. These bio-oil categories were compared across varying lignin content and reactor temperature as shown below in Figure 4.4. When looking at the speciation of bio-oil and product distribution in Figures 4.4 and 4.5a and b,

it is observed that with increasing temperature (for most poplar samples) the lignin-derived phenolics present in the bio-oil increases approximately 20%. The exception to this trend is the poplar sample at 20.5% lignin which exhibited a slight decrease in phenolics in the bio-oil with increasing pyrolysis temperature (Figure 4.5b). Within this study, the poplar species (603) with 22% lignin has the highest average amount of lignin containing compounds present in the bio-oil and does have one of the highest average bio-oil yields from the experiments at 550°C, as shown in Figure 4.2. Aside from more lignin containing compounds being present in the bio-oil at 600°C, the product distribution of gas, char and water, for poplar sample 603, is nearly identical at 550°C and 600°C, as shown in Figure 4.4. Therefore, from our study 550 °C may be the most favorable fast-pyrolysis conditions for enhancing both bio-oil yield and phenolics present in the bio-oil for these hybrid poplar samples

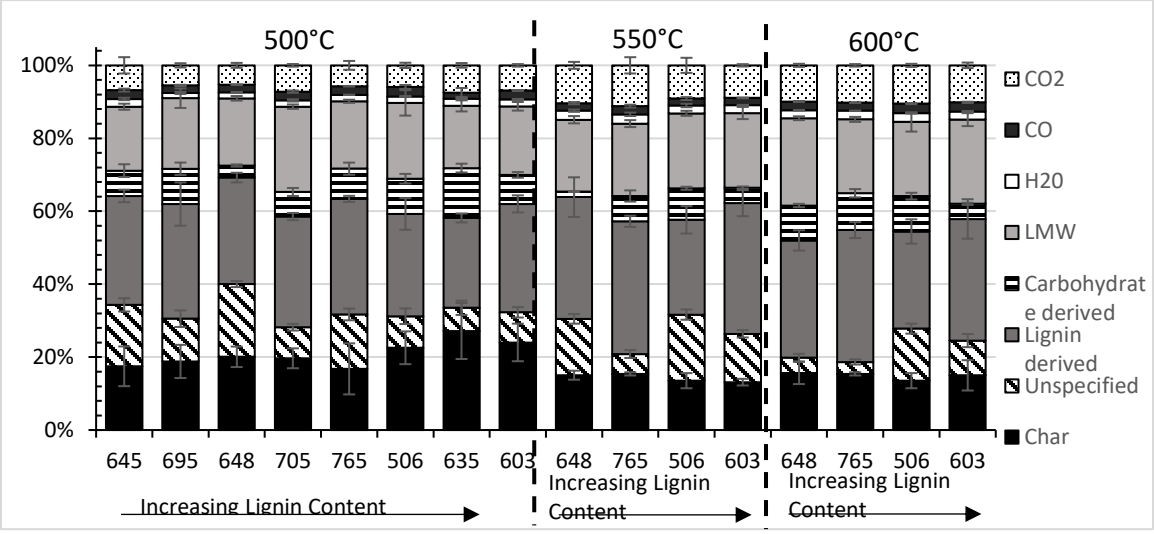

Figure 4.4: Relative amounts of compounds in the bio-oil and gas and char yield compared against samples with increasing lignin content (645 is the lowest and 603 is the highest) and increasing temperature as shown by the dashed lines. LMW refers to the low molecular weight bio-oil species.

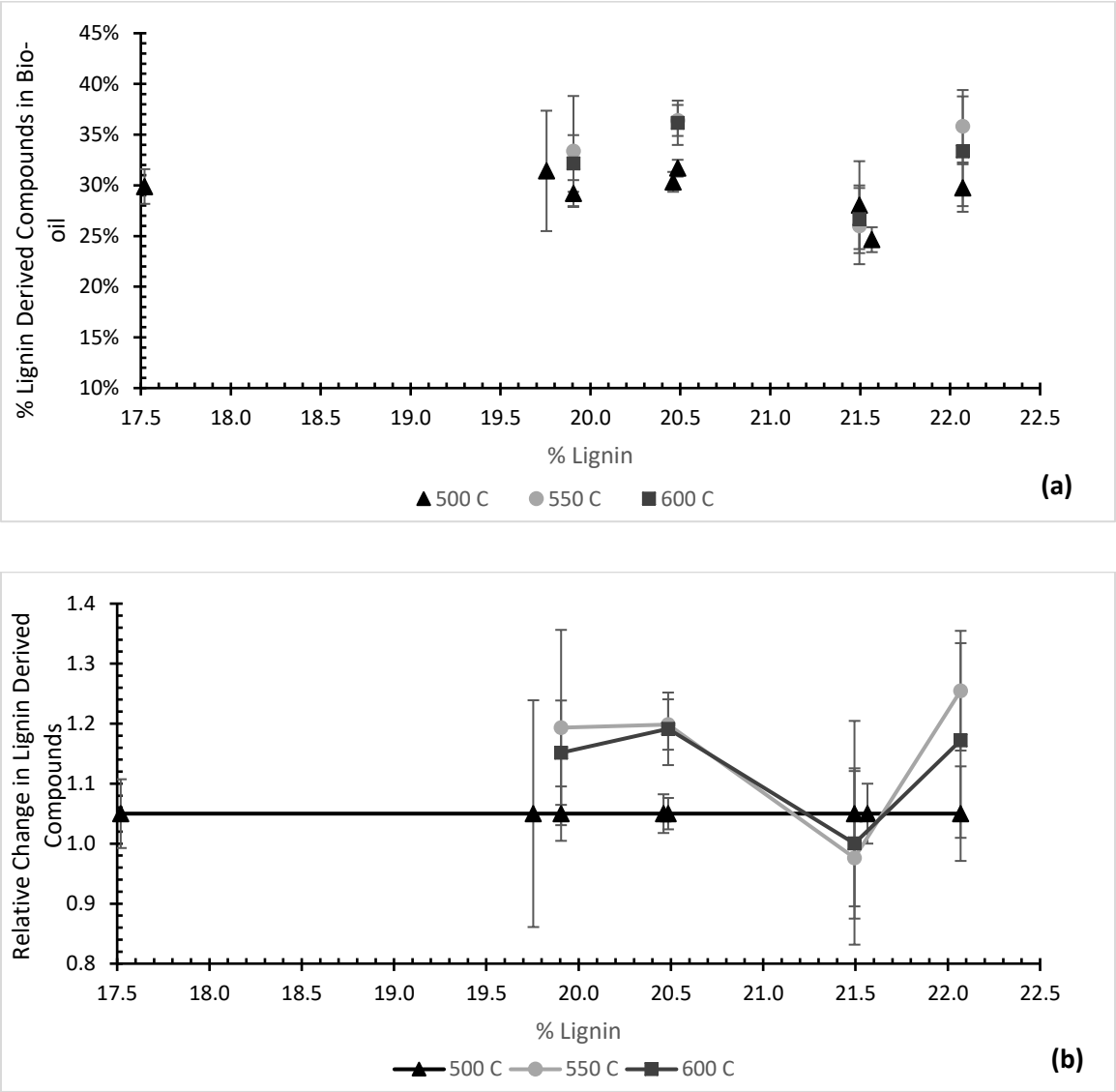

Figure 4.5 : a)Relative amount of lignin derived compounds in the bio-oil yield with respect to varying lignin content pyrolyzed at 500°C, 550°C, 600°C. b) Relative change of lignin derived compounds within the bio-oil with respect to 500°C

While the lignin content in the bio-oil was shown to increase with increasing temperature, it is expected that relative amounts of other compounds would change in the bio-oil with increasing lignin and temperature. One of the largest relative changes was the decrease in

the carbohydrate fraction with increasing temperature, and the increasing amount of CO_2 and CO generated, as shown in Figure 4.4. At the higher temperatures, the hemicellulose is likely converted into gases instead of generating more small carbohydrate compounds such as furans. The increase in pyrolysis gas formed with respect to increase in temperature can also be evidence for the degradation of the lignin structure[18].

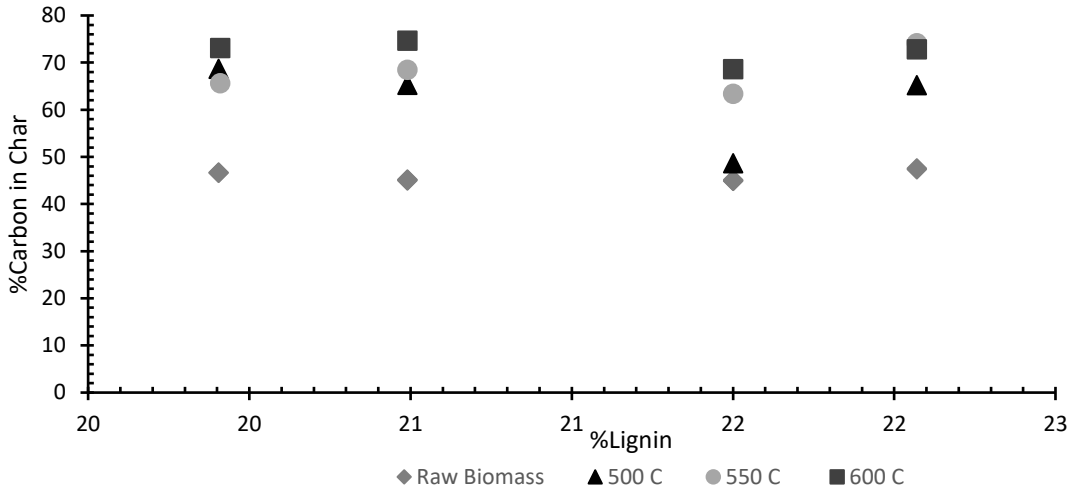

Figure 4.6: The amount of carbon present in the raw biomass and pyrolysis char from various reaction temperatures, with respect to biomass lignin content.

As the pyrolysis reaction temperature is increased from 500 to 600°C, Figure 4.6 shows by an elemental analysis that percent carbon within the char increased by about 20-30% compared to raw biomass. This increase in C content is fairly consistent across all lignin contents in the poplar samples. This trend is in agreement with previous studies[14,16,22] in that as the biomass is pyrolyzed the molecular structure of the remaining solid char changes with severity of pyrolysis to increase C and reduce O. During pyrolysis while

the biomass is volatizing, the biomass structure is continuously rearranging to develop a more stable structure. It is suggested that with increasing temperatures more carbon-carbon bonds form, generating a more carbonaceous char[4]. For three of the four biomass samples, pyrolysis at 600°C produced char with the highest C percent, but any conclusions about effects of pyrolysis temperature on char composition are preliminary due to lack of replicate measurements.

Although some trends with respect to poplar lignin content and fast-pyrolysis temperature were observed in these experiments, the interpretations are not so broadly applicable due to the limited range of lignin content. Therefore, it is recommended that more experiments be conducted over a wider range of lignin for poplar and for other types of woody biomass species. Another consideration for interpreting these results is the manner that fast-pyrolysis was conducted in these experiments. The residence time of pyrolysis vapors in the reactor zone is very short because of the configuration of the pyro-probe within the reaction interface of the micro-pyrolysis reactor. Helium gas sweeps vapors quickly from the hot pyrolysis reaction zone into a cooler environment in the transfer line to the gc-ms. The reactions measured in these experiments must be interpreted as the primary reactions that liberate volatile vapors from the biomass solid, and not secondary reactions that would occur in the gas phase with longer reaction residence time in the reactor. Future experiments may gain additional insights into the fundamental pyrolysis reactions and mechanisms by re-configuring micropyrolysis reactions to gain control over reaction residence time and study secondary reactions that occur. These results focus on the primary products formed with respect to varying lignin content and reaction temperatures. Understanding how lignin and temperature affect the

product distribution of the bio-oil allow for a more mechanistic understanding of the thermochemical degradation of biomass.

4.5 Conclusion

The main conclusion from this study is that increasing the amount of lignin in hybrid poplar has the potential to increase the amount of lignin-derived phenolics present in the bio-oil, but only with the assistance of increasing pyrolysis temperature of up to 600°C. However, at typical fast pyrolysis temperature of 500°C, increasing lignin in the raw biomass produced more char rather than bio-oil with a tendency for more of the lignin to be retained in the solid char. For this study, sample 603 produced the most amount of phenolics in the bio-oil at a temperature of 600 °C but had the highest bio-oil yield at 550 ºC and was the poplar species with the highest lignin content. This indicates that biomass structures with increased amounts of lignin, can generate large bio-oil yields, with temperature optimization. When considering varying feedstocks for the generation of pyrolysis bio-oil, micro-pyrolysis allows for a rapid screening process to identify optimum conditions.

4.6 Acknowledgments

The authors would like to gratefully acknowledge the National Science Foundation grant MSP/CHE-ENG/ECCS-1230803 for support of this work through a sustainable Energy Pathways Grants, and the Richard and Bonnie Robbins Endowment.

4.7 References

1. Bridgwater AV. Principles and practice of biomass fast pyrolysis processes for liquids. Journal of Analytical and Applied Pyrolysis 1999;51(1–2):3-22.
2. Bridgwater AV. Review of fast pyrolysis of biomass and product upgrading. Biomass and Bioenergy 2012;38:68-94.
3. Caballero JA, Conesa JA, Font R, Marcilla A. Pyrolysis kinetics of almond shells and olive stones considering their organic fractions. Journal of Analytical and Applied Pyrolysis 1997;42(2):159-175.
4. Collard F-X, Blin J. A review on pyrolysis of biomass constituents: Mechanisms and composition of the products obtained from the conversion of cellulose, hemicelluloses and lignin. Renewable and Sustainable Energy Reviews 2014;38:594-608.
5. de Wit M, Faaij A. European biomass resource potential and costs. Biomass and Bioenergy 2010;34(2):188-202.
6. Di Blasi C, Branca C, Santoro A, Hernandez EG. Pyrolytic behavior and products of some wood varieties. Combustion and Flame 2001;124(1):165-177.
7. DOE U. US billion-ton update: biomass supply for a bioenergy and bioproducts industry. ORNL/TM-2011/224 2011.
8. Elliott DC, Beckman D, Bridgwater AV, Diebold JP, Gevert SB, Solantausta Y. Developments in direct thermochemical liquefaction of biomass: 1983-1990. Energy & Fuels 1991;5(3):399-410.

9. Fahmi R, Bridgwater AV, Donnison I, Yates N, Jones J. The effect of lignin and inorganic species in biomass on pyrolysis oil yields, quality and stability. Fuel 2008;87(7):1230-1240.

10. Gani A, Naruse I. Effect of cellulose and lignin content on pyrolysis and combustion characteristics for several types of biomass. Renewable Energy 2007;32(4):649-661.

11. Hilten RN, Speir RA, Kastner JR, Mani S, Das K. Effect of torrefaction on bio-oil upgrading over HZSM-5. Part 1: Product yield, product quality, and catalyst effectiveness for benzene, toluene, ethylbenzene, and xylene production. Energy & Fuels 2013;27(2):830-843.

12. Hosoya T, Kawamoto H, Saka S. Cellulose–hemicellulose and cellulose–lignin interactions in wood pyrolysis at gasification temperature. Journal of Analytical and Applied Pyrolysis 2007;80(1):118-125.

13. Jia L, Le-Brech Y, Shrestha B, Frowein MB-v, Ehlert S, Mauviel G, Zimmermann R, Dufour A. Fast Pyrolysis in a Microfluidized Bed Reactor: Effect of Biomass Properties and Operating Conditions on Volatiles Composition as Analyzed by Online Single Photoionization Mass Spectrometry. Energy & Fuels 2015;29(11):7364-7374.

14. Kan T, Strezov V, Evans TJ. Lignocellulosic biomass pyrolysis: A review of product properties and effects of pyrolysis parameters. Renewable and Sustainable Energy Reviews 2016;57:1126-1140.

15. Klinger J, Bar-Ziv E, Shonnard D. Kinetic study of aspen during torrefaction. Journal of Analytical and Applied Pyrolysis 2013;104:146-152.

16. Mohan D, Pittman CU, Steele PH. Pyrolysis of wood/biomass for bio-oil: a critical review. Energy & Fuels 2006;20(3):848-889.

17. Muley PD, Henkel C, Abdollahi KK, Marculescu C, Boldor D. A critical comparison of pyrolysis of cellulose, lignin, and pine sawdust using an induction heating reactor. Energy Conversion and Management 2016;117:273-280.

18. Newalkar G, Iisa K, D'Amico AD, Sievers C, Agrawal P. Effect of Temperature, Pressure, and Residence Time on Pyrolysis of Pine in an Entrained Flow Reactor. Energy & Fuels 2014;28(8):5144-5157.

19. Nik-Azar M, Hajaligol M, Sohrabi M, Dabir B. Mineral matter effects in rapid pyrolysis of beech wood. Fuel Processing Technology 1997;51(1):7-17.

20. Novaes E, Osorio L, Drost DR, Miles BL, Boaventura-Novaes CR, Benedict C, Dervinis C, Yu Q, Sykes R, Davis M. Quantitative genetic analysis of biomass and wood chemistry of Populus under different nitrogen levels. New Phytologist 2009;182(4):878-890.

21. Oasmaa A, Kuoppala E. Fast pyrolysis of forestry residue. 3. Storage stability of liquid fuel. Energy & Fuels 2003;17(4):1075-1084.

22. Patwardhan PR. Understanding the product distribution from biomass fast pyrolysis. 2010.

23. Patwardhan PR, Brown RC, Shanks BH. Product distribution from the fast pyrolysis of hemicellulose. ChemSusChem 2011;4(5):636-643.

24. Perlack RD, Wright LL, Turhollow AF, Graham RL, Stokes BJ, Erbach DC. Biomass as feedstock for a bioenergy and bioproducts industry: the technical feasibility of a billion-ton annual supply. DTIC Document; 2005.

25. Sharma RK, Wooten JB, Baliga VL, Lin X, Chan WG, Hajaligol MR. Characterization of chars from pyrolysis of lignin. Fuel 2004;83(11):1469-1482.

26. Stein SE. Mass Spectra. In: Linstron PJ, Mallard, W.G., editor. NIST Chemistry WebBook, NIST Standard Reference Database Number 69. Gaithersburg, MD 20899: National Institute of Standards and Technology

27. U.S. Bioenergy Statistics [Internet]. 2016 [updated cited Available from: http://www.ers.usda.gov/data-products/us-bioenergy-statistics.aspx

28. Wang S, Guo X, Wang K, Luo Z. Influence of the interaction of components on the pyrolysis behavior of biomass. Journal of Analytical and Applied Pyrolysis 2011;91(1):183-189.

29. Wannapeera J, Worasuwannarak N, Pipatmanomai S. Product yields and characteristics of rice husk, rice straw and corncob during fast pyrolysis in a drop-tube/fixed-bed reactor. Songklanakarin Journal of Science and Technology 2008;30(3):393.

30. Yang H, Yan R, Chen H, Lee DH, Zheng C. Characteristics of hemicellulose, cellulose and lignin pyrolysis. Fuel 2007;86(12):1781-1788.

5. A Kinetic Study of the Fast Micro-Pyrolysis of Hybrid Poplar

Submitted to JOURNAL OF ANALYTICAL AND APPLIED PYROLYSIS KLEMETSRUD, B, KLINGER , J, BAR ZIV E, SHONNARD, D A KINETIC STUDY OF THE FAST MICRO-PYROLYSIS OF HYBRID POPLAR. JOURNAL OF ANALYTICAL AND APPLIED PYROLYSIS [4]

5.1 Abstract

Hybrid poplar from the clone DN34 was studied to determine the rate of production of bio-oil species with respect to time during the pyrolysis process. 300-660 ug samples were pyrolyzed using a micropyrolzer at 500ºC at very high heating rates. Individual poplar samples were run in triplicate at discrete time points ranging from 1-20 seconds. Several bio-oil compounds from each individual sample were analyzed using GC/MS. The bio-oil compounds that were used to determine the degradation of the biomass were quantified using standards to determine the weight percent relative to the original raw biomass produced with respect to time. Acetic acid, glycolic acid, acetol, furfural, methyl syringol and guiacol were used to understand the degradation of biomass with respect to bio-oil production. Pyrolysis kinetic reaction models were fit to this experimental data in order to determine suitability of each model. A first order exponential decay model for degradation of the solid biomass was used to fit the data along with a six-step

[4] The material in this chapter was submitted to *Journal of Analytical and Applied Pyrolysis*

consecutive degradation model previously developed by Klinger et al. 2015. The experimental data suggests that compounds derived from the hemicellulose are produced at faster rates than that of the lignin or cellulose fractions of the wood, consistent with prior data from thermogravimetric analysis (TGA). When applying the first order exponential decay model, the reaction rates calculated did prove that holocellulose compounds reaction rates were approximately twice that of the lignin compounds reaction rate but did not provide a good fit. The application of the six-step degradation model, provided a good fit and gained insight with the fitted stoichiometric variables into the biomass degradation. Using the stoichiometric variables within the model, we were able to show that certain parts of the biomass are degraded at earlier times in the pyrolysis process, like acetic acid from the degradation of hemicellulose, whereas compounds derived from lignin take more time to degrade.

5.2 Introduction

Thermochemical conversion of biomass has been identified as a means in which to generate renewable liquid, solid, and gaseous fuels from various types of biomass[1, 2]. Thermochemical conversion is the thermal degradation of biomass in the absence of oxygen into an energy dense solid, liquid, or gaseous product. Fast pyrolysis, one among many thermochemical conversions, is one viable method for maximizing the production of an energy rich liquid from biomass. Pyrolysis occurs at temperatures of 400-600°C in an inert atmosphere with generally short residence times (1-2 seconds)[1, 3]. Unlike biochemical conversion, most biomass types can be thermochemically converted in a similar manner and don’t require biomass-specific inputs. Reaction conditions may

change, however the configuration of thermochemical conversion remains the same for nearly all biomass. In 2014, approximately 4.8 quadrillion BTUs of many forms of renewable energy were produced from biomass with half of that being generated as liquid transportation biofuels , with nearly 95% of it being produced from the production of ethanol [4]. With the vast resources of biomass available in the United States [5], it is estimated that biomass could account for the production of about 100 billion gallons of fuel a year [6].To be able to achieve this considerable goal, a better understanding of thermochemical degradation is needed.

Several review articles have appeared which summarize different aspects of biomass pyrolysis kinetics [3, 7-10]. These review articles focus on three main types of reactions: 1) single component model, often based off of mass loss data, 2) multicomponent models and 3) activation energy distribution models. Each of these models is useful in understanding phenomenological observations of how biomass degrades. Often single component models are used with respect to the rate of volatilization from biomass or biomass constituents studied using TGA [11-14]. An example of this model, shown below in Figure 5.1a, was described by the Shafizadeh and Chin model[14] used to describe the macroscopic behavior observed from the pyrolysis of wood. These types of models are useful in deciphering how the biomass is degrading with respect to temperature, and especially when evaluating the biomass individual components (hemicellulose, cellulose, lignin). Generally speaking, these models are in the form of a first order exponential decay.

Multicomponent models are useful in understanding multiple or sequential reactions that occur within the biomass, and they allow for a better understanding of the intermediates occurring within the biomass with respect to time and temperature. Di Blasi and Lanzetta first developed this model by evaluating the thermal degradation of xylan using TGA data [15], it was further evaluated by Lanzetta and Di Blasi from their study of corn straw and wheat [16]. The refined model states that the original biomass is degraded to an intermediate (B) and is then degraded into its final char product. For each reaction there is the production of volatiles. [16]. These models assume that the first reaction occurs much faster than consecutive reactions. These multicomponent models were the basis for developing the six consecutive reaction model by Klinger et al. [17]and a schematic of this model is shown below in Figure 5.1b. The six step degradation model takes a similar approach as Di Blasi and Lanzetta, however instead of one intermediate there are five intermediates to capture the biomass degradation. The six step degradation model was developed and explored through a range of temperatures from 260 °C to 425°C.

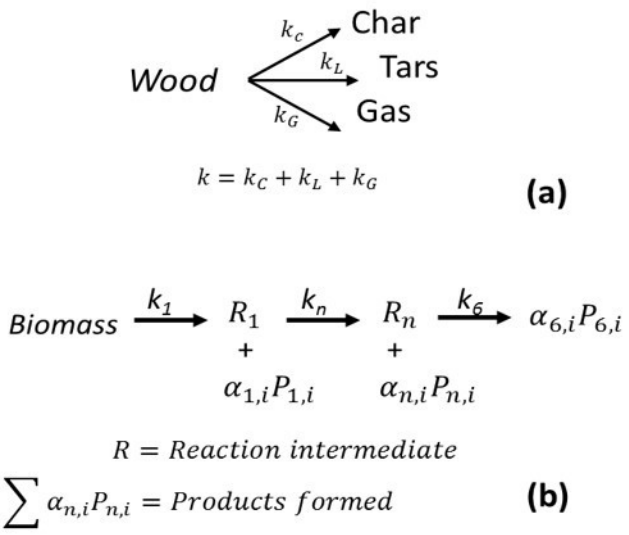

Figure 5.1: a) single component model adapted from [14] **b)** multicomponent model developed by Klinger et al. [17]

The distributed activation energy model (DAEM) assumes that there are numerous parallel first order reactions occurring within the model and that all reactions have the same activation energy. This model has been used to study the individual biomass components (hemicellulose, cellulose and lignin) and then combines them in a superposition model to represent the actual biomass.

These models are useful in predicting the amount of volatiles produced, but do not allow for any knowledge of intrinsic behavior of the biomass degrading with respect to time. Most of these models were developed using TGA. TGA is a useful tool to evaluate thermal degradation, but due to its low heating rates (typical maximum value of 100°C/min) cannot be considered fast pyrolysis. These results and kinetic data are not necessarily indicative of what happens during fast pyrolysis. One concern with slower heating rates is that when the biomass is volatilized, the solid residual is able to form

strong bonds within the remaining char, and ultimately producing less volatiles through a change of chemical mechanisms[11]. Generally, these models are based off of individual biomass components decomposing, but do not look at the biomass as a whole or understand the interactions occurring with biomass degradation.

Previously Klinger et al. [17], developed a six step consecutive reaction model that predicted the rate at which species evolve from the biomass based on the many types of biomass intermediates that occur during torrefaction and pyrolysis. This model was developed using the instantaneous generation of bio-oil compound ions detected by a mass spectrometer. Aside from looking at relative contributions from unique ions specific to the hemicellulose, cellulose and lignin, it did not focus on quantification of any individual bio-oil species produced with respect to time. This model assumes that the biomass is degraded into 5 intermediate solids and then produces the final char product. The model assumes that each sequential reaction step has the same approximate reaction rate constant for any of the species generated from that intermediate and lumps them into an approximate reaction stage, or, that the biomass as a whole degrades at the same rate. As the degradation occurs these reactions get slower with respect to time. The model uses scaling parameters to adjust for the magnitude of species production.

The continual development and study of pyrolysis has allowed for a greater understanding of how bio-oil is produced. However, previous understanding of pyrolysis and models have either focused on the speciation of bio-oil produced from cellulose, hemicellulose, lignin and/or various biomass [1, 2, 18-22] or looked at empirical or semi-empirical models that focused on char degradation and volatile and/or gas production

[12-14, 17, 23]. These individual understandings are useful in piecing together biomass degradation, however little has been done to look at bio-oil speciation within the context of pyrolysis kinetics.

Kinetic work has been done using TGA, due its ability to be coupled with gas analyzers and DSC and to measure the mass loss with respect to time [16, 24-27]. However as mentioned above TGA has limitations because it is not a fast-pyrolysis process and this technique tracks total mass loss rather than following the time course of individual chemical species that volatilize from the solid. Pilot plant reactors have been used to measure yields from fast-pyrolysis and have described the effects of secondary reactions by varying residence time within the reactor and evaluating bio-oil composition [13, 28-34]. However, in pilot scale reactions it is difficult to control the reaction environment due to heat, mass, and momentum transfer limitations and therefore to uncover fundamental reaction mechanisms and intrinsic kinetics. Micropyrolysis GC/MS experiments have primarily been used as a rapid screening process to show what type of bio-oil compound are produced but have not been used extensively for intrinsic kinetic work [20, 21, 35-37] . The novel aspect of this work is that the bio-oil speciation of fast-pyrolysis was evaluated with respect to time to study intrinsic kinetics of primary reactions, allowing various models to be applied to the data generated. This type of dynamic prediction of chemical species formation allows for a better understanding of the mechanisms of biomass degradation.

The main objectives of this research is to: 1) gain a better understanding of fast-pyrolysis reactions of biomass by measuring production of bio-oil species over time 2) evaluate

previous kinetic models of pyrolysis existing in literature, and 3) develop a greater knowledge of the relative rates of degradation of the biomass components of hemicellulose, cellulose and lignin.

5.3 Methods

DN34 hybrid polar was thermochemically treated using fast micro-pyrolysis up to different time points, and key bio-oil compounds were detected and quantified to understand how rapidly the biomass breaks down as a whole and with respect to the individual biomass constituents of hemicellulose, cellulose, and lignin.

5.3.1 Py-GC/MS Experiments

To understand the intrinsic kinetics of biomass degradation, fast micro-pyrolysis experiments were conducted at several time intervals, in triplicate at 500 °C. Pyrolysis experiments were conducted for 1 s, 2 s, 3 s, 5 s, 7 s, 10 s, 15 s, and 20s to understand biomass degradation with respect to time and the production of bio-oil chemical species changed with respect to time. Fast pyrolysis experiments were conducted and analyzed using a CDS 5200 HP pyroprobe coupled with gas chromatography (GC Trace Ultra, Thermofisher) and mass spectroscopy (DSQ II, Thermofisher). The experimental set up is shown below in Figure 5.2. The pyrolysis experiments took place at 500ºC within an interface zone kept at 300ºC. Due to the very short residence time (0.009) seconds, see Appendix C for calculation) of pyrolysis vapors within the zone of pyrolysis, these reactions are interpreted as the primary reactions forming vapors from the solid with a

minimum effect of secondary reactions that could otherwise occur with longer residence times.

The sample probe shown in Figure 5.2 was heated to a temperature of 500°C at a rate of 1000°C/sec for the various reaction times discussed above. 300-660 µg of hybrid poplar (DN34) with a particle size of 180 – 250 microns (80-60 Tyler mesh) were loaded into a quartz reactor vial between two glass wool plugs and placed in the sample probe. The sample was then dried at 120 °C for 10 minutes to ensure that any water produced during pyrolysis were not from bound moisture within the biomass but rather were from reaction water generation. Some samples were weighed before and after drying and no detectable mass change was observed, confirming that most samples tested were at zero moisture content. After drying, the interface was then heated to a temperature of 300°C. Upon reaching the interface temperature, the sample probe was then heated to 500°C for its designated time. The reaction zone was kept inert by ultra-high purity helium (99.999%) at a flow rate of 20 mL/min. Pyrolysis vapors were swept from the reaction zone through a heated transfer line kept at 300°C into the gas chromatograph kept initially at 35ºC.

The transfer line was connected to the inlet of the GC and kept at a temperature of 275°C. The pyrolysis vapors then condensed on the inlet of the column (Restek, Rxi-5ms, 30m x 0.25 mm, 0.25 um film thickness) which was kept at 35°C in the GC oven for 2 minutes. The column was then heated at a rate of 5°C/min until it reached 150°C where it then underwent a heating rate of 10°C upon reaching 275°C at which it was held for 2 minutes to ensure larger compounds were eluted through the column. Compounds were detected using the MS with the ion source kept at 275°C with an ionization potential of 70 eV.

Data was recorded using Thermofisher's Xcalibur software. Chromatograms and mass ionization specrtra was analyzed using this software. The char was then weighed using a microbalance with a readability of 10 ug (Mettler Toledo XS105DU)

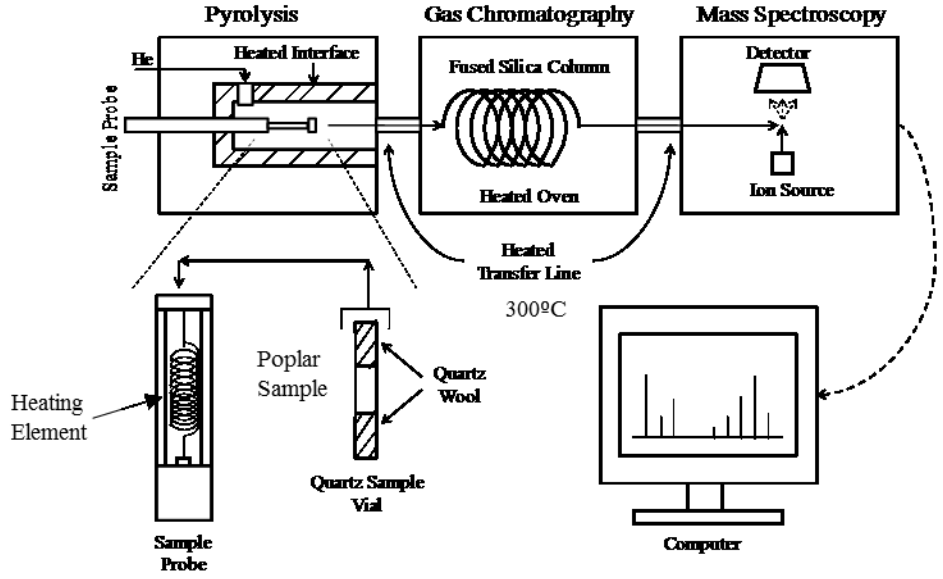

Figure 5.2: Experimental diagram for fast pyrolysis kinetic experiments conducted in this study[38]

5.3.2 Peak Identification

Compounds were identified using the library within the Xcalibur software or with the use of the NIST webbook [39]. Bio-oil species were categorized based on being representative of their parent component's (hemicellulose, cellulose, and lignin) degradation. Therefore acetic acid and furfural, were chosen to represent the degradation of the holocellulose within the biomass [25, 40-42]. Methyl syringol and guacicol were identified and used to show the degradation of the two different kinds of lignin present within the biomass, the syringyl monomer and the gualacyl monomer respectively.

Acetol was chosen to represent the degradation of the cellulose [36].concentrations [21, 36] . Levoglucosan was not detected in the initial chromatograms, but was detected during cleaning runs between samples. These results are shown in Appendix C.

5.3.3 Standards

Six chemical standards were run on the GC/MS: acetic acid, furfural, guaciol, methyl syringol, m-cresol and levoglucosan were run at concentrations of 0.15-40 ug/uL. All standards except for levoglucosan were mixed together with acetonitrile. 2 mL each of the liquid samples (acetic acid, furfural, guaiacol and m-cresol) and 1 g of methyl syringol were mixed with 48 mL of acetonitrile to generate the stock solution. The stock solution was then further diluted with acetonitrile in the following ratios) 1:1, 2:1, 5:1, 10:1, 50:1 and 100:1. The levoglucosan was prepared in a similar manner but was dissolved in DMSO. 1 g of levoglucosan was dissolved in 30 mL of DMSO and then diluted to the same ratios listed above. 2 mL of each stock solution was placed in an autosampler vial. 1 uL of each sample was injected into the GC/MS using an AI 1310 autosampler (Thermofisher), this was done in triplicate. The samples were identified using their unique mass charge fragmentation and analyzed using Thermofisher's Xcalibur software. The peak area detected for each compound within the stock solutions was calculated and plotted (x-axis) against its respective mass injected (y-axis). The response factor was calculated by taking the slope of that line. The response factor was then used to quantify the samples detected in this study. The levoglucosan standard was unable to be calibrated properly, therefore the response factor used in our previous work [20] was used and adjusted based on the ratios of the response factors for the 5 other

compounds to the response factors in previous work. The acetic acid standard was used to determine the mass of the glycolic acid and the acetol due to lower molecular weight species having similar response factors. The calibration curves and their response factors are shown in Appendix C in Table C.1 and Figure C.1.

5.3.4 Kinetic Modelling

Two kinetic models were used to fit to the experimental data. The first model was one commonly employed using TGA. It is a first order exponential decay with the weight loss curve escribed as

$$\frac{d(\alpha)}{(1-\alpha)} = kdt$$

Where α is the ratio of biomass reacted compared to the total biomass reacted and is given by the equation,

$$\alpha = \frac{w_o - w}{w_o - w_f}.$$

Where w_o is the initial biomass, w is the mass of the biomass at any time and w_f is the final mass of the reacted biomass. Inversely, this can be related to the amount of volatiles produced at any given time (V), versus the total amount of volatiles produced (V_t), therefore

$$\alpha = \frac{V}{V_t}.$$

This model is primarily used for weight loss curves, but can be applied to the production of bio-oil species if the final amount of volatiles produced is known. In this work is was

assumed that the pyrolysis experiments run at 20 seconds give the final total amount of each compound produced (V_t). The volatiles produced for the model compounds (acetic acid, glycolic acid, acetol, methyl syringol and guaiacol) were normalized by their final weight percent of compounds produced and the model described above was applied. This normalization places the data on a basis such that the degradation dynamics can be interpreted without weight-impacts of the ash, fixed carbon, or other recalcitrant structures at these reaction conditions. The reaction rate was calculated by fitting the model to the data and minimizing the summed squared error by changing the k value using Excel's solver function.. The k value was then applied within the first order model and plotted against the normalized data to determine if a first order decay model is a good fit for the experimental data produced in this study.

The second type of model applied was the multicomponent model developed previously by Klinger et al. [17]. The multicomponent model uses a lumped approach to approximate biomass degradation through six consecutive reactions. The model assumes that the biomass proceeds through a series of solid quasi-intermediates that represent partially degraded constituents. These solid structures are not necessarily distinct intermediates, but represent average solid residuals over the range of degradation. At each of these reaction stages, volatiles are produced through the same reaction rate constant and thus presents a lumped approach to approximating many simultaneous reactions that occur with similar kinetics. The magnitude of chemical species production is controlled through so-called stoichiometric factors, and represent how much of a compound is produced in the respective reaction stages. The model is shown below.

$$Biomass \xrightarrow{k_{1,i}} R_1 + \sum \alpha_{1,i} P_{1,i} \qquad \text{Rxn 1}$$

$$R_{j-1} \xrightarrow{k_{j,i}} R_j + \sum \alpha_{j,i} P_{j,i} \qquad \text{Rxn (2-6)}$$

R_j represents the biomass intermediate and α is a stoichiometric parameter representing the amount of that specific product (i) formed from each biomass intermediate. Some pyrolysis products may or may not be formed in significant quantities from certain reactions of the biomass intermediate degrading.

The six stage consecutive model was developed and reported as a kinetic rate model, therefore in this work the integral of the model was taken to match the production data in this study. The char data was used to fit the rate constant values because char mass was a direct measurement, and we believe has higher accuracy than the bio-oil species measurements. In addition, volatile species may or may not be formed at each of the respective reaction stages. The degradation of the solid material, however, shows the overall or summative release of all the volatile species and is affected significantly through each reaction stage. Although the previous study investigated lower pyrolysis temperatures, the Arrhenius parameters reported in Klinger et al. [17]were used to extrapolate initial guesses to fit the model kinetics to the char data. The model fitting was done by minimizing the summed square error between the experimental data and the model by changing the model parameters.

After the rate constant values were determined from the fit to the char data, these constants were assumed to represent the lumped kinetics of volatiles production, and were used in the fitting of individual bio-oil species production. The reaction rates remain

the same for all species produced, however the values of α were changed to allow for different production rates among the species for each reaction step. The α's were fit to the data by minimizing the error between the model and the experimental data.

5.4 Results

5.4.1 Experimental Results

Pyrolysis experiments were done in triplicate at various discreet time points as described above in the methods section. The weight percent of these compounds are shown below in Figures 5.3 and 5.4**.** The figures are categorized into compounds derived from holocellulose and lignin. For the holocellulose derived compounds the most rapidly produced species is acetic acid. The initial concentration spikes to 2.7 wt% and between 3-5 seconds plateaus at approximately 3.3%. The data indicates that most of the acetic acid is produced nearly instantaneously at the beginning of pyrolysis. Furfural and glycolic acid behave similarly. They are produced in significant quantities initially, as shown below in Figure 5.3 b and c**,** however the time at which the production rate stops is approximately 5-7 seconds indicating that it takes a longer time to generate these compounds compared to acetic acid.

The lignin compounds behave very differently compared to the hemicellulose-derived compounds in bio-oil. The lignin compounds studied were methyl syringol and guiacol to represent the monomers that are produced through the depolymerization of the lignin structure of hardwoods[43-45]. The initial production with time of these monomers is very slow, especially compared to furfural and acetic acid. The maximum amount of

product produced happens between 7-10 seconds, after the hemicellulose has plateaued its production of low molecular weight species and furans. This suggests that the lignin does not begin to depolymerize to form volatile products at a fast rate until the hemicellulose structure begins its degradation.

Acetol behaves in a different manner compared to the other lower molecular weight species and is generally derived from the degradation of cellulose. Initially, very little acetol is produced, 0.41% at 1 s and at a slower rate continues to produce acetol until 7 seconds where it plateaus at approximately 2%. Even though similar amounts of acetic acid hydroxyl and acetol are being produced after 7 seconds, the rate at which they are initially produced is very different, indicating that cellulose doesn't degrade until a later time in the pyrolysis process. Compared to the hemicellulose-derived compounds, the methyl syringol, guaiacol and acetol have a delayed production response, reach their maximum production between 7-10 seconds after the hemicellulose has fully degraded and the hemicellulose derived products plateau in production.

Hemicellulose is thought of as "the glue" that holds the biomass together. Therefore, it may be difficult for the lignin or cellulose to begin degrading until the hemicellulose has degraded, allowing for these monomers to be volatilized. Previous TGA models have looked at the biomass degradation as a whole and tried to interpret it within the context of individual biomass components degrading, however due to lack of speciation or knowing production rates of bio-oil compounds, it is difficult to ascertain. This data, like that of TGA data, suggests that the production of bio-oil compounds occurs at different rates depending on its original parent material. Therefore, it is important to understand the

reaction rates with respect to the mechanistic degradation of the individual components within the biomass structure.

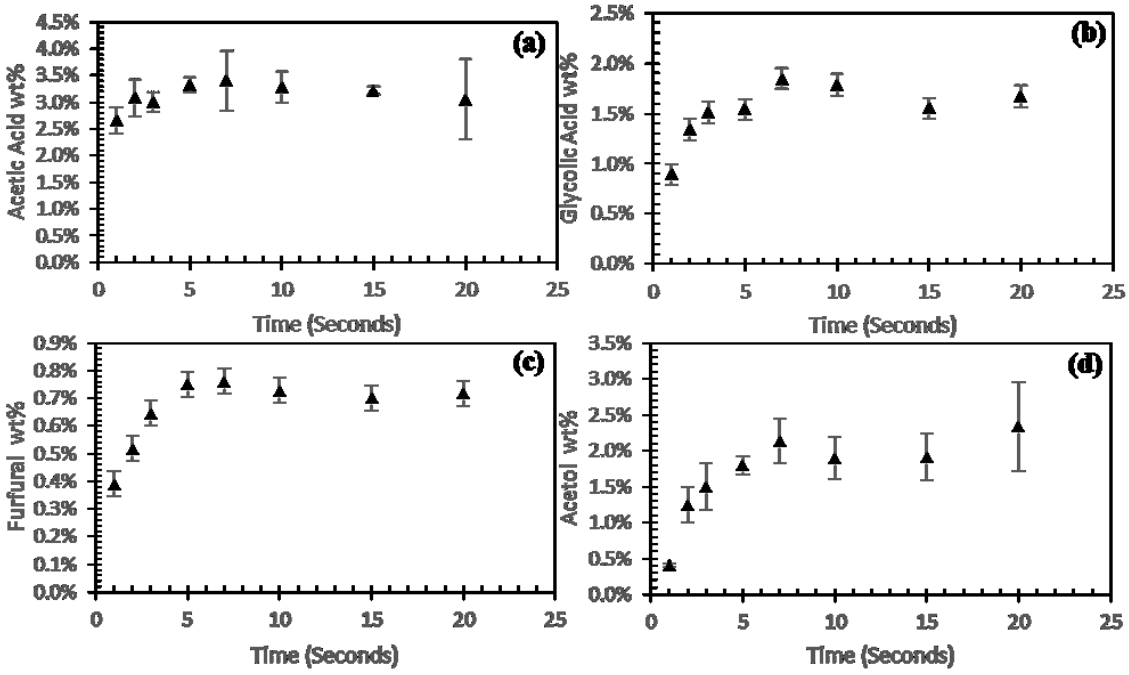

Figure 5.3: Production of bio-oil compounds generated from the holocellulose with respect to the original biomass a) acetic acid, b) glycolic acid, c) furfural, d) acetol

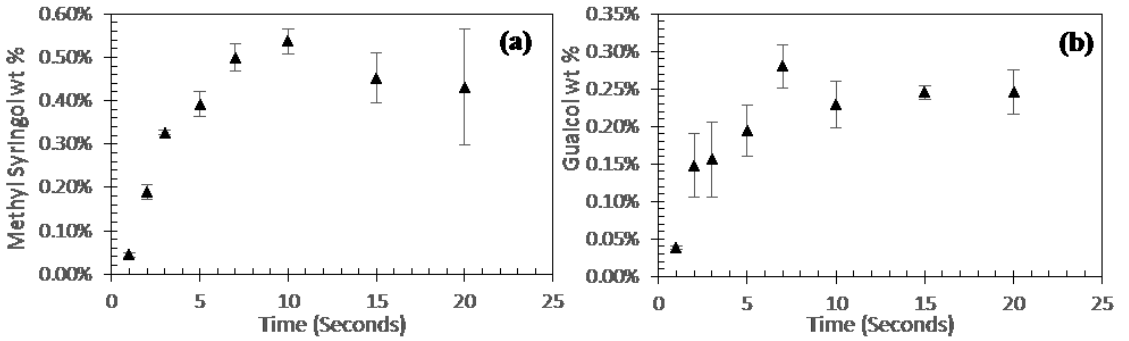

Figure 5.4: Production of bio-oil compounds generated form the lignin with respect to the original biomass a) methyl syringol, b) guaciol

5.4.2 Modelling Results

5.4.2.1 First order decay model

The first order decay model was fit to the data. The data was normalized to allow for a comparison among the k values. As expected from the experimental results the hemicellulose compounds, acetic acid, glycolic acid and furfural, had the highest reaction rate *k* values, whereas acetol and the lignin compounds had lower *k* values. This shows that the acetic acid is being produced the fastest and that it takes longer to produce the lignin-derived compounds. These first order decay models are generally used with TGA data and therefore when comparing the reaction rates, the values in this work are much faster than those within the TGA literature.

Using this model matches the overall time-dependent trends in the data, but does not closely match at early times for either the species that exhibit a delay or over predicts the intermediate data when the compounds are produced rapidly. The first order decay model was also fit to the char data. The char data visually resembles TGA mass loss data seen in literature where there is a rapid decrease with severity and then plateaus [16, 46]. As observed below in Figure 5.7 the kinetic data behaves similarly to that observed in the bio-oil produced, this model has a difficult time capturing the intermediate time dynamics. The exponential decay model over predicts the amount of char and volatiles produces from 5-10 seconds, indicating that more than one reaction may be occurring.

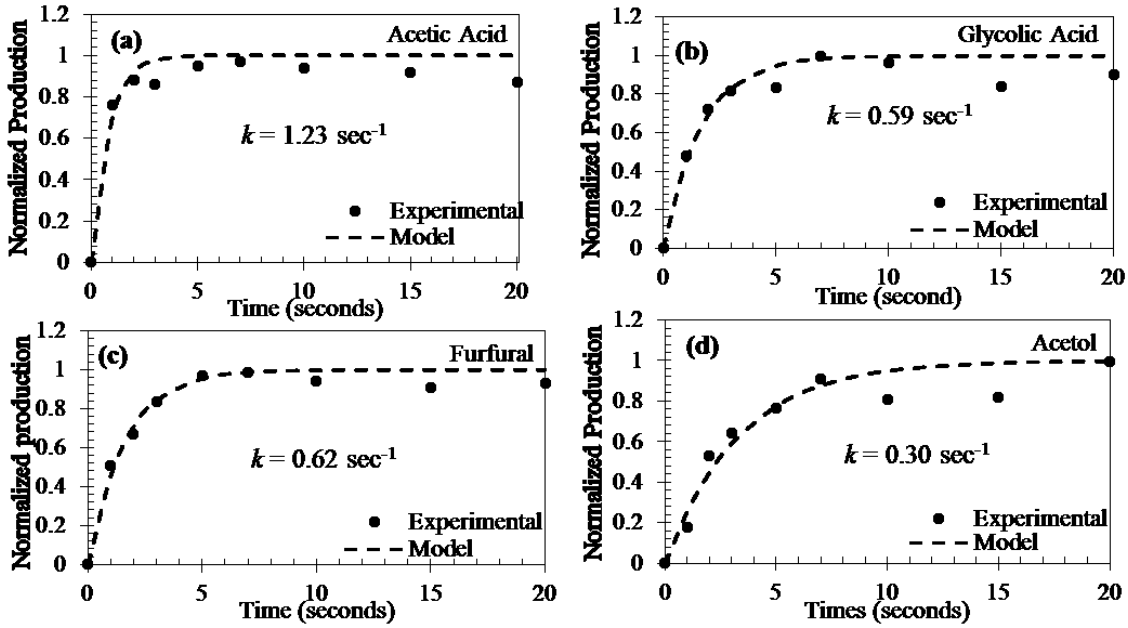

Figure 5.5: Normalized production fit with a first order decay model for compounds derived from the degradation of holocellulose a) acetic acid, b) glycolic acid, c) furfural and d) acetol

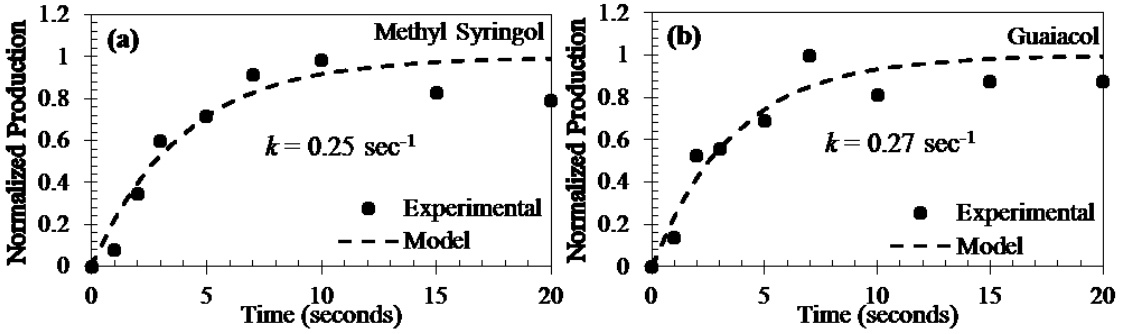

Figure 5.6: Normalized production fitted with a first order decay model for compounds derived from the degradation of lignin a) methyl syringol and b) guaiacol

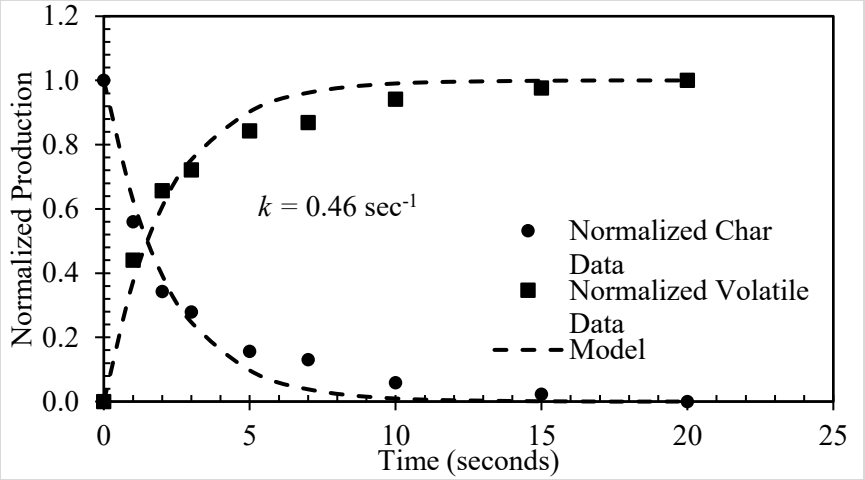

Figure 5.7: Normalized production of total volatiles and mass loss with respect to time fit to the first order exponential

5.4.2.2 Six-Step Degradation Model

A six consecutive reaction model previously developed by Klinger, et al. [17]was applied to the experimental results. The reaction rates were extrapolated from previous work as described above in the methods section. The extrapolated reaction rates were used as initial guesses in the model fitting and are shown in Table 1. The reaction rate constants were then fit to the char data as shown below in Figure 8. The difference in the extrapolated *k's* vary from the calculated *k's* due to smaller errors being magnified due the exponential form of the Arrhenius Kinetics. These reaction rates were then used for all species and the α's were fit to each species individually and are shown in Table 1. The fit of the six-step sequential model to the char data is shown in Figure 8. It is important to note that as the reaction temperature increases more reaction intermediates may be needed to account for the changing biomass. This model was originally generated at a maximum temperature of 425°C and as we continue to increase the temperature a 7th

reaction may be needed. However, this degradation model fits the data very well with six reactions and is superior than the exponential decay model fit shown in Figure 7. The sum squared difference between the six-step degradation model and the experimental char data was a factor of 24 times smaller than that of the exponential decay model and the char data, 0.023 and 0.00096 respectively.

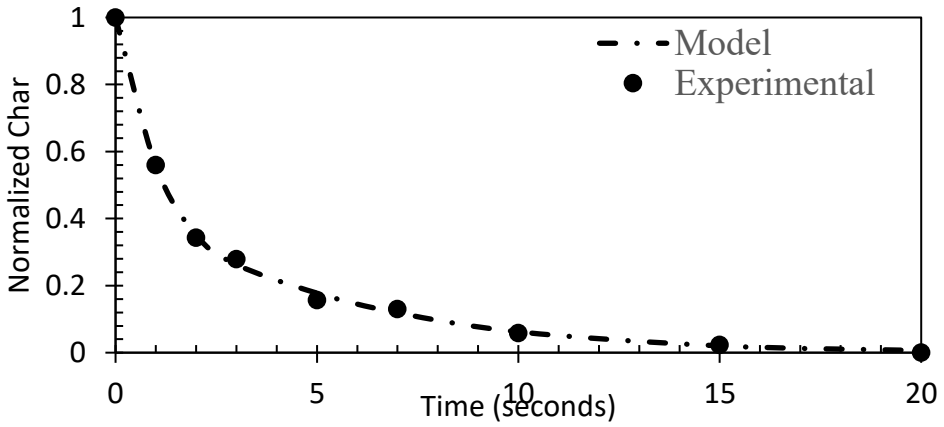

Figure 5.8: Normalized char data fit to the 6 step consecutive model to determine the k values as shown in Table 1.

The experimental data, shown in the figures above, suggests that hemicellulose degrades much quicker than the lignin derived compounds as well as the cellulose-derived acetol. From previous TGA literature it is known that hemicellulose degrades at temperatures of 220-315°C, cellulose begins to degrade at 315-400°C and lignin degrades over a long temperature range[11, 47]. TGA data shown in the literature of the pyrolysis of these individual biomass constituents supports the data from this study. However, when looking at the literature no reaction mechanism has been able to illustrate this concept. When fitting the six consecutive reaction model the α's, or the stoichiometric values, were calculated for each species and are used to observe which reaction or reactions are

contributing the most to the degradation of the biomass occurring. The model fits for the experimental data are shown in Figures 5.9 and 5.10.

The six step degradation model fits the experimental data very well. As observed in Figure 5.9, this model is able to predict the amount of bio-oil produced for each compound derived from the holocellulose as shown by the shape of the model curve going through nearly all of the experimental data points. This model is able to capture the very quick production of acetic acid and can still capture the delay in acetol production as well. When modelling the compounds derived from lignin, the model is able to capture the delayed production on methyl syringol, and still captures the delay in guiacol and large increase in production from 1-2 seconds as shown in Figure 5.10b. The model is not able to go through all of the data points, but still captures the general trend of guaiacol production with respect to time.

To understand how the biomass is being degraded, or conversely how the bio-oil compounds are produced, the α's (stoichiometric coefficients for each reaction step) provide insight into the mechanisms of the biomass degradation. The α values for each bio-oil compounds studied are shown in Table 5.2. In general, the α values for hemicellulose-derived bio-oil compounds such as acetic acid and furfural are higher in reaction steps 1-3 and lower in reaction steps 4-6, indicating that these compounds are produced earlier in the sequence of pyrolysis reactions. Lignin and cellulose-derived compounds in bio-oil are in general produced later in the sequence of reactions.

The normalized α's that were fit to this kinetic experimental data are shown for all of the compounds below in Figure 5.11. α_i represents the amount (weight percent produced in

each reaction step) of each compound produced for each reaction step i, therefore normalizing α_i by the total weight percent produced for each species ($\sum_1^6 \alpha_i$) allows for an accurate determination of which reaction step produced the majority of the compound. Figure 5.11 allows for a comparison across all compounds studied of what reaction steps contributed to the production of each bio-oil compound.

Table 5.1: Kinetic values determined from fitting the six step consecutive model to the normalized char data

Reaction	*Extrapolated k (min^{-1})*	*Calculated k* (min^{-1})
1	303	315
2	286	270
3	251	144
4	203	76
5	166	45
6	50	13.5

Figure 5.10 and Table 5.2 allow for a better understanding of how the biomass is degrading with respect to time. We can also refer to it as the biomass degrading with respect to increasing severity with time as the main severity axis for a constant temperature experiment. The hemicellulose degrades at shorter times, or with less severe conditions, as shown by the large normalized α1, α2 and α3 values. Nearly 90% of acetic acid is derived within the first three reactions. Furfural, which also is derived from the degradation of hemicellulose is substantial within those first 3 reactions, approximately 50% of furfural has degraded within the first 3 reactions. Cellulose degradation, as observed by the acetol, occurs quite substantially within reaction 4 as indicated by 70% of the acetol produced in reaction 4 as shown by *α4.* The $\alpha's$ originally calculated for the

six-step degradation model show that species from each biomass constituent react throughout the entire reaction. The hemicellulose primarily degrades within the first three reactions, however some guaiacol is produced within that first reaction as well. Though the majority of the hemicellulose degrades within (Rxn 1-3) 10% of the acetic acid and 25% of the glycolic acid are produced in Rxn 5.The $\alpha's$ show that the lignin and cellulose compounds degrade more substantially with later reactions (Rxn 3- 6), with over 50% of the guiacol and methyl syringol being produced in Rxn 5. This data shows that the hemicellulose needs to begin degradation before other biomass components can start to fully degrade. This micro-pyrolysis gc/ms data mirrors the understanding of TGA data in which the hemicellulose degrades first with time, followed by the cellulose, and the lignin degrades throughout the entire temperature profile [47], but mostly at later times in the reaction.

Table 5.2: α's determined for the experimental data for the bio-oil compounds. α's represent the amount of each species produced with the specified reaction

Compound	α_1	α_2	α_3	α_4	α_5	α_6
Acetic Acid	0.0139	0.0066	0.0091	1 E-6	0.0029	1 E-6
Glycolic Acid	2 E-6	2 E-6	0.0120	0.0007	0.0041	0.0002
Furfural	0.0024	0.0009	4 E-6	0.0026	0.0013	0.0002
Acetol	1 E -6	1 E -6	1 E -6	0.0153	0.0018	0.0043
Guaciol	0.0003	0.0002	0.0001	0.0004	0.0014	0.0005
Methyl Syringol	1 E -6	2 E -6	0.0002	0.0016	0.0025	0.0005

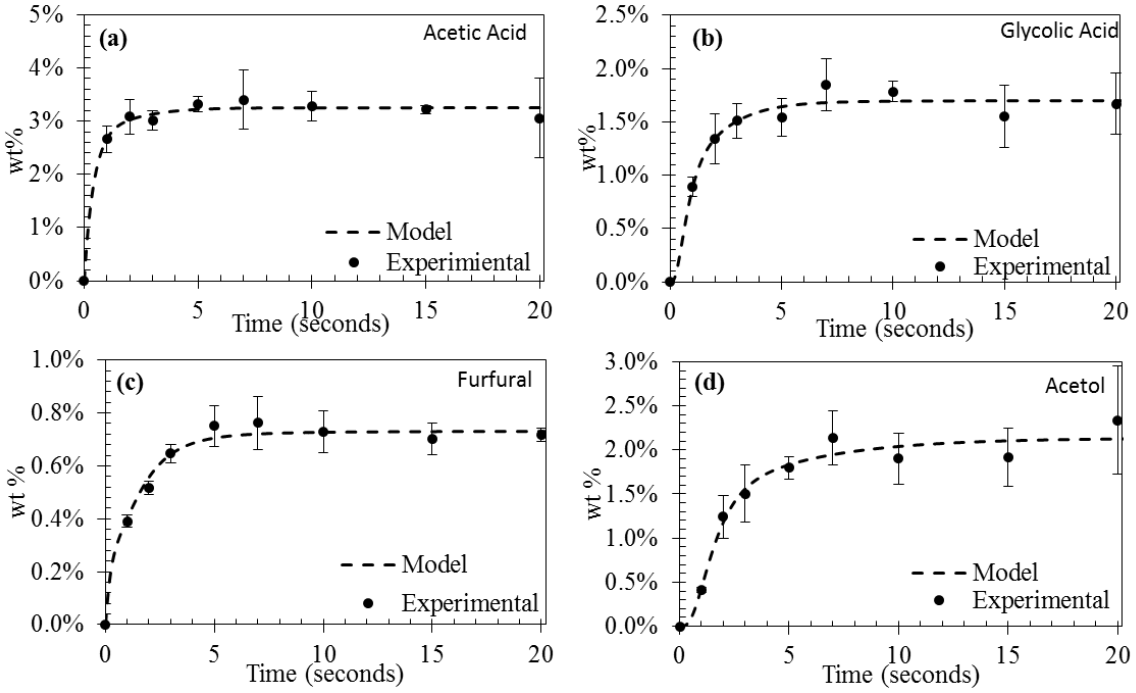

Figure 5.9 Experimental data fitted to the six consecutive reaction model for compounds derived from the degradation of hollocellulose a) acetic acid, b) glycolic acid, c) furfural and d) acetol (from cellulose)

The lignin needs more severe conditions to degrade, or at these constant temperature experiments, a longer amount of time as shown by the experimental results. This is illustrated with the use of this six consecutive degradation model with the large normalized α4 and α5 values. Reaction 6 is a culmination of the last final remains of the biomass degrading. Therefore, with respect to this six consecutive step model we can think of the degradation as follows:

$$k_1 to\ k_3 = dominated\ by\ hemicellulose\ degradation$$

$$k_4 = cellulose\ degradation > lignin\ degrdation$$

$$k_5 = lignin\ degradation > cellulose\ degradation$$

$$k_6 = final\ degradation\ of\ the\ biomass$$

This experimental data, which measured bio-oil species at different time points allows for a way to test and evaluate various types of pyrolysis kinetic models. The six consecutive reaction model gives a very good fit with the experimental data and allows for a better understanding of the biomass degradation, as shown in Figures 5.9 - 5.11. The kinetic data in these experiments allowed for the six consecutive reaction model to be independently tested with individual bio-oil species. Application of the six-step degradation model to this experimental data allows for better insight and knowledge of this model. The model was originally developed using the rate of production of ions instead of quantified bio-oil species. This experimental kinetic data allows for more accurate kinetic parameters to be obtained. The six consecutive reaction model is adaptable to various data collected, along with the ability to be applied to various biomass with different thermal degradation severities.

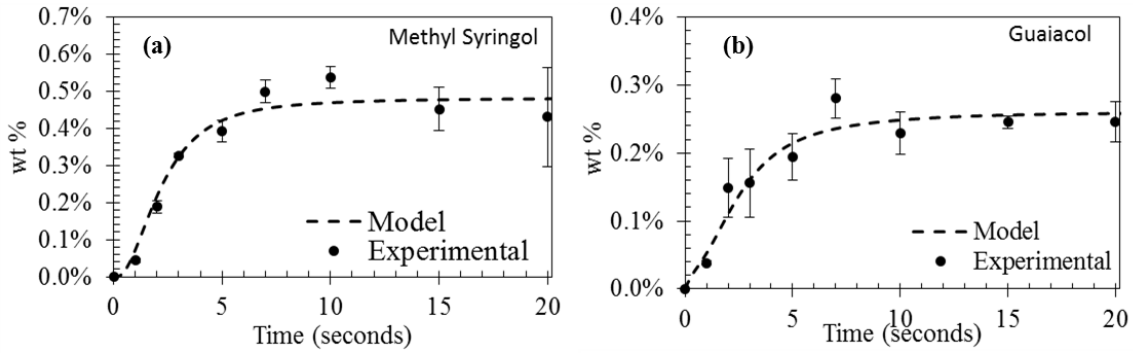

Figure 5.10 Experimental data fitted to the six consecutive reaction model for compounds derived from the degradation of lignin a) methyl syringol b) guaiacol

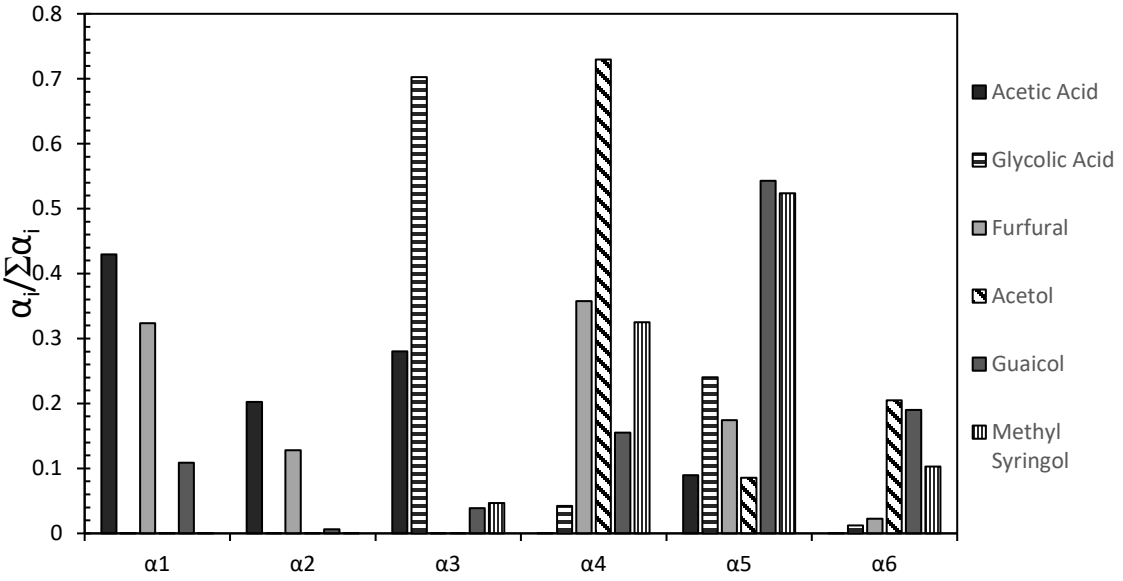

Figure 5.11: Alphas for each model compound normalized to the total amount produced for each of the compounds.

5.5 Conclusion

The results from this study provide a novel set of data compared to the prior pyrolysis literature for measuring the rates of production of specific bio-oil compounds and to evaluate intrinsic kinetic models. The key novel aspect is that the experimental data represents integrated production of individual bio-oil compounds over a controlled period of reaction time. Most prior experiments measured biomass loss or followed rates of production of bio-oil ion fragments, which may have emerged from different bio-oil species. These experimental results give a better understanding bio-oil speciation and production of compounds with respect to discrete time points. In addition, this study allowed for a better understanding of how rapidly components in biomass degrade with respect to time. The first order exponential decay model fit the char and bio-oil compounds data trends reasonably well, but had a difficult time capturing fast reactions

initially or delays in production, like that of the acetic acid and guaiacol, respectively. The first order exponential decay models did show that certain compounds were produced faster with the higher reaction rates that were fit to the data, however no mechanistic behavior of the biomass degradation was able to be determined. The six step consecutive reaction model was able to fit the data the best. It was able to capture the initial fast production of acetic acid and accurately predict the relatively slow production of compounds like guaiacol. This work independently confirms the six step consecutive reaction model developed previously, by applying a set of data to the model, resulting in a good fit. This work allows for a better understanding of the model with respect to bio-oil compounds produced and allows for a understanding of the mechanisms of biomass degradation. The α values plotted in Figure 5.11, mathematically show that different parts of the biomass degrade with respect to its individual components as previously observed from TGA data. This work allows for a new set of experimental data to compare kinetic models to and validates the six step consecutive model.

5.6 Acknowledgments

The authors would like to gratefully acknowledge the National Science Foundation grant MSP/CHE-ENG/ECCS-1230803 for support of this work through a sustainable Energy Pathways Grants, and the Richard and Bonnie Robbins Endowment.

5.7 References

1. Mohan, D., C.U. Pittman, and P.H. Steele, *Pyrolysis of wood/biomass for bio-oil: a critical review.* Energy & Fuels, 2006. **20**(3): p. 848-889.
2. Kan, T., V. Strezov, and T.J. Evans, *Lignocellulosic biomass pyrolysis: A review of product properties and effects of pyrolysis parameters.* Renewable and Sustainable Energy Reviews, 2016. **57**: p. 1126-1140.
3. Bridgwater, A.V., *Review of fast pyrolysis of biomass and product upgrading.* Biomass and Bioenergy, 2012. **38**: p. 68-94.
4. Adminstration, U.S.E.I., *Monthly Energy Review (March 2015)*, EIA, Editor. 2014: eia.gov.
5. Perlack, R.D., et al., *Biomass as feedstock for a bioenergy and bioproducts industry: the technical feasibility of a billion-ton annual supply*. 2005, DTIC Document.
6. Energy, U.S.D.o., *U.S. Billion-Ton Update: Biomass Supply for a Bioenergy and Bioproducts Industry*, R.D.P.a.B.J.S. (Leads), Editor. 2011: Oak Ridge National Laboratory, Oak Ridge, TN. p. 227.
7. Sharma, A., V. Pareek, and D. Zhang, *Biomass pyrolysis—A review of modelling, process parameters and catalytic studies.* Renewable and Sustainable Energy Reviews, 2015. **50**: p. 1081-1096.
8. Di Blasi, C., *Modeling chemical and physical processes of wood and biomass pyrolysis.* Progress in Energy and Combustion Science, 2008. **34**(1): p. 47-90.

9. White, J.E., W.J. Catallo, and B.L. Legendre, *Biomass pyrolysis kinetics: A comparative critical review with relevant agricultural residue case studies.* Journal of Analytical and Applied Pyrolysis, 2011. **91**(1): p. 1-33.

10. Papari, S. and K. Hawboldt, *A review on the pyrolysis of woody biomass to bio-oil: Focus on kinetic models.* Renewable and Sustainable Energy Reviews, 2015. **52**: p. 1580-1595.

11. Collard, F.-X. and J. Blin, *A review on pyrolysis of biomass constituents: Mechanisms and composition of the products obtained from the conversion of cellulose, hemicelluloses and lignin.* Renewable and Sustainable Energy Reviews, 2014. **38**: p. 594-608.

12. Thurner, F. and U. Mann, *Kinetic investigation of wood pyrolysis.* Industrial & Engineering Chemistry Process Design and Development, 1981. **20**(3): p. 482-488.

13. Gorton, C. and J. Knight. *Oil from biomass by entrained-flow pyrolysis*. in *6. symposium on biotechnology for fuels and chemicals. Gatlinburg, Ten.(USA). 15-18 May 1984.* 1984.

14. Shafizadeh, F. and P.P. Chin. *Thermal deterioration of wood*. in *ACS Symposium Series American Chemical Society*. 1977.

15. Di Blasi, C. and M. Lanzetta, *Intrinsic kinetics of isothermal xylan degradation in inert atmosphere.* Journal of Analytical and Applied Pyrolysis, 1997. **40**: p. 287-303.

16. Lanzetta, M. and C. Di Blasi, *Pyrolysis kinetics of wheat and corn straw.* Journal of Analytical and Applied Pyrolysis, 1998. **44**(2): p. 181-192.

17. Klinger, J., E. Bar-Ziv, and D. Shonnard, *Unified kinetic model for torrefaction–pyrolysis.* Fuel Processing Technology, 2015. **138**: p. 175-183.

18. Caballero, J.A., et al., *Pyrolysis kinetics of almond shells and olive stones considering their organic fractions.* Journal of Analytical and Applied Pyrolysis, 1997. **42**(2): p. 159-175.

19. Di Blasi, C., et al., *Pyrolytic behavior and products of some wood varieties.* Combustion and Flame, 2001. **124**(1): p. 165-177.

20. Klemetsrud, B., et al., *Characterization of Products from Fast Micropyrolysis of Municipal Solid Waste Biomass.* ACS Sustainable Chemistry & Engineering, 2016. **4**(10): p. 5415-5423.

21. Patwardhan, P.R., R.C. Brown, and B.H. Shanks, *Product distribution from the fast pyrolysis of hemicellulose.* ChemSusChem, 2011. **4**(5): p. 636-643.

22. Stefanidis, S.D., et al., *A study of lignocellulosic biomass pyrolysis via the pyrolysis of cellulose, hemicellulose and lignin.* Journal of Analytical and Applied Pyrolysis, 2014. **105**: p. 143-150.

23. Di Blasi, C. and C. Branca, *Kinetics of primary product formation from wood pyrolysis.* Industrial & engineering chemistry research, 2001. **40**(23): p. 5547-5556.

24. Slopiecka, K., P. Bartocci, and F. Fantozzi, *Thermogravimetric analysis and kinetic study of poplar wood pyrolysis.* Applied Energy, 2012. **97**: p. 491-497.

25. Shen, D., S. Gu, and A.V. Bridgwater, *Study on the pyrolytic behaviour of xylan-based hemicellulose using TG–FTIR and Py–GC–FTIR.* Journal of analytical and applied pyrolysis, 2010. **87**(2): p. 199-206.

26. Worasuwannarak, N., T. Sonobe, and W. Tanthapanichakoon, *Pyrolysis behaviors of rice straw, rice husk, and corncob by TG-MS technique.* Journal of Analytical and Applied Pyrolysis, 2007. **78**(2): p. 265-271.

27. Liu, Q., et al., *Mechanism study of wood lignin pyrolysis by using TG–FTIR analysis.* Journal of Analytical and Applied Pyrolysis, 2008. **82**(1): p. 170-177.

28. Newalkar, G., et al., *Effect of Temperature, Pressure, and Residence Time on Pyrolysis of Pine in an Entrained Flow Reactor.* Energy & Fuels, 2014. **28**(8): p. 5144-5157.

29. Jia, L., et al., *Fast Pyrolysis in a Microfluidized Bed Reactor: Effect of Biomass Properties and Operating Conditions on Volatiles Composition as Analyzed by Online Single Photoionization Mass Spectrometry.* Energy & Fuels, 2015. **29**(11): p. 7364-7374.

30. de Diego, L.F., et al., *Modeling of the devolatilization of nonspherical wet pine wood particles in fluidized beds.* Industrial & engineering chemistry research, 2002. **41**(15): p. 3642-3650.

31. Jand, N. and P.U. Foscolo, *Decomposition of wood particles in fluidized beds.* Industrial & engineering chemistry research, 2005. **44**(14): p. 5079-5089.

32. Saastamoinen, J., *Simplified model for calculation of devolatilization in fluidized beds.* Fuel, 2006. **85**(17): p. 2388-2395.

33. Di Blasi, C., *Modelling the fast pyrolysis of cellulosic particles in fluid-bed reactors.* Chemical Engineering Science, 2000. **55**(24): p. 5999-6013.

34. Di Blasi, C., *Modeling intra-and extra-particle processes of wood fast pyrolysis.* AIChE journal, 2002. **48**(10): p. 2386-2397.

35. Patwardhan, P.R., R.C. Brown, and B.H. Shanks, *Understanding the fast pyrolysis of lignin.* ChemSusChem, 2011. **4**(11): p. 1629-1636.

36. Patwardhan, P.R., et al., *Product distribution from fast pyrolysis of glucose-based carbohydrates.* Journal of Analytical and Applied Pyrolysis, 2009. **86**(2): p. 323-330.

37. Patwardhan, P.R., et al., *Influence of inorganic salts on the primary pyrolysis products of cellulose.* Bioresource Technology, 2010. **101**(12): p. 4646-4655.

38. Klinger, J., E. Bar-Ziv, and D. Shonnard, *Kinetic study of aspen during torrefaction.* Journal of Analytical and Applied Pyrolysis, 2013. **104**: p. 146-152.

39. Stein, S.E., *Mass Spectra*, in *NIST Chemistry WebBook, NIST Standard Reference Database Number 69*, P.J. Linstron, Mallard, W.G., Editor., National Institute of Standards and Technology Gaithersburg, MD 20899.

40. Shen, D. and S. Gu, *The mechanism for thermal decomposition of cellulose and its main products.* Bioresource Technology, 2009. **100**(24): p. 6496-6504.

41. Peng, Y. and S. Wu, *The structural and thermal characteristics of wheat straw hemicellulose.* Journal of Analytical and Applied Pyrolysis, 2010. **88**(2): p. 134-139.

42. Wu, Y.-m., et al., *Low temperature pyrolysis characteristics of major components of biomass.* Journal of Fuel Chemistry and Technology, 2009. **37**(4): p. 427-432.

43. Huang, Y., et al., *Study on structure and pyrolysis behavior of lignin derived from corncob acid hydrolysis residue.* Journal of Analytical and Applied Pyrolysis, 2012. **93**: p. 153-159.

44. Mu, W., et al., *Lignin pyrolysis components and upgrading—technology review.* BioEnergy Research, 2013. **6**(4): p. 1183-1204.

45. Kibet, J., L. Khachatryan, and B. Dellinger, *Molecular products and radicals from pyrolysis of lignin.* Environmental science & technology, 2012. **46**(23): p. 12994-13001.

46. Branca, C. and C. Di Blasi, *Kinetics of the isothermal degradation of wood in the temperature range 528–708 K.* Journal of Analytical and Applied Pyrolysis, 2003. **67**(2): p. 207-219.

47. Yang, H., et al., *Characteristics of hemicellulose, cellulose and lignin pyrolysis.* Fuel, 2007. **86**(12): p. 1781-1788.

6. Conclusions and Recommendations for Future Work

This dissertation research investigated the experimental and intrinsic kinetic modeling of thermochemical reactions of a variety of advanced feedstocks for production of pyrolysis bio-oil, which is an intermediate for production of hydrocarbon biofuels and potentially high value chemicals. In addition, this research covered broader sustainability issues of advanced biofuels through a literature review and critical analysis of previous environmental life cycle assessments in the literature within the Pan American region.

Understanding how production distributions (char, gas and bio-oil yields) are affected by different biomass feedstocks and varying process conditions (i.e temperature, acid washing) allows for a better assessment of the sustainability of pyrolysis based biofuels during the conversion stage of an LCA. Higher bio-oil yields from hybrid poplar convey that less biomass is needed, reducing the impacts from the cultivation stage for the final biofuel product. However if a better quality bio-oil can be produced (less oxygen, reduced amounts of acidic compounds, higher average molecular weight) can be achieved it can reduce the amount of hydrogen needed within the upgrading step of the bio-oil, decreasing the impacts from the upgrading step. The tradeoff to a better quality bio-oil is that the overall bio-oil yield is reduced thereby increasing the impacts from the cultivation stage. To have a better understanding of these tradeoffs (lower upgrading impacts vs higher cultivation impacts) future process simulations derived from this experimental work coupled with LCA's will allow for an overall better assessment of the

sustainability of pyrolysis based biofuels. The following paragraphs provide a summary of key findings and recommendations for future research.

This research evaluated the theoretical sustainability of biofuels across the Pan American region through the analysis of different policy frameworks used across the Americas. The differences in methodological choices gave way to large differences in greenhouse gas emissions as shown in Chapter 2. As illustrated by the case study, policy differences play a large role in GHG emissions and compliance with one policy or certification scheme does not mean compliance with the other. Life cycle assessments in the Pan American region vary greatly due to, feedstocks used, geographical changes, impacts studied, system boundaries used, allocation methods chosen and policy adhered to. One of the largest emissions for greenhouse gas emission came from the agricultural stage. One way to avoid emissions would be the use of waste as material for biofuel production.

As shown in Chapter 3, municipal solid waste (MSW) and construction and demolition (C&D) waste materials are viable feedstocks for the production of advanced biofuels. The woody waste had similar bio-oil compositions as that of traditional woody material (hybrid poplar). Speciation of grass clipping bio-oil was similar to that of switchgrass due to its similar lignocellulosic properties, however due to the large mineral content, had a lower yield. Waste paper had very little lignin derived compounds (due to the removal of lignin from the Kraft process) in the bio-oil and generated a large amount of lower molecular weight species due to its large mineral content. The grass clippings and waste paper were washed in dilute acid and the bio-oil yields were increased significantly from 58% to 73% for the grass clippings and 67% to 73% for the waste paper. There was an

increase in levoglucosan production for both biomass samples after dilute acid washing which agreed with literature. The woody waste though similar to hybrid poplar varied in bio-oil speciation due to differences in the woody feedstock. Therefore, in order to understand how feedstock affects woody waste a systematic understanding of varied feedstock needed to be studied.

Chapter 4 evaluated the effects of changes in lignin content of hybrid poplar that were crossbred to produce biomass with varied lignin content on properties of pyrolysis bioo-oils, char, and gas. The lignin content varied from 17% to 22%. When evaluating lignin content with respect to bio-oil yield at pyrolysis temperatures of 500°C the relative bio-oil yield decreased from 73% to 65%. Indicating that more of the lignin is remaining in the char likely due to the increase of the syringol monomer within the lignin structure for these samples. To volatilize the lignin monomers from the char, higher temperatures were needed. An increase from 500°C to 550°C decreased the char yield from 27% to 13%. There was little change in char yield from 550°C to 600°C indicating nearly all of the lignin was volatilized from the char at 550°C. The amount of lignin derived compounds in the bio-oil increased with increasing lignin content and increasing temperatures, again indicating that the lignin is going from being fixed in the char to being degraded into single monomers present in the bio-oil and thereby increasing the bio-oil yield. Depending on market conditions and what the char is used for as a co-product it may be beneficial to use the high lignin content biomass species as 500ºC to generate more char, if the economics of the process are more favorable. These results help to understand biomass degradation with respect to the lignin content; more severe conditions are needed

to degrade the lignin and generate a higher bio-oil yield. However, a good understanding of intrinsic biomass degradation is not well known.

Chapter 5 focuses on a novel way of obtaining experimental kinetic data from micropyrolysis GC/MS. Previous work for micropyrolsyis GC/MS had only used it as a rapid screening tool for bio-oil speciation and yields with little consideration of rates of production and intrinsic kinetics. The data collected from this experimental set up gains insight into biomass degradation with respect to what bio-oil compounds are being produced first with respect to time. This data shows that hemicellulose derived compounds are produced the fastest and that cellulose and lignin derived compounds are slightly delayed. This data was then compared against a first order exponential decay model and a six step degradation model. The first order exponential decay model fit the data well overall, however was unable to capture the rapid production of compounds like acetic acid or delayed production of compounds like guaiacol. The six step degradation model was applied and fit the data extremely well. The stoichiometric parameters allowed for a better understanding of biomass degradation. These parameters showed that hemicellulose compounds are produced within the first 3 reaction steps, whereas compounds from cellulose and lignin are not significantly produced until reactions 4-6. Some lignin gradually degrades initially, but lignin derived compounds are not produced in much higher quantities until later reactions. The cellulose degrades primarily in reaction 4 as indicated by 70% of the production of acetol occurring within that reaction. These stoichiometric parameters mirror that of TGA degradation data found in literature, allowing for an understanding of the mechanisms of biomass degradation with respect to a semi-empirical model.

The work in this dissertation has addressed many of the limitations and technological barriers of biofuel production in the United States and Pan American region. By having a firm understanding of policy and how sustainability assessments are conducted within this region we know where the greatest challenges exist in biofuels meeting policies and certification schemes. This work contributes to the overall knowledge of biomass degradation and its ability to be converted to an energy rich liquid through pyrolysis.

In order for the advancement of biofuels to continue there needs to be work from governing bodies to adhere to a single type of certification scheme or to make parallels between these policies and certificates to allow for a better comparison. A better understanding of how these frameworks affect life cycle assessment results is needed to help move the biofuel industry forward.

In order to overcome technological barriers more work is needed on understanding biomass degradation with respect to bio-oil production as initially shown in Chapter 5. More bio-oil compounds should be evaluated, along with having a better understanding of cellulose degradation within a modified experimental set up so that anhydrosugars can be quantified and detected. The six step degradation model should also be expanded with experimental results from higher temperatures within the pyrolysis range to evaluate if the Arrhenius parameters remain constant for the entirety of biomass degradation as initially shown when the six step degradation model was developed.

Along with evaluating different temperatures and bio-oil compounds within the context of the six step degradation model, different biomass feedstocks should also be evaluated.

Different biomass feedstocks allow for a better understand of how cellulose, hemicellulose and lignin affect product distribution or the rate of production. Being able to compare stoichiometric values of compounds derived from individual components may allow for an improvement to the six step degradation. The experimental set-up of these experiments allowed for the understanding and analysis of primary reactions. There should be efforts made to go beyond initial primary reactions that occur in micropyrolysis to experiments where control of both reaction temperature and residence time of the pyrolysis vapors is achieved and varied in a systematic way.

Appendix A: A Review of Environmental Life Cycle Assessment of Liquid Transportation Biofuels in the Pan American Region Supplementary Material

A.1 Supplementary material from Chapter 2

This additional information is categorized to reflect the headings from chapter 2 of this dissertation.

Table A.1 Overview of articles evaluated in this study

Paper	Country	Feedstock				Biofuel	Functional Unit	Allocation	System Boundary			
		Starch Crops	Oil Crops	Ligno-cellulosic	Waste				Agri-culture	Trans-portation	Con-version	Use
Acreche and Valeiro 2013	AR	SC				Et	LA	EN	x		x	
Agusdinita and others 2010	US		CM,AG	SG	CS	HRJ	VOL	SE	x	x	x	
Amores and others 2013	AR	SC				Et	MA	MA, EN, EC	x		x	
Bailis and Baka 2010	BR		JT			HRJ	EN	EN, MA, SE	x	x	x	x
Bailis and Kavlak 2013	BR		JT			HRJ	EN	EC, EN, MA, SE	x	x	x	x
Bote and others 2011	CO	CV				Et	VOL	NA	x	x	x	x
Bruinsma 2009	PE		PM, JT			BD	MA	MA	x		x	
Castanheira and Freire, 2009	CO		PM			BD	EN	EN, MA, EC	x	x	x	
Cavalett and others 2012	BR	SC				Et	EN	EN	x	x	x	x
Chavez-Rogriguez and Nebra 2010	BR, US	SC				Et	EN	NA	x	x	x	
Chiu and others 2009	US	CN				Et	VOL	NA	x		x	
Chiu and others 2012	US	CN				Et	VOL	NA				
Clarens and others 2010	US		AG			BM	EN	None	x			
Concocio CUE 2012	CL	SC	PM			Et, BD	DI	EC, EN	x	x	x	x
da Costa and others 2006	BR, CO		PM			BD	MA	NA	x		x	
da Silva and others 2010	BR		SB			BM	MA	None	x	x		
de Oliveira and others 2005	BR, US	SC, CN				Et	LA, DI	NA	x	x	x	
de Souza and others 2010	BR		PM			BD	LA	Mass	x	x	x	x
Emmeneggar and others 2011	AR		RS			BD	EN	EC	x	x	x	x

Fan and others 2013	US		PC		HRJ,BD	EN	SE, EN, EC	x	x	x	x
Fu and others 2003	CA			FR	Et	DI	NA	x		x	x
Garcia and others 2011	MX	SC			Et	EN	EN	x	x	x	
Graefe and others 2011	CR, EC			BN	Et	VOL	NA	x	x	x	
Grillo and others 2011	BR			SB	Me	MA	EN	x	x	x	
Hertel and others 2010	US	CN			Et	EN	NA				
Hilbert and others 2009	AR		SB		BD	EN	NA	x	x	x	
Huo and others 2008	US		SB		BD, RG	EN	SE, EN, EC, HY	x	x	x	x
Iriarte and Vilalobos 2013	CL		SF		BD	DI	EN	x	x	x	x
Iriarteand others 2010	CL		RS, SF		BM	MA	None	x	x		
Iriarteand others 2012	CL		RS		BD	DI	EN, MA, SE	x	x	x	x
Kauffman and others 2011	US	CN		CS	Et, RG	LA	SE	x	x	x	
Kim and Dale 2005b	US	CN	SB		Et, BD	LA	SE, MA	x	x	x	
Kim and Dale 2005a	US	CN			Et	MA, EN	SE, MA	x	x	x	
Kim and Dale 2006	US	CN			Et	MA, EN	SE	x	x	x	x
Kim and Dale 2008	US	CN			Et	MA	SE	x	x	x	x
Kim and Dale 2009	US	CN	SB		Et, SO	MA	SE, MA	x	x	x	
Kim and others 2009	US	CN			BM	MA	SE, MA		x	x	
Koch 2003	CR		PM		BD	MA	EC	x	x	x	x
Krohn and Fripp 2012	US		CM		BD	EN	MA, EC, SE	x	x	x	
Liska and others 2009	US	CN			Et	EN	SE	x	x	x	
Luo and others 2009	US			CS	Et	DI	SE, MA, EC	x	x	x	x
Luo and others 2009	BR	SC			Et	DI	EC	x	x	x	x
Macedo and others 2008	BR	SC			Et	VOL	SE	x	x	x	

Mishra and Yeh 2011	US	CN				Et	DI	SE	x	x	x	
Molino 2008	MX	SC				Et	NA	MA	x		x	
Neupane and others 2011	US			WC		Et	VOL	MA	x	x	x	
Ometto and others 2009	BR	SC				Et	DI	NA	x	x	x	x
Panichelli and others 2008	AR		SB			BD	DI	EC, EN, MA	x	x	x	x
Pivotto and others 2011	BR		SB			BD	NA	NA				x
Pradhan and others 2011	US		SB			BD	EN	MA	x	x	x	
Queiroz and others 2012	BR		PM			BD	EN	NA	x		x	
Quinteto and others 2008	CO	SC				Et	MA	NA		x		
Ramirez 2011	BR	SC				Et	MA	NA	x	x	x	
Reijinders and Huijbredgts 2008	BR		SB			BD	LA	EC	x			
Rodriguez and others 2012	MX				AF	BD	MA	None		x	x	
Sander and Murthy 2010	US		AG			BD	EN	SE	x	x	x	
Scown and others 2012	US			MS		Et	EN	SE	x	x	x	
Souzaand others 2012	BR	SC	PM			Et, BD	VOL	NA	x	x	x	
Spatari and others 2005	CA			SG	CS	Et	DI	SE	x	x	x	x
Tsao and others 2012	BR	SC	SB			Et, BD	EN	NA				
Turdera 2013	BR	SC				Et	LA	NA	x	x	x	
Vargas-Gomez 2009	CO		PM			PO	MA	NA	x	x	x	
Velasquez and others 2010	CO	BN				Et	MA	NA	x		x	
Wang and others 2007a	BR	SC				Et	EN	NA	x	x	x	x
Wang and others 2007b	US	CN				Et	EN	NA	x	x	x	x

Wang and others 2011	US	CN		SG	FR	Et	EN	SE	x	x	x	x
Wang and others 2012	US	CN, SC		MS, SG	CS	Et	EN	SE, EN	x	x	x	x
Wu and others 2006	US	CN			CS, FR	Et	EN	EN	x	x	x	x
Yanez and others 2004	BR, CO		PM			BD	MA	NA	x	x	x	
Yang 2013	US	CN				Et	DI	EC	x	x	x	x
Yang and others 2012	US	CN				Et	DI	EC	x	x	x	x
Yang and others 2010	US		AG			BD	MA	NA	x		x	
Zaimes and Khanna 2013	US		AG			BM	EN	None	x			
Zumalacárregui, and others 2008	CU	SC				Et	MA	NA	x	x	x	x

EN: Energy, MA: Mass, DI: Distance, VOL: Volume, LA: Land, SE: System Expansion, EC: Economic, HY: Hybrid approach, NA: Not Available, CN: Corn, CS: Corn Stover, SC: Sugarcane, CM: Camelina, CV: Cassava PM: Palm, AG: Algae, SB: Soybean, RS: Rapeseed, SF: Sunflower, MS: Miscanthus, SG: Switchgrass, FR: Forest Residue, AF: Animal Fat, SB: Sugarcane Bagasse, BN: Banana BD: Banana Discard, WC: Woody Crops, Et: Ethanol, BD: Biodiesel, PO: Palm Oil, BM: Biomass, SO: Soy Oil, HRJ: Hydrorenewable Jet Fuel,

A.4.5 Biofuel pathway inputs and sources of inventory data

LCA tools such as SimaPro, GREET, GaBi, etc., take input data, transform them into inventories, have embedded emission factors within the inventories and convert the emission factors into impacts using an impact methodology. The LCA tool is what culminates: allocation, inputs, inventory, impact assessments and then generates the final results. The tool that is chosen is important due to emission factors embedded within in the program, timeliness and availability of inventory data and the geographical context of the tool itself. Using different tools will yield similar results, but they do differ. Therefore when conducting an LCA the tool used must be mentioned so that good comparison between studies can be upheld.

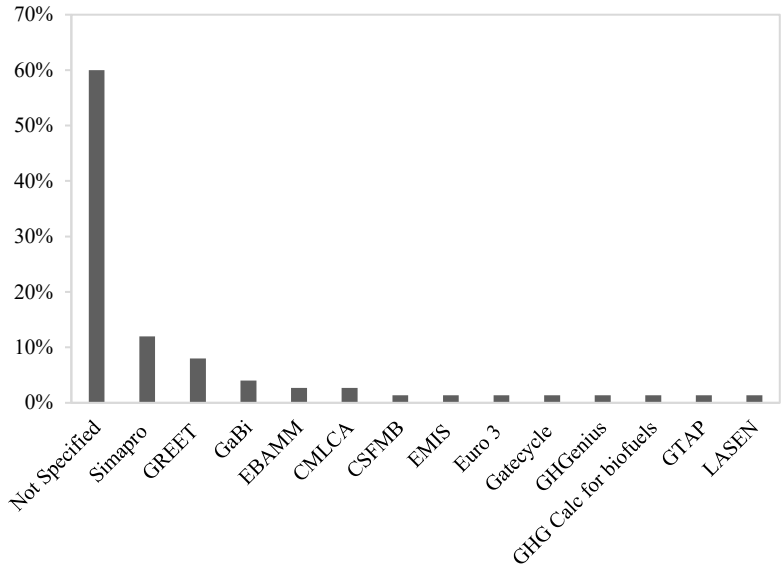

Figure A.1 Tools used within this evaluation.

There are a vast amount of tools are also used for conducting LCA Figure A.1 shows the percentage of what tools were used with in this evaluation. Over half of the articles did not report the tool used to conduct the LCA. The most commonly reported tool used was

SimaPro but this only represented 12% of the studies evaluated. These LCA tools provide a means of organizing and conducting a LCA, often they provide data and impact methodology built into the program. Some tools are versatile and come with their own inventory data and impact methodology as discussed in section 2.4.3.

A.4.6 Impact assessment categories and methods

Table A.2: Impacts evaluated by articles within this study

Paper	Impacts																
	GWP	EC	dLUC	AP	EP	HT	WE	WC	PCOP	ET	ODP	ABD	TE	LO	iLUC	RD	BD
Acreche and Valeiro 2013	x	x															
Agusdinita and others 2010	x																
Amores and others 2013	x		x														
Bailis and Baka 2010	x		x														
Bailis and Kavlak 2013	x		x														
Bote and others 2011	x	x															
Bruinsma 2009	x	x	x														
Castanheira and Freire, 2009	x		x	x	x				x		x						
Cavalett and others 2012	x			x	x	x	x	x	x	x	x	x	x	x		x	
Chavez-Rogriguez and Nebra 2010	x		x					x		x							
Chiu and others 2009								x									
Chiu and others 2012			x	x	x			x		x							
Clarens and others 2010	x	x			x			x						x			
Concocio CUE 2012	x	x	x	x	x	x			x	x							
da Costa and others 2006		x															
da Silva and others 2010	x	x	x	x	x								x	x			
de Oliveira and others 2005	x	x	x							x							x
de Souza and others 2010	x	x															
Emmeneggar and others 2011	x					x		x		x		x				x	
Fan and others 2013	x	x													x		
Fu and others 2003	x	x		x	x	x			x		x						
Garcia and others 2011	x	x	x														
Graefe and others 2011	x	x															
Grillo and others 2011	x	x		x	x	x	x		x		x	x	x	x			

Hertel and others 2010	x	x	x														
Hilbert and others 2009	x	x															
Huo and others 2008	x	x															
Iriarte and Vilalobos 2013	x	x	x														
Iriarte and others 2010	x	x	x	x	x	x	x	x	x		x	x	x				
Iriarte and others 2012	x	x	x	x	x	x	x	x	x		x	x	x				
Kauffman and others 2011	x		x												x		
Kim and Dale 2005b	x	x															
Kim and Dale 2005a	x	x		x	x												
Kim and Dale 2006	x	x		x	x												
Kim and Dale 2008	x	x		x			x		x								
Kim and Dale 2009	x		x														
Kim and others 2009	x			x	x												
Koch 2003	x	x		x	x						x						
Krohn and Fripp 2012	x	x	x														
Liska and others 2009	x	x															
Luo and others 2009	x			x	x	x			x	x	x	x					
Luo and others 2009	x			x	x	x			x	x	x	x					
Macedo and others 2008	x	x															
Mishra and Yeh 2011								x									
Molino 2008	x	x															
Neupane and others 2011	x			x	x	x				x	x	x		x		x	
Ometto and others 2009	x	x		x	x	x		x	x				x				
Panichelli and others 2008	x	x	x	x	x	x	x						x	x			
Pivotto and others 2011	x																
Pradhan and others 2011		x															
Queiroz and others 2012		x															
Quinteto and others 2008	x			x		x	x		x				x				

Ramirez 2011		x															
Reijinders and Huijbredgts 2008	x		x														
Rodriguez and others 2012	x	x															
Sander and Murthy 2010	x	x															
Scown and others 2012	x	x	x														
Souzaand others 2012	x	x	x														
Spatari and others 2005	x																
Tsao and others 2012	x		x														
Turdera 2013	x	x															
Vargas-Gomez 2009	x																
Velasquez and others 2010		x															
Wang and others 2007a	x	x															
Wang and others 2007b	x	x	x														
Wang and others 2011	x	x	x														x
Wang and others 2012	x	x	x														
Wu and others 2006	x	x															
Yanez and others 2004		x															
Yang 2013						x	x										
Yang and others 2012								x									
Yang and others 2010	x	x		x	x	x		x	x		x	x				x	x
Zaimes and Khanna 2013	x	x						x									
Zumalacárregui, and others 2008	x																

GWP; Global Warming Potentional, EC; Energy Consumption, dLUC; direct Land Use Change, AP; Acidification Potential, EP; Eutrophication Potential, HT; Human Toxiciity, WE; Water Ecotoxicity, WC; Water Consumption, PCOP; Photochemical Oxidant Formation Potential, ET; Ecosystem Toxicity, ODP; Ozone Layer Depletion Potential, ABD; Abiotic Depletion Potential, TE; Terrestrial Ecotoxicity; LO; Land Occupation, iLUC; indirect Land Use Change, RD; Resource Depletion, BD; Biodiversity

A.5.1 Global-warming potential

Figure A.2 shows the breakdown of GHG emissions by production stages without including the direct land-use change (dLUC) effects. For comparison purposes we have gathered the different described stages in only three. The first is the agricultural stage includes which includes the GHG emissions from the fertilizers production and application, and the emissions from cultivation purposes (harvesting, diesel for irrigation, etc.). The second is the industrial stage which refers to all the transformation processes performed on the biomass for biofuel production. Transport refers to the transportation from farm to factory gate and also the distribution of the resulting fuel. Except for lignocellulosic feedstock, agricultural stage seems to contribute the most to the net GHG emissions. A similar situation occurs with the microalgae-based biofuels due to the high amount of energy required for its cultivation

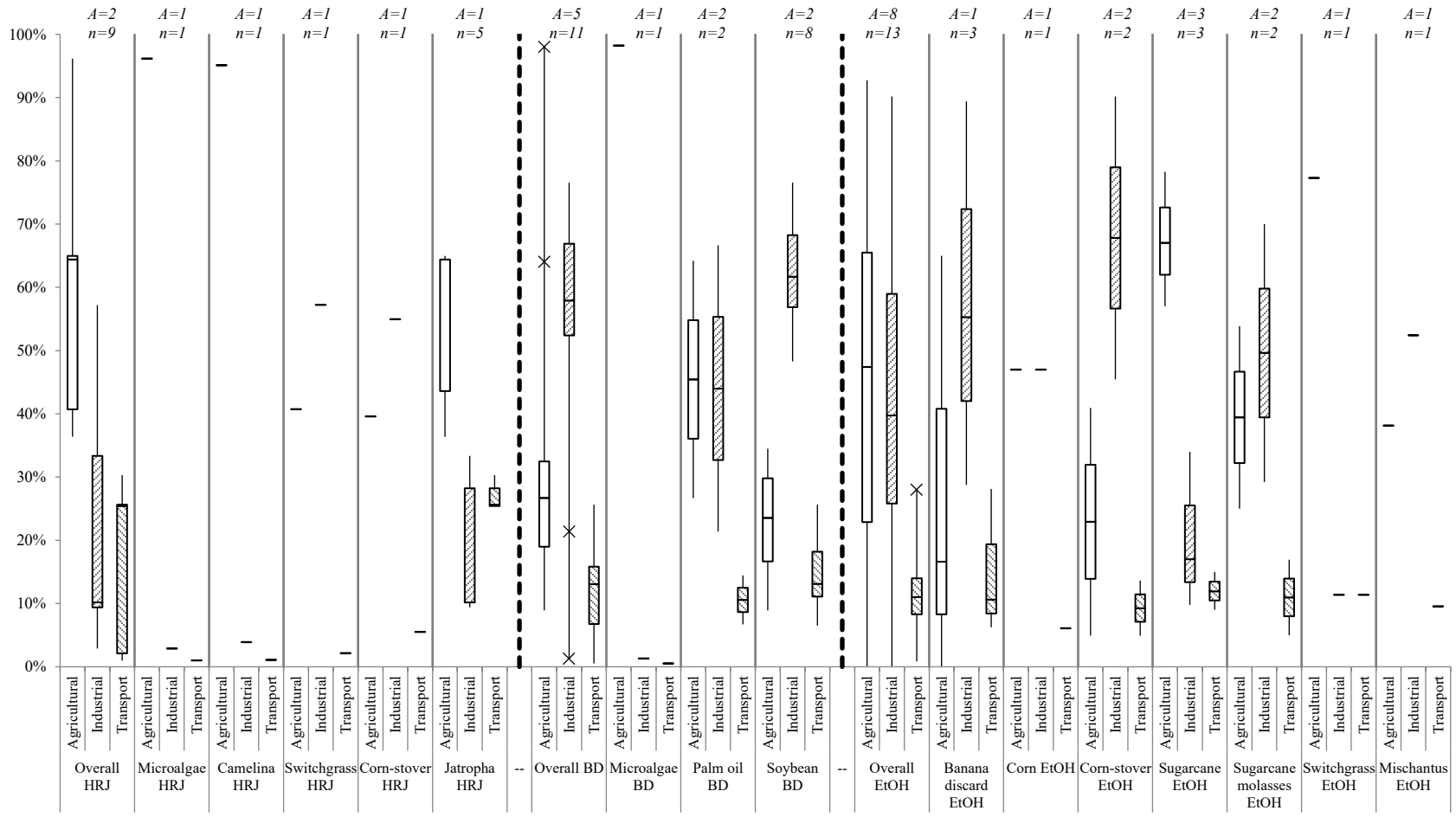

Figure A.2 Box and Whisker plot with the breakdown of GHG emissions by production stages without including the LUC effect. *A* refers to the number of articles and *n* to the number of analyses. HRJ, BD, and EtOH mean hydrorenewable jet, biodiesel, and ethanol, respectively.

A.5.2 Direct land-use change (dLUC) effect on the GHG emissions

Figire A.3 shows the breakdown of the GHG emissions by production stages. For comparison purposes we have gathered the different described stages in only three: agricultural stage, industrial stage, and transportation stage. The emissions from the dLUC were assigned to the agricultural stage. Agricultural stage contributes the most to the net GHG emission except for corn and corn stover. In the case of corn, assuming old industrial conditions that require coal explains the high contribution of the industrial stage (Kim and Dale 2005). However, the use of more recent data that reflect the current corn-based ethanol production leads to a different trend where the agricultural stage is the major contributor to the net GHG emissions (Wang and others 2011; Wang and others 2012). The corn stover is treated as a residue and the resulting GHG emissions come mainly from the supplement of fertilizers to compensate the nutrient loss from the stover removal (Wang and others 2012) .

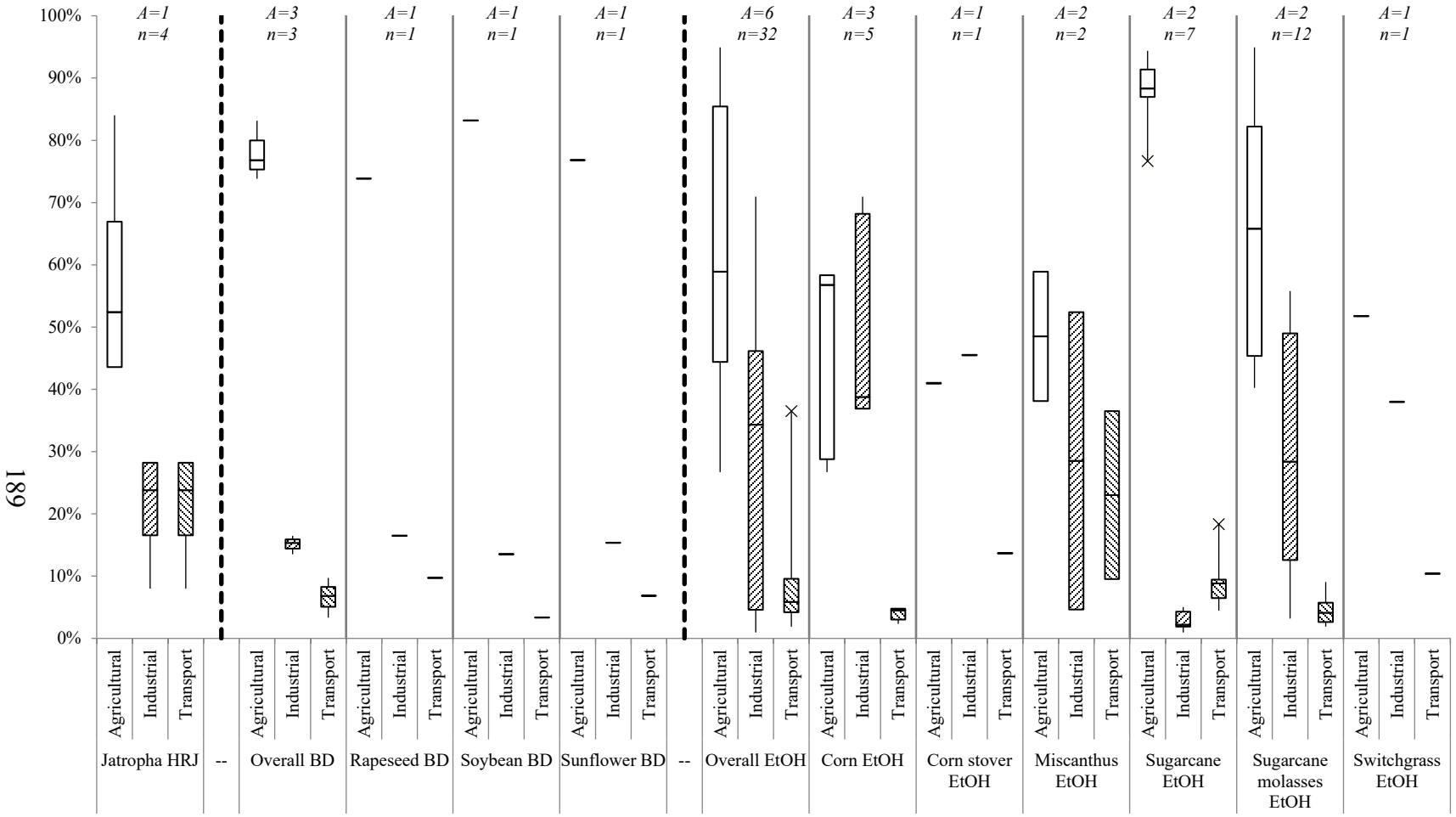

Figure A.3 Box and Whisker plot with the breakdown of GHG emissions by production stages including the dLUC effect. *A* refers to the number of articles and *n* to the number of analysis. HRJ, BD, and EtOH refer to hydrorenewable jet, biodiesel, and ethanol, respectively. Corn, corn stover, miscanthus, and switchgrass include also the iLUC effect.

A.5.3 Regulatory frameworks and certification schemes for biofuels production

The EU-RED and the RSB require a GHG-emission reduction based on a fossil comparator of 83.8 (RED 2009) and 90 gCO_{2eq}/MJ (RSB 2013), respectively. Furthermore, the EU-RED requires energy allocation while the RSB an economic allocation. Therefore, the comparison of the results should be as close as possible to the metrics stated by these initiatives.

Figure A.4 shows the GHG emissions of the biofuels production under energy allocation criteria including the dLUC effect. Jatropha-based HRJ fuel may fulfill the EU-RED metrics if cultivation takes place on pastureland (Bailis and Baka 2010). Biodiesel derived from either sunflower (Iriarte and Villalobos 2013) or rapeseed (Iriarte and others 2012) does not achieve the EU-RED requirements. Palm oil biodiesel may fulfill the EU-RED requirements when cultivation takes place on savannah (Castanheira and Freire 2011). Sugarcane-based ethanol might fulfill the EU-RED requirements. However, more studies are necessary to fully conclude that. Sugarcane molasses-based ethanol production under Argentinean (Amores and others 2013) and Mexican (Garcia and others 2011) conditions could not fulfill the EU-RED metrics due to the large effect of the dLUC (deforestation).

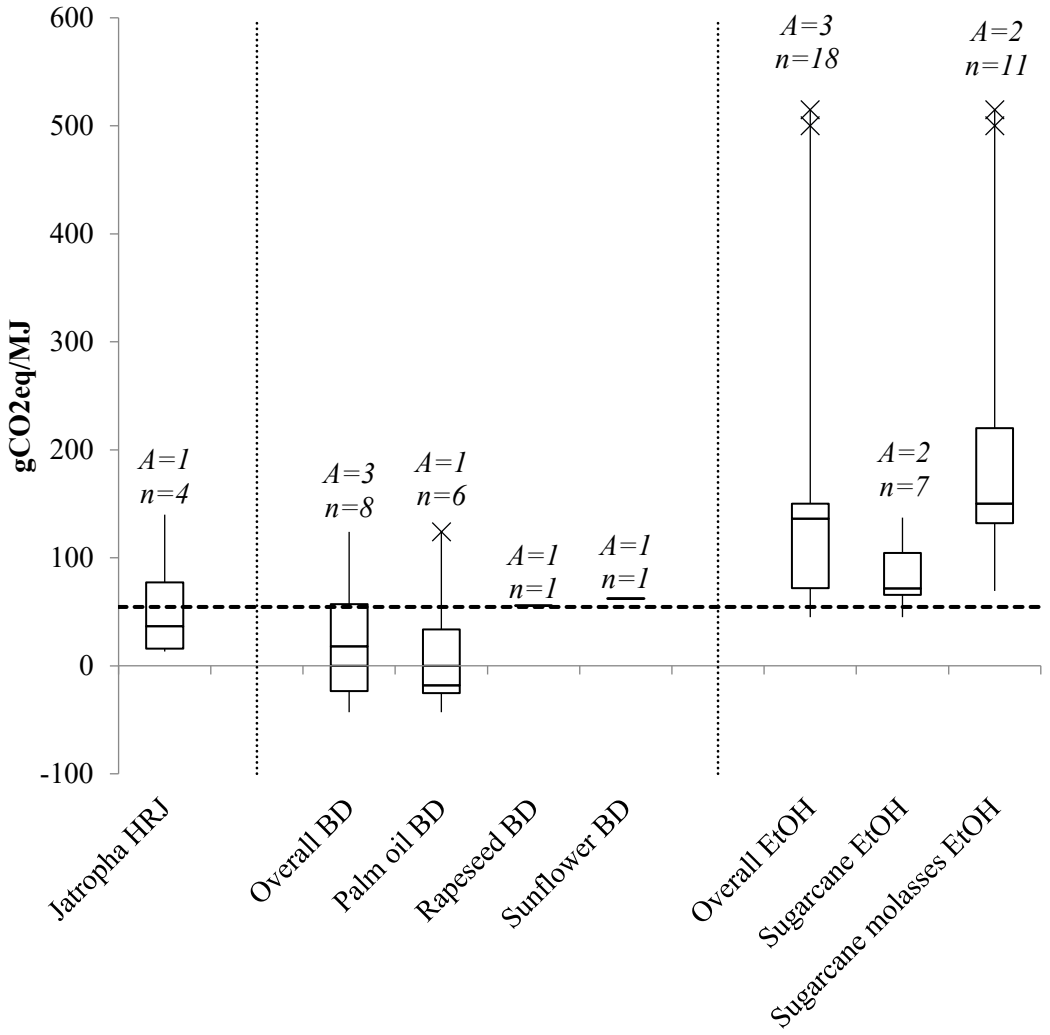

Figure A.4 GHG emissions including dLUC effects under energy allocation criteria. *A* refers to the number of articles and *n* to the number of analysis. HRJ, BD, and EtOH mean hydrorenewable jet, biodiesel, and ethanol, respectively. The dash line represents the EU-RED threshold.

Few studies analyze the dLUC effect on the GHG emissions of biofuels production under economic allocation criteria (Amores and others 2013; Consorcio 2012; Galbusera and Hilbert 2011). Sugarcane molassess-based ethanol production under Colombian conditions might fulfill the RSB requirements if cultivation takes place on shrubberies (Consorcio 2012). Direct deforestation leads to a large amount of GHG emissions for the sugarcane-molassess-based ethanol production under Argentinean conditions what avoids achieving

the RSB metrics (Amores and others 2013). A study on the GHG emissions derived from the soybean-based biodiesel production (Galbusera and Hilbert 2011) indicates that the resulting GHG emissions fulfill the RSB target. However, this study does not consider the GHG emissions from the fertilizers production.

A.6 Case study: Jatropha biofuel production in the Yucatan state of Mexico

Direct land use change

Direct land use change (dLUC) emissions of CO_2 are also included in the base case analysis. To calculate dLUC emissions on an annualized basis, the following formula was used;

$$dLUC\ Emissions\ [tons\ CO_2/yr]\ =\ Plantation\ Area * (CS_i - CS_j) * 44/12/40$$

where CS_i is the carbon stocks of the land prior to jatropha planting [tons C/ha], CS_j is carbon stock after maturation of jatropha plantation [tons C/ha], 44/12 is ratio of molecular weight of CO_2 to C, and 40 represents the plantation life in years.

Table A.3 Land category classes of native vegetation of the green bordered area from Figure 1, as well as of proposed jatropha plantations in this area.

Canopy Cover Classes	Carbon Content (tons C/ha)	Plantation Area (ha)	dLUC (tons CO_2/yr)
≤ 10% tree canopy cover	2.4	11,501	-15919
10-20% tree canopy cover	10	21,726	-8962
20-30% tree canopy cover	20	21,773	4990
Jatropha plantation cover	17.5	55,000	

The dLUC value for the first land class (10% or less) is calculated according to the equation above as (11,501 ha*(2.4-17.5) tons C/ha*44/12)/40 = -15919 tons CO_2/yr. The dLUC for the other two land classes are calculated similarly. The dLUC values from above are added together, divided by the total energy content of HRJ produced in 1 year (4,694,471,387 MJ = 106,692,532 kg HRJ * 44 MJ/kg HRJ), multiplied by 10^6 to convert to grams, and multiplied by the energy allocation factor for HRJ of 0.197, yielding -0.8 g CO_2 eq./MJ HRJ, which is the value listed in Table 10.

Inputs and inventory data

In the tables below, the full set of inputs for the base case analysis at each life cycle stage are presented without considering energy allocation (section 3.2). The application of energy allocation factors for the HRJ life cycle will be described subsequently. Table 4 below lists the material and energy inputs for the base case analysis at the cultivation stage and any emissions on the plantation due to fertilizer application or fuel combustion. Table 5 provides input data for jatropha biomass transport to Uman, Table 4 shows data for the oil extraction stage, Table 5 is for oil transport to Cancún, and Table 6 lists input materials and energy for the HRJ production stage.

Table A.4 Annual Inputs for Material and Energy for Cultivation and Harvesting.

Materials	Ecoprofiles (ecoinvent™)	Value	Units
Diesel	Diesel, low-sulphur, at regional storage/RER S	$2.26x10^5$	kg
N	Diammonium phosphate, as N, at regional storehouse/RER S	$4.07x10^5$	kg
N	Ammonium nitrate, as N, at regional storehouse/RER S	$8.25x10^4$	kg
P	Single superphosphate, as P_2O_5, at regional storehouse/RER S	$8.25x10^4$	kg
K	Potassium sulphate, as K_2O, at regional storehouse/RER S	$8.25x10^4$	kg
	Processes	**Value**	**Units**
Diesel Combustion Emissions (3.17 kg CO_2 / kg diesel) * →		$2.26x10^5$	kg
N Fertilizer N_2O emissions (.01325*44/28) kg N_2O/kg N * →		$2.01x10^6$	kg
Heat, nat. gas, at industrial furnace low-NOx >100kW/RER S		$2.67x10^8$	MJ
Yucatan electricity for irrigation of pig farm waste water		$6.67x10^5$	kWh

Diesel fuel values in Table 4 for cultivation are derived from KUO Bionergía data indicating that 26 tractors working an 8 hour day will consume 4 L/hr (per tractor) of diesel fuel of density 0.85 kg/L. Diammonium phosphate (DAP) and NPK (macronutrient fertilizer containing nitrogen (N), phosphorus (P) and potassium (K)) are applied to augment nitrogen inputs from manure/waste water associated with affiliated pig farms. The analysis utilized ammonium nitrate, single superphosphate and potassium phosphate data of the ecoinvent database to calculate emissions associated with NPK production. For this study the assumption is that the seeds are dried with heat from the combustion of natural gas from a moisture content of 20% to a moisture content of 8% in a heating plant that is 55% efficient. Specific heat input is based upon a heat of vaporization of .271 MJ/kg seed. Installation of plantation irrigation system was not included on the justification that infrastructure impacts are generally minor.

The resulting seed and shell ($1.43x10^6$ tons) is transported to Uman for oil exraction and combustion of biomass for electricity production as shown in Table 5. The dried seed and

associated shell are transported to Uman (round trip mileage of 95 km*2=190 km) with 27 ton trucks that consume fuel at a rate of .37 liters/km. Emissions of greenhouse gases were included for the production of diesel fuel using econivent data in SimaPro7.2 and for combustion using an emission factor of 3.17 kg CO_2 / kg diesel combusted, which is an emission factor based on carbon content of petroleum diesel.

Table A.5 Annual Inputs for Material and Energy for Seed and Shell Transport to Uman.

Parameter		Value	Units
Jatropha seed and shell transported to Uman by Truck		$1.43x10^6$	ton
Materials	**Ecoprofiles (ecoinvent™)**		
Diesel	Diesel, low-sulphur, at regional storage/RER S (2.21 kg diesel / ton seed and shell transported)	$3.23x10^6$	kg
	Processes		
Diesel Combustion Emissions (3.17 kg CO_2 / kg diesel) * →		$3.23x10^6$	kg

The study assumes a jatropha oil content of the seed of 40% (based on moist seed) and that recovery efficiency of oil is 100%, which will require $5.33x10^5$ kg of hexane solvent (3.7 l/ton of oil), as shown in Table 6. While the hexane is expected to be recycled in the extraction process, this study conservatively assumes that all of the annual input of hexane will be lost due to emissions or other release processes over a 1-year period and produce CO_2 emissions from hexane oxidation in the environment. From data provided by KUO, $2.86x10^8$ MJ (1.3 MJ/kg oil) of heat is required to heat the plant and other extractive processes. Based upon data provided by KUO Bionergía, a biomass electricity generation plant will produce $3.24x10^7$ kWh for internal consumption and an excess above oil extraction process needs of $7.68x10^8$ kWh of power from the combustion of residual jatropha biomass (seed cake(meal), husks, shells).

Table A.6 Annual Inputs for Material and Energy for Oil Extraction at Uman.

Materials	Ecoprofiles (ecoinvent™)	Value	Units
Diesel	Hexane, at plant/RER S	$5.33x10^5$	kg
	Processes		
Heat, nat. gas, at industrial furnace low-NOx >100kW/RER S		$2.86x10^8$	MJ
Electricity generated in and used by oil extraction process		$3.24x10^7$	kWh
Electricity generated in and exported by oil extraction process		$7.68x10^8$	kWh
Hexane emissions of CO_2 from microbial metabolism (3.0 kg CO_2 / kg hexane) * →		$5.33x10^5$	kg

The jatropha oil ($2.2x10^5$ tons) is transported to Cancún where the oil will be converted to HRJ using the UOP LLC process. Inputs for this transportation step are shown in Table 7. The round trip distance is calculated as (round trip mileage of 320 km*2=640 km) with 27 ton trucks that consume fuel at a rate of .37 liters/km. Emissions of greenhouse gases were included for the production of diesel fuel using econivent data in SimaPro7.2 and for combustion using an emission factor of 3.17 kg CO_2 / kg diesel combusted, which is an emission factor based on carbon content of petroleum diesel.

Table A.7 Annual Inputs for Material and Energy for Jatropha Oil Transport to Cancún.

Parameter		Value	Units
Jatropha oil transported to Uman by Truck		$2.20x10^5$	ton
Materials	**Ecoprofiles (ecoinvent™)**		
Diesel	Diesel, low-sulphur, at regional storage/RER S (2.21 kg diesel / ton jatropha oil transported)	$4.86x10^5$	kg
	Processes		
Diesel Combustion Emissions (3.17 kg CO_2 / kg diesel) * →		$4.86x10^5$	kg

Table A.8 shows the inventory of input data for production of HRJ using the UOP LLC process in amounts sufficient to process the entire amount of jatropha oil from the Yucatan plantations of 55,000 ha. In this analysis, H_2 production is assumed to be from a steam reformer unit processing methane and using data from UOP LLC. Hydrogen from a petroleum refinery platformer unit is not possible in the future because of the existing and future demands on hydrogen from fuel desulfurization processing. The HRJ process utilizes softened water for boiler operations and cooling. Two proprietary chemicals are used in the HRJproduction reactions, but their inputs are relatively small. Heat is required for the HRJ reactions and separation processes and this process energy is provided by refinery gas and also natural gas. A separate combustion emission profile was created for refinery gas use based on an assumed composition of propane and butane. Additional heat inputs were included using steam, and a small production of steam is also a part of the HRJ production stage as is a generation of an energy stream in the form of process water condensate. A small environmental credit was provided for this condensate stream assuming that the warm liquid water stream would reduce energy demand for steam production using natural gas (boiler efficiency of 80%). Jatropha oil is refined in order to eliminate contaminants using inputs of electricity and steam. Wastewater and a solid waste stream combined to generate 1.9×10^7 kg/yr, with over 99% wastewater. Emissions of GHGs from these waste treatment processes were included using unit processes from the ecoinvent database in SimaPro7.2.

TableA. 8 Inputs for material and energy for the HRJ production stage.

Materials	Value	Units
H_2 from steam reforming of natural gas	UOP Confidential Information	kg
Boiler feed water	UOP Confidential Information	kg
Cooling water	UOP Confidential Information	kg
Chemical 1 (proprietary)	UOP Confidential Information	kg
Chemical 2 (proprietary)	UOP Confidential Information	kg
Refinery gas (for heat input)	UOP Confidential Information	kg
Process Inputs for HRJ production stage		
Processes	**Value**	**Units**
Yucatan electricity	UOP Confidential Information	kWh
Heat from natural gas	UOP Confidential Information	MJ
Fuel gas combustion emissions	UOP Confidential Information	kg
On-site steam use	UOP Confidential Information	kg
On-site steam credit	UOP Confidential Information	kg
Heat from natural gas, credit for condensate recycle	UOP Confidential Information	MJ
UOP CONCAWE Raw Oil to Refined Oil	UOP Confidential Information	kg
Wastewater treatment and solid waste	UOP Confidential Information	kg

Allocation Methods

In this study, *energy allocation* is used as the base case method because this allocation approach is adopted by the European Community in its current Renewable Energy Directive (Council of The European Union (2009)). Fig. 8 in the main article shows the allocation of environmental impact by energy. The red bars in Fig. 8 indicate greenhouse gas (GHG) emission impacts and height of each bar is proportional to the magnitude of

impact. Impacts accumulate as material moves through the life cycle due to the input and use of material and energy (key inputs are shown below each stage). Impacts exit the HRJ product life cycle when co-products are created and exported. Impacts are allocated to HRJ and also to the co-products electricity and fuels using energy allocation, by considering the material flows of products/co-products and each material's lower heating value. For example, at the oil extraction stage, jatropha oil is the main product and electricity is the co-product. An energy allocation factor (EAF_{JO}) for jatropha oil (JO) is calculated using the energy allocation method as shown in the equation below,

$$EAF_{JO} = \frac{M_{JO}\ LHV_{JO}}{M_{JO}\ LHV_{JO} + M_{JB}\ LHV_{JB}}$$

where M_{JO} and M_{JB} are the annual mass production amounts of jatropha oil and jatropha biomass (JB) (seed meal, husks, shell in kilograms, kg) and HLV_{JO} and LHV_{JB} are lower heating values of oil and biomass (MJ/kg). The accumulated impacts up to and including oil extraction, for example also the prior stages of cultivation / harvesting and transport of jatropha biomass, are allocated to jatropha oil by multiplying the impacts by the EAF_{JO} in the equation above (EAF_{JO} = 0.37). The same energy allocation approach is used at the HRJ production stage, and in this case the energy allocation factor for HRJ is EAF_{HRJ} = 0.53.

These energy allocation factors for HRJ life cycle were applied to the inventory data in Tables A.4 through A.8 as shown in Table A.9. The units of "p" indicate that the full annual amounts of inventory data are called in the analysis, multiplied by the indicated energy allocation factors. For example, 19.7% of the impacts for inventory data from cultivation /

harvesting, transport to Uman, and oil extraction at Uman are allocated to HRJ. For the stages of oil transport to Cancún and for HRJ production at Cancún 53.3% of the impact of these stages is allocated to HRJ. It is clear from this table, that most of the environmental impacts of the HRJ production life cycle are exported out of the system to co-products electricity and green fuels.

Table A.9 Energy allocation factors (EAF) for the HRJ life cycle.

Assemblies	EAF	Units
Jatropha Cultivation and Harvesting	0.37*0.533 = 0.197	p
Jatropha Transport to Uman	0.37*0.533 = 0.197	p
Jatropha Oil Extraction at Uman	0.37*0.533 = 0.197	p
Jatropha Oil Transport to Cancún	0.533	p
HRJ Production production from Jatropha Oil	0.533	p

A second allocation approach that is frequently used in biofuel life cycle assessments is called *displacement allocation*. Figure A.5 shows displacement allocation applied to the jatropha HRJ life cycle. The red bars indicate greenhouse gas (GHG) emission impacts and green bars indicate credits of impact allocated to HRJ. GHG emission impacts accumulate as material moves through the life cycle due to the input and use of material and energy (key inputs are shown below each stage), and all of the GHG emissions are assigned to HRJ. Environmental impact credit is allocated to HRJ by avoiding production and use of products in the Mexican economy by substituting the co-products produced in the life cycle. Table 10 shows that the full impacts of each stage of HRJ production are allocated to HRJ, plus avoided emission credits for co-products exported from the product system are also allocated to HRJ.

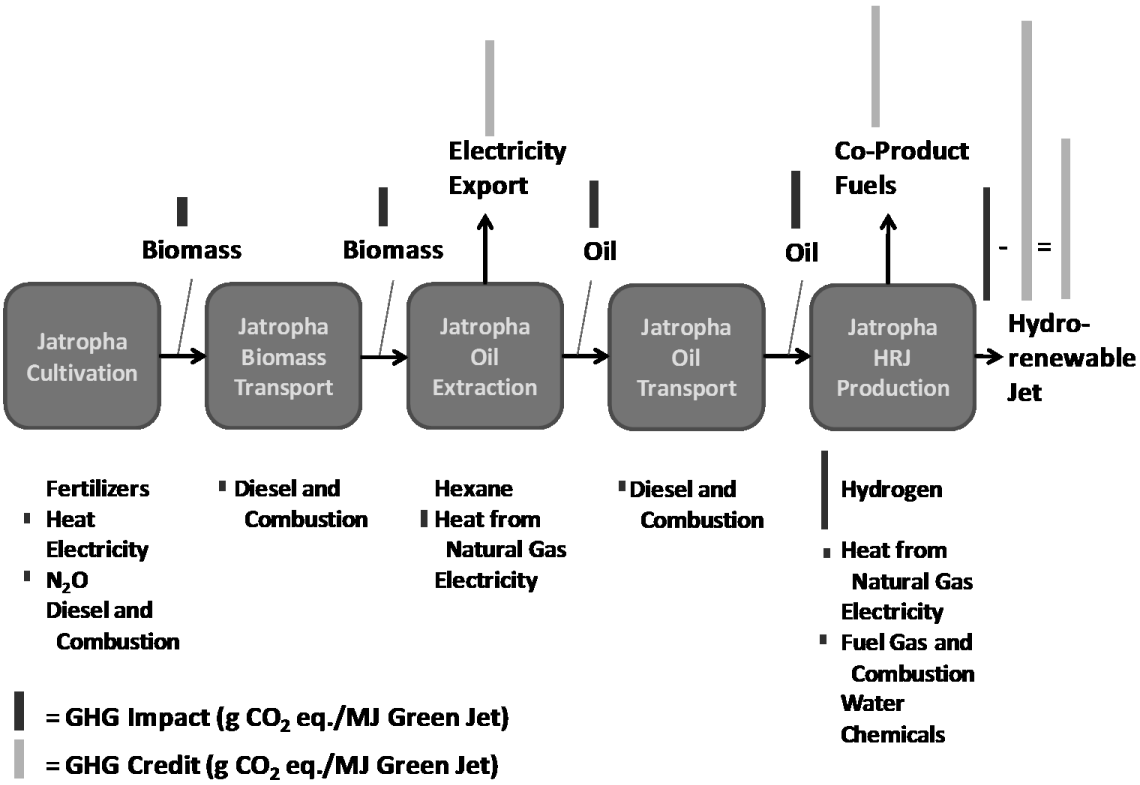

Figure A.5 Life cycle stages for the analysis of HRJ from jatropha using system expansion (displacement) allocation. The red bars indicate greenhouse gas (GHG) emission impacts and height of bar is proportional to the degree of impact. Green bars indicate credits of impact given to HRJ. GHG impacts accumulate as material moves through the life cycle due to the input and use of material and energy (shown below each stage), and all of the impact is assigned to HRJ. Environmental impact credit is allocated to HRJ by avoiding production and use of products in the Mexican economy by the co-products produced in the life cycle.

Table A.10 Displacement allocation factors (DAF) for the HRJ life cycle.

Assemblies	DAF	Units
Jatropha cultivation and harvesting	1	p
Jatropha transport to Uman	1	p
Jatropha oil extraction at Uman	1	p
Jatropha oil transport to Cancún	1	p
HRJ production from jatropha oil	1	p
Jatropha oil extraction Yucatan electricity credit	1	p
HRJ co-product fuel credits	1	p

The choice of allocation method is a subject of some discussion among life cycle practitioners, and most biofuels studies include more than one method, possibly including other methods such as mass allocation and market value allocation. Because of the preference of the European Community regulators for energy allocation, in this study energy allocation is the base case method.

Energy allocation according to the EU-RED

After presenting final results to staff members of KUO Bionergia in Merida, Mexico on February 21, 2011, a final set of changes to the jatropha green jet and green diesel LCAs were identified. The most important change is to have the analysis comply with European Commission mandates with respect to energy allocation, in particular, the treatment of oil extraction residue (husk and meal) as waste. As such, it is not allowed to consider this waste in energy allocation calculations. A list of final variants is shown below in order of life cycle stage, beginning with jatropha cultivation and harvesting. Other than these listed changes, inventory data provided by KUO Bionergia was used, as shown in the main article.

1. Harvesting and Cultivation: Solar drying of jatropha seeds at the plantation was assumed and therefore natural gas inputs for drying were eliminated. Transportation back to the plantation is already included in transportation inputs.
2. Transport of Seed to Uman: Only seed is assumed to be transported to Uman for oil extraction. No shell is transported from the plantation to Uman, but shell is returned to the plantation soil after seed separation to serve as a soil enhancer and fertilizer nutrient provider.

3. Oil Extraction at Uman: Heat and power is generated on site at Uman from husk and meal to satisfy all process demands. Therefore, Yucatan electricity and natural gas inputs from the base case were eliminated from the analysis. Any export of electricity cannot be included in energy allocation calculations. There is no energy allocation at this stage as stated in the European Commission rules (Council of the European Union, 2009).
4. Transport of Jatropha Oil to HRJ Production: There is no change in these inputs compared to the base case analyses.
5. HRJ Production: No changes compared to the base case. Energy allocation factors were as follows: natural gas H_2 HRJ = .533.
6. Other Changes: dLUC emissions of CO_2 were recalculated based on updated C stocks data from KUO Bionergia for native vegetation on three categories of land in the Yucatan (Table 11)

Energy allocation factors for this EU-RED case for each life cycle stage are displayed in Table A.1

Table A.11 Updated land category classes of native vegetation of the green bordered area from Figure 1, as well as of future jatropha plantations planted in this area.

Canopy Cover Classes	Carbon Content (tons C/ha)	Plantation Area (ha)
10% or less tree canopy cover	4.8	11,501
10-20% or tree canopy cover	13.65	21,726
20-30% or tree canopy cover	21	21,773
Jatropha plantation cover	17.5	55,000

Table A.12 Energy allocation factors (EAF) for the HRJ life-cycle for the EU-RED case.

Assemblies	EAF	Units
Jatropha cultivation and harvesting	0.533	p
Jatropha transport to Uman	0.533	p
Jatropha oil extraction at Uman	0.533	p
Jatropha oil transport to Cancún	0.533	p
HRJ production from jatropha oil	0.533	p

Global Warming Potentials from the European Commission were used in these new calculations: CO_2=1, N_2O=296, CH_4=23.

A.2 Glossary

Tool	Definition	Link to More Information
EcoInvent	Life Cycle Inventory Data	http://www.ecoinvent.org/
IPCC	Intergovernmental Panel on Climate Change	http://www.ipcc.ch/
EPA	Environmental Protection Agency	http://www.epa.gov/otaq/fuels/renewablefuels/index.htm
GREET	Greenhouse Gases, Regulated Emissions and Energy Use in Transportation Model	https://greet.es.anl.gov/
SimaPro	LCA software tool	http://www.pre-sustainability.com/simapro
USLCI	United States Life Cycle Inventory Database	http://www.nrel.gov/lci/
Ecobilan	Company that specializes in sustainable development	https://ecobilan.pwc.fr/
Office of Industrial Technology	Provide energy and environmental profiles of U.S. Industries	http://energy.gov/eere/amo/advanced-manufacturing-office
EIPRO	Environmental Impacts of Products	http://ipts.jrc.ec.europa.eu/publications/pub.cfm?id=1429
National Climatic Data Center	Provides climate and historical weather data for the United States	http://www.ncdc.noaa.gov/
SQCB	Sustainable Quick Check for Biofuels	http://www.sqcb.org/
CLIMWAT	Climatic database compiled by FAO (Food and Agriculture Organization of the UN)	http://www.fao.org/nr/water/infores_databases_climwat.html

CEDA	Comprehensive Environmental Data Archive	http://cedainformation.net/
EMIS	Environmental Management Information System	http://www.ess.co.at/EMIS/
Franklin	Life cycle inventory data based upon experience of companies operating in the USA	http://www.fal.com/lifecycle-services.html
GHGenius	A model for lifecycle assessment of transportation fuels in Canada	http://www.ghgenius.ca/
Maine Forest Service	Provide information about biomass resources	www.maineforestservice.gov/
NREL	National Renewable Energy Laboratory	www.nrel.gov/
USDA	US Department of Agriculture	www.usda.gov/
PestLCI	Model for estimating field emissions of pesticides in agricultural LCA	Morten Birkved, Michael Z. Hauschild, PestLCI—A model for estimating field emissions of pesticides in agricultural LCA, Ecological Modelling, Volume 198, Issues 3–4, 15 October 2006, Pages 433-451.
CML 2001	Impact Assessment Method	http://cml.leiden.edu/software/data-cmlia.html
TRACI	Tool for the Reduction and Assessment of Chemical and other Environmental Impacts	http://www.epa.gov/nrmrl/std/traci/traci.html
IPCC GWP 100a	Impact method used to calculate global warming potential	http://www.ipcc.ch/publications_and_data/ar4/wg1/en/ch2s2-10-2.html

EBAMM	ERG Biofuel Analysis Meta-Model	http://rael.berkeley.edu/sites/default/files/EBAMM/
EDIP	Environmental Development of Industrial Products	http://database-documentation.gabi-software.com/support/gabi/gabi-lcia-documentation/edip-2003/
IMPACT	Midpoint Impact Assessment Method	http://www.impactmodeling.net/
Ecological Scarcity	Midpoint Impact Assessment Methodology	http://www.esu-services.ch/projects/ubp06/
Eco-Indicator 99	Endpoint Impact Assessment Methodology	http://www.pre-sustainability.com/eco-indicator-99-manuals
Ecological Footprint	Endpoint impact assessment methodology	The Ecological Footprint Atlas 2008. Ewing, B.; Goldfinger, S.; Wackernagel, M.; Stechbart, M.; Stechbart, S.; Rizk, M.; Reed, A.; Kitzes, J.; Global Footprint Network: 2008.
USEtox	Endpoint impact assessment methodology	http://www.usetox.org/
ReCiPe	Endpoint impact assessment methodology	http://www.lcia-recipe.net/

A.3 References

Acreche MM, Valeiro AH (2013) Greenhouse gasses emissions and energy balances of a non-vertically integrated sugar and ethanol supply chain: A case study in Argentina Energy 54:146-154 doi:http://dx.doi.org/10.1016/j.energy.2012.12.046

Agusdinata D. B., Zhao F., Ileleji K., DeLaurentis D. (2011) Life cycle assessment of potential biojet fuel production in the United States Environmental Science & Technology 45:9133-9143 doi:10.1021/es202148g; 10.1021/es202148g

Amores M. J., Mele F. D., Jimenez Laureano, Castells Francesc (2013) Life cycle assessment of fuel ethanol from sugarcane in Argentina The International Journal of Life Cycle Assessment 18:1344-1357 doi:10.1007/s11367-013-0584-2

Bailis R, Kavlak G (2013) Environmental Implications of Jatropha Biofuel from a Silvi-Pastoral Production System in Central-West Brazil Environmental science & technology 47:8042-8050 doi:10.1021/es303954g

Bailis RE, Baka JE (2010) Greenhouse gas emissions and land use change from Jatropha curcas-based jet fuel in Brazil Environmental science & technology 44:8684-8691 doi:10.1021/es1019178; 10.1021/es1019178

Botero A, Jaime,, Castano P, Hader., Naranjo M, Carlos. (2011) Life Cycle Assessment for bioethanol produced from cassava in Colombia Produccion + Limpia 6:69-77

Bruinsma B (2009) Producción de biodiesel de palma aceitera y jatropha en la Amazona del Peru y el impacto para la sostenibilidad. Open Universiteit Nederland

Castanheira EG, Freire FM Environmental performance of palm oil biodiesel - a life cycle persepctive In: IEEE International Symposium on Sustainable Systems and Technology (ISSST), 2011. pp 1-6. doi:10.1109/ISSST.2011.5936843

Cavalett O, Chagas M, Seabra JEA, Bonomi A (2013) Comparative LCA of ethanol versus gasoline in Brazil using different LCIA methods The International Journal of Life Cycle Assessment 18:647-658 doi:10.1007/s11367-012-0465-0

Chavez-Rodriguez MF, Nebra SA (2010) Assessing GHG emissions, ecological footprint, and water linkage for different fuels Environmental science & technology 44:9252-9257 doi:10.1021/es101187h; 10.1021/es101187h

Chiu Y, Wen., Suh S, Pfister S, Hellweg S, Koehler A (2012) Measuring ecological impact of water consumption by bioethanol using life cycle impact assessment The International Journal of Life Cycle Assessment 17:16-24 doi:10.1007/s11367-011-0328-0

Chiu YW, Walseth B, Suh S (2009) Water embodied in bioethanol in the United States Environmental science & technology 43:2688-2692

Clarens AF, Resurreccion EP, White MA, Colosi LM (2010) Environmental life cycle comparison of algae to other bioenergy feedstocks Environmental science & technology 44:1813-1819 doi:10.1021/es902838n; 10.1021/es902838n

Consorcio C. U. E. (2012) Evaluacion del ciclo de vida de la cadena de produccion de biocombustibles en Colombia vol ATN/JC-10826-CO y ATN/JF-10827-CO. Medellin

da Costa E. R., Yanez E., Torres E. A. (2006) The energy balance in the production of palm oil biodiesel-two case studies: Brazil and Colombia:1-5

da Silva PV, van der Werf HMG, Spies A, Soares SR (2010) Variability in environmental impacts of Brazilian soybean according to crop production and transport scenarios

Journal of environmental management 91:1831-1839 doi:http://dx.doi.org/10.1016/j.jenvman.2010.04.001

de Oliveira D, Vaughan BE, Rykiel EJ (2005) Ethanol as fuel: energy, Carbon dioxide balances, and ecological footprint Bioscience 55:593-602 doi:10.1641/0006-3568(2005)0550593:EAFECD]2.0.CO;2; M3: doi: 10.1641/0006-3568(2005)0550593:EAFECD]2.0.CO;2; 02

10.1641/0006-3568(2005)055[0593:EAFECD]2.0.CO;2

de Souza SP, Pacca S, Turra dAM, Borges J, Luiz, B, (2010) Greenhouse gas emissions and energy balance of palm oil biofuel Renewable Energy 35:2552-2561 doi:http://dx.doi.org/10.1016/j.renene.2010.03.028

Emmenegger FM, Pfister S, Koehler A, Giovanetti L, Arena AP, Zah R (2011) Taking into account water use impacts in the LCA of biofuels: an Argentinean case study The International Journal of Life Cycle Assessment 16:869-877 doi:10.1007/s11367-011-0327-1

Fan J, Handler, R.M., Shonnard, D.R., Kalnes, T.N. (2012) A review of life cycle greenhouse gas emissions of hydroprocessed jet fuels from renewable oil and fats International Journal of Environmental Science and Engineering Research (IJESER) 3:114-138

Fu GZ, Chan AW, Minns DE (2003) Life cycle assessment of bio-ethanol derived from cellulose The international journal of life cycle assessment 8:137-141

Galbusera S, Hilbert JA (2011) Analisis de emisiones de gases de efecto invernadero de la produccion agricola extensiva y estudio de la "huella de carbono" de los productos derivados de la soja en la Republica de Argentina. INTA, Argentina

Garcia CA, Fuentes A, Hennecke A, Riegelhaupt E, Manzini F, Masera O (2011) Life-cycle greenhouse gas emissions and energy balances of sugarcane ethanol production in Mexico Applied Energy 88:2088-2097 doi:http://dx.doi.org/10.1016/j.apenergy.2010.12.072

Graefe Sand others (2011) Energy and carbon footprints of ethanol production using banana and cooking banana discard: A case study from Costa Rica and Ecuador Biomass and Bioenergy 35:2640-2649 doi:http://dx.doi.org/10.1016/j.biombioe.2011.02.051

Grillo R, Maria, Luiza,, Lora E, Eduardo, Silva,, Escobar P, Jose, Carlos,, Venturini O, Jose,, Buchgeister J, Almazan O (2011) A LCA (life cycle assessment) of the methanol production from sugarcane bagasse ECOS 2009 36:3716-3726 doi:http://dx.doi.org/10.1016/j.energy.2010.12.010

Hertel T, Golub AA, Jones AD, O'Hare M, Plevin RJ, Kammen DM (2010) Effects of US maize ethanol on global land use and greenhouse gas emissions: Estimating market-mediated responses Bioscience 60:223 doi:10.1525/bio.2010.60.3.8

Hilbert JA, Donato LB, Muzio J, Huerga I (2009) Analisis comparativo del consumo energetico y las emisiones de gases efecto invernadero de la produccion de biodiesel a base de soja bajo manejos de siembra directa y labranza convencional vol IIR-BC-INF-06-09. Instituto Nacional de Tecnologia Agropecuaria, Argentina

Huo H, Wang M, Bloyd C, Putsche V (2008) Life-cycle assessment of energy and greenhouse gas effects of soybean-derived biodiesel and renewable fuels.

Iriarte A, Rieradevall J, Gabarrell X (2010) Life cycle assessment of sunflower and rapeseed as energy crops under Chilean conditions Journal of Cleaner Production 18:336-345 doi:http://dx.doi.org/10.1016/j.jclepro.2009.11.004

Iriarte A, Rieradevall J, Gabarrell X (2012) Transition towards a more environmentally sustainable biodiesel in South America: The case of Chile Applied Energy 91:263-273 doi:http://dx.doi.org/10.1016/j.apenergy.2011.09.024

Iriarte A, Villalobos P (2013) Greenhouse gas emissions and energy balance of sunflower biodiesel: Identification of its key factors in the supply chain Resources, Conservation and Recycling 73:46-52 doi:http://dx.doi.org/10.1016/j.resconrec.2013.01.014

Kauffman N, Hayes D, Brown R (2011) A life cycle assessment of advanced biofuel production from a hectare of corn Fuel 90:3306-3314

Kim S, Dale B (2006) Ethanol fuels: E10 or E85 - Life cycle perspectives The International Journal of Life Cycle Assessment 11:117-121 doi:10.1065/lca2005.02.201

Kim S, Dale B (2009) Regional variations in greenhouse gas emissions of biobased products in the United States - corn-based ethanol and soybean oil The International Journal of Life Cycle Assessment 14:540-546 doi:10.1007/s11367-009-0106-4

Kim S, Dale BE (2005a) Environmental aspects of ethanol derived from no-tilled corn grain: nonrenewable energy consumption and greenhouse gas emissions Biomass and Bioenergy 28:475-489 doi:http://dx.doi.org/10.1016/j.biombioe.2004.11.005

Kim S, Dale BE (2005b) Life cycle assessment of various cropping systems utilized for producing biofuels: Bioethanol and biodiesel Biomass and Bioenergy 29:426-439 doi:http://dx.doi.org/10.1016/j.biombioe.2005.06.004

Kim S, Dale BE (2008) Life cycle assessment of fuel ethanol derived from corn grain via dry milling Cellulose Conversion in Dry Grind Plants 99:5250-5260 doi:http://dx.doi.org/10.1016/j.biortech.2007.09.034

Kim S, Dale BE, Jenkins R (2009) Life cycle assessment of corn grain and corn stover in the United States The International Journal of Life Cycle Assessment 14:160-174 doi:10.1007/s11367-008-0054-4

Koch S (2003) LCA of biodiesel in Costa Rica: An environmental study on the manufacturing and use of palm oil methyl ester. San Jose

Krohn BJ, Fripp M (2012) A life cycle assessment of biodiesel derived from the "niche filling" energy crop camelina in the USA Applied Energy 92:92-98 doi:http://dx.doi.org/10.1016/j.apenergy.2011.10.025

Liska AJ, Yang HS, Bremer VR, Klopfenstein TJ, Walters DT, Erickson GE, Cassman KG (2009) Improvements in life cycle energy efficiency and greenhouse gas emissions of corn-ethanol Journal of Industrial Ecology 13:58-74 doi:10.1111/j.1530-9290.2008.00105.x

Luo L, van der Voet E, Huppes G (2009a) Life cycle assessment and life cycle costing of bioethanol from sugarcane in Brazil Renewable and Sustainable Energy Reviews 13:1613-1619 doi:http://dx.doi.org/10.1016/j.rser.2008.09.024

Luo L, Voet E, Huppes G, Udo de Haes H (2009b) Allocation issues in LCA methodology: a case study of corn stover-based fuel ethanol The International Journal of Life Cycle Assessment 14:529-539 doi:10.1007/s11367-009-0112-6

Macedo IC, Seabra JEA, Silva JEAR (2008) Green house gases emissions in the production and use of ethanol from sugarcane in Brazil: The 2005/2006 averages and a

prediction for 2020 Biomass and Bioenergy 32:582-595 doi:http://dx.doi.org/10.1016/j.biombioe.2007.12.006

Mishra GS, Yeh S (2011) Life cycle water consumption and withdrawal requirements of ethanol from corn grain and residues Environmental science & technology 45:4563-4569 doi:10.1021/es104145m; 10.1021/es104145m

Molina CM (2008) Aplicacion del Modelo EBAMM para Estimar el Impacto Ambiental y Energetico de la Produccion de Bioetanol a Partir de Ca~na de Azucar en Mexico desde la Perspectiva de Ciclo de Vida.

Neupane B, Halog A, Dhungel S (2011) Attributional life cycle assessment of woodchips for bioethanol production Journal of Cleaner Production 19:733-741 doi:http://dx.doi.org/10.1016/j.jclepro.2010.12.002

Ometto AR, Hauschild MZ, Nelson Lopes RW (2009) Lifecycle assessment of fuel ethanol from sugarcane in Brazil The International Journal of Life Cycle Assessment 14:236-247 doi:10.1007/s11367-009-0065-9

Panichelli L, Dauriat A, Gnansounou E (2009) Life cycle assessment of soybean-based biodiesel in Argentina for export The International Journal of Life Cycle Assessment 14:144-159 doi:10.1007/s11367-008-0050-8

Pivotto F, Lamano Ferreira M, Lamano Ferreira APN (2011) Analise do ciclo de vida do biodiesel no mercado brasileiro e quantificacao das emissoes liberadas pelo uso desse combustivel Exacta 9:293-300

Pradhan A, Shrestha DS, McAloon A, Yee W, Hass M, Duffield JA (2011) Energy life-cycle assessment of soybean biodiesel revisited American Society of Agricultural and Biological Engineers 5:1031-1039

Queiroz AG, Franca L, Ponte MX (2012) The life cycle assessment of biodiesel from palm oil ("dende") in the Amazon Biomass and Bioenergy 36:50-59 doi:http://dx.doi.org/10.1016/j.biombioe.2011.10.007

Quintero JA, Montoya MI, Sanchez OJ, Giraldo OH, Cardona CA (2008) Fuel ethanol production from sugarcane and corn: Comparative analysis for a Colombian case Energy 33:385-399 doi:http://dx.doi.org/10.1016/j.energy.2007.10.001

Ramirez T, Carlos A (2011) Energetics of Brazilian ethanol: Comparison between assessment approaches At the Crossroads: Pathways of Renewable and Nuclear Energy Policy in North Africa 39:4605-4613 doi:http://dx.doi.org/10.1016/j.enpol.2011.05.001

RED (2009) Directive 2009/28/EC of the European Parliament and of the Council of 23 April 2009 on the promotion of the use of energy from renewable sources and amending and subsequently repealing Directives 2001/77/EC and 2003/30/EC vol 2013.

Reijnders L, Huijbregts MAJ (2008) Biogenic greenhouse gas emissions linked to the life cycles of biodiesel derived from European rapeseed and Brazilian soybeans Journal of Cleaner Production 16:1943-1948 doi:http://dx.doi.org/10.1016/j.jclepro.2008.01.012

Rodriguez Ibarra JJ (2012) Analisis del ciclo de vida de la produccion de biodiesel a partir del descarne procedente de la industria de la curtiduria Acta Universitaria 22:5-13

RSB (2013) RSB fossil fuel baseline calculation methodology vol 2013.

Sander K, Murthy G (2010) Life cycle analysis of algae biodiesel The International Journal of Life Cycle Assessment 15:704-714 doi:10.1007/s11367-010-0194-1

Scown CDand others (2012) Corrigendum: Lifecycle greenhouse gas implications of US national scenarios for cellulosic ethanol production Environmental Research Letters 7:019502

Souza S, Pereira, de Avila M, Turra,, Pacca S (2012) Life cycle assessment of sugarcane ethanol and palm oil biodiesel joint production Biomass and Bioenergy 44:70-79 doi:http://dx.doi.org/10.1016/j.biombioe.2012.04.018

Spatari S, Zhang Y, MacLean HL (2005) Life cycle assessment of switchgrass-and corn stover-derived ethanol-fueled automobiles Environmental science & technology 39:9750-9758

Tsao CC, Campbell JE, Mena-Carrasco M, Spak SN, Carmichael GR, Chen Y (2012) Biofuels that cause land-use change may have much larger non-GHG air quality emissions than fossil fuels Environmental science & technology 46:10835-10841 doi:10.1021/es301851x; 10.1021/es301851x

Turdera MV (2013) Energy balance, forecasting of bioelectricity generation and greenhouse gas emission balance in the ethanol production at sugarcane mills in the state of Mato Grosso do Sul Renewable and Sustainable Energy Reviews 19:582-588 doi:http://dx.doi.org/10.1016/j.rser.2012.11.055

Vargas-Gómez C-A (2009) Life Cycle Analysis of Carbon for Palm Oil in Colombia Científica 13:69-75

Velásquez HI, Ruiz AA, Oliveira Sd (2010) Análisis energético y exergético del proceso de obtención de etanol a partir de la fruta del banano Revista Facultad de Ingenieria Universidad de Antioquia 51:87-96

Wang M, Han J, Dunn JB, Cai H, Elgowainy A (2012) Well-to-wheels energy use and greenhouse gas emissions of ethanol from corn, sugarcane and cellulosic biomass for US use Environmental Research Letters 7:045905

Wang M, Han J, Haq Z, Tyner WE, Wu M, Elgowainy A (2011) Energy and greenhouse gas emission effects of corn and cellulosic ethanol with technology improvements and land use changes Biomass and Bioenergy 35:1885-1896 doi:http://dx.doi.org/10.1016/j.biombioe.2011.01.028

Wang M, Wu M, Huo H (2007a) Life-cycle energy and greenhouse gas emission impacts of different corn ethanol plant types Environmental Research Letters 2:024001

Wang M, Wu M, Huo H, Liu J (2007b) Well-to-Wheels Energy Use and Greenhouse Gas Emissions of Brazilian Sugarcane Ethanol Production Simulated by Using the GREET Model vol 1.

Wu M, Wang M, Huo H (2006) Fuel-cycle assessment of selected bioethanol production pathways in the United States. Oak Ridge

Yanez Angarita EE, Silva Lora EE, da Costa RE, Torres EA (2009) The energy balance in the Palm Oil-Derived Methyl Ester (PME) life cycle for the cases in Brazil and Colombia Renewable Energy 34:2905-2913 doi:http://dx.doi.org/10.1016/j.renene.2009.05.007

Yang J, Xu M, Zhang X, Hu Q, Sommerfeld M, Chen Y (2011) Life-cycle analysis on biodiesel production from microalgae: Water footprint and nutrients balance Special Issue: Biofuels - II: Algal Biofuels and Microbial Fuel Cells 102:159-165 doi:http://dx.doi.org/10.1016/j.biortech.2010.07.017

Yang Y (2013) Life cycle freshwater ecotoxicity, human health cancer, and noncancer impacts of corn ethanol and gasoline in the U.S Journal of Cleaner Production 53:149-157 doi:http://dx.doi.org/10.1016/j.jclepro.2013.04.009

Yang Y, Bae J, Kim J, Suh S (2012) Replacing gasoline with corn ethanol results in significant environmental problem-shifting Environmental science & technology 46:3671-3678 doi:10.1021/es203641p; 10.1021/es203641p

Zaimes GG, Khanna V (2013) Microalgal biomass production pathways: evaluation of life cycle environmental impacts Biotechnology for biofuels 6:88

Zumalacárregui L, Zumalacárregui B (2011) Cálculo del beneficio ambiental de la caña de azúcar para la producción de etanol combustible Revista Ingeniería y Competitividad 10:65-71

Appendix B. Characterization of Products from Fast Micro-Pyrolysis of Municipal Solid Waste (MSW)

B.1 Bio-Oil Composition

Table B.1: Total bio-oil mass (above the 0.5% peak area percent cutoff) from fiberboard

Compounds	Mass average (microgram)	Mass percent (%)	Mass average STDV
Small molecular weight compounds	***12.63***	***6.58***	***2.19***
Acetone	1.19	0.62	0.14
Acetaldehyde, hydroxy-	3.40	1.77	0.95
Acetic acid	3.94	2.05	0.57
2-Propanone, 1-hydroxy	1.87	0.97	0.31
Acetic acid, (acetyloxy)-	2.24	1.16	0.35
2-hydroxy-2-cyclopenten-1-	1.09	0.57	0.15
2-Cyclopenten-1-one, 2-hydroxy-3-methyl-	0.53	0.28	0.07
Light Sugars	***1.44***	***0.75***	***0.28***
3-Furaldehyde	0.87	0.45	0.20
5-Hydroxymethylfurfural	0.57	0.29	0.09
Lignin	***5.22***	***2.72***	***0.77***
2-Methoxy phenol	0.37	0.19	0.04
Creosol	0.64	0.34	0.13
2-Methoxy-4-vinylphenol	0.54	0.28	0.07
Phenol, 2-methoxy-4-(1-propenyl)-	0.35	0.18	0.05
Acetic acid, (4-hydroxy-3-methoxyphenyl)-	0.75	0.39	0.26
Phenol, 2,6-dimethoxy-4-(2-propenyl)-	1.12	0.58	0.14
Phenol, 2,6-dimethoxy-	0.42	0.22	0.01
4-((1E)-3-Hydroxy-1-propenyl)-2-methoxyphenol	0.85	0.44	0.13
Phenol, 4-acetyl-2-methoxy	0.18	0.10	0.03
Sugars	***6.48***	***3.37***	***1.02***
Levoglucosan	6.48	3.37	1.02
Unknown compounds	***30.18***	***15.72***	***1.90***
Unknown Low MW (1 data)	0.46	0.24	0.09
Unknown Light Sugar (4 data)	2.39	1.24	0.18
Unknown Sugar (from 6 data)	33.71	17.56	3.75
Unknown Phenolic (from 14 data)	3.56	1.86	3.08
Unknown (from 12 data)	-	-	-
Total bio-oil mass	***63.04***	***32.83***	***10.04***

Table B.2: Total bio-oil mass (above the 1% peak area percent cutoff) from grass clippings

Compounds	Mass average (microgram)	Mass percent (%)	Mass average STDV
Small molecular weight compounds	***7.17***	***3.79***	***1.75***
Acetone	0.58	0.31	0.06
Acetaldehyde, hydroxy-	0.91	0.48	0.25
Acetic acid	2.12	1.12	0.67
Acetic acid, (acetyloxy)-	2.65	1.40	0.94
2-hydroxy-2-cyclopenten-1-	0.52	0.27	0.14
2-Cyclopenten-1-one, 2-hydroxy-3-methyl-	0.38	0.20	0.07
Light sugars	***1.55***	***0.82***	***0.50***
3-Furaldehyde	0.35	0.19	0.15
2-Furanmethanol	0.30	0.16	0.12
2(5H)-Furanone	0.48	0.25	0.15
5-Hydroxymethylfurfural	0.42	0.22	0.13
Lignin	***1.90***	***1.01***	***0.50***
Phenol	0.34	0.18	0.04
2-Methoxy phenol	0.19	0.10	0.09
Creosol	0.20	0.11	0.04
Phenol, 4-ethyl-2-methoxy-	0.18	0.10	0.13
2-Methoxy-4-vinylphenol	0.16	0.09	0.05
Phenol, 2-methoxy-4-(1-propenyl)-	0.14	0.07	0.04
Benzaldehyde, 4-hydroxy-3,5-dimethoxy-	0.35	0.18	0.04
4-((1E)-3-Hydroxy-1-propenyl)-2-methoxyphenol	0.35	0.18	0.10
Unknown compounds	***56.98***	***30.10***	***7.17***
Unknown furfural (from 1 data)	0.27	0.14	0.09
Unknown sugars (from 17 data)	49.50	26.14	6.29
Unknown phenolic (from 12 data)	7.22	3.81	0.89
Unknown (from 19 data)	-	-	-
Total bio-oil mass	***67.61***	***35.71***	***9.67***

Table B.3: Total bio-oil mass (above the 1% peak area percent cutoff) from acid washing of grass clippings

Compounds	Mass average (microgram)	Mass percent (%)	Mass average STDV
Small molecular weight compounds	***2.53***	***1.93***	***0.23***
Acetone	0.45	0.34	0.04
Acetic acid	1.56	1.19	0.21
1,2-Cyclopentanedione	0.29	0.22	0.02
3-Pyridinol	0.24	0.18	0.01
Light sugars	***2.39***	***1.83***	***0.13***
2(5H)-Furanone	0.42	0.32	0.00
3-Furaldehyde	0.83	0.63	0.08
2(3H)-Furanone, 3-butyldihydro-	*0.65*	*0.49*	*0.03*
Benzofuran, 2,3-dihydro-	0.49	0.38	0.03
Lignin	***0.89***	***0.68***	***0.03***
p-Cresol	0.31	0.24	0.02
2-Methoxy-4-vinylphenol	0.57	0.44	0.02
Sugars	***38.53***	***29.49***	***6.97***
Levoglucosenone	0.66	0.50	0.03
β-D-Glucopyranose	*4.67*	*3.57*	*0.46*
Levoglucosan	33.21	25.41	6.84
Unknown compounds	***65.52***	***50.14***	***7.88***
Unknown furan (from 1 data)	0.60	0.46	0.06
Unknown sugars (from 10 data)	62.86	48.10	7.64
Unknown phenolic (from 3 data)	2.06	1.57	0.32
Unknown (from 4 data)	-	-	-
Total bio-oil mass	***109.85***	***84.07***	***13.96***

Table B.4: Total bio-oil mass (above the 1% peak area percent cutoff) from Microllam

Compounds	Mass average (microgram)	Mass percent (%)	Mass average STDV
Small molecular weight compounds	***9.39***	***6.21***	***1.87***
Acetone	0.96	0.61	0.26
Acetaldehyde, hydroxy-	4.16	2.61	1.06
Acetic acid	2.74	1.72	0.65
2-hydroxy-2-cyclopenten-1-	1.06	0.67	0.31
2-Cyclopenten-1-one, 2-hydroxy-3-methyl-	0.46	0.29	0.52
Light sugars	***3.20***	***2.01***	***0.88***
2-Furanmethanol	2.62	1.65	0.59
2(5H)-Furanone	0.58	0.36	0.29
Lignin	***7.00***	***4.39***	***1.65***
2-Methoxy phenol	0.29	0.18	0.08
Creosol	0.33	0.21	0.13
Phenol, 4-ethyl-2-methoxy-	0.29	0.18	0.09
2-Methoxy-4-vinylphenol	0.46	0.29	0.14
Phenol, 2-methoxy-4-(2-propenyl)-	0.22	0.14	0.09
4-Hydroxy-2-methoxybenaldehyde	0.36	0.23	0.12
Phenol, 2-methoxy-4-(1-propenyl)-	1.82	1.14	0.33
Phenol, 4-acetyl-2-methoxy	1.10	0.69	0.49
Acetic acid, (4-hydroxy-3-methoxyphenyl)-	0.46	0.29	0.12
4-((1E)-3-Hydroxy-1-propenyl)-2-methoxyphenol	1.67	1.05	0.32
Sugars	***3.89***	***2.44***	***2.06***
Levoglucosan	3.89	2.44	2.06
Unknown compounds	***48.31***	***30.32***	***16.93***
Unknown phenolic (from 4 data)	3.30	2.07	1.38
Unknown sugars (from 6 data)	45.01	28.25	15.55
Unknown large tar (from 3 data)	-	-	-
Unknown (from 2 data)	-	-	-
Total bio-oil mass	***71.78***	***45.05***	***22.89***

Table B.5: Total bio-oil mass (above the 1% peak area percent cutoff) from waste paper

Compounds	Mass average (microgram)	Mass percent (%)	Mass average STDV
Small molecular weight compounds	***14.20***	***10.49***	***4.40***
Acetone	0.90	0.67	0.21
Acetaldehyde, hydroxy-	4.75	3.51	0.98
Acetic acid ethenyl ester	0.63	0.46	0.13
Acetic acid	1.83	1.35	1.02
2-Propanone, 1-hydroxy	1.70	1.26	0.37
Acetic acid, (acetyloxy)-	1.01	0.75	0.27
Acetic anhydride	1.84	1.36	2.16
2-hydroxy-2-cyclopenten-1-	0.64	0.47	0.14
2-Cyclopenten-1-one, 2-hydroxy-3-methyl-	0.89	0.66	1.19
Light sugars	***1.51***	***1.12***	***0.56***
3-Furaldehyde	0.58	0.43	0.12
2(5H)-Furanone	0.37	0.27	0.08
5-Hydroxymethylfurfural	0.56	0.42	0.49
Lignin	***1.43***	***1.06***	***0.60***
2-Methoxy phenol	0.23	0.17	0.06
Creosol	0.26	0.19	0.11
2-Methoxy-4-vinylphenol	0.20	0.15	0.15
Phenol, 2-methoxy-4-(1-propenyl)-	0.09	0.07	0.08
4-((1E)-3-Hydroxy-1-propenyl)-2-methoxyphenol	0.33	0.24	0.29
Styrene	0.32	0.24	0.12
Sugars	***6.90***	***5.10***	***2.79***
Levoglucosan	6.90	5.10	2.79
Unknown compounds	***40.51***	***29.93***	***10.18***
Unknown aldehyde/acid (from 2 data)	1.78	1.31	0.39
Unknown sugars (from 7 data)	38.73	28.62	10.14
Unknown large tar (from 1 data)	-	-	-
Total bio-oil mass	***64.55***	***47.70***	***14.09***

Table B.6: Total bio-oil mass (above the 1% peak area percent cutoff) from acid washing of waste paper

Compounds	Mass average (microgram)	Mass percent (%)	Mass average STDV
Small molecular weight compounds	***5.06***	***4.22***	***1.42***
Acetone	0.97	0.81	0.03
Acetaldehyde, hydroxy-	2.85	2.38	1.19
1-Pentanol, 2,3-dimethyl-	1.24	1.03	0.23
Light sugars	***3.87***	***3.22***	***1.12***
3-Furaldehyde	0.79	0.66	0.20
2(3H)-Furanone, 3-butyldihydro-	0.35	0.29	0.11
5-Hydroxymethylfurfural	1.13	0.94	0.26
2(3H)-Furanone, dihydro-3-(thioacetyl)-	1.60	1.33	0.58
Lignin	***0.29***	***0.24***	***0.18***
Styrene	0.17	0.14	0.02
4-((1E)-3-Hydroxy-1-propenyl)-2-methoxyphenol	0.12	0.10	0.17
Sugars	***44.56***	***37.13***	***4.98***
Methyl-α-d-ribofuranoside	13.35	11.12	3.42
D-Allose	3.18	2.65	0.33
Levoglucosan	28.03	23.36	1.85
Unknown compounds	***35.69***	***29.74***	***2.37***
Unknown aldehyde/acid (from 1 data)	0.73	0.61	0.46
Unknown phenolic (from 1 data)	0.29	0.24	0.07
Unknown sugar (from 3 data)	34.67	28.89	2.35
Total bio-oil mass	***89.47***	***74.56***	***6.29***

Table B.7: Total bio-oil mass (above the 1% peak area percent cutoff) from plywood

Compounds	Mass average (microgram)	Mass percent (%)	Mass average STDV
Small molecular weight compounds	***21.09***	***11.46***	***3.18***
Acetone	1.49	0.81	0.31
Acetaldehyde, hydroxy-	7.11	3.87	0.53
Acetic acid	3.61	1.96	0.21
2-Propanone, 1-hydroxy	4.15	2.25	1.32
Acetic acid, (acetyloxy)-	3.06	1.66	0.51
2-hydroxy-2-cyclopenten-1-	1.14	0.62	0.23
2-Cyclopenten-1-one, 2-hydroxy-3-methyl-	0.52	0.28	0.11
Light sugars	***3.62***	***1.97***	***0.21***
3-Furaldehyde	1.08	0.58	0.19
2-Furanmethanol	0.50	0.27	0.04
2(5H)-Furanone	0.57	0.31	0.08
5-Hydroxymethylfurfural	1.48	0.80	0.48
Lignin	***8.17***	***4.44***	***1.15***
Phenol	0.15	0.08	0.17
2-Methoxy phenol	0.52	0.28	0.04
Creosol	1.06	0.57	0.21
2-Methoxy-4-vinylphenol	0.84	0.46	0.07
Phenol, 2,6-dimethoxy-	0.29	0.16	0.48
Phenol, 2-methoxy-4-(2-propenyl)-	0.31	0.17	0.03
4-Hydroxy-2-methoxybenaldehyde	0.30	0.16	0.03
Phenol, 4-acetyl-2-methoxy	0.31	0.17	0.07
Acetic acid, (4-hydroxy-3-methoxyphenyl)-	0.55	0.30	0.22
Benzaldehyde, 4-hydroxy-3,5-dimethoxy-	0.21	0.11	0.36
Phenol, 2,6-dimethoxy-4-(2-propenyl)-	0.42	0.23	0.45
4-((1E)-3-Hydroxy-1-propenyl)-2-methoxyphenol	2.10	1.14	0.27
Phenol, 2-methoxy-4-(1-propenyl)-	1.09	0.59	0.28
Sugars	***14.69***	***7.98***	***6.25***
Levoglucosan	14.69	7.98	6.25
Unknown compounds	***76.37***	***41.50***	***6.54***
Unknown Low MW (from 2 data)	3.99	2.17	0.47
Unknown Furan	0.73	0.40	0.21
Unknown Phenolic (from 8 data)	36.28	19.72	12.06
Unknown Sugar (from 5 data)	35.36	19.22	10.79
Unknown (from 4 data)	-	-	-
Total bio-oil mass	***123.93***	***67.35***	***7.12***

Table B.8: Total bio-oil mass (above the 1% peak area percent cutoff) from waferboard

Compounds	Mass average (microgram)	Mass percent (%)	Mass average STDV
Small molecular weight compounds	***18.33***	***12.76***	***2.21***
Acetone	1.47	1.02	0.33
Acetaldehyde, hydroxy-	5.61	3.91	0.90
Acetic acid	4.55	3.16	0.87
2-Propanone, 1-hydroxy	1.81	1.26	0.45
Acetic acid, (acetyloxy)-	3.09	2.15	0.77
2-hydroxy-2-cyclopenten-1-	1.27	0.88	0.28
2-Cyclopenten-1-one, 2-hydroxy-3-methyl-	0.53	0.37	0.14
Light sugars	***1.83***	***1.27***	***0.56***
3-Furaldehyde	1.10	0.77	0.28
5-Hydroxymethylfurfural	0.73	0.51	0.34
Lignin	***6.71***	***4.67***	***1.09***
Phenol	0.62	0.43	0.13
2-Methoxy phenol	0.36	0.25	0.02
Creosol	0.40	0.28	0.09
2-Methoxy-4-vinylphenol	0.39	0.27	0.08
Phenol, 2,6-dimethoxy-	0.90	0.63	0.20
Phenol, 2-methoxy-4-(1-propenyl)-	0.29	0.20	0.07
Phenol, 4-acetyl-2-methoxy	0.57	0.40	0.09
Benzaldehyde, 4-hydroxy-3,5-dimethoxy-	0.62	0.43	0.13
Phenol, 2,6-dimethoxy-4-(2-propenyl)-	1.02	0.71	0.17
4-((1E)-3-Hydroxy-1-propenyl)-2-methoxyphenol	1.54	1.07	0.36
Sugars	***2.89***	***2.01***	***1.45***
Levoglucosan	2.89	2.01	1.45
Unknown compounds	***49.69***	***34.59***	***4.19***
Unknown aldehyde/acid (from 2 data)	3.75	2.61	0.74
Unknown phenolic (from 5 data)	4.05	2.82	0.95
Unknown sugar (from 3 data)	41.89	29.16	3.46
Unknown large tar (from 2 data)	-	-	-
Unknown (from 2 data)	-	-	-
Total bio-oil mass	***79.45***	***55.30***	***6.07***

Table B.9: Total bio-oil mass (above the 1% peak area percent cutoff) from corn stover

Compounds	Mass average (microgram)	Mass percent (%)	Mass average STDV
Small molecular weight compounds	***13.60***	***8.89***	***7.74***
Acetone	1.10	0.72	0.67
Acetaldehyde, hydroxy-	4.31	2.82	2.39
Acetic acid	5.42	3.54	3.75
2-hydroxy-2-cyclopenten-1-	0.20	0.13	0.08
2-Cyclopenten-1-one, 2-hydroxy-3-methyl-	0.36	0.23	0.26
Propanoic acid, 1-methylpropyl ester	0.58	0.38	0.31
Acetic acid, (acetyloxy)-	1.62	1.06	1.18
Light Sugars	***2.64***	***1.73***	***1.44***
2(5H)-Furanone	2.34	1.53	1.24
5-Hydroxymethylfurfural	0.30	0.20	0.21
Lignin	***6.15***	***4.02***	***3.55***
Phenol	0.54	0.36	0.30
2-Methoxy phenol	0.28	0.18	0.17
Creosol	0.48	0.31	0.28
Phenol, 4-ethyl-2-methoxy-	0.31	0.20	0.20
2-Methoxy-4-vinylphenol	1.16	0.75	0.69
Phenol, 2,6-dimethoxy-	0.34	0.22	0.19
4-Hydroxy-2-methoxybenaldehyde	0.66	0.43	0.37
2,5-Dimethoxybenzyl alcohol	0.29	0.19	0.17
Phenol, 2-methoxy-4-(1-propenyl)-	0.25	0.16	0.04
Phenol, 3-(1,1-dimethylethyl)-4-methoxy-	0.11	0.07	0.09
4-((1E)-3-Hydroxy-1-propenyl)-2-methoxyphenol	0.99	0.65	0.65
Phenol, 2,6-dimethoxy-4-(2-propenyl)-	0.76	0.49	0.44
Unknown compounds	***62.43***	***40.80***	***37.19***
Unknown Phenolic (from 8 data)	2.36	1.54	1.37
Unknown sugar (from 13 data)	60.07	39.26	35.88
Unknown large tar (from 3 data)	-	-	-
Unknown (from 11 data)	-	-	-
Total bio-oil mass	***84.82***	***55.44***	***49.53***

Table B.10: Total bio-oil mass (above the 1% peak area percent cutoff) from switchgrass

Compounds	Mass average (microgram)	Mass percent (%)	Mass average STDV
Small molecular weight compounds	***13.79***	***8.55***	***1.69***
Acetone	0.77	0.48	0.67
Acetaldehyde, hydroxy-	4.13	2.56	0.65
Acetic acid	3.62	2.24	0.88
2-Propanone, 1-hydroxy	1.91	1.18	0.57
Acetic acid, (acetyloxy)-	1.85	1.15	0.19
2-hydroxy-2-cyclopenten-1-	1.01	0.63	0.19
2-Cyclopenten-1-one, 2-hydroxy-3-methyl-	0.50	0.31	0.14
Light sugars	***2.23***	***1.38***	***0.49***
3-Furaldehyde	1.26	0.78	0.26
2-Furanmethanol	0.52	0.32	0.05
5-Hydroxymethylfurfural	0.46	0.29	0.20
Lignin	***4.93***	***3.05***	***0.77***
4-((1E)-3-Hydroxy-1-propenyl)-2-methoxyphenol	0.33	0.21	0.13
2-Methoxy phenol	0.36	0.22	0.08
Creosol	0.42	0.26	0.09
2-Methoxy-4-vinylphenol	1.03	0.64	0.35
Phenol, 2,6-dimethoxy-	0.76	0.47	0.30
Phenol, 2-methoxy-4-(1-propenyl)-	0.26	0.16	0.07
Phenol, 4-acetyl-2-methoxy	0.51	0.31	0.02
Phenol, 2,6-dimethoxy-4-(2-propenyl)-	0.38	0.24	0.15
4-((1E)-3-Hydroxy-1-propenyl)-2-methoxyphenol	0.87	0.54	0.26
Sugars	***1.06***	***0.66***	***0.72***
Levoglucosan	1.06	0.66	0.72
Unknown compounds	***40.01***	***24.80***	***6.11***
Unknown aldehyde/acid (from 2 data)	2.75	1.71	0.53
Unknown furfural (from 1 data)	3.79	2.35	0.39
Unknown phenolic (from 1 data)	0.48	0.30	0.20
Unknown sugars (from 5 data)	32.99	20.45	5.57
Unknown large tar (from 1data)	-	-	-
Unknown (from 1 data)	-	-	-
Total bio-oil mass	***62.02***	***38.44***	***9.09***

Table B.11: Mass percentage of identified bio-oil composition (above the 1% peak area percent cutoff) between grass clippings and acid washed grass clippings.

Compounds	Bio-oil mass percentage (%)	
	Grass clippings	**Acid washed grass clippings**
Small molecular weight compounds	***3.79***	***1.93***
Acetone	0.31	0.34
Acetaldehyde, hydroxy-	0.48	-
Acetic acid	1.12	1.19
Acetic acid, (acetyloxy)-	1.40	-
2-hydroxy-2-cyclopenten-1-	0.27	-
2-Cyclopenten-1-one, 2-hydroxy-3-methyl-	0.20	-
1,2-Cyclopentanedione	-	0.22
3-Pyridinol	-	0.18
Light sugars	***0.82***	***1.83***
3-Furaldehyde	0.19	0.63
2-Furanmethanol	0.16	-
2(5H)-Furanone	0.25	0.32
5-Hydroxymethylfurfural	0.22	-
2(3H)-Furanone, 3-butyldihydro-	-	*0.49*
Benzofuran, 2,3-dihydro-	-	0.38
Lignin	***1.01***	***0.68***
Phenol	0.18	-
2-Methoxy phenol	0.10	-
Creosol	0.11	-
Phenol, 4-ethyl-2-methoxy-	0.10	-
2-Methoxy-4-vinylphenol	0.09	0.44
Phenol, 2-methoxy-4-(1-propenyl)-	0.07	-
Benzaldehyde, 4-hydroxy-3,5-dimethoxy-	0.18	-
4-((1E)-3-Hydroxy-1-propenyl)-2-methoxyphenol	0.18	-
p-Cresol	-	0.24
Sugars	***-***	***29.49***
Levoglucosenone	***-***	0.50
β-D-Glucopyranose	***-***	*3.57*
Levoglucosan	***-***	25.41
Unknown compounds	***30.48***	***50.14***
Unknown furan	0.14	0.46
Unknown sugars	26.53	48.10
Unknown phenolic	3.81	1.57
Total bio-oil mass (%)	***36.34***	***69.08***

Table B.12: Mass percentage of identified bio-oil composition (above the 1% peak area percent cutoff) between waste paper and acid washed waste paper.

Compounds	Bio-oil mass percentage (%)	
	Waste Paper	**Acid Washed Waste Paper**
Small molecular weight compounds	***10.49***	***4.22***
Acetone	0.67	0.81
Acetaldehyde, hydroxy-	3.51	2.38
Acetic acid ethenyl ester	0.46	-
Acetic acid	1.35	-
2-Propanone, 1-hydroxy	1.26	-
Acetic acid, (acetyloxy)-	0.75	-
Acetic anhydride	1.36	-
2-hydroxy-2-cyclopenten-1-	0.47	-
2-Cyclopenten-1-one, 2-hydroxy-3-methyl-	0.66	-
1-Pentanal, 2,3-dimethyl-	-	1.03
Light sugar	***1.12***	***3.22***
3-Furaldehyde	0.43	0.66
2(5H)-Furanone	0.27	-
5-Hydroxymethylfurfural	0.42	0.94
2(3H)-Furanone, 3-butyldihydro-	-	0.29
2(3H)-Furanone, dihydro-3-(thioacetyl)-	-	1.33
Lignin	***1.06***	***0.24***
2-Methoxy phenol	0.17	-
Creosol	0.19	-
2-Methoxy-4-vinylphenol	0.15	-
Phenol, 2-methoxy-4-(1-propenyl)-	0.07	-
4-((1E)-3-Hydroxy-1-propenyl)-2-methoxyphenol	0.24	0.10
Styrene	0.24	0.14
Sugars	***5.10***	***37.13***
Levoglucosan	5.10	23.36
Methyl-α-d-ribofuranoside	**-**	11.12
D-Allose	**-**	2.65
Unknown compounds	***29.93***	***29.74***
Unknown aldehyde/acid	1.31	0.61
Unknown sugars	28.62	28.89
Unknown phenolic	**-**	0.24
Total bio-oil mass (%)	***47.70***	***74.56***

B.2 The effects of acid washing on fast pyrolysis products

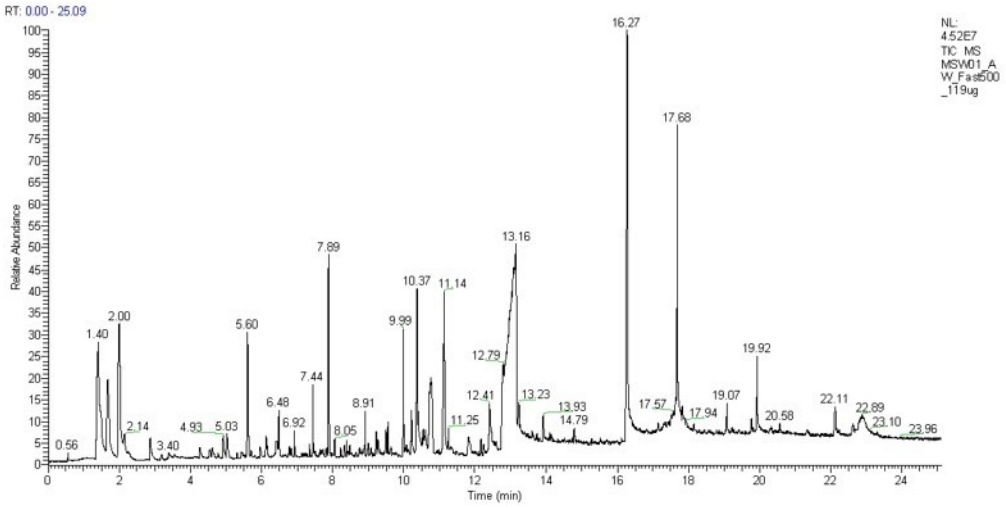

Figure B.1: Acid Washed Waste Paper chromatogram.

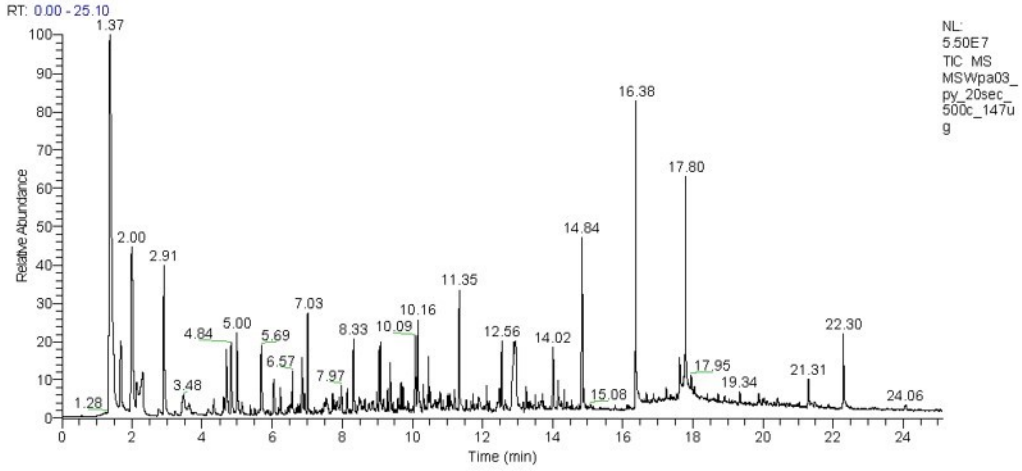

Figure B.2: Waste Paper chromatogram without acid washing

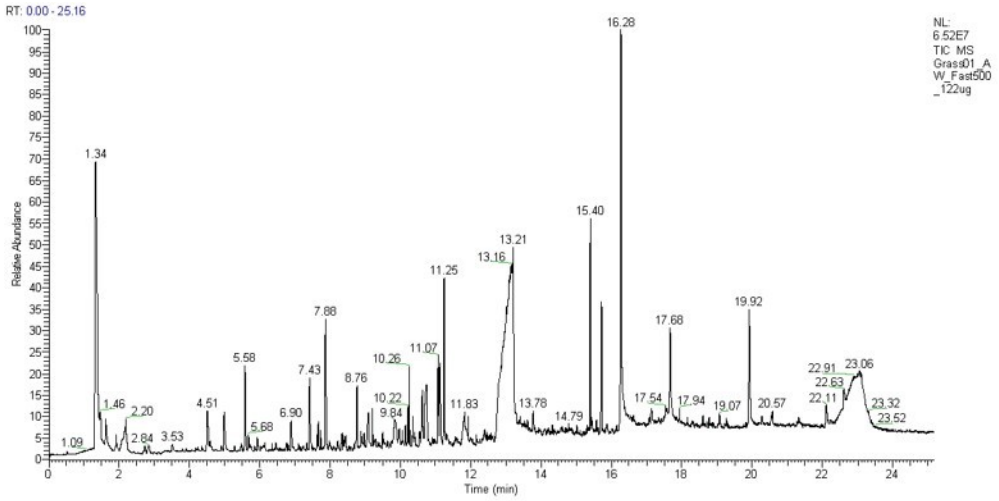

Figure B.3: Acid washed Grass Clipping chromatogram

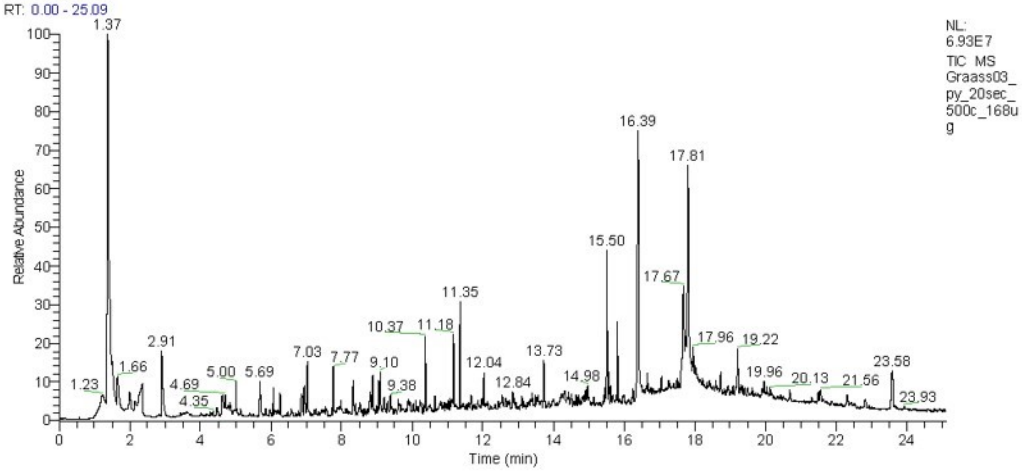

Figure B.4: Grass clipping without acid washing chromatogram

Appendix C: Kinetic Study of the Fast Micro-Pyrolysis of Hybrid Poplar

C.1: Residence Time Calculation

The residence time of vapors in the micro-pyrolysis reactor was approximated by use of the ideal gas law. The vapors are envisioned as forming very quickly from the rapid heating rate and forming a "cloud" in the gas phase that pushes the molecules out of the reaction vial with a pressure driven wave mechanism against the prevailing background He flow. It was assumed that the average molecular weight of the bio-oil produced within the first 1 second of pyrolysis was 60 g/mol (assuming primarily hemicellulose degradation, as verified in the results). The dimensions of the reactor vial are 2.5 cm long and 0.2 cm in diameter, resulting in a cross sectional rea of 0.03 cm^2 and a reactor volume of 0.08 cm^3. The biomass is loaded so that it is centered within the reaction vial. The pressure and temperature of the reactor during pyrolysis are 1 atm and 500°C (773.15 K), respectively. Assuming the average mass of biomass used for the pyrolysis experiments, which is 480 ug, and knowing from Figure 5.7 that 45% of the biomass is degraded within the first second the molar flow rate of volatilized product is shown below

$$\text{Amount volatilized in first second of pyrolysis} = 480\ ug \times 45\% = 216\frac{ug}{second}$$

$$\dot{n} = \frac{\left(216\frac{ug}{second}\right)}{60\ g/mol} \times 10^{-6}\frac{g}{ug} = 3.6 \times 10^{-6}\ \frac{moles}{seconds}$$

Therefore, when applying the ideal gas law the volumetric flow rate for the first 1 second of pyrolysis with 45% biomass degraded is 4.4 cm^3/s as shown below

$$\dot{V} = \frac{P}{nRT} = \frac{1\ \dot{atm}}{3.6\frac{moles}{second} \times 82.1\ \frac{cm^3\ atm}{K\ mol} \times 773.15\ K} = 4.4\frac{cm^3}{second}.$$

Diving the volumetric flow rate by the cross sectional area the superficial velocity is 139 cm/sec. Assuming the volatiles only travel half the length of the reactor due to be centered, the residence time is 0.009 second, the calculation is shown below.

$$\tau = \frac{(A \times L_{traveled})}{\dot{V}} = \frac{0.03\ cm^2 \times \left(\frac{2.5cm}{2}\right)}{4.4\frac{cm^3}{second}} = 0.009\ seconds$$

This residence time of vapors within the 500°C reaction zone is 2 orders of magnitude lower than fast pyrolysis conducted within pilot scale reactors, proving that only primary reactions were measured in this study.

C.2 Standards

Known masses of bio-oil compounds ranging from 0.15 to 40 ug were analyzed using gc-ms to determine the response factors for quantification of the bio-oil compounds produced via fast pyrolysis.

Table C.1 Response factors for bio-oil compounds studied with

Compound	Response Factor	R^2
Acetic Acid	3.49e-9	0.9
Furfural	2.8 E-9	0.99
m-cresol	1.73e-6	0.96
Guaiacol	1.91 e-9	0.96
Methyl Syringol	7.76e-9	0.97
Levoglucosan	1.22 e-8	n/a

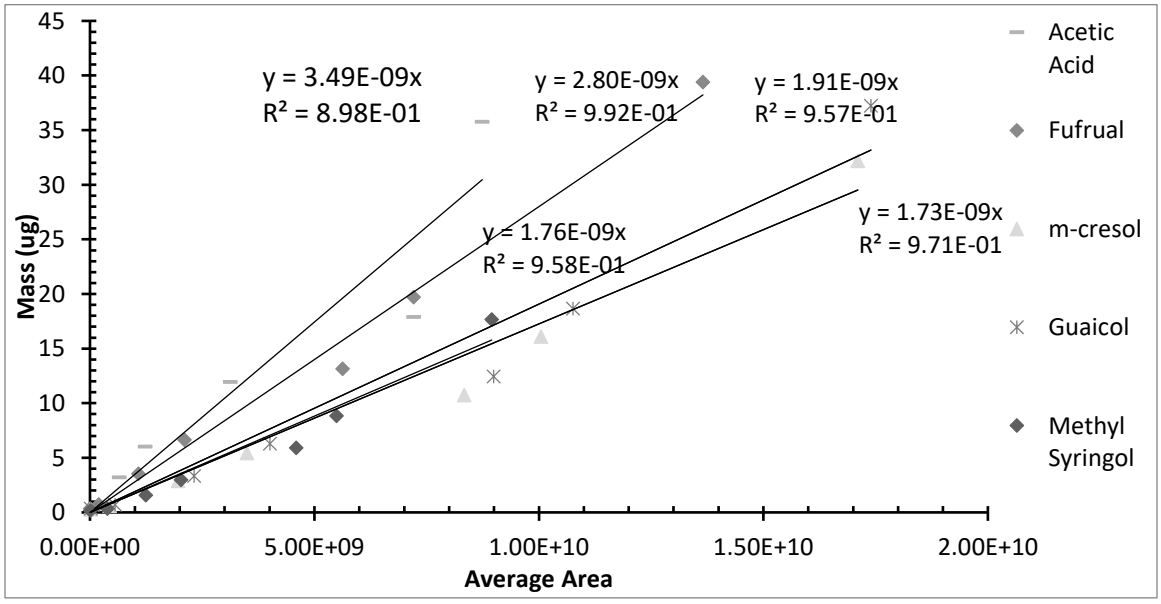

Figure C.1: Calibration curves for standards run for bio-oil compounds

C.3 Levoglucosan Results

The levoglucosan was not detected during the analysis of the bio-oil produced from the fast pyrolysis of the hybrid poplar. However, when the system was cleaned in-between pyrolysis runs, levoglucosan was detected. The levoglucosan peak was easily identified and the area of that peak calculated. The levoglucosan standard was unable to be calibrated properly, therefore the response factor used in our previous work [1] was used and adjusted based on the ratios of the response factors for the 5 other compounds to the response factors in previous work. The experimental results from this method are shown below in Figure C.1. There is large error in the mass of levoglucosan calculated at later times, likely due to more production of it and a difficulty in detection within our experimental set-up. The overall behavior of the data is similar to that of lignin and acetol; where there is delay in production and then in between 7-10 seconds begins to plateau.

The six step degradation model was applied in the same manner as the bio-oil compounds in the main body of this paper. The model fits the data quite well. It is able to capture the production delay and then the increase in production at later times. The α s fit to the levoglucosan data are shown below in Table C.2**.** As shown by the normalized α s 90% of the production of levoglucosan happens in the last 2 reactions. Evaluating the acetol we know that it is produced primarily in reaction 3, which could indicate when the cellulose is first beginning degradation and then continues degrading to produce levoglucosan. This experimental data is in good agreement with the main body of results,

however due to the large uncertainty of these results and how they were obtained, they were not directly compared in the main body of the work.

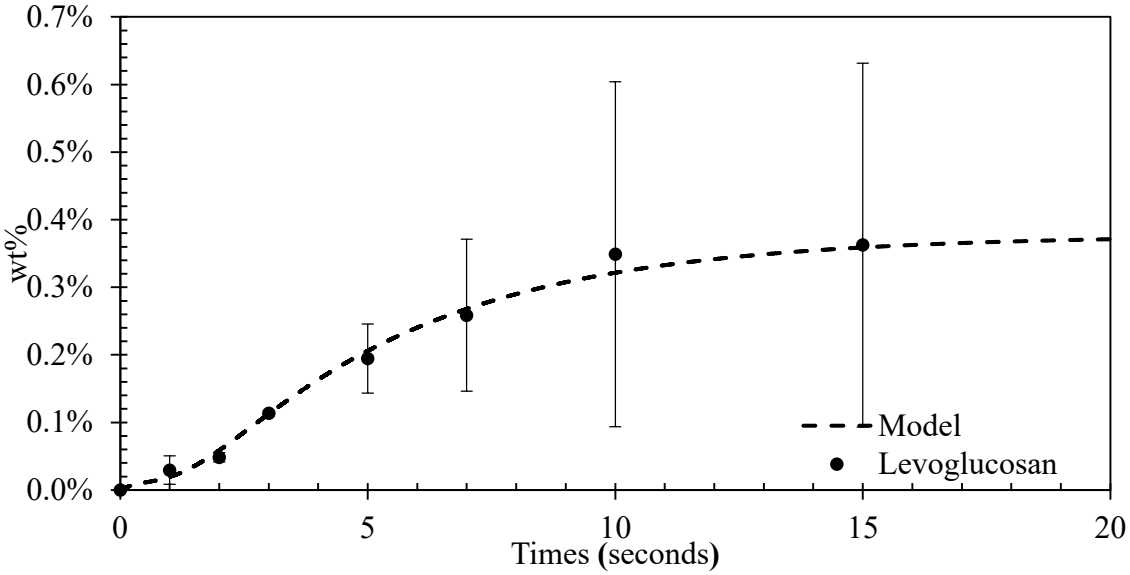

Figure C.2 Experimental data fitted to the six consecutive reaction model for levoglucosan.

Table C.2: Stoichiometric parameters for levoglucosan

Reaction	Amount Produced	Normalized Production
$\boldsymbol{\alpha_1}$	0.000070	0.017
$\boldsymbol{\alpha_2}$	0.000058	0.015
$\boldsymbol{\alpha_3}$	0.000001	0.0003
$\boldsymbol{\alpha_4}$	0.000001	0.0003
$\boldsymbol{\alpha_5}$	0.001137	0.30
$\boldsymbol{\alpha_6}$	0.002502	0.66

C.4 References

1. Klemetsrud, B., et al., *Characterization of Products from Fast Micropyrolysis of Municipal Solid Waste Biomass.* ACS Sustainable Chemistry & Engineering, 2016. **4**(10): p. 5415-5423.

Appendix D: Copyright Clearance

ELSEVIER LICENSE
TERMS AND CONDITIONS

Nov 07, 2016

This Agreement between Bethany J Klemetsrud ("You") and Elsevier ("Elsevier") consists of your license details and the terms and conditions provided by Elsevier and Copyright Clearance Center.

License Number	3983810109714
License date	Nov 07, 2016
Licensed Content Publisher	Elsevier
Licensed Content Publication	Journal of Analytical and Applied Pyrolysis
Licensed Content Title	Kinetic study of aspen during torrefaction
Licensed Content Author	Jordan Klinger,Ezra Bar-Ziv,David Shonnard
Licensed Content Date	November 2013
Licensed Content Volume Number	104
Licensed Content Issue Number	n/a
Licensed Content Pages	7
Start Page	146
End Page	152
Type of Use	reuse in a thesis/dissertation
Portion	figures/tables/illustrations
Number of figures/tables/illustrations	1
Format	both print and electronic
Are you the author of this Elsevier article?	No
Will you be translating?	No
Order reference number	
Original figure numbers	Fig 1
Title of your thesis/dissertation	EXPERIMENTAL AND THEORETICAL INVESTIGATION OF SUSTAINABLE FAST PYROLYSIS BIOFUELS FROM WOODY BIOMASS
Expected completion date	Dec 2016
Estimated size (number of pages)	200
Elsevier VAT number	GB 494 6272 12
Requestor Location	Bethany J Klemetsrud 1400 Townsend Dr 308 Chem Sci HOUGHTON, MI 49931 United States Attn: Bethany J Klemetsrud
Total	0.00 USD

Figure D.1: Copyright clearance for Figures 3.1, 4.1 and 5.2

SPRINGER LICENSE
TERMS AND CONDITIONS

Oct 27, 2016

This Agreement between Bethany J Klemetsrud ("You") and Springer ("Springer") consists of your license details and the terms and conditions provided by Springer and Copyright Clearance Center.

License Number	3977090672193
License date	Oct 27, 2016
Licensed Content Publisher	Springer
Licensed Content Publication	Environmental Management
Licensed Content Title	A Review of Environmental Life Cycle Assessments of Liquid Transportation Biofuels in the Pan American Region
Licensed Content Author	David R. Shonnard
Licensed Content Date	Jan 1, 2015
Licensed Content Volume Number	56
Licensed Content Issue Number	6
Type of Use	Thesis/Dissertation
Portion	Full text
Number of copies	
Author of this Springer article	Yes and you are the sole author of the new work
Order reference number	
Title of your thesis / dissertation	EXPERIMENTAL AND THEORETICAL INVESTIGATION OF SUSTAINABLE FAST PYROLYSIS BIOFUELS FROM WOODY BIOMASS
Expected completion date	Dec 2016
Estimated size(pages)	200
Requestor Location	Bethany J Klemetsrud 1400 Townsend Dr 308 Chem Sci HOUGHTON, MI 49931 United States Attn: Bethany J Klemetsrud
Billing Type	Invoice
Billing Address	Bethany J Klemetsrud 1400 Townsend Dr 308 Chem Sci HOUGHTON, MI 49931 United States Attn: Bethany J Klemetsrud
Total	0.00 USD
Terms and Conditions	

Figure D.2: Copyright clearance for Chapter 2

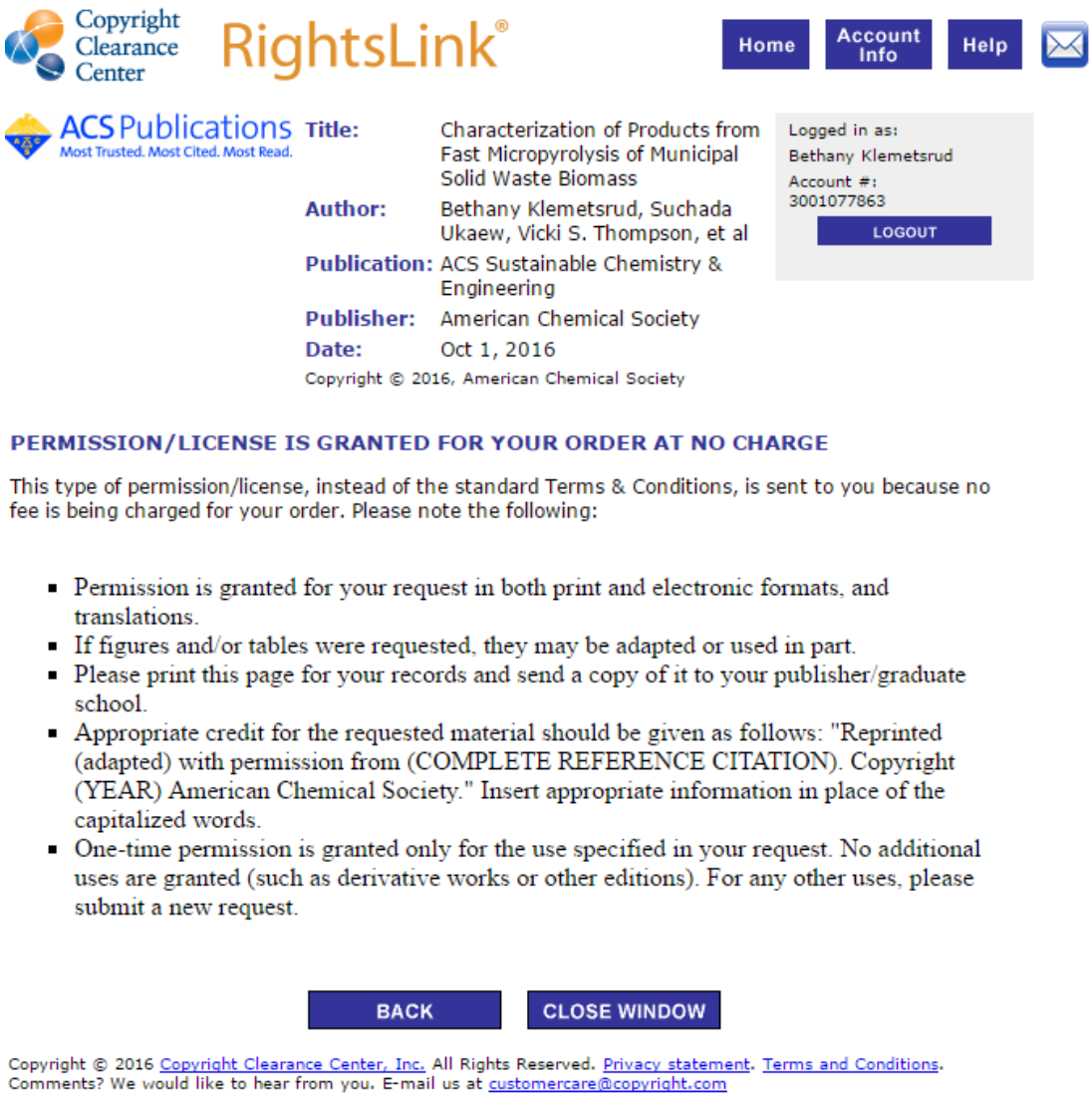

Copyright Clearance Center RightsLink®

Home | Account Info | Help

ACS Publications
Most Trusted. Most Cited. Most Read.

Title:	Characterization of Products from Fast Micropyrolysis of Municipal Solid Waste Biomass
Author:	Bethany Klemetsrud, Suchada Ukaew, Vicki S. Thompson, et al
Publication:	ACS Sustainable Chemistry & Engineering
Publisher:	American Chemical Society
Date:	Oct 1, 2016

Copyright © 2016, American Chemical Society

Logged in as:
Bethany Klemetsrud
Account #:
3001077863
LOGOUT

PERMISSION/LICENSE IS GRANTED FOR YOUR ORDER AT NO CHARGE

This type of permission/license, instead of the standard Terms & Conditions, is sent to you because no fee is being charged for your order. Please note the following:

- Permission is granted for your request in both print and electronic formats, and translations.
- If figures and/or tables were requested, they may be adapted or used in part.
- Please print this page for your records and send a copy of it to your publisher/graduate school.
- Appropriate credit for the requested material should be given as follows: "Reprinted (adapted) with permission from (COMPLETE REFERENCE CITATION). Copyright (YEAR) American Chemical Society." Insert appropriate information in place of the capitalized words.
- One-time permission is granted only for the use specified in your request. No additional uses are granted (such as derivative works or other editions). For any other uses, please submit a new request.

BACK | CLOSE WINDOW

Copyright © 2016 Copyright Clearance Center, Inc. All Rights Reserved. Privacy statement. Terms and Conditions.
Comments? We would like to hear from you. E-mail us at customercare@copyright.com

Figure D.3: Copyright clearance for Chapter 3